

---

# **NOVEL    BIOACTIVE    PRODUCTS**

# **FROM ANTARCTIC BACTERIA**

---

**Filomena Sannino**

Dottorato in Scienze Biotecnologiche – XXVIII ciclo

Indirizzo Biotecnologie Industriali e Molecolari

Università di Napoli Federico II







Dottorato in Scienze Biotecnologiche – XXVIII ciclo

Indirizzo Biotecnologie Industriali e Molecolari

Università di Napoli Federico II



---

# **NOVEL      BIOACTIVE      PRODUCTS**

# **FROM ANTARCTIC BACTERIA**

---

**Filomena Sannino**

Dottorando:              Filomena Sannino

Relatore:                  Prof. Maria Luisa Tutino

Coordinatore:            Prof. Giovanni Sannia

*Beneath the placid ice floes and under the calm  
water pools the old universal warfare is raging  
incessantly in the struggle for existence*

*(Robert Falcon Scott)*

*A chi non ha mai smesso di credere in me...*



## INDEX

<b>SUMMARY</b>	pag. 1
<b>RIASSUNTO</b>	pag. 3
<b>GENERAL INTRODUCTION</b>	
1. Marine Biotechnologies	pag. 9
2. Polar bacteria as a source of bioactive natural products	pag. 11
3. The cold-adapted model microorganisms	
3.1 <i>Pseudoalteromonas haloplanktis</i> TAC125	pag. 12
3.2 <i>Colwellia psychrerythraea</i> 34H	pag. 13
4. Aim of the study	pag. 13
<b>CHAPTER I – Antimicrobial volatile organic compounds</b>	
1. Topic Introduction	pag. 15
1.1 Paper I: A novel synthetic medium for sub-zero growth and recombinant protein production in <i>Pseudoalteromonas haloplanktis</i> TAC125	pag. 17
1.2 Paper II: <i>Pseudoalteromonas haloplanktis</i> TAC125 produces methylamine, a volatile compound active against <i>Burkholderia cepacia</i> complex strains	pag. 34
<b>CHAPTER II – Anti-biofilm molecules</b>	
2. Topic Introduction	pag. 51
2.1 Paper I: Anti-biofilm activity of <i>Pseudoalteromonas haloplanktis</i> TAC125 against <i>Staphylococcus epidermidis</i> biofilm: evidence of a signal molecule involvement?	pag. 53
2.2 Paper II: Anti-Biofilm activities from marine cold-adapted bacteria against Staphylococci and <i>Pseudomonas aeruginosa</i>	pag. 63
2.3 Paper III: Biofilm cultivation of Antarctic bacterium <i>P. haloplanktis</i> TAC125: physiologic studies and biotechnological applications	pag. 71
<b>CHAPTER II – Anti-biofilm molecules</b>	
3. Topic Introduction	pag. 82
3.1 Paper I: A unique capsular polysaccharide from the psychrophilic marine bacterium <i>Colwellia psychrerythraea</i> 34H that mimics antifreeze (glyco)	pag. 83
<b>REFERENCES</b>	pag. 94
<b>CONCLUSIONS</b>	pag. 99
<b>PUBLICATIONS AND COMMUNICATIONS</b>	pag. 100
<b>EXPERIENCES IN FOREIGN LABORATORIES</b>	pag. 101



## SUMMARY

Marine bacteria have considerable importance as sources of biologically active products. Marine microorganisms that live in cold regions have been largely underexplored, and may be endowed with interesting chemical repertoire. The microorganisms that thrive in these cold environments are referred to as psychrophiles or cold-adapted bacteria and are able to produce a large number of bioactive compounds, such as antimicrobial, anti-fouling and various pharmaceutically-relevant activities.

In this context, the aim of my PhD project was the research of new bioactive compounds of biotechnological interest from Polar marine bacteria. In particular, I focused my attention on three classes of molecules:

- I. Antimicrobial volatile organic compounds (VOCs);
- II. Anti-biofilm molecules;
- III. Cryoprotectant compounds.

### • **Part I**

In order to explore the *Pseudoalteromonas haloplanktis* TAC125 (*P.haloplanktis* TAC125) chemical diversity as source of bioactive compounds, a suitable synthetic growth medium was developed, containing D-gluconate and L-glutamate as carbon, nitrogen and energy sources (GG medium). The definition of a synthetic medium is necessary for the scale up of *P. haloplanktis* TAC125 growth in automatic bioreactors. Moreover, a defined “minimum” medium could enhance the secondary metabolites production, and it surely makes their purification easier. Preliminary studies demonstrated that some Antarctic marine bacteria are able to produce volatile organic compounds (VOCs) that specifically inhibit the growth of *Burkholderia cepacia* complex (Bcc) strains. Amongst the tested Antarctic marine bacteria, *P.haloplanktis* TAC125 was further investigated. It is known that the *P.haloplanktis* TAC125 production of VOCs changes with growth medium composition. With the aim to identify the anti-Bcc VOCs, a suitable capture trap for volatile compounds was developed. A bioactive compound was identified, the methylamine, and its anti-Bcc activity was demonstrated by defining the Minimum Volatile Inhibitory Concentration (MVIC) on a panel of Bcc strains.

### • **Part II**

Anti-biofilm molecules may have interesting biomedical applications in targeting adhesive properties of several insidious human pathogens. Previous results showed that the cell-free supernatant of *P.haloplanktis* TAC125 grown in static condition strongly inhibited bacterial adhesion. In particular, *Staphylococcus epidermidis* showed the highest susceptibility to the treatment. During this part of my PhD project the best conditions in which *P.haloplanktis* TAC125 produces the anti-biofilm compound/s were searched and a preliminary purification scheme was set up. In particular, the effect of growth mode, culture medium composition, growth phase and temperature was explored. The best production conditions were set as a benchmark for the scale-up of *P.haloplanktis* TAC125 anti-biofilm molecule/s in bioreactor.

- **Part III**

Marine cold-adapted microorganisms may be also source of another interesting class of chemical compounds, known as cryoprotectors, as they are able to avoid ice crystal formation inside living cells. Freeze-thaw cycles are quite common in the cold regions, especially in Polar one. Cold-adapted microorganisms are accustomed to being frozen within their habitats. Such organisms are also expected to have evolved adaptations to survive repeated freezing and thawing, as these processes tend to damage living cells and attenuate cell viability. The cold-adapted bacterium *Colwellia psychrerythraea* strain 34H (*C. psychrerythraea* 34H), attracted particular attention because it was reported to physically interact with sea ice crystals and secrete cryoprotectants of polysaccharidic nature in culture medium as a survival strategy.

During my project, it was demonstrated that *C. psychrerythraea* 34H cells are covered by a capsula: the determination of chemical composition of purified capsular material revealed a novel polysaccharidic structure. Indeed the capsula was made by a linear tetrasaccharide repeating unit containing two amino sugars and two uronic acid, one of which is amidated by a threonine. The presence of an amminoacidic decoration of the capsular polysaccharide is quite uncommon in marine bacteria, but more intriguing is the decoration with Thr residues, as glycosilated Thr residues are essential for the interaction of anti-freeze glycoproteins (AFGPs) with ice crystals. In line with this indirect observation, in vitro assays demonstrated that the *C. psychrerythraea* 34H capsular polysaccharide is endowed with ice re-crystallization inhibition activity.

## RIASSUNTO

### Premesse scientifiche:

I microrganismi che colonizzano gli habitat marini sono produttori di un variegato numero di metaboliti secondari. Ad oggi è nota la struttura di almeno 17.000 biomolecole di origine marina, ma la maggior parte di queste proviene da organismi che vivono in ambienti temperati o tropicali. Meno del 3% del totale, invece, proviene da organismi che vivono in ambienti estremi come gli ecosistemi polari, la cui biodiversità è ancora largamente inesplorata.

Le regioni polari rappresentano, quindi, dei laboratori unici per lo studio dei meccanismi molecolari che gli organismi utilizzano per sopravvivere e adattarsi a condizioni estreme. Microrganismi che vivono in queste regioni sono chiamati psicrofili o adattati al freddo.

Particolarmente interessante e oggetto di studio presso il laboratorio dove è stato svolto il mio progetto di dottorato è il batterio psicrofilo Gram-negativo *Pseudoalteromonas haloplanktis* TAC125 (*P.haloplanktis* TAC125) il cui genoma è stato completamente sequenziato e annotato nel 2005 da Medigue et al. Questo batterio, per il quale sono già disponibili sistemi genetici per l'espressione ricombinante di geni e per la creazione di mutanti genomici per inserzione e sostituzione, è in grado di crescere in un ampio intervallo di temperature e concentrazioni saline raggiungendo alte densità cellulari. Attualmente viene anche utilizzato come piattaforma tecnologica per la produzione di svariati tipi di proteine ricombinate tra cui alcuni anticorpi e proteine di interesse biomedico. Hanno catturato la nostra attenzione anche i microrganismi appartenenti al genere *Colwellia*, in modo particolare *Colwellia psychrerythraea* 34H (*C.psychrerythraea* 34H), che è stato isolato da sedimenti del mare Artico ed è considerato un organismo modello per lo studio degli adattamenti al freddo. Produce molecole di elevato interesse biotecnologico tra cui enzimi extracellulari e crioprotettori.

Il mio progetto di dottorato si inserisce nell'ambito della ricerca di nuove molecole bioattive da microrganismi adattati al freddo. In particolare mi sono occupata di molecole volatili ad attività antimicrobica, molecole anti-biofilm e di composti ad attività crioprotettrice.

### Obiettivi:

Il mio progetto di dottorato si è incentrato su tre aspetti principali:

#### Parte I

La ricerca di molecole volatili bioattive ad attività anti-microbica prodotte da *P.haloplanktis* TAC125 capaci di inibire la crescita di ceppi appartenenti al cosiddetto *Burkholderia cepacia* complex (Bcc).

#### Parte II

Ricerca di molecole ad attività anti-biofilm prodotte da *P.haloplanktis* TAC125 che sono in grado di eradicare il biofilm di *Staphylococcus epidermidis*. Inoltre valutare come potenziali produttori di molecole anti-biofilm batteri marini Polari appartenenti ad altri generi.

#### Parte III

Studiare le molecole ad attività crioprotettrice prodotte da *C.psychrerythraea* 34H



## Risultati e Discussione:

### Parte I

Poiché la capacità dei microrganismi di produrre metaboliti bioattivi è spesso condizionata dalla composizione e natura del terreno di coltura, si è scelto di sviluppare un nuovo mezzo per *P.haloplanktis* TAC125. È stato quindi formulato il mezzo di coltura minimo e definito GG, il quale contiene D-gluconato ed L-glutammato quali fonti di carbonio ed energia, scelti alla luce delle preferenze del microrganismo verso substrati di natura amminoacidica. Il GG non solo è ottimale per la crescita di *P.haloplanktis* TAC125 ma ha reso possibile anche lo sviluppo di processi di produzione in bioreattore automatizzato. Inoltre la scelta del terreno definito potrebbe portare ad un aumento della produzione dei metaboliti secondari e facilitarne la loro purificazione per la sua minore complessità rispetto ad un terreno ricco.

È stato dimostrato che alcuni microrganismi marini Antartici, appartenenti al genere *Pseudoalteromonas*, sono capaci di produrre molecole volatili bioattive (*Volatile Organic Compound/s*, VOCs), che hanno la capacità di inibire la crescita di alcuni ceppi di *Burkholderia cepacia* complex (Bcc). I ceppi appartenenti al genere Bcc sono patogeni opportunistici responsabili delle infezioni polmonari in pazienti affetti da Fibrosi Cistica (FC) e sono particolarmente resistenti alla maggior parte degli antibiotici attualmente in commercio. Solitamente i pazienti affetti da FC sono trattati con combinazioni di due o più antibiotici, ma neppure questa è parsa fino ad oggi una strategia ottimale per abbattere la carica microbica. Da qui nasce la necessità di trovare altre molecole ad azione antimicrobica specifiche per le Bcc.

È noto da letteratura che quando *P.haloplanktis* TAC125 cresce su un terreno agarizzato è in grado di produrre molecole volatili bioattive contro le Bcc, quindi il primo obiettivo è stato quello di verificare la produzione di VOCs attivi anche quando il batterio era cresciuto in terreno liquido.

Per valutare la produzione di molecole volatili attive durante la crescita in liquido, è stato utilizzato un bioreattore automatizzato nel quale *P.haloplanktis* TAC125 è stato cresciuto in un convenzionale terreno complesso, dimostrando il rilascio di un numero elevato di VOCs attivi. Il passo successivo è stato lo sviluppo di un sistema efficiente per la cattura e l'accumulo delle molecole volatili prodotte dal microrganismo. Per realizzare ciò, è stato progettato una trappola per la cattura e l'accumulo dei VOCs che ha previsto la condensazione dei gas in uscita da un fermentatore inoculato con *P.haloplanktis* TAC125. Analisi di SPME-GC-MS hanno dimostrato che *P.haloplanktis* TAC125 è in grado di produrre un numero discreto di molecole volatili appartenenti a svariate classi chimiche. Data la complessità della "lista" dei VOCs prodotti dal microrganismo in terreno ricco, è stato utilizzato il terreno GG in precedenza ottimizzato come mezzo di crescita. È stato dimostrato che *P.haloplanktis* TAC125 non è in grado di inibire la crescita delle Bcc se cresciuto in GG, ciò conferma la dipendenza della produzione dei VOCs dalla composizione del terreno di coltura. La mancanza di produzione dei VOCs attivi in GG ci ha permesso di formulare un nuovo terreno di coltura il GG-metionina, ottenuto aggiungendo al GG la metionina. L'aggiunta dell'amminoacido come fonte di carbonio/azoto al terreno definito GG ha ripristinato la capacità inibente da parte di *P.haloplanktis* TAC125 sulle Bcc. Grazie alla disponibilità del sistema di cattura sono state identificate le molecole volatili, prodotte in questa condizione attraverso analisi di SPME-GC-MS, e tra le molecole identificate abbiamo focalizzato la nostra

attenzione sulla metilammina a causa della sua bassa tossicità per l'uomo e la facilità di manipolazione in laboratorio. Per valutare la tossicità della metilammina sulle Bcc è stato messo a punto un sistema per la valutazione della Minima Concentrazione Inibente della molecola Volatile (MVIC). Ed è stata valutata la MVIC della metilammina su un pannello più ampio di Bcc.

## Parte II

Il biofilm può essere considerato come una comunità multicellulare, costituita sia da procarioti che da eucarioti, immersa in una matrice che in parte è sintetizzata dalle cellule stesse. I biofilm batterici sono responsabili, nell'uomo, della maggior parte delle infezioni persistenti. Infatti, i biofilm possono ostruire cateteri e causano infezioni negli impianti ortopedici.

La causa più frequente d'infezione di protesi è a carico degli Staphilococchi perché sono microrganismi già presenti sulla pelle umana e nelle mucose. La virulenza a carico degli Staphilococchi è dovuta alla capacità di questi di formare biofilm su superfici sia biotiche sia abiotiche. Tra tutti gli staphilococchi, *Staphylococcus epidermidis* (*S.epidermidis*) è particolarmente difficile da eradicare ed è coinvolto nella maggior parte delle infezioni croniche a carico del biofilm. Nasce quindi la necessità di studiare nuove molecole ad attività anti-biofilm mirate a non intaccare la vitalità cellulare per evitare la comparsa di mutanti resistenti.

La ricerca di nuove molecole ad attività anti-biofilm è il presupposto nel quale si inserisce la seconda parte del mio lavoro di tesi. È già stato dimostrato che il surnatante di *P.haloplanktis* TAC125 cresciuto in statico è in grado di inibire la formazione del biofilm di *S.epidermidis*.

Al fine di rendere possibile la purificazione della/e molecole bioattive, è stato essenziale definire le condizioni di processo ottimali per la sua massima produzione. In particolare, sono stati oggetto di valutazione ed ottimizzazione i seguenti parametri di processo: la temperatura di crescita, la natura chimica del supporto; le modalità di crescita stessa; l'effetto della composizione del terreno di coltura.

Le informazioni così ottenute sono state poi direttamente utilizzate nello sviluppo di un processo su larga scala in un bioreattore automatizzato da tre litri. La produzione in fermentatore permette non solo di ottenere grandi quantità di surnatante, ma anche di recuperare le cellule cresciute in biofilm per studi di tipo fisiologico. Per la crescita di *P.haloplanktis* TAC125 in fermentatore in biofilm, sono stati appositamente studiati supporti di polistirene, che hanno permesso la formazione del biofilm all'interfaccia tra aria e liquido. Questa strategia ha permesso una produzione su larga scala della molecola d'interesse e di capire la diversa fisiologia delle cellule cresciute in biofilm o in planctonico. In particolare per gli studi fisiologici, è stato analizzato il lipopolisaccaride.

Poi si è passati ad uno *screening* preliminare di microrganismi appartenenti al genere *Pseudoalteromonas*, *Psychrobacter*, e *Psychromonas* allo scopo di valutare la loro eventuale capacità di produzione di molecole anti biofilm su altri patogeni.

In particolare sono state eseguite delle crescite in sessile e in planctonico di una piccola collezione di batteri psicrofili polari. I surnatanti di queste crescite, sono stati utilizzati per valutare l'inibizione della formazione di biofilm su differenti specie di patogeni tra cui *S.epidermidis*, *P. aeruginosa* PAO1 e tre *strains* appartenenti al genere *Staphylococcus aureus* (*S. aureus*).

Soltanto alcuni dei ceppi hanno mostrato avere attività, in modo particolare *Psychrobacter* sp. TAD1, *P.haloplanktis* TAE79, *P.haloplanktis* TAE80, *Psychrobacter articus* 273-4 e *Psychromonas artica*, sono capaci di produrre molecole anti-biofilm.

Sui surnatanti di queste crescite sono state fatte delle preliminari caratterizzazioni chimiche e si è visto che ciascuno di loro può produrre molecole di natura differente a seconda della modalità di crescita (plantonico o sessile). Ancora, ciascuno di questi ceppi può produrre molecole attive di differente natura chimica a seconda del ceppo bersaglio su cui va ad agire. È stata inoltre fatta una caratterizzazione chimico-fisica che ha confermato la differente natura di ciascuna delle molecole anti-biofilm.

### Parte III

I batteri freddo adattati sono capaci di produrre un'altra classe di molecole interessanti a livello industriale: i crioprotettori. Questa classe di molecole è essenziale per la sopravvivenza in ambienti estremi in quanto non permette la formazione di ghiaccio nella cellula evitandone il congelamento. I crioprotettori di origine naturale hanno svariate applicazioni biotecnologiche che vanno dall'industria alimentare a quella medica come la crioconservazione degli embrioni.

Tra i vari batteri psicrofili notevole interesse lo ha suscitato *Colwellia psychrerythraea* 34H (*C.psychrerythraea* 34H) della quale è stato sequenziato e annotato il genoma nel 2005.

*C.psychrerythraea* 34H è in grado di produrre molecole ad attività crioprotettrice come strategia di sopravvivenza per l'adattamento al freddo. In questo scenario, s'inserisce l'ultima parte del mio progetto di dottorato: la ricerca di molecole ad attività crioprotettrice da batteri adattati al freddo.

Sono state messe a punto le condizioni di crescita per il batterio *C.psychrerythraea* 34H con il fine di ottenere elevate biomasse per la successiva caratterizzazione chimica delle molecole di interesse.

Le analisi chimiche hanno mostrato che *C.psychrerythraea* 34H è dotata di una capsula di natura polisaccaridica che mostra una struttura del tutto inusuale tra quelle note. In particolare, si presenta come un polimero la cui unità ripetitiva è costituita da un tetrasaccaride contenente due ammino zuccheri e due acidi uronici di cui uno ha legato un residuo di treonina. La decorazione amminoacidica su uno zucchero è una struttura del tutto nuova e inusuale tra i batteri. È noto in letteratura che le proteine *anti-freeze* di alcuni organismi superiori possono essere caratterizzate dalla presenza di treonina che ne permettono l'interazione con il ghiaccio.

Sulla capsula di *C.psychrerythraea* 34H sono stati effettuati saggi di ricristallizzazione con il ghiaccio i quali hanno mostrato che la capsula di è capace di interferire con la cristallizzazione del ghiaccio stesso.

### Risultati conseguiti:

È stato ottimizzato un terreno definito per *P.haloplanktis* TAC125: il GG.

L'ottimizzazione del GG ha permesso di studiare i metaboliti secondari prodotti da *P.haloplanktis* TAC125. Il GG ci ha consentito non solo di fare delle crescite in fermentatore, ma anche di facilitare la purificazione dei metaboliti secondari prodotti da *P.haloplanktis* TAC125.

È stata trovata la prima molecola volatile ad attività antimicrobica specifica contro le Bcc da *P.haloplanktis* TAC125: la metilammina. Di tale molecola è stata valutata la minima concentrazione inibente sulle Bcc

Sono state ottimizzate le condizioni di produzione della molecola anti-biofilm da *P.haloplanktis* TAC125 contro *S.epidermidis*. In particolare sono state esplorati vari terreni di crescita, temperature e supporti.

*P.haloplanktis* TAC125 produce biofilm su supporti di polistirene, la produzione della molecola anti-biofilm è dipendente dal terreno di coltura, al contrario non dipende dalla temperatura. Inoltre è stato definito un sistema per la crescita in biofilm in fermentatore che ha permesso da un lato di ottenere grosse quantità di campione per la purificazione, dall'altro di ottenere cellule cresciute in biofilm da utilizzare per studi fisiologici.

È stato dimostrato che *C.psychrerythraea* 34H è un microrganismo capace di produrre una capsula. La struttura è di natura polisaccaridica con decorazioni amminoacidiche. Tale molecola, la cui struttura è del tutto nuova, presenta attività crioprotettrice poiché è in grado di inibire il processo di cristallizzazione del ghiaccio.



## **GENERAL INTRODUCTION**

## 1. Marine Biotechnologies

More than 70% of the Earth's surface is covered by the ocean which contains a vast collection of diverse microbial communities, all interacting with each other and with the environment around them. In fact, it is estimated that the ocean contains the highest percentage of prokaryotic cells on Earth, with a reported  $3.67 \times 10^{30}$  cells [1]. It is believed that specific physiochemical properties of the marine environment, such as pressure, temperature, pH, osmolarity, and uncommon functional groups (such as isonitrile, dichloroimine, isocyanate, and halogenated functional groups) may result in the production of bioactive substances with different properties from those found in terrestrial habitats [2].

Therefore, the marine habitat continues to be a source of unique natural products used for pharmaceutical and biotechnological applications [3]. In fact, the Roman philosopher Plinius first described the use of marine natural organisms such as sponges in medicinal applications, such as for the treatment of wounds, sunstroke and infections, around 2000 years ago [4]. More than 20,000 structurally diverse marine natural products have been isolated from marine organisms [5].

Major pharmaceutical companies have been exploring marine compounds for several decades, but their investments and interest ceased when synthetic combinatorial compound libraries emerged since they were simpler and more cost-efficient for the high-throughput screening. However, the combinatorial chemistry approach failed to produce enough new drug entities, and in the recent years, there has been an emergence of small biotechnology companies marketing marine-based drugs [6]. Examples of approved drugs and potential therapeutic compounds derived from marine sources are given in **Table 1**.

Therapeutic class	Compound	Chemical classification	Source organism
Cancer	Aplidine, plitidepsin (Aplidin®)	Depsipeptide	Tunicate Aplidium alpicans
	Brentuximab vedotin (Adcetris™)	Antibody-drug conjugate	Monomethyl auristatin E, synthetic, based on dolastatin 10, sea hare <i>Dolabella auricularia</i> /cyanobacteria
	Cytarabine, Ara-C (Cytosar-U, Depocyt)	Pyrimidine nucleoside	Sponge <i>Cryptotheca crypta</i>
	Elisidepsin (Irvalec®)	Depsipeptide	Synthetic, based on kahalalide F, mollusc <i>Elysia rufescens</i>
	Eribulin mesylate (Halaven®)	Macrolide	Synthetic, based on halichondrin B, sponge <i>Halichondria</i>
	Trabectedin (Yondelis®)	Alkaloid	Tunicate <i>Ecteinascidia turbinata</i>

Therapeutic class	Compound	Chemical classification	Source organism
	Jorumycin (Zalypsis®)	Alkaloid	Mollusc <i>Jorunna funebris</i>
Schizophrenia	DMXBA (GTS-21) anabaseine derivative	Alkaloid	Synthetic, based on anabaseine, marine worm <i>Paranemertes peregrine</i>
Pain	Ziconotide (Prialt®)	Peptide	Cone snail <i>Conus magus</i>
	Tetrodotoxin (Tectin®)	Alkaloid	Pufferfish Tetraodontidae

**Table 1: Approved drugs and potential therapeutic compounds derived from marine sources.** Source: <http://marinepharmacology.midwestern.edu/clinPipeline.htm>

Moreover, the importance of marine organisms as source of new natural products promotes the launch of large scale marine biotechnology projects, in the European Union. Horizon 2020 program is strongly supporting the investments in marine research and innovation started during the previous 7th Framework Program, in which several marine biotechnology projects based on drug discovery were founded: MAREX – Exploring marine resources for bioactive compounds: from discovery to sustainable production and industrial applications (2010–2014), BAMMBO – Sustainable production of biologically active molecules of marine based origin (2011–2014), PharmaSea – Increasing value and flow in the marine biodiscovery pipeline (2012–2016), SeaBioTech – From sea-bed to test-bed: harvesting the potential of marine microbes for industrial biotechnology (2012–2016).

Amongst marine organisms that are excellent sources for many industrial products, marine microorganisms continue to be a major focus of many natural product research efforts, with a 10% increase in the number of compounds reported from 2011 to 2012 [7].

Marine bacteria include archaea and eubacteria: archaea is an interesting group of bacteria since many of them are extremophiles, organisms that live in extreme conditions, e.g., deep sea, thermal vents, low temperature, or chemically challenging environment (salinity, pH, heavy metals). Marine eubacteria consist of Gram-positive actinomycetes and bacilli, Gram-negative  $\alpha$ -proteobacteria and  $\gamma$ -proteobacteria and several anoxygenic anaerobes [8]. Marine bacteria as well as marine fungi, cyanobacteria and some microalgae are living as symbionts in sediment, sponges or other invertebrates [9]. Several marine bacteria can be grown in laboratory cultures and thus only small amounts of sample are required for cultivation, or metagenomic approaches can be used to build libraries [10].

Sometimes, marine bacteria live in association with other organisms, which lack obvious structural defense mechanisms, and thus rely on chemical defense by production of bioactive secondary metabolites, either by themselves or by associated microflora, to survive in their extreme habitat. In the last decades, the number of



reported secondary metabolites from marine bacteria has strongly increased, thus reflecting the growing attention by research groups from academia and industry [5]. Marine bacteria produce several classes of compounds. Around 100 novel compounds (e.g., polyketides, alkaloids, fatty acids, peptides and terpenes) are isolated from marine bacteria per year [8]. Bacterial metabolites are probably the most promising source for novel antibacterial, [11], is a potential antibiotic against MRSA (Methicillin-Resistant *Staphylococcus aureus* ) and vancomycin-resistant enterococci.

## **2. Polar bacteria as source of bioactive natural products**

We know that the marine habitat is extremely complex and contains a vast diversity of life forms, considering that the water column of oceans contains about  $10^6$  bacterial cells per milliliter [12].

The majority of marine organisms studied have originated from tropical and temperate waters. As a consequence, fewer than 3% of reported marine natural products originate from organisms collected in Polar habitats, despite the fact that one entire continent and a significant portion of global shallow-water habitat are found at polar latitudes.

Cold-water microbial biodiversity is largely unexplored but recent efforts to characterize Polar marine microbial communities have demonstrated them to be rich and often uncharacterized [13]. The microorganisms that thrive in these cold environments are referred to as psychrophiles or cold-adapted. Cold-adapted bacteria are microorganisms able to survive in habitats where the average temperatures are permanently or transiently below 15 °C (temperature: -2-15°C).

These low temperature conditions impose several challenges to living organisms, especially the unicellular ones, such as the exponential decrease of biochemical reaction rates, change in medium viscosity which makes reaction rate more slowly, changes in membrane fluidity and protein conformation, nutrient availability, ability to reproduce and protection against freezing condition [14, 15]. Even in this condition, cold-tolerant organisms manage to survive due to modification made to cytoplasmic membrane, supramolecular assembly processes, secondary structure of nucleic acid and to adaptations in either extra- or intracellular enzymes [14].

Most cellular adaptations to low temperatures and the underlying molecular mechanisms are not fully understood. This includes studies on the regulation of membrane fluidity, the maintenance of protein synthesis and the production of cold-acclimation proteins, and the mechanisms of freeze tolerance [16]. In psychrophilic bacteria the presence of cryoprotective molecules [17], antifreeze proteins [18] and exopolymers [19] can buffer these organisms against the damaging effects of intracellular ice formation. Enzymatic structural adaptations, [20] including a reduction in protein residues displaying ion-pairing, hydrogen bonding and even  $\pi$ -stacking aromatic interactions, [21] have enabled these organisms to maintain metabolic rates commensurate with their mesophilic congeners [22].

Protected against ice formation and enzymatically adapted to function most efficiently at low temperature, psychrophiles are subject to switch metabolic energy and other secondary metabolic resources to chemical defence as are mesophiles.

Following this raising of interest concerning cold-adapted marine bacteria, in the very recent years few papers reported their ability to produce a large number of bioactive compounds. A preliminary characterization of these molecules demonstrate that are

endowed with antimicrobial, anti-fouling and various pharmaceutically-relevant activities [23, 24].

Amongst the Polar marine bacteria that are able to produce bioactive products, *Pseudoalteromonas haloplanktis* TAC125 (*P.haloplanktis* TAC125) and *Colwellia psychrerythraea* 34H (*C.psychrerythraea* 34H) have been deeply investigated.

### 3. The cold-adapted model microorganisms

#### 3.1 *Pseudoalteromonas haloplanktis* TAC125

*P.haloplanktis* TAC125 is a Gram-negative bacterium isolated from an Antarctic coastal seawater sample collected in the vicinity of the French Antarctic station Dumont D'Urville, Terre Adélie (66°40' S; 140° 01' E). It can be classified as a eurypsychrophile and was the first Antarctic Gram-negative bacterium of which the genome was fully sequenced and carefully annotated. Several exceptional genomic and metabolic features were derived from the genome sequence of this bacterium, showing adaptation to periodic situations of nutrient abundance. *P.haloplanktis* TAC125 is one of the most intensively investigated, as the bacterium is one of the fastest growing psychrophiles characterized so far and it is able to grow in a quite wide temperature range (0-25°C) [25]. Furthermore, *P.haloplanktis* TAC125 is considered to be one of the model organisms of cold-adapted bacteria and it is the first Antarctic marine bacterium for which a genome-scale metabolic reconstruction is also available [26]. The determination of *P.haloplanktis* TAC125 genome revealed that the bacterial genome is characterized by a quite high number of rRNA and tRNA genes (106, sometimes organized in long runs of repeated sequences), which may account for its relevant capacity for translation and fast growth performances at low temperatures. Fast growth rates, combined with the ability of *P.haloplanktis* TAC125 to reach very high cell densities even under laboratory growth conditions and to be easily transformed by intergeneric conjugation [27], made this bacterium an attractive host for the development of an efficient gene expression system at low temperatures [28]. Indeed *P.haloplanktis* TAC125 has been suggested as an alternative host for the soluble overproduction of heterologous proteins [29, 30]. In view of its application for industrial purposes, laboratory-scale fermentation processes have been developed, demonstrating the feasibility of *P.haloplanktis* TAC125 growth in batch [31], in a C-limited chemostat cultivation [32], and in fed-batch fermentations [29]. The efficiency of cold-adapted expression systems was also validated by the successful production of difficult proteins and biopharmaceuticals [30, 32, 33, 34]. The increasing interest in *P.haloplanktis* TAC125 has led to the accumulation of different data types for this bacterium in the last few years, including its complete genome sequence [25], its proteome [35, 36] and detailed growth phenotypes [29]. Thus, it is now possible to integrate such different data sources and perform a system-level investigation of *P.haloplanktis* TAC125 metabolism. Furthermore, bacteria belonging to the genus *Pseudoalteromonas* are known to possess an inhibitory activity against human pathogens belonging to the *Burkholderia cepacia* complex (Bcc) and to be able to produce anti-biofilm molecules [24, 37], thus revealing the interesting biotechnological potential and metabolic biodiversity of this microorganism.

### 3.2 *Colwellia psychrerythraea* 34H

Among the cold-adapted bacteria, the genus *Colwellia* is strictly psychrophilic. In particular, *C. psychrerythraea* 34H isolated from Arctic marine sediments represents the type species of the genus *Colwellia* [38]. *C. psychrerythraea* 34H has been considered as a model for the study of life in permanently cold environments, reveals capabilities important to carbon and nutrient cycling, bioremediation, production of secondary metabolites, and cold adapted enzymes. It grows reliably in heterotrophic media over a temperature range of approximately 1°C to 10°C, with cardinal growth temperatures ranking among the lowest for all characterized bacteria. From a genome-level perspective, adaptations potentially beneficial to life in cold environments can be seen in several broad categories. The determination of *C. psychrerythraea* 34H genome revealed that several of the adaptive strategies appear to increase fitness by effectively overcoming multiple obstacles at low temperature, including temperature-dependent barriers to carbon and nitrogen uptake. These strategies are reflected in expansions of gene families related to cell membrane synthesis, a capacity for uptake or synthesis of compounds that in part may confer cryotolerance, including PHAs (which may also aid in pressure adaptation), cyanophycin-like compounds, and glycine betaine, as well as the capacity to produce large quantities of extracellular enzymes [39]. Majority of organic matter in marine environments is composed of high-molecular-weight compounds that are largely unavailable for direct uptake by heterotrophic bacteria, the hydrolytic activity of extracellular enzymes plays a crucial role in bacterial acquisition of dissolved organic matter. The role of this activity is thought to be particularly important in low-temperature environments, in which bacterial activity is believed to require higher levels of dissolved organic matter than the bacterial activity in warmer environments requires. *C. psychrerythraea* 34H also produces extracellular polysaccharides [40]. Usually extracellular polysaccharides can serve as cryoprotectants and extracellular enzyme production may represent another mechanism for overcoming threshold requirements for dissolved organic carbon in cold environments. The production of EPS from *C. psychrerythraea* strain 34H was tested in extreme life conditions (up to -14°C, 200 atm and 100% of salinity); the results obtained from Marx et al. in 2009 [40] showed a dramatic increase of EPS production when the life conditions get worse. *C. psychrerythraea* 34H was selected as a model organism for genomic studies of bacterial cold adaptation.

### 4. Aims of the study

In this contest, the aim of my PhD project is the identification and characterization of new bioactive molecule/s from marine microorganisms to be implemented in industrial processes. There are three groups of bioactive molecules that have attracted our attention: volatile organic compounds VOCs, anti-biofilm molecules and cryoprotectant compounds.

For the sake of clarity, the results of my project will be described in three different sections:

- i. Research of bioactive volatile organic compound/s against *Burkholderia cepacia* complex.
- ii. Identification of anti-biofilm molecules against *Staphylococcus epidermidis*.
- iii. Study of “cryoprotectant” molecules for biotechnological application.



## **CHAPTER I**

### **Antimicrobial volatile organic compounds**

## Topic I: Antimicrobial volatile organic compounds (VOCs) from Antarctic microorganism against Bcc complex

Inappropriate or unnecessary antibiotic uses (either in human or in veterinary applications) appear to be the key contributors to the emergence of antibiotic resistance. The increasing threat of multidrug resistant pathogens and the continuing evolution of resistance make paramount the need to develop new antimicrobial therapies [41].

In this contest, natural products play an important role in drug discovery, as many approved therapeutics as well as drug candidates are derived from natural sources. Particular interest for biotechnological applications is the inhibitory effects of microbial volatiles against the growth of the others microorganisms.

Microorganisms usually produce a wide range of compounds, many of which are volatile. The most of microorganisms produce unique reproducible volatile organic compounds profile (VOCs) under specific conditions (e.g. medium composition). Generally VOCs belong to several chemical classes (aldehydes, alcohols, esters, lactones, terpenes and sulphur compounds) and are characterized by low molecular weight [42, 43].

Some Antarctic marine bacteria are able to produce volatile organic compounds (VOCs), probably in response to environmental pressure, that specifically inhibit the growth of *Burkholderia cepacia* complex (Bcc) strains [44].

Most Bcc species are also opportunistic human pathogens, being particularly problematic for immuno-compromised individuals (including Cystic Fibrosis patients) since they are often multidrug resistant. There is therefore a need for novel and effective antimicrobial agents against Bcc strains.

*P. haloplanktis* TAC125 is able to produce antimicrobial volatile compounds able to inhibit the growth of Bcc complex strains.

In particular, in this section of my PhD dissertation you will find two papers:

- In the first paper, the optimization of a defined medium GG (D-gluconate and L-glutamate) is described. In GG broth, *P. haloplanktis* TAC125 is capable to growth with a good biomass yield and quite fast specific growth rate even at sub-zero temperatures and it will be fundamental in the definition of survival strategies, used by *P. haloplanktis* TAC125, to face sub-zero temperature conditions. Besides use of *P. haloplanktis* TAC125 as cell factory for recombinant protein production, the bacterium does share with many other Pseudoalteromonales the striking ability to produce bioactive secondary metabolites of biotechnological relevance, such as anti-biofilm molecules [24] and volatile organic compounds (VOCs), active against a group of human opportunistic pathogen called *Burkholderia cepacia* complex (Bcc) [37]. In order to explore the *P. haloplanktis* TAC125 potentiality as source of bioactive compounds and non-conventional systems for the recombinant protein production, it is necessary to develop a synthetic medium for growth at low temperature. The definition of a medium is the requirement for scale up of the *P. haloplanktis* TAC125 growth in automatic bioreactors. Moreover, a defined “minimum” medium could enhances the secondary metabolites production and it surely makes easier their purification from extracellular medium.
- In the second paper, the strategy set up for the capture and identification of *P. haloplanktis* TAC125 VOCs is described. Confirming the tight dependence of their production on the specific growth medium composition, results reported

in the paper demonstrate that the bacterium grown in GG medium is not able to produce any VOCs active against Bcc strains. Starting from this concept, a new medium was developed adding methionine to GG. When grown in GG supplemented with L-methionine, *P. haloplanktis* TAC125 recovered largely its inhibitory potential. Further, the paper describes the set up of a suitable VOCs capture trap and accumulation of condensed VOCs allowed their analysis by SPME-GC-MS. We reported for the first time the identification of methylamine as one of the VOCs responsible to inhibition of Bcc growth and the minimum Inhibitory methylamine concentration was established.

**A novel synthetic medium for sub-zero growth and recombinant protein production in *Pseudoalteromonas haloplanktis* TAC125**

Sannino F.<sup>1</sup>, Giuliani M.<sup>2</sup>, Salvatore U.<sup>1</sup>, Apuzzo G.A.<sup>1</sup>, De Pascale D.<sup>3</sup>, Fani R.<sup>4</sup>, Fondi M.<sup>4</sup>, Marino G.<sup>1</sup>, Tutino M.L.<sup>1</sup>, Parrilli E.<sup>1\*</sup>

<sup>1</sup> Department of Chemical Sciences, University of Naples Federico II, Complesso Universitario Monte Sant'Angelo, Via Cinthia, 80126 Napoli-Italy

<sup>2</sup> Novartis Vaccines and Diagnostics, Via Fiorentina 1, 53100, Siena Italy

<sup>3</sup> Institute of Protein Biochemistry, National Research Council, Via Pietro Castellino, 111, 80126 Naples-Italy.

<sup>4</sup> Laboratory of Microbial and Molecular Evolution, Department of Biology, University of Florence, via Madonna del Piano 6, I-50018 Sesto F.no (Florence), Italy.

\*Author to whom correspondence should be addressed; E-mail: erparril@unina.it; tel +39 081 674003; fax +39 081 674313.

**Acknowledgments**

This work was supported by the EU-KBBE 2012-2016 project PharmaSea, grant N° 312184 to DdP, and Programma Nazionale di Ricerche in Antartide grants PNRA 2013 AZ1.04 to RF and PNRA 2013/B1.04 to MLT.

**Abstract**

The Antarctic bacterium *Pseudoalteromonas haloplanktis* TAC125 is a model organisms of cold-adapted bacteria and it has a great biotechnological potential as non-conventional systems for the recombinant protein production and as source of bioactive compounds. In this paper, in order to deeply explore *P. haloplanktis* TAC125 biotechnological potential, a synthetic medium for bacterium growth at very low temperature was developed. The new medium containing D-gluconate and L-glutamate allowed *P. haloplanktis* TAC125 growth in a range of temperatures from 15°C to -2,5°C. The growth kinetic parameters of the bacterium in GG medium at subzero temperature confirm that the Antarctic bacterium is well adapted to cold environment and pave the way to the definition of strategies, used by *P. haloplanktis* TAC125, to face sub-zero temperature conditions. Moreover, in this paper we reports the setup of a finely regulated expression system inducible by D-galactose to produce recombinant protein in GG synthetic medium at low temperatures. Thanks to the new expression systems we obtained, for the first time, the production of a recombinant protein at minus 2,5°C, providing a new tool for investigating basic science issues and for the recombinant production of “difficult” proteins.

**Keywords**

*P. haloplanktis* TAC125, sub-zero growth temperature, recombinant protein production, cold-adapted bacteria.

**Introduction**

*Pseudoalteromonas haloplanktis* TAC125 (*P. haloplanktis* TAC125), a Gram-negative psychrotolerant marine bacterium, is one of the best studied cultivable representatives of the marine bacterioplankton and it can be considered a model



organisms of cold-adapted bacteria (Medigue et al. 2005; Feller et al 2003). Indeed, the increasing interest in *P. haloplanktis* TAC125 has led to the accumulation of different data types for this bacterium in the last few years, including its complete genome sequence (Medigue et al. 2005), its proteome (Piette et al. 2010; Piette et al. 2011), detailed growth phenotypes (Wilmes et al., 2010; Giuliani, 2011) and a genome scale metabolic model (Fondi et al 2015).

Genomic and metabolic features of this bacterium, accounting for its notable versatility and fast growth compared with other bacteria from marine environments, were revealed by combining genome sequencing and further *in silico* and *in vivo* studies. It is worth mentioning that the bacterium is well adapted to protection against reactive oxygen species (ROS) under cold condition (Wilmes et al. 2010; Parrilli et al. 2010a). Moreover the *in silico* proteome composition revealed a specific bias that is responsible for its ability to resist to protein aging features involving asparagine cyclization and deamidation (Weintraub and Manson 2004). The bacterial genome is characterized by a quite high number of rRNA and tRNA genes, which may account for its relevant capacity for translation in the cold (Medigue et al., 2005).

*P. haloplanktis* TAC125 was also the first Antarctic bacterium in which an efficient gene-expression technology was set up (Parrilli et al. 2008a). Several generations of cold-adapted gene-expression vectors allow the production of recombinant proteins either by constitutive or inducible systems (Papa et al. 2007; Giuliani et al. 2011 ), and to address the product towards any cell compartment or to the extra-cellular medium (Parrilli et al. 2008b). This cold-adapted protein production platform, compared to the conventional mesophilic *E. coli*, offers favourable effects described during the production of some “difficult proteins”, such as: antibody fragments (Dragosits et al. 2011; Giuliani et al. 2011; Giuliani et al. 2014; Giuliani et al. 2015), human nerve growth factor (h-NGF), (Vigentini et al. 2006), alpha-glucosidase from *S. cerevisiae* (Papa et al. 2007) and human alpha-galactosidase (Unzueta et al. 2015). The versatility of *P. haloplanktis* TAC125 as host for recombinant protein production was widened by the development of an efficient genetic scheme, allowing the construction of genome targeted insertion/deletion mutants and permitting to create genetically engineered strains with improved features regarding protein production (Parrilli et al. 2010b).

Besides the above mentioned use of *P. haloplanktis* TAC125 as cell factory for recombinant protein production, the bacterium does share with many other *Pseudoalteromonales* the striking ability to produce bioactive secondary metabolites of biotechnological relevance, such as anti-biofilm molecules (Papa et al. 2013; Parrilli et al. 2015) and volatile organic compounds (VOCs), active against a group of human opportunistic pathogen called *Burkholderia cepacia* complex (Bcc) (Papaleo et al. 2013).

In order to widen and deeply explore the *P. haloplanktis* TAC125 potentiality as source of bioactive compounds and non-conventional systems for the recombinant protein production, it is necessary to develop a synthetic medium for growth at low temperature. The definition of a low cost synthetic medium is the requirement for scale up of the *P. haloplanktis* TAC125 growth in automatic bioreactors. Moreover, a defined “minimum” medium could enhance the secondary metabolites production and it surely makes their purification from extracellular medium easier.

*P. haloplanktis* TAC125 does not possess a phosphoenolpyruvate-dependent phosphotransferase system (PTS) for the transport and first metabolic step of carbohydrate degradation (Medigue et al. 2005) therefore it does not grow on D-glucose, and it doesn't grow on glucose related sugars (e.g. D-fructose or D-xylose)

(Papa et al. 2006). The Antarctic bacterium seems to be well adapted to growth on rich media containing amino acids, used as carbon and nitrogen source. Genomic (Medigue et al. 2005) and proteomic (Wilmes et al. 2010) analysis reveals the presence of all metabolic pathways for amino acids biosynthesis and degradation. Starting from this observation, a defined medium composed by L-leucine, L-isoleucine and L-valine (LIV) was previously formulated and optimised for the production of recombinant proteins (Giuliani et al. 2011). LIV medium allowed an over sevenfold increase of reporter enzyme production and threefold of biomass yield with respect to the previously optimized conditions, moreover the synthetic medium was also tested for the production of a recombinant antibody fragment in batch and chemostat cultivations (Giuliani et al. 2011). However, in this synthetic medium *P. haloplanktis* TAC125 displays a very low specific growth rate already at 4°C (Giuliani et al. 2011) and it is not able to grow at lower temperature. This is a severe limit either for the use of Antarctic bacterium as host for recombinant protein production or as source of bioactive compounds. Moreover, the use of L-leucine, L-isoleucine and L-valine substrates is unprofitable for a large scale production process due to their high cost and their very poor solubility in water.

## Materials and methods

### Bacterial strains and culture conditions

*Escherichia coli* DH5 $\alpha$  [*supE44*,  $\Delta$ *lacU169* ( $\Phi$ 80 *lacZ* $\Delta$ M15) *hsdR17*, *recA1*, *endA1*, *gyrA96*, *thi-1*, *relA1*] (Hanahan 1983) was used as host for the gene cloning. *E. coli* strain S17-1( $\lambda$ *pir*) [*thi*, *pro*, *hsd* (*r-m+*) *recA::RP4-2-TCr::Mu Kmr::Tn7*, *Tpr*, *Smr*, *λpir*] (Tascon 1993) was used as donor in intergeneric conjugation experiments (Parrilli et al. 2008a). *E. coli* cells were routinely grown in LB broth containing 100  $\mu$ g mL<sup>-1</sup> of ampicillin if transformed.

The Gram-negative Antarctic bacterial strain *P. haloplanktis* TAC125 was isolated from Antarctic sea water (Medigue et al., 2005) and it is deposited and available at the Institut Pasteur Collection (CIP 108707). TAC125. Different media were used for the *P. haloplanktis* cultivations: 1) D-Gluconate 5-10-20 g L<sup>-1</sup> as single carbon source, 2) L-Glutamate 10g L<sup>-1</sup> as single carbon and nitrogen source 3) GG medium (L-glutamate 10 g L<sup>-1</sup>, D-gluconate 10 g L<sup>-1</sup>). All media was complemented with a marine salts mix K<sub>2</sub>HPO<sub>4</sub> 1 gL<sup>-1</sup> 10 g L<sup>-1</sup> NaCl, 1 g L<sup>-1</sup> NH<sub>4</sub>NO<sub>3</sub>, 200 mg L<sup>-1</sup> MgSO<sub>4</sub>·7H<sub>2</sub>O, 5 mg L<sup>-1</sup> FeSO<sub>4</sub>·7H<sub>2</sub>O, 5 mg L<sup>-1</sup> CaCl<sub>2</sub>·2H<sub>2</sub>O resulting in a final of pH 7.5.

The bacterium was grown in GG at various temperatures (15, 4, 0 -2,5°C) with shaking at 250 rpm in Nüve-Cooled incubator (model ES120). Absorbance at 600 nm was monitored over time. Growth rates at exponential phase were calculated by standard methods.

Recombinant strain *P. haloplanktis* TAC125 (pMAV-*lacZ*) was grown in GG medium in presence of 100  $\mu$ g mL<sup>-1</sup> ampicillin (Sigma) at 15°C and 4°C, and in presence of 50  $\mu$ g mL<sup>-1</sup> ampicillin (Sigma) at 0°C and -2,5°C.

### Biomass determination

For biomass determination suitable sample volumes were washed in demineralised water, collected and dried on pre-weighed filter paper discs and dried at 110°C until

constant weight. The dry cell weight was correlated with OD at 600nm throughout the following equation:

At 15°C Dry cell weight ( $\text{g L}^{-1}$ ) =  $0,74 \times \text{OD}_{600\text{nm}}$

At 4°C Dry cell weight ( $\text{g L}^{-1}$ ) =  $0,74 \times \text{OD}_{600\text{nm}}$

At 0°C Dry cell weight ( $\text{g L}^{-1}$ ) =  $0,66 \times \text{OD}_{600\text{nm}}$

At -2.5°C Dry cell weight ( $\text{g L}^{-1}$ ) =  $0,41 \times \text{OD}_{600\text{nm}}$

### **Construction of pMAV and pMAV-*lacZ* plasmids**

DNA manipulation and analysis were performed according to standard methods (Sambrook and Russell 2001). Plasmidic DNA extraction and fragments purification are carried out with the QIAprep Spin Miniprep Kit and Qiaquick gel extraction kit from Qiagen, respectively. Restriction enzymes, T4 DNA ligase, alkaline phosphatase, Phusion High-Fidelity DNA Polymerase were supplied by Promega, Boehringer-Roche, Fermentas or Finnzyme.

The *galTK* operon upstream region was amplified from *P. haloplanktis* TAC125 genome by polymerase chain reaction (PCR).

The primers used mavfw (5'-ACACAAGCTTATGGGCTATTTTGTACTC-3') and mavrv (5'-GCGCCATATGAAGTATCTCAAATGTGG-3') were designed on the basis of the *P. haloplanktis* TAC125-genome sequence and sequences corresponding to the *HindIII* site and a *NdeI* site were introduced in the forward and reverse primers, respectively.

The amplifications were performed in a mixture containing 80 ng of *P. haloplanktis* TAC125-genomic DNA as template, 50 pmol of each oligonucleotide primer, 1.8 mM  $\text{MgCl}_2$ , 50 mM KCl, 20 mM Tris-HCl pH 8.3, 0.1% gelatine, 200  $\mu\text{M}$  dNTP in a final volume of 50  $\mu\text{l}$ . The mixtures were incubated at 95°C for 10 min, then 1.25 units of Taq DNA polymerase were added. Twenty cycles of amplification (consisting in 1 min at 95°C, 1.5 min at 60°C and 1 min plus 5sec/cycle at 72°C) were carried out and followed by a cycle in which the extension reaction at 72°C was prolonged for 15 min in order to complete DNA synthesis. The amplified fragment was cloned and its nucleotide sequence checked to rule out the occurrence of any mutation during synthesis.

The amplified region (MAV promoter) was hydrolysed with *Hind III* restriction enzyme and a fill in reaction at the 3' extremity was performed, after that a *NdeI* hydrolysis was performed. The amplified region was cloned into a psychrophilic vector. In detail, the pPM13 plasmid (Duilio et al. 2004) was hydrolysed with *EcoRV* and *NdeI* restriction enzymes in order to remove the DNA fragment corresponding to promoter 13 and to introduce MAV promoter. The fragment amplified region was subcloned into pPM13 obtaining the plasmid pMAV.

A fragment (964 bp) of psychrophilic *lacZ* was amplified from cloneQ-*lacZ*(ref) plasmid by polymerase chain reaction (PCR).

The primers used were galfw (5'-AGCACATATGACCTCTTTACAGCAC-3') and galrv (5'-TGTTATAGGCTTCAACGTCGACTG-3') and sequences corresponding to the *NdeI* site and a *SaI* site were introduced in the forward and reverse primers, respectively. The amplified fragment was hydrolysed with *NdeI* and *SaI* restriction enzymes. The cloneQ-*lacZ* plasmid was hydrolysed with *SaI* and *PstI* restriction enzymes to obtain the remaining fragment of the psychrophilic *lacZ* gene. The pMAV plasmid was hydrolysed with *NdeI* and *PstI* restriction enzymes and a ligase was performed to clone the two fragments of the psychrophilic *lacZ* gene in pMAV plasmid. The resulting pMAV-*lacZ* plasmid was verified by DNA sequencing.

## RNA preparation and RT

Total RNA was isolated from pellets corresponding to 500  $\mu$ l of *P. haloplanktis* TAC125 cell culture (RNasy Mini kit, Qiagen) and subjected to in-column DNase treatment (Rnase-Free Dnase Set, Qiagen). Quality of the RNA isolation was checked by gel electrophoresis followed by quantification in spectrophotometer according to Sambrook and Russell, 2001. Only samples showing a A260nm/A280nm ratio = 0,8 were used for further experiments. Reverse transcription (RT) reactions were performed using SuperScript II RNase H Reverse Transcriptase (Invitrogen) according to the manufacturer's instructions using 100 pmol of specific primers on approximately 5  $\mu$ g of total purified RNA. In addition, RT negative control reactions were performed where water was added instead of template.

## Analysis of mRNA by qRT-PCR

The qRT-PCR method was used to determine the relative amount of specific transcriptional products in the presence/absence of 10 mM D-galactose. The qRT-PCR was performed with cDNAs prepared from 2 separate cultures per treatment. Each of the four cDNA samples obtained was amplified in triplicate experiments. A total of 12 data were obtained.

Real-time PCR was carried out using a StepOne™ Real Time PCR System (Applied Biosystems) and the amplification of the target sequences was detected using SYBR-Green technology. The housekeeping gene *ihfB* was chosen as an internal control to correct for variations of mRNA amounts and cDNA synthesis efficiency.

The primers for specific amplification were designed by Primer Express Software Version 3.0 (Applied Biosystems) *IhfB*-fw-PSHAa1426 5'-

TTGAGATCAGAGGTTTTGGTAGTTTTT-3', *IhfB*-rv-PSHAa1426 5'-

TTCCGCCAGTCTTAGGGTTACG-3', *LacZ*-fw 5'-CCTTCTCGCCCCAGTGCAA-3',

*LacZ*-rv 5'-CGGGAGTACATTGGGCAAAT-3') qRT-PCR amplification mixtures

(20  $\mu$ l) contained 2  $\mu$ l template cDNA, 2x SYBR® Green I Master Mix (10  $\mu$ l) (Applied Biosystems) and 300 nM forward and reverse primer. A non-template control reaction mixture was included for each gene. The PCR cycling programme was as follows: holding stage, 1 cycle of 95°C for 10 min; cycling stage, 40 cycles at 95°C for 15 s, 60°C for 60 s; melting curve stage 1 cycle at 95°C for 15 s, 60°C for 60 s, 95°C for 15 s with a temperature increment of +0,3°C. Specificity of the reaction was checked by analysis of the melting curve of the final amplified product. Experiments and data analysis were performed using StepOne™ Software v2.0 by  $\Delta\Delta C_t$  method (Applied Biosystems User Bulletin, 1997).

## Cell lysis and enzymatic assays

For recombinant  $\beta$ -galactosidase production analysis aliquots of bacterial pellet corresponding to 1 mL culture volume were resuspended in 1mL Lysis buffer (Na phosphate buffer 0,1M pH 7,8, EDTA 2 mM, DTT 1 mM, Triton X-100 1% v/v, lysozyme 5 mg mL<sup>-1</sup>, PMSF 1 mM) and incubated at 15°C for 30'. The suspension was then centrifuged at 10000 rpm for 15 mins at 4°C and the supernatant used for activity assays.

Recombinant cold-active  $\beta$ -galactosidase was assayed spectrophotometrically at 25°C as previously reported (Hoyoux et al. 2001). Calculation were performed on the basis of the extinction coefficient for o-nitrophenol at 410 nm (3.5mM<sup>-1</sup> cm<sup>-1</sup>) and the

specific activity of purified enzyme, 138.2 U mg<sup>-1</sup> (Hoyoux et al. 2001). Kinetics were registered with a DU7500 spectrophotometer (Beckman). Protein concentration was determined with the Bio-Rad protein assay (Bradford, 1976), using bovine serum albumin as standard.

### Determination of concentration of D-Gluconate and L-Glutamate

Aliquots of the supernatant deriving from cell cultures were assayed to determine the concentration of D-gluconate, and L-glutamate residue, by Megazyme kits D-gluconic acid/ D-glucono- $\delta$ -lactone k-gate 11/05l and L-glutamic acid k-glut 03/06.

### Statistic calculation

Data are reported as means of at least four independent experiments with its uncertainty s expressed as standard deviations. Propagation of errors was calculated using simpler average errors (add all the relative errors to get the relative error in the result).

## Results

### Selection of suitable carbon sources

Previously reported data (Wilmes et al. 2010; Giuliani et al. 2011) suggested that sodium glutamate is an important carbon and nitrogen source for *P. haloplanktis* TAC125. Therefore we started our search of suitable carbon sources focusing our attention on L-glutamate. Our analysis was firstly focused on glutamate uptake system in the Antarctic bacterium, *in silico* genome scanning pointed to a putative sodium dependent transporter gene (PSHAa2084, a glutamate transporter *PhGltS*). This gene displays an 47% sequence identity with *V. cholerae* glutamate transporter and 30% sequence identity with *Aphanothece halophytica* *AhGltS* gene coding for a L-glutamate sodium dependent carrier (Boonburapong et al. 2012). In order to assess if in *P. haloplanktis* TAC125 the glutamate uptake is sodium dependent we analyzed the bacterium growth performance in three different media differing in NaCl concentration (5, 10, 15 g L<sup>-1</sup>). As shown in Table S1 the specific growth rate depends on NaCl concentration used in growth medium., at least in the range between 5 and 10 g L<sup>-1</sup>. The biomass yields in the three media is almost the same indicating that the NaCl concentration influences only the glutamate uptake and suggests that *PhTAC125 GltS* transporter is sodium dependent. Since the growth parameters recorded in presence of 15 or 10 g L<sup>-1</sup> NaCl resulted to be identical, we choose as salt source a mineral medium (see material and methods section) that contains NaCl 10g L<sup>-1</sup>.

The analysis of *P. haloplanktis* TAC125 genome highlighted the occurrence of the Entner-Doudoroff pathway (Medigue et al. 2005) as central catabolic pathway for carbon metabolism. *In silico* analysis revealed that genes for all enzymatic functions required in Entner-Doudoroff pathway are present in *P. haloplanktis* TAC125 genome. In order to evaluate the *P. haloplanktis* TAC125 growth performances in a medium containing D-gluconate as sole carbon and energy source, we analysed three media differing in D-gluconate concentration. As reported in Table S1 *P. haloplanktis* TAC125 is able to growth in a mineral medium supplemented with gluconate, and the gluconate concentration has no evident effect on specific growth

rate and has only a slight positive effect on the maximum biomass obtained (Table S1).

Also in case of glutamate uptake, an *in silico* analysis of *P. haloplanktis* TAC125 genome was carried out. D-gluconate is likely to be uptaken from the medium by a gluconate transporter, encoded by the PSHAb0479 gene, homologous to *E. coli* GntU (Izu et al. 1997). In *E. coli* *gntU* is repressed by GntR in the absence of gluconate. As *P. haloplanktis* genome contains a *gntR* homologous, PSHAb0478, a real time PCR analysis of PSHAb0479 transcription demonstrated its expression only in the presence of D-gluconate in the medium (data not shown).

## **GG Medium**

Numerous trials have been carried out looking for the best combination between L-glutamate, D-gluconate, other mineral nutrients and final pH value. The medium that led to the best growth performance was named GG (mineral medium supplemented with 10g L<sup>-1</sup> L-glutamate and 10g L<sup>-1</sup> D-gluconate, see material and methods). As shown in Fig.1, *P. haloplanktis* TAC125 growth profiles at 15°C and 4°C in GG are characterized by the absence of lag phase and by a simultaneous consumption of the two substrates, a condition which allows its use for a fed-batch process development. As reported in Table 1 the GG medium resulted to be more efficient than medium containing only either L-glutamate or D-gluconate, in terms of biomass yields. This improvement is more noticeable at 4°C, at this temperature Antarctic bacterium was able to growth with a biomass yields of 0,44, thus indicating that GG medium is suitable for *P. haloplanktis* TAC125 growth at low temperature.

## ***P. haloplanktis* TAC125 growth in GG at sub-zero temperature**

As previously described (Medigue et al. 2005) a remarkable feature of *P. haloplanktis* TAC125 is that, when provided with sufficient nutrients and aeration, it grows to very high density under laboratory settings, even at 0°C. Since in GG *P. haloplanktis* TAC125 was able to growth with a good biomass yield and specific growth rate at 4°C, we tested the Antarctic bacterium growth at lower temperatures i.e. at 0°C and at -2,5°C (Fig. S1) and the recorded growth parameters are shown in Table 1, in the synthetic medium *P. haloplanktis* TAC125 was able to growth at 0°C and at -2,5°C also. Surprisingly when grown at 0°C *P. haloplanktis* TAC125 reaches a biomass concentration higher than that obtained growing the bacterium in media containing only L-glutamate at 15°C or at 4°C. Moreover, specific growth rate at -2,5°C is comparable with the value obtained growing *P. haloplanktis* TAC125 in media containing only D-gluconate at 4°C (Table 1).

## **Construction of a novel psychrophilic inducible gene expression system (pMAV) for recombinant protein production in GG medium**

To enlarge *P. haloplanktis* TAC125 available genetic tools for the recombinant protein production system, it is necessary to set up a finely regulated expression system to allow the production of toxic proteins for the host cells. This goal can be achieved by the identification of new regulated psychrophilic promoter to be used in the new synthetic medium GG.

*P. haloplanktis* TAC125 is able to grow on mineral medium containing D-galactose (data not shown) thus indicating the presence of a functional Leloir pathway (Frey et

al. 1996), which catalyses the conversion of D-galactose to the more metabolically useful version of the sugar, D-glucose-6-phosphate. Aiming at the identification of new regulated promoters, the regulation of genes responsible for D-galactose catabolism in *P. haloplanktis* TAC125 was studied *in silico*. In *E. coli*, the genes responsible for D-galactose metabolism (*gal*ETKM operon) and for its high affinity transport (*mg*/BAC operon) are repressed, in absence of D-galactose, by the repressor GalR and the isorepressor GalS (Weickert and Adhya 1993; Von Wilcken-Bergmann and Muller-Hill 1982). In *P. haloplanktis* TAC125 *gal* operon shows a different organisation compared to the one of *E. coli*, the *PhgaIE* gene (*PSHAa0469*) is not included in the cluster and between *PhgaIK* and *PhgaIM* there is a gene (*PSHAa1768*) predicted to encode a putative sodium/hexose co-transport protein (Fig.2). Moreover a *galR* homologous was found showing 42,7% identity to *EcgalR*, this gene, named *PhgalR* (*PSHAa1771*) is located downstream the *galT* sequence in the opposite direction (Fig. 2). In *P. haloplanktis* TAC125 genome neither the *mg*/BAC operon nor the *galS* isorepressor are present. The intergenic distances between *P. haloplanktis* TAC125 *gal* genes could suggest that only *galT* and *galK* can be included in *gal* operon. Those two genes are in fact overlapped (-1bp distance) showing the typical intergenic region structure of translationally coupled *P. haloplanktis* TAC125 genes. Starting from the above consideration, we decided to construct an expression vector using the DNA region upstream *PhgaITK* operon, the DNA sequence containing *PhgaITK* promoter and the gene coding for *PhGalR* (Fig. 2) the resulting region was called MAV promoter.

The MAV promoter region was suitably PCR-amplified and used to construct the psychrophilic pMAV vector. In order to assess if pMAV expression system was finely regulated by D-galactose, *lacZ* gene, coding for cold-adapted  $\beta$ -galactosidase from *Pseudoalteromonas haloplanktis* TAE 79 (Hoyoux et al. 2001), was cloned under the control of MAV promoter (see Material and Methods section). Then *P. haloplanktis* TAC125 (pMAV-*lacZ*) recombinant cells were grown both in the presence and in absence of 5g L<sup>-1</sup> D-galactose (28 mM) in the GG medium, at 15°C. A real-time PCR was performed, to compare the relative amount of *lacZ* mRNA produced both in the presence and in the absence of D-galactose (Fig. 3). In absence of D-galactose the *lacZ* transcript was almost negligible, while it was observed a 40-fold enhancement upon induction (Fig. 3).

*P. haloplanktis* TAC125 pMAV-*lacZ* recombinant strain was grown in GG in the absence and in the presence of 10 mM D-galactose, added at middle exponential phase, at different temperatures and  $\beta$ -galactosidase catalytic activity was assayed in the cell lysates as previously described (Hoyoux et al. 2001). In absence of the inducer no  $\beta$ -galactosidase activity was recorded. As reported in Table 2 recombinant  $\beta$ -galactosidase is produced at all tested temperatures and surprisingly at 0°C the production yield is comparable with that obtained at 15°C and 4°C.

## Discussion

Previously reported data (Wilmes et al 2010; Giuliani et al 2011) suggested that sodium glutamate is an important carbon and nitrogen source for *P. haloplanktis* TAC125. Therefore we started our search of suitable carbon sources for *P. haloplanktis* TAC125 focusing our attention on L-glutamate, although reported results confirmed the validity of glutamate as carbon and nitrogen source, we formulated a new medium adding the gluconate to glutamate.

The ED route is proficient in generation of reducing power, in particular NADPH (Conway et al. 1992; Kim et al. 2008), this cofactor has many metabolic functions, out of which synthesis of various amino acids and counteracting oxidative stress predominate (Chavarría et al. 2013; Singh et al. 2007). As oxygen solubility increases with a decline in temperature, the employment of a ED substrate for *P. haloplanktis* TAC125 growth may represent a feasible means, not only for the production of energy (ATP) and generation of various building blocks for cellular functions, but also for providing the organism with better oxidative stress adaptation under low-temperatures life. These observations prompted us to test D-gluconate as carbon source for *P. haloplanktis* TAC125, and to formulate a new medium combining D-gluconate and L-glutamate. In detail, glutamate catabolism provides the bulk of cellular energy and various building blocks for cellular functions through TCA, while gluconate metabolism provides a reductive environment (generating NADPH) to nullify the reactive oxygen species (Singh et al. 2007). In GG the Antarctic bacterium resulted to be able to growth at 4°C with the best biomass yield ever reported (0,44), and to efficiently grow at sub-zero temperatures (0°C and -2.5°C), displaying a doubling time of about 23h at -2,5°C. In previously reported papers (Nunnet al. 2015; Mykytczuk et al. 2013 ) describing bacteria growth at sub-zero temperature the time reported for duplication are usually several weeks, these results clearly confirm that *P. haloplanktis* TAC125 is well adapted to cold environment and suggest that GG medium allows a fine balance between NADPH, ATP and NADH in *P. haloplanktis* TAC125 cells at low temperature. GG medium is the first, to the best of knowledge, described synthetic medium used to characterize growth kinetic parameter of bacterium in pure culture at subzero temperature and it will be fundamental in the definition of strategies, used by *P. haloplanktis* TAC125, to face sub-zero temperature conditions. Moreover, surely GG medium will be decisive to deeply explore the *P. haloplanktis* TAC125 potentiality as source of bioactive molecules allowing the analysis of never described secondary metabolites produced at 0 °C and -2.5°C.

In order to exploit GG synthetic medium not only for physiologic studies but also for the recombinant protein production, a suitable expression system was constructed. The development of an cold expression system to produce recombinant protein at sub-zero temperature needed an *ad hoc* regulated promoter since previously described *P. haloplanktis* TAC125 genetic systems (Papa et al. 2007; Giuliani et al. 2011) resulted to be not compatible with GG medium. As previously reported in Giuliani et al. 2011, the L-malate inducible psychrophilic expression system (Papa et al. 2007 ) in presence of L-glutamate is not functional and a negative interference between the L-glutamate and L-malate (the inducer) was suggested. Transcription activation by L-malate is also inhibited when L-glutamate are used in combination with other amino acid (Giuliani et al. 2011).

Aiming at the identification of new regulated promoters, the analysis of *P. haloplanktis* TAC125 genome was carried out in order to identify genes and/or operons whose transcription is expected to be up-regulated in the presence of particular carbon sources. This kind of analysis was not easy since in bacteria genes involved in primary metabolism processes are generally finely regulated in response to the nutrients availability, but in environments where excess of several easily metabolised carbon sources are present simultaneously, it is unlikely, as in Antarctic sea water, that the catabolite repression is an the exception rather than the rule. Our attention was captured by genes involved in D-galactose catabolism since our unpublished results clearly indicate that *P. haloplanktis* TAC125 is able to grow on D-



galactose (data not shown), thus indicating the presence of a functional Leloir pathway (Frey et al. 1996). The analysis indicated in *P. haloplanktis* TAC125 the presence of a *gal* gene cluster with a different structural organisation compared to best studied *E. coli* one. In the mesophilic bacterium, the transcription regulation of *gal* operon is complex (Lewis and Adhya 2015) and involve cAMP, its receptor protein CRP, and GalS, all components that are not present in *P. haloplanktis* TAC125 genome. However, the Antarctic bacterium possess a gene coding for a *E. coli* GalR homologue, *PhgalR* (PSHAa1771), which is located upstream the *PhgalT* but in the opposite direction. In order to obtain a finely regulated expression system, DNA sequence containing *galTK* promoter and the gene coding for *PhGalR* was cloned in the pMAV vector. The new expression system resulted to be repressed in absence and induced in presence of D-galactose, and therefore it could be used for the production of toxic proteins for the host cells. In this paper the new expression system was used to produce a cold-adapted  $\beta$ -galactosidase at different temperatures from 15°C to -2,5°C, surprisingly at 0°C we obtained more enzyme than at 4°C. Although this surprising result could be due to several factors, in any case it is reasonable to think that optimal induction conditions (different amount of D-galactose, growth induction phase, time of induction ecc,...) may be different for each growth temperature and have to be defined. However, the expression system described in this paper (GG medium and pMAV vector) allowed, for the first time, the recombinant protein production at sub-zero temperature, this result not only will be used to further investigate some basic science issues, i.e the relation between protein folding and temperature, but will be instrumental for the recombinant production of “difficult” proteins. As previously reported (Corcero et al; Piette et al. 2010), cellular physicochemical conditions and/or folding processes in *P. haloplanktis* TAC125 are quite different from those observed in canonical mesophilic hosts, therefore the possibility to produce proteins at a range of temperature from 15°C to -2.5°C enhance the chances to improve the conformational quality and solubility of difficult-to-express protein products.

## References

- Boonburapong B, Laloknam S, Yamada N, Incharoensakdi A, Takabe T (2012) Sodium-dependent uptake of glutamate by novel ApGltS enhanced growth under salt stress of halotolerant cyanobacterium *Aphanothece halophytica*. *Biosci Biotechnol Biochem* 76(9):1702-7. doi: 10.1271/bbb.120309.
- Bradford MM (1976) A rapid and sensitive method for the quantitation of micro gram quantities of protein utilizing the principle of protein–dye binding. *Anal Biochem* 72(1–2):248–54. doi: 10.1016/0003-2697(76)90527-3.
- Conway T (1992) The Entner–Doudoroff pathway: history, physiology and molecular biology. *FEMS Microbiol Rev* 9:1–27. doi: 10.1111/j.1574-6968.1992.tb05822.x.
- Dragosits M, Frascotti G, Bernard-Granger L, Vázquez F, Giuliani M, Baumann K, Rodríguez-Carmona E, Tokkanen J, Parrilli E, Wiebe MG, Kunert R, Maurer M, Gasser B, Sauer M, Branduardi P, Pakula T, Saloheimo M, Penttilä M, Ferrer P, Luisa Tutino M, Villaverde A, Porro D, Mattanovich D (2011) Influence of growth temperature on the production of antibody Fab fragments in different microbes: a host comparative analysis. *Biotechnol Prog* 27(1):38-46. doi: 10.1002/btpr.524.

Duilio A, Madonna S, Tutino ML, Pirozzi M, Sannia G, Marino G (2004) Promoters from a cold-adapted bacterium: definition of a consensus motif and molecular characterization of UP regulative elements. *Extremophiles* 8:125–32. doi: 10.1007/s00792-003-0371-2.

Feller G, Gerday C (2003) Psychrophilic enzymes: hot topics in cold adaptation. *Nat Rev Microbiol* 1(3):200-8. doi: 10.1038/nrmicro773.

Frey P (1996) The Leloir pathway: a mechanistic imperative for three enzymes to change the stereochemical configuration of a single carbon in galactose. *FASEB J* 10(4):461-70.

Giuliani M, Parrilli E, Ferrer P, Baumann K, Marino G, Tutino ML (2011) Process optimization for recombinant protein production in the psychrophilic bacterium *Pseudoalteromonas haloplanktis*. *Process Biochemistry* 46(4):953-959. doi: 10.1016/j.procbio.2011.01.011.

Giuliani M, Parrilli E, Sannino F, Apuzzo G, Marino G, Tutino ML (2015) Soluble Recombinant Protein Production in *Pseudoalteromonas haloplanktis* TAC125. In: Elena García-Fruitós E (ed) *Insoluble Proteins Methods in Molecular Biology*, Springer Science Business, Media New York Volume 1258, pp 243-257.

Hoyoux A, Jennes I, Dubois P, Genicot S, Dubail F, Francois JM, Baise E, Feller G, Gerday C (2001) Cold adapted beta-galactosidase from the Antarctic psychrophile *Pseudoalteromonas haloplanktis*. *Appl Environ Microbiol* 67:1529–35. doi: 10.1128/AEM.67.4.1529-1535.2001.

Izu H, Adachi O, Yamada M (1997) Gene organization and transcriptional regulation of the gntRKU operon involved in gluconate uptake and catabolism of *Escherichia coli*. *J Mol Biol* 267(4):778-93. doi: 10.1006/jmbi.1996.0913.

Izu H, Kawai T, Yamada Y, Aoshima H, Adachi O, Yamada M (1997) Characterization of the gntT gene encoding a high-affinity gluconate permease in *Escherichia coli*. *Gene* 199(1-2):203-10. doi: 10.1016/S0378-1119(97)00368-5.

Kim J, Jeon CO, Park W (2008) Dual regulation of zwf-1 by both 2-keto-3-deoxy-6-phosphogluconate and oxidative stress in *Pseudomonas putida*. *Microbiology* 154:3905–3916. doi: 10.1099/mic.0.2008/020362-0.

Lewis DE, Adhya S (2015) Molecular Mechanisms of Transcription Initiation at gal Promoters and their Multi-Level Regulation by GalR, CRP and DNA Loop. *Biomolecules* 5(4):2782-807. doi: 10.3390/biom5042782.

Chavarría M, Nikel PI, Pérez-Pantoja D, de Lorenzo V (2013) The Entner–Doudoroff pathway empowers *Pseudomonas putida* KT2440 with a high tolerance to oxidative stress. *Environmental Microbiology* 15(6):1772–1785. doi: 10.1046/j.1462-2920.2002.00365.x.

Médigue C, Krin E, Pascal G, Barbe V, Bernsel A, Bertin PN, Cheung F, Cruveiller S, D'Amico S, Duilio A, Fang G, Feller G, Ho C, Mangenot S, Marino G, Nilsson J,

Parrilli E, Rocha EP, Rouy Z, Sekowska A, Tutino ML, Vallenet, von Heijne G, Danchin A (2005) Coping with cold: the genome of the versatile marine Antarctica bacterium *Pseudoalteromonas haloplanktis* TAC125. *Genome Res* 15(10):1325–35. doi: 10.1101/gr.4126905.

Mykytczuk NC, Foote SJ, Omelon CR, Southam G, Greer CW, Whyte LG (2013) Bacterial growth at -15 °C; molecular insights from the permafrost bacterium *Planococcus halocryophilus* Or1. *ISME J* 7(6):1211-26. doi: 10.1038/ismej.2013.8.

Nunn BL, Slattey KV, Cameron KA, Timmins-Schiffman E, Junge K (2015) Proteomics of *Colwellia psychrerythraea* at subzero temperatures - a life with limited movement, flexible membranes and vital DNA repair. *Environ Microbiol* 17(7):2319-35. doi: 10.1111/1462-2920.12691.

Papa R, Glagla S, Danchin A, Schweder T, Marino G, Duilio A (2006) Proteomic identification of a two-component regulatory system in *Pseudoalteromonas haloplanktis* TAC125. *Extremophiles* 10(6):483-91. doi: 10.1007/s00792-006-0525-0.

Papa R, Parrilli E, Sannino F, Barbato G, Tutino ML, Artini M, Selan L (2013) Anti-biofilm activity of the Antarctic marine bacterium *Pseudoalteromonas haloplanktis* TAC125. *Research in Microbiology* 164 (5):450–456. doi: 10.1007/s00792-006-0525-0.

Papa R, Rippa V, Sannia G, Marino G, Duilio A (2007) An effective cold inducible expression system developed in *Pseudoalteromonas haloplanktis* TAC125. *J Biotechnol* 127(2):199–210. doi: 10.1016/j.jbiotec.2006.07.003.

Papaleo MC, Romoli R, Bartolucci G, Maida I, Perrin E, Fondi M, Orlandini V, Mengoni A, Emiliani G, Tutino ML, Parrilli E, de Pascale D, Michaud L, Lo Giudice A, Fani R (2013) Bioactive volatile organic compounds from Antarctic (sponges) bacteria. *N Biotechnol* 30(6):824-38. doi: 10.1016/j.nbt.2013.03.011.

Parrilli E, De Vizio D, Cirulli C, Tutino ML (2008) Development of an improved *Pseudoalteromonas haloplanktis* TAC125 strain for recombinant protein secretion at low temperature. *Microb Cell Fact* 7:2. doi: 10.1186/1475-2859-7-2.

Parrilli E, Duilio A, Tutino ML (2008) Heterologous protein expression in psychrophilic hosts. In: Margesin R, Schinner F, Marx JC, Gerday C(ed) *Psychrophiles: from biodiversity to biotechnology*. Berlin Heidelberg: Springer-Verlag; 2008. p. 365–79.

Parrilli E, Giuliani M, Giordano D, Russo R, Marino G, Verde C, Tutino ML (2010) The role of a 2-on-2 haemoglobin in oxidative and nitrosative stress resistance of Antarctic *Pseudoalteromonas haloplanktis* TAC125. *Biochimie* 92(8):1003-9. doi: 10.1016/j.biochi.2010.04.018.

Parrilli E, Papa R, Carillo S, Tilotta M, Casillo A, Sannino F, Cellini A, Artini M, Selan L, Corsaro MM, Tutino ML (2015) Anti-biofilm activity of *Pseudoalteromonas haloplanktis* TAC125 against *Staphylococcus epidermidis* biofilm: Evidence of a signal molecule involvement? *Int J Immunopathol Pharmacol* 28(1):104-13. doi: 10.1177/0394632015572751.

Piette F, D'Amico S, Mazzucchelli G, Danchin A, Leprince P, Feller G (2011) Life in the cold: a proteomic study of cold-repressed proteins in the antarctic bacterium *Pseudoalteromonas haloplanktis* TAC125. *Appl Environ Microbiol* 77(11):3881-3. doi: 10.1128/AEM.02757-10.

Piette F, D'Amico S, Struvay C, Mazzucchelli G, Renaut J, Tutino ML, Danchin A, Leprince P, Feller G (2010) Proteomics of life at low temperatures: trigger factor is the primary chaperone in the Antarctic bacterium *Pseudoalteromonas haloplanktis* TAC125. *Mol Microbiol* 76(1):120-32. doi: 10.1111/j.1365-2958.2010.07084.x.

Singh R, Mailloux RJ, Puiseux-Dao S, Appanna VD (2007) Oxidative Stress Evokes a Metabolic Adaptation That Favors Increased NADPH Synthesis and Decreased NADH Production in *Pseudomonas fluorescens*. *Bacteriol* 189(18): 6665–6675. doi: 10.1128/JB.00555-07.

Sambrook J, Russell DW (2001) Molecular cloning in a laboratory manual. Cold Spring Harbor, NY.

Singh R, Mailloux RJ, Puiseux-Dao S, Appanna VD (2007) Oxidative stress evokes a metabolic adaptation that favors increased NADPH synthesis and decreased NADH production in *Pseudomonas fluorescens*. *J Bacteriol* 189:6665–6675. doi: 10.1128/JB.00555-07.

Unzueta U, Vázquez F, Accardi G, Mendoza R, Toledo-Rubio V, Giuliani M, Sannino F, Parrilli E, Abasolo I, Schwartz S Jr, Tutino ML, Villaverde A, Corchero JL, Ferrer-Miralles N (2015) Strategies for the production of difficult-to-express full-length eukaryotic proteins using microbial cell factories: production of human alpha-galactosidase A. *Appl Microbiol Biotechnol* 99(14):5863-74. doi: 10.1007/s00253-014-6328-9.

Vigentini I, Merico A, Tutino ML, Compagno C, Marino G (2006) Optimization of recombinant human nerve growth factor production in the psychrophilic *Pseudoalteromonas haloplanktis*. *J Biotechnol* 127(1):141-50. doi: 10.1016/j.jbiotec.2006.05.019.

von Wilcken-Bergmann B, Müller-Hill B (1982) Sequence of *galR* gene indicates a common evolutionary origin of *lac* and *gal* repressor in *Escherichia coli*. *Proc Natl Acad Sci U S A* 79(8):2427-31.

Weickert MJ, Adhya S (1993) Control of transcription of *gal* repressor and isorepressor genes in *Escherichia coli*. *J. Bacteriol* 175: 251–258.

Weickert MJ, Adhya S (1993) The galactose regulon of *Escherichia coli*. *Mol Microbiol* 10(2):245-51. doi: 10.1111/j.1365-2958.1993.tb01950.x.

Weintraub SJ, Manson SR (2004) Asparagine deamidation: a regulatory hourglass. *Mech Ageing Dev* 125(4):255-7. doi: 10.1016/j.mad.2004.03.002.

Wilmes B, Hartung A, Lalk M, Liebeke M, Schweder T, Neubauer P (2010) Fed-batch process for the psychrotolerant marine bacterium *Pseudoalteromonas haloplanktis*. *Microb Cell Fact* 21:9-72. doi: 10.1186/1475-2859-9-72.

## TABLES:

**Table 1: *P. haloplanktis* specific growth rate ( $\mu_{\max}$ ), maximum biomass concentration, biomass yield ( $Y_{x/s}$ ) in selected synthetic media.** Means and standard deviations have been calculated from four independent experiments; .  $\pm$ : standard error of the mean; dcw stands for dry cell weight; \* values obtained by error propagation procedure and assuming that the g carbon source are  $10\text{g}\pm 0,1$  (in case of medium containing gluconate or glutamate only) and  $20\text{g}\pm 0,1$  in case of GG medium.

Temperature	Medium	$\mu_{\max}$ ( $\text{h}^{-1}$ )	maximum biomass concentration ( $\text{g}_{\text{dcw}} \text{L}^{-1}$ )	$Y_{x/s}$ ( $\text{g}_{\text{dcw}} \text{g}_{\text{carbon}}^{-1}$ )
15°C	10 g L <sup>-1</sup> L-glutamate	0,23 $\pm$ 0,03	2,44 $\pm$ 0,07	0,24 $\pm$ 0,07*
4°C	10 g L <sup>-1</sup> L-glutamate	0,087 $\pm$ 0,02	3,65 $\pm$ 0,013	0,365 $\pm$ 0,011*
15°C	10 g L <sup>-1</sup> D-gluconate	0,13 $\pm$ 0,02	1,63 $\pm$ 0,03	0,16 $\pm$ 0,004*
4°C	10 g L <sup>-1</sup> D-gluconate	0,035 $\pm$ 0,005	2,05 $\pm$ 0,014	0,05 $\pm$ 0,003*
15°C	GG	0,28 $\pm$ 0,02	5,40 $\pm$ 0,01	0,27 $\pm$ 0,03*
4°C	GG	0,16 $\pm$ 0,01	8,89 $\pm$ 0,03	0,44 $\pm$ 0,05*
0°C	GG	0,037 $\pm$ 0,002	3,20 $\pm$ 0,03	0,16 $\pm$ 0,03*
-2.5°	GG	0,030 $\pm$ 0,002	1,86 $\pm$ 0,06	0,093 $\pm$ 0,004*

**Table 2: Recombinant  $\beta$ -galactosidase production at different temperatures:**  $\beta$ -galactosidase activity recovered in cell extracts of *P. haloplanktis* TAC125 (pMAV-LacZ) cells grown in GG in shaken flasks at 4°C, 15°C, 0°C and -2,5°C. Galactosidase induction was performed by 10mM D-galactose addition in middle exponential phase, samples were collected 24 h after in case of *P. haloplanktis* TAC125 (pMAV-LacZ) growth at 4°C and 15°C., after 72h at 0°C and after 120h at -2,5°C. Means and standard deviations have been calculated from three independent assays.  $\pm$ : standard error of the mean; dcw: dry cell weight; \* values obtained by error propagation procedure.

Temperature	[ $\beta$ -gal] ( $\text{mg L}^{-1}$ )	final biomass concentration ( $\text{g L}^{-1}$ )	$Y_{P/X}$ ( $\text{g g}_{\text{dcw}}^{-1}$ )
15°C	119,3 $\pm$ 0,1	1,85 $\pm$ 0,1	0,064 $\pm$ 0,003*
4°C	34,5 $\pm$ 0,1	1,80 $\pm$ 0,3	0,02 $\pm$ 0,003*
0°C	82,84 $\pm$ 0,8	1,65 $\pm$ 0,1	0,05 $\pm$ 0,003*
-2,5°C	6,52 $\pm$ 0,01	1,22 $\pm$ 0,2	0,0051 $\pm$ 0,008*

## FIGURE

**Fig. 1: Growth of *P.halopanktis* TAC125 in GG medium at 15°C and 4°C:**

**Panel a**, *P.halopanktis* TAC125 growth profile at 15°C in GG. The black line indicates growth profile at 15°C, the gray continue line shows L-glutamate consumption, the black hatched line shows D-gluconate consumption.

**Panel b**, *P.halopanktis* TAC125 growth profile at 4°C in GG. The black line indicates growth profile at 4°C, the gray continue line shows L-glutamate consumption, the black hatched line shows D-gluconate consumption.

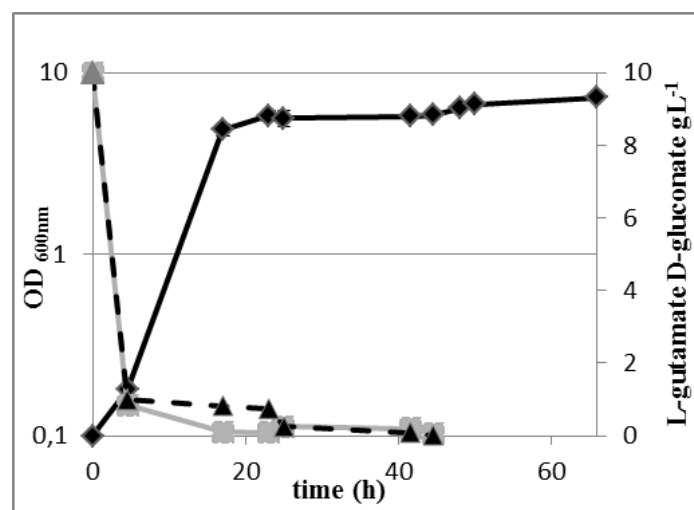


**Fig. 2:** Schematic organization of in *P.halopanktis* TAC125 gal operon, the region PCR amplified and cloned in pMAV is highlighted. OriC: pUC18-derived origin of replication; OriR: pMtBL-derived autonomous replication sequence; Amp<sup>R</sup>-β-lactamase encoding gene; OriT: conjugational DNA transfer origin; Tasp, *PhTAC125* aspC transcriptional terminator; MAV DNA sequence containing *galTK* promoter and the gene coding for *PhGalR*.

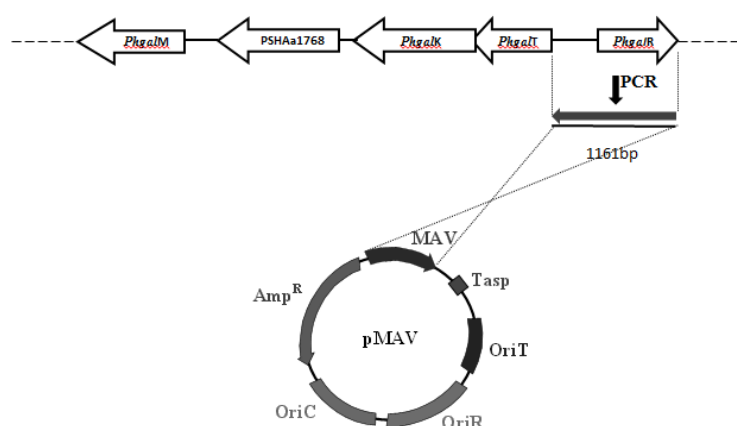
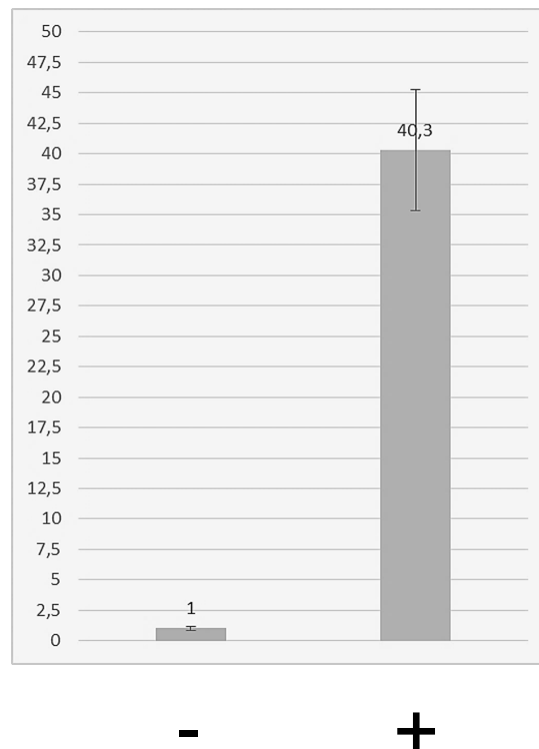
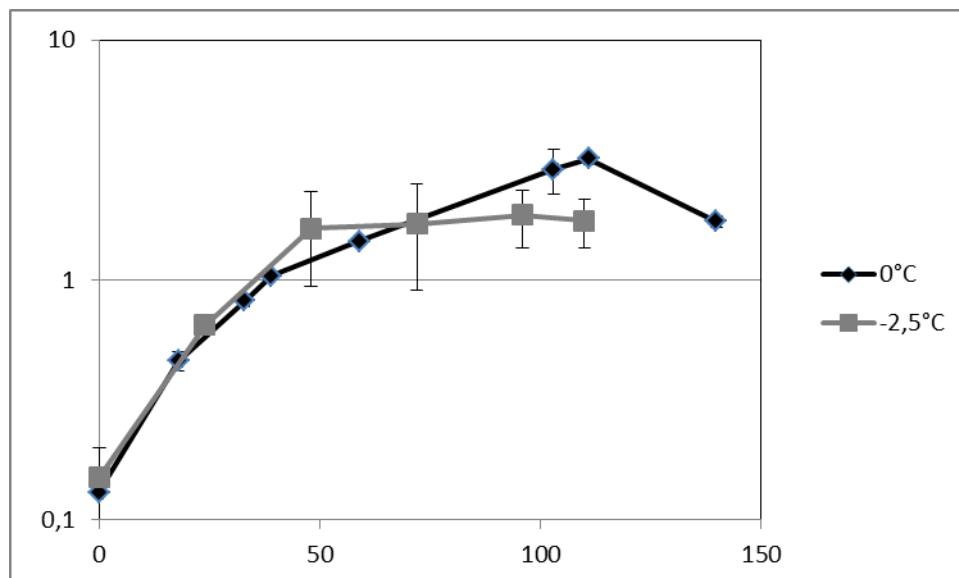


**Fig. 3:** Real Time PCR relative quantification of *P. haloplanktis* TAC125 (pMAV-lacZ) at 15°C in GG when induced by galactose. On X-axis are reported *lacZ* mRNA in the presence (+) or absence (-) of D-galactose, an Y-axis are reported the relative quantification RQ.



## SUPPLEMENTARY MATHIERIAL

**Fig. S1:** Growth profile of *P.halopanktis* TAC125 in GG at 0 °C and -2,5°C.





***Pseudoalteromonas haloplanktis* produces methylamine, a volatile compound active against *Burkholderia cepacia* complex strains**

Filomena Sannino<sup>1</sup>, Ermenegilda Parrilli<sup>1</sup>, Gennaro Antonio Apuzzo<sup>1</sup>, Donatella de Pascale<sup>2</sup>, Pietro Tedesco<sup>2</sup>, Isabel Maida<sup>3</sup>, Elena Perrin<sup>3</sup>, Marco Fondi<sup>3</sup>, Renato Fani<sup>3</sup>, Gennaro Marino<sup>1</sup> and Maria Luisa Tutino<sup>1,\*</sup>

<sup>1,\*</sup> Department of Chemical Sciences, University of Naples Federico II, Complesso Universitario Monte Sant'Angelo, Via Cinthia, 80126 Napoli- Italy; E-Mail: filomena.sannino2@unina.it; gen.apuzzo@gmail.com; erparril@unina.it ; gmarino@unina.it; tutino@unina.it

<sup>2</sup> Institute of Protein Biochemistry, National Research Council, Via Pietro Castellino, 111, 80126 Naples-Italy; E-Mail: d.depascale@ibp.cnr.it ; p.tedesco@ibp.cnr.it

<sup>3</sup> Laboratory of Microbial and Molecular Evolution, Department of Biology, University of Florence, via Madonna del Piano 6, I-50018 Sesto F.no (Florence), Italy; E-Mail: isabel.maida@unifi.it ; marco.fondi@unifi.it; renato.fani@unifi.it; elena.perrin@unifi.it;

\* Author to whom correspondence should be addressed; E-mail: tutino@unina.it; Tel.: +39-081-674317; Fax: +39-081-674313.

**Abstract:**

The Antarctic marine bacterium *Pseudoalteromonas haloplanktis* TAC125 has been reported to produce several Volatile Organic Compounds (VOCs), which are able to inhibit the growth of *Burkholderia cepacia* complex (Bcc) strains, opportunistic pathogens infecting immune-compromised patients. Growth media composition influenced the produced VOCs profiles and, conversely, effectiveness and number of pathogen strains inhibited. In this paper we report the definition of a synthetic medium (containing D-gluconate and L-glutamate as carbon and energy sources), in which the Antarctic bacterium displays good growth parameters but is unable to inhibit Bcc strains. The single addition of several amino acids to the medium restores the *P. haloplanktis* TAC125 inhibition ability. Therefore, with the aim of identifying specific volatile compound/s responsible for Bcc inhibition, we used a methodology for VOCs capture, accumulation, and storage by coupling the growth of the Antarctic bacterium in an automatic fermenter with the application of a cooling system to the exhaust air outlet. This approach allowed the identification of methylamine as a VOC produced by *P. haloplanktis* TAC125 when grown in the synthetic medium supplemented with methionine and demonstrated that this molecule is able to inhibit the growth of several Bcc strains in dose-dependent way. This is the first paper in which the antibacterial effect of one specific identified volatile compound produced by an Antarctic marine bacterium was demonstrated.

**Keywords:** *Pseudoalteromonas haloplanktis* TAC125, methylamine, Volatile organic compounds, *Burkholderia cepacia* complex

**Introduction:**

Microbial resistance to antibiotics has spread dramatically in the last 50 years, leading to an increasing number of deaths due to infectious diseases. The massive and often inappropriate use of antibiotics in hospitals and in livestock industries led to the creation of a group of multi-drug Resistant (MDR) microorganisms, which represent a major global health issue [1]. Hence, there is an urgent need to identify novel antibiotics to counteract these hazardous microorganisms [2, 3]; in this context

the discovery of novel natural drugs might represent one of the possible solutions. Indeed, natural products have been the main source of antibacterial drugs in the past, and today they still represent the two-third of the new antibiotics released in the last 20 years [4, 5].

Particular interest for biotechnological applications are the inhibitory effects of microbial volatile compounds against the growth of the others microorganisms.

Volatile Organic Compounds (VOCs) are a class of heterogeneous natural molecules that have recently acquired a notable interest. Various bacteria from different environments synthesise VOCs [6, 7] through both primary and secondary metabolic pathways; however, their biological function has not been clearly defined yet. It was initially proposed that these compounds might represent waste material or end products of various biological processes. Further studies demonstrated that VOCs are able to influence the growth of other bacteria, in a sort of chemical at-a-distance cross-talk [8, 7].

We have previously demonstrated that marine Antarctic bacteria belonging to different genera/species are able to synthesise VOCs of different chemical classes, including sulphur compounds [9, 10, 11, 12,]. Interestingly, VOCs synthesised by several Antarctic bacteria specifically inhibit the growth on solid media of strains belonging to the *Burkholderia cepacia* complex (Bcc) [9, 10, 11], a group of opportunistic human pathogens most of which characterized by multi drug resistance. Outcomes from our previous reports demonstrated that VOCs are constitutively synthesised by Antarctic bacteria [11] and that Antarctic strains belonging to different species/genera apparently synthesize the same VOCs, as their respective VOCs profiles are quite similar [9, 11]. Interestingly, relative concentration of each VOC may vary between different strains [9, 11] and/or in the same strain grown in different media [13, 11].

Therefore, combining the above information with the consideration that we never observed the appearance of Bcc mutants resistant to Antarctic VOCs, we suggested that the antagonistic activity exhibited by the Antarctic strains was very likely due to the combination of different VOCs rather than to the effect of a single molecule [13, 11]. On the other side, reported complexity in VOCs produced by Antarctic bacteria let quite difficult to test each identified molecule (and eventually their different combinations) for Bcc inhibition activity. Therefore, all our previous reports described the VOCs chemical diversity, not aiming at defining the association between the anti-Bcc activity and a single volatile compound.

One of the Antarctic bacteria tested for the ability to synthesize anti-Bcc VOCs is *Pseudoalteromonas haloplanktis* TAC125 (*P. haloplanktis* TAC125), which is the first Antarctic marine strain whose genome was sequenced and carefully annotated [14]. *P. haloplanktis* TAC125 represents a model system for the study of bacterial cold-adaptation due to: a) the availability of efficient genetic schemes for genome targeted insertion/deletion [15]; b) the availability of a well-settled technology for homologous/heterologous gene expression [16, 17]; c) the development of efficient schemes for bacterial cultivation in automatic fermenters, either in batch or in chemostat modalities [18,19]; and d) the availability of a genome-scale model of its metabolism [20]. Furthermore, it has also been demonstrated that this bacterium is able of producing an anti-biofilm compound targeting *Staphylococcus epidermidis* [21, 22].

Since it was demonstrated that the ability of *P. haloplanktis* TAC125 to inhibit the growth of Bcc strains was influenced by the specific growth medium composition [11], the aim of this work was to explore the ability of this bacterium to synthesize anti-Bcc

VOCs when grown in different cultivation conditions and synthetic media. We demonstrated that when *P. haloplanktis* TAC125 was grown in a specific synthetic medium it was unable to inhibit the Bcc growth, while when grown in the same synthetic medium enriched by single selected amino acids, such as L-methionine, the bacterium was able to inhibit the growth of tested Bcc strains by VOCs production. Then, we set up a methodology, based on the use of an automatic fermenter, to produce, capture, and accumulate VOCs, which allowed us to identify the methylamine as one of VOCs produced by the bacterium grown in presence of L-methionine. Finally, we evaluated methylamine antimicrobial activity against several Bcc strains

## Material and Methods:

### Bacterial strains and growth conditions

*P. haloplanktis* TAC125 was grown at 20°C on agar-containing (15 g/L) GG medium (10 g/L L-glutammate, 10 g/L D-gluconate, K<sub>2</sub>HPO<sub>4</sub> 1 g/L 10 g/L NaCl, 1 g/L NH<sub>4</sub>NO<sub>3</sub>, 200 mg/L MgSO<sub>4</sub>•7H<sub>2</sub>O, 5 mg/L FeSO<sub>4</sub>•7H<sub>2</sub>O, 5 mg/L CaCl<sub>2</sub>•2H<sub>2</sub>O pH 7.5) or GG+amino acid medium (final concentration of amino acids in medium was 0.04M ). Bcc strains (Table 1) and *Escherichia coli* K12 were grown at 20°C or 37°C (depending on the specific assay to be carried out) on TYP medium (16 g/L yeast extract, 16 g/L bacto peptone, 10 g/L NaCl) containing 15 g/L agar.

Each of the ten Bcc strain used in this work (Table 1) was grown on TYP solid medium or on buffered TYP at different pH values. Buffering of TYP medium was obtained by adding 20mM Tris buffer at different pH; in this way buffered TYP media with a different pH (7.0, 7.5, 8.0, 8.5, and 9.0) were obtained.

Species	Strain	Source
<i>B. arboris</i>	LMG 24066	Soil
<i>B. cenocepacia</i>	LMG 16654	Cystic Fibrosis Patient
<i>B. cenocepacia</i>	LMG 19230	Environmental
<i>B. contaminans</i>	LMG 23361	Animal infection
<i>B. latens</i>	LMG 24064	Cystic Fibrosis Patient
<i>B. metallica</i>	LMG 24068	Cystic Fibrosis Patient
<i>B. multivorans</i>	LMG 13010	Cystic Fibrosis Patient
<i>B. pseudomultivorans</i>	LMG 26863	Cystic Fibrosis Patient
<i>B. stabilis</i>	LMG 14294	Cystic Fibrosis Patient
<i>B. ubonensis</i>	LMG 20358	Soil

**Table 1.** List of Bcc strains used in this work

### **Cross-streaking assays**

Cross-streaking experiments were carried out as previously described [9] by using Petri dishes with a septum separating the two hemi-cycles, to permit the growth of the tester (*P. haloplanktis* TAC125) and target strains (*Burkholderia cenocepacia* LMG 19230 and LMG 16654 and *E. coli* K12) on different media without any physical contact. *P. haloplanktis* TAC125 was grown on GG agar or GG+amino acid (final concentration of amino acids in medium was 0.04M) agar media for 4 days at 20°C; then the target strains were streaked onto the TYP agar medium on the opposite hemi-cycle of the Petri dish with septum, and incubated at 20°C for 2 days and at 37°C for two additional days.

### ***P. haloplanktis* TAC125 cultivation in automatic fermenter**

The Antarctic bacterium was grown in a Sixfors HT automatic fermenter (INFORS) containing 1/3 TYP liquid medium (5.3 g/L yeast extract, 5.3 g/L bacto peptone, 10 g/L NaCl), or GG medium with or without the addition of 40 mM L-methionine. The cultures were grown in a volume of 250 mL at 20 °C in aerobic conditions (Dissolved Oxygen Tension DOT $\geq$ 30 %), by keeping the inlet airflow of 20 L/h and a stirring rate of 250 rpm.

### **VOCs condensation system and molecules identification by Solid-phase Micro extraction Gas Chromatography -Mass Spectrometry (SPME-GC-MS)**

The condensation and preliminary identification experiments were carried out in triplicate in the following conditions: a) uninoculated GG medium; b) *P. haloplanktis* TAC125 inoculated GG medium; c) *P. haloplanktis* TAC125 inoculated GG-Met medium. Gas stream coming out from the fermentation vessel was forced to pass through a water trap, consisting in a bottle filled by hygroscopic salts (i.e. anhydrous magnesium sulfate and sodium chloride in a 1:1 w/w ratio), to eliminate as much water molecules as possible. Dehydrated gas was then conveyed to a distillation equipment located inside a cooling system (average temperature of -20°C), allowing the condensation of Volatile Organic Compounds eventually present in the gas mixture. Identification of condensed VOCs was carried out by Solid-phase Micro extraction Gas Chromatography - Mass Spectrometry (SPME-GC-MS), at the Servizio di Spettrometria di Massa at the Department of Chemical Sciences-Federico II University of Naples. The gas chromatographic analyses were performed with an Agilent 6890 Series GC, coupled to a detector MS 5973. The column used was a DB-5ms capillary column (30 m  $\times$  0.25mm ID, 0.25 $\mu$ m film, 5% phenyl 95% polydimethylsiloxane). Helium was used as carrier gas, with a flow of 1.0 mL/min. Solid-phase micro extraction was performed by using DVB/CAR/PDMS 50/30  $\mu$ m fibre, connected to the top of the bottle containing the condensed VOCs, and the bottle (and its content) was heated at 230°C and exposed for 45 min in the headspace of the flask (adsorption). Subsequently the fibre was exposed in the injector of the GC, maintained at a temperature of 230°C for 3 min (desorption). The gradient used for analysis was as follows: 45°C for 3 min, 150°C to 12 °C/min, 230°C to 18°C/min, 250°C to 19°C/min. The analyzer of the GC is maintained at 250°C. The collision energy in the source has been set to a value of 70 eV; fragment ions generated were analyzed in the range of 30-450 mass m/z.

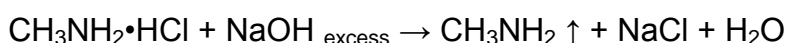
A preliminary identification of the molecules synthesized was performed by SPME-GC-MS. In detail, the tentative identification of the volatile components was based on comparison of their mass spectra with those of NIST 2.0 as well as by comparison of

their retention indexes with the literature data. As for methylamine, each condensed molecule was identified by its fragmentation mass spectrum and comparison between its retention time (1.58) and the retention time of a standard.

### **Definition of Bcc strains sensitivity to methylamine and determination of Minimum Volatile Inhibitory Concentration (MVIC)**

Minimum Volatile Inhibitory Concentration (MVIC) is defined as the lowest methylamine concentration that showed no visible growth of the streaked tester strain after 96 hrs at 20°C.

The gaseous methylamine was obtained through *in situ* acid-base reaction between sodium hydroxide and methylamine hydrochloride salt (SIGMA code: M0505):



The number of moles of methylamine hydrochloride ( $\text{CH}_3\text{NH}_2\cdot\text{HCl}$ ), which are placed to react with the base solution, corresponds to the number of gaseous methylamine ( $\text{CH}_3\text{NH}_2\uparrow$ ) moles released. To define the final gaseous methylamine concentration, we consider the volume of the hermetically sealed incubation box (2L). For instance, to test on Bcc strains a final concentration of 10 mM gaseous methylamine in a 2 L sealed box, 1.35 g (corresponding to 20 mM) of methylamine hydrochloride salt were dissolved in a 1 mL of distilled water; then 200  $\mu\text{L}$  of sodium hydroxide 10 M were added, developing 20 mM of gaseous methylamine. The boxes containing the target strains were incubated at 20°C for 4 days. Then the plates were recovered and placed at 37°C for further 2 days, to allow cells to grow on solid medium.

### **Measurement of pH**

The pH of TYP liquid medium (1 mL volume) exposed to methylamine in the hermetically sealed incubation (Fig.4 (a)) was determined using Instruments XS, pHmeter Orto lab S.n.c.

## **Results**

### ***P. haloplanktis* TAC125 is able to produce VOCs active against *Burkholderia cepacia* complex strains when grown in liquid culture**

With the aim of developing a methodology for VOCs capture from the outlet air stream from a bioreactor, *P. haloplanktis* TAC125 was grown in a multi-vessel automatic fermenter at 20°C in a complex rich medium (see methods section) where the bacterium exerts its maximal inhibitory activity against Bcc strains in conventional cross-streaking experiments [11]. The culture was continuously supplemented by a sterile air inlet (20 L/hr). The outlet gas stream during the bacterial growth was conveyed towards a culture bottle filled by TYP–agar medium and streaked with two Bcc strains (*Burkholderia cenocepacia* LMG 16654 and LMG 19230), which were inhibited by *P. haloplanktis* TAC125 VOCs when tested in cross-streaking experiments [11]. As a control, a bottle containing the same agar medium and same strains was subjected to the outlet gas coming from another vessel containing uninoculated sterile liquid medium. The outlet gases were conveyed towards culture bottles for at least 2 days and during this period the room temperature was fixed at 20°C. A schematic representation of the experimental setup is shown in Fig. 1(a). Data obtained revealed that the growth of both Bcc strains was inhibited when exposed to the outlet gas from *P. haloplanktis* TAC125 culture (Fig. 1(b)), thus

demonstrating that this bacterium produces anti-Bcc VOCs even when grown in liquid medium.

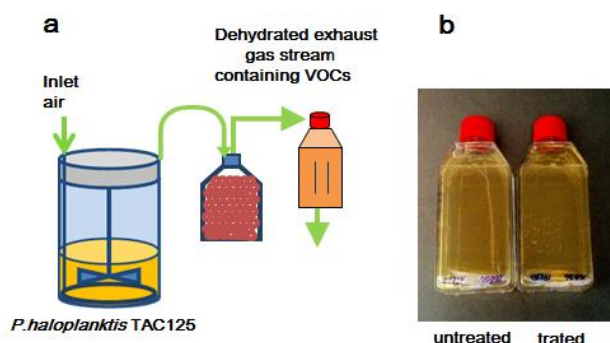


**Fig. 1: *P. haloplanktis* TAC125 is able to produce VOCs when grown in liquid culture.** Outlet gas from the *P. haloplanktis* TAC125 growth contains VOCs able to inhibit the growth of two Bcc strains. (a) Diagram describing the experimental setup; (b) Culture bottles, containing TYP-agar medium and streaked with the strains *B. cenocepacia* LMG 16654 and LMG 19230, exposed (treated) or not exposed (untreated) to the exhaust gas stream outlet coming out from the vessel in which the *P. haloplanktis* TAC125 is growing in exponential/stationary phase. Please, note that a hole was introduced in both bottles to avoid the over-pressure due to the gas stream.

### Development of an efficient VOCs trap for capturing the volatile compounds produced by *P. haloplanktis* TAC125

Once established that anti-Bcc VOCs are produced when the Antarctic bacterium is grown in automatic fermenter, we developed a system to capture VOCs produced during *P. haloplanktis* TAC125 growth. As schematically shown in Fig. 2, the gas stream coming out from a *P. haloplanktis* TAC125 inoculated vessel was conveyed into a chemical water trap (for water elimination), then the gas stream was cooled at -20°C and forced to pass into a distillation equipment, aimed at obtaining the condensation of all volatile molecules eventually contained. To evaluate the condensation efficiency of this VOCs trap, *P. haloplanktis* TAC125 was grown in rich medium at 20°C and the outlet exhaust gas were condensed. A culture bottle containing a streak of two Bcc target strains (LMG 19230 and LMG 16654) was exposed to the gas stream coming out from the VOCs trap. No growth inhibition of the Bcc strains was observed in this case (data not shown); confirming that the VOCs trap is effective in the condensation of anti-Bcc VOCs.

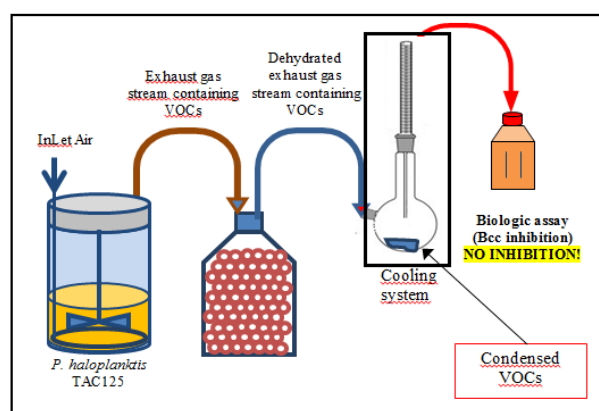


**Fig. 2: Experimental setup for the capture of VOCs produced by *P. haloplanktis* TAC125 when grown in batch in automatic fermenter.** See text for a detailed description.

### Effect of the growth medium composition on *P. haloplanktis* TAC125 anti-Bcc VOCs producing ability

The capability of the Antarctic bacterium to inhibit the growth of Bcc strains is influenced by the specific growth medium composition [11], therefore we tested the ability of *P. haloplanktis* TAC125 to synthesize anti-Bcc VOCs when grown in a synthetic (GG) defined medium. This medium contains D-gluconate and L-glutamate as carbon, nitrogen and energy sources, while a salts mixture was used as mineral base. *P. haloplanktis* TAC125 growth in GG medium resulted to be well balanced, as calculated growth parameters (in terms of specific growth rate and biomass yield) resulted to be comparable to those recorded when the bacterium grows in rich complex media (unpublished data).

The ability of *P. haloplanktis* TAC125 to inhibit the growth of two Bcc strains (*B. cenocepacia* LMG 16654 and LMG 19230) was tested by a cross-streaking experiment. When the Antarctic bacterium was grown on GG solid medium, it was unable to inhibit the growth of the Bcc target strains (Fig. S1 (a)). This result paved the way to test the effect of the addition of several different amino acids to restore the *P. haloplanktis* TAC125 inhibition ability. To this purpose cross-streaking experiments were carried out using GG medium containing different amino acids and the addition of some of them restored the *P. haloplanktis* TAC125 Bcc inhibition ability (Table 2; Fig. S1). This finding suggested that degradation of different amino acids appeared to produce VOCs able to inhibit the growth of Bcc strains; however, since we have previously demonstrated that at least some of the anti-Bcc VOCs were sulfur-containing compounds [10; 12], we focused our attention on GG-L-methionine condition (we excluded cysteine as *P. haloplanktis* TAC125 growth in GG+Cys liquid medium is very poor (data not shown)).

Then we investigated on *P. haloplanktis* TAC125 growth behaviour when cultivated in GG medium either in the presence or in the absence of L-methionine in an automatic fermenter. Two batch fermentation processes were carried out at 20°C, and the relative growth curves are shown in Fig. 3. The addition of L-methionine to the GG medium resulted in a reduction of the *P. haloplanktis* TAC125 specific growth rate (from 0.24 to 0.11 h<sup>-1</sup>). However, in line with the addition of an extra carbon, nitrogen and eventually energy source, the final biomass produced by *P. haloplanktis* TAC125 in GG-Met medium was about 15% higher than that produced in GG (Fig. 3, supplementary). These results strongly suggest the actual use of L-methionine as growth substrate for the Antarctic bacterium.

Amino acid	<i>E. coli</i> K12	<i>B. cenocepacia</i> LMG 16654	<i>B. cenocepacia</i> LMG 19230
L-alanine	+	-	+
L-asparagine	+	-	-
L-aspartate	+	-	-
L-cysteine	+	±	±
Glycine	+	±	-
L-serine	+	-	-
L-histidine	+	-	-
L-methionine	+	±	-
L-isoleucine	+	+	+

Amino acid	<i>E. coli</i> K12	<i>B. cenocepacia</i> LMG 16654	<i>B. cenocepacia</i> LMG 19230
L-leucine	+	±	+
L-phenylalanine	+	-	-
L-valine	+	+	+
L-proline	+	-	-
L-lysine	+	-	-

Symbols: + growth; ± reduced growth; - no growth.

**Table 2. Growth of *B. cenocepacia* LMG 16654 and LMG 19230 and *E. coli* K12 in the presence of *P. haloplanktis* TAC125 grown on GG solid medium containing different amino acids.** The inhibition ability of the Antarctic bacterium grown on GG solid medium, supplemented with different amino acids, was tested by cross-streaking experiments in Petri dishes with septum, using the Bcc strains LMG 19230 and LMG 16654 and *E. coli* K12 as target strains.

### Identification of methylamine as a VOC produced by *P. haloplanktis* TAC125

VOCs capture experiments were carried out, condensing the outlet gas from a culture of *P. haloplanktis* TAC125 grown in GG medium or GG-Met medium, respectively. In both growth conditions, condensation was carried out for 48 hours, starting from the medium exponential growth phase and continuing over the stationary phase. As corresponding negative control, VOCs capture was also performed on the outlet gas from un-inoculated media. Condensed VOCs were kept at -20°C until the following identification procedure. A suitable probe for the Solid-phase Micro extraction Gas-Chromatography - Mass Spectrometry (SPME-GC-MS) analysis was connected to the top of the bottle containing the condensed volatile molecules. The bottle (and its content) was heated to let the VOCs to interact with the probe. After 45 minutes exposure, the probe was connected to the mass spectrometer and the tentative identification analysis was carried out. Interestingly, when *P. haloplanktis* TAC125 is grown in GG medium the only volatile molecule identified is carbon dioxide (data not shown), thus supporting our preliminary observations about the absence of Bcc strain inhibition in a classical cross-streaking experiment (Fig. S1 (a)). The addition of L-methionine to the growth medium results in the production of some compounds (data not shown); one of the detected compounds was methylamine, whose identification was confirmed by comparison with a standard. Interestingly this compound has never been reported to have antibacterial activity, although its anti-fungi activity was previously described [23] and it has low toxicity towards human cells, which might allow handling this molecule even in uncontained laboratory conditions.

### Methylamine inhibits Bcc strains at different Minimal Volatile Inhibitory Concentrations (MVIC)

To evaluate the antibacterial activity eventually exerted by methylamine on *B. cenocepacia* LMG 19230 and LMG 16654 strains a suitable experimental procedure was set up. As shown in Fig. 4(a), the target Bcc strains (and *E. coli* K12 as control) were streaked onto two TYP-agar Petri dishes, one of which was placed into a box in which a defined molar amount of methylamine was released by a stoichiometric reaction between methyl-ammonium hydrochloride and an excess of sodium hydroxide (see Materials and Methods for details). The box was then hermetically sealed and incubated at 20°C for 4 days, to allow the growth of bacteria. As positive



control the second Petri dish was placed in a similar hermetically sealed box, without the addition of methylamine, and incubated in the same conditions. Both plates were then recovered from the sealed boxes and further incubated at 37°C for 2 days to allow a better bacterial growth on solid medium, if any.

The sensitivity of *B. cenocepacia* LMG 19230 and LMG 16654 strains was evaluated in the range of methylamine concentration between 1 and 10 mM, aiming at observing a dose-dependent growth inhibition and defining their Minimum Volatile Inhibitory Concentration (MVIC). Both strains displayed a MVIC of 10 mM, while *E. coli* K12 was able to grow when exposed to the same methylamine concentration (Fig. 4). Then, we applied the methylamine inhibition assay to a panel of Bcc strains, representative of some of the species belonging to the complex, with the aim of determining their respective MVIC.

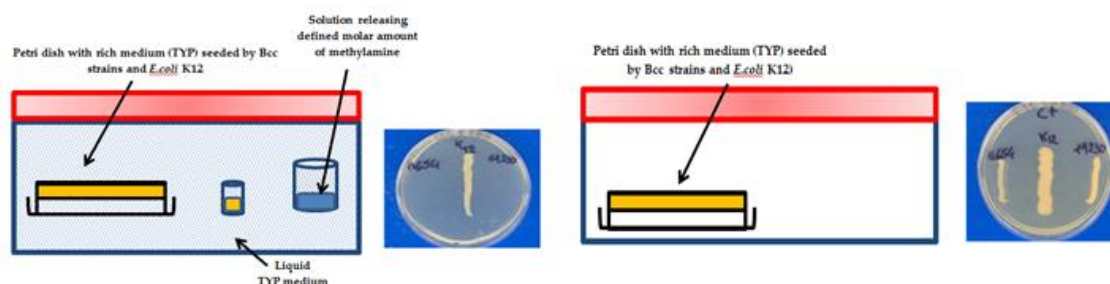


**Fig. 4: Methylamine inhibition assay.** Bcc strains LMG 19230, LMG 16654 and *E. coli* strain K12 (control) were streaked onto two Petri dishes containing TYP-agar medium. One plate was placed into a box with a solution releasing a stoichiometric quantity of methylamine, the other one (positive control) was placed in a similar box without any gaseous addition. Bcc strains LMG 19230, LMG 16654 and *E. coli* strain K12 streaked onto two Petri dishes containing TYP-agar medium exposed to methylamine. The plates were incubated 4 days at 20°C, then recovered from the boxes and incubated at 37°C for further 2 days.

Data obtained are reported in Table 3. Most of the analysed Bcc strains display a methylamine MVIC of 20 mM, while *B. latens* LMG 24064 is more resistant to the volatile molecule, as the methylamine MVIC is above 35 mM, concentration at which the *E. coli* K12 growth is inhibited.

A recent paper reports that several volatile compounds, in particular, trimethylamine (TMA), modify the antibiotic resistance profiles of different bacteria and that the TMA mode of action consists in a not specific transient alteration of antibiotic uptake due to pH increase in the environment of bacteria aerielly exposed to the VOC [24]. In order to evaluate if the observed Bcc growth inhibition could be due to alkalization of growth medium induced by methylamine aerial exposure, we followed the strategy reported in [24]. We measured the pH of 1 mL TYP liquid medium exposed to methylamine in the same conditions used for the MVIC test (Fig. 4(a)). Before any methylamine treatment, TYP liquid medium pH is  $6.7 \pm 0.1$ . Aerial exposure to 10 mM methylamine enhances TYP medium pH to  $8.2 \pm 0.2$ , while 20 mM methylamine treatment increases medium final pH to  $8.8 \pm 0.2$ . Then, we evaluated the ability of tested Bcc strains to grow on a modified TYP solid media buffered at different pHs (in the range 7.0 to 9.0) and results are shown in Table 3. With the notable exception of *B. multivorans* LMG 13010, all the Bcc strains used in this work are able to grow up to 8.5 and six over ten do grow at pH 9.0. Combining the information reported in Table 3, it is clear that the methylamine sensitivity spectrum of tested Bcc strains is not in agreement with their respective ability to grow at alkaline pHs. Therefore, although in case of *B. multivorans* LMG 13010 we cannot exclude the possibility that

the methylamine mode of action consists in a not permissive pH increase of growth medium, the other tested Bcc strains seem to be inhibited by methylamine regardless of pH variation.

Species	Strain	Methylamine MVIC (mM)	pH				
			7.0	7.5	8.0	8.5	9.0
<i>B. arboris</i>	LMG 24066	20	+	+	+	+	-
<i>B. cenocepacia</i>	LMG 16654	10	+	+	+	+	+
<i>B. cenocepacia</i>	LMG 19230	10	+	+	+	+	+
<i>B. contaminans</i>	LMG 23361	20	+	+	+	+	-
<i>B. latens</i>	LMG 24064	>35	+	+	+	+	+
<i>B. metallica</i>	LMG 24068	20	+	+	+	+	-
<i>B. multivorans</i>	LMG 13010	20	+	+	±	-	-
<i>B. pseudomultivorans</i>	LMG 26863	20	+	+	+	+	+
<i>B. stabilis</i>	LMG 14294	20	+	+	+	+	+
<i>B. ubonensis</i>	LMG 20358	20	+	+	+	+	+
<i>E. coli</i>	K12	35	+	+	+	+	+

Symbols: + growth; ± reduced growth; - no growth.

**Table 3. Bcc strains Methylamine MVIC and ability to growth at different pH.** For each *Burkholderia* species the list contains indication of strain number, the methylamine Minimum Volatile Inhibitory Concentration (MVIC) and the ability to growth on buffered TYP agar medium at different pH.

### Discussion:

Over the last years, we have reported the ability of many marine Antarctic strains, including the model organism *P. haloplanktis* TAC125, to produce VOCs able to inhibit the growth of *B. cepacia* complex strains. This inhibition ability was demonstrated using the classical cross-streaking experimental conditions [9, 11], which implies the growth of the Antarctic strains on solid medium. In the present paper, we demonstrated that *P. haloplanktis* TAC125 has the ability to produce anti-Bcc VOCs even when growing in liquid culture. Based on these results, we set up a methodology for VOCs capture, accumulation and storage by coupling the growth of the Antarctic bacterium in an automatic fermenter with the application of a cooling system to the exhaust air outlet.

Previously reported data demonstrated that the ability of *P. haloplanktis* TAC125 [11] and other marine Antarctic bacteria [13] to inhibit the growth of Bcc strains was influenced by the growth medium composition. We demonstrated that when the Antarctic bacterium is grown on GG solid medium, it is unable to inhibit the growth of

the Bcc target strains. This result confirmed the tight dependence of anti-Bcc VOCs production on *P. haloplanktis* TAC125 culture medium composition, and allowed us to test the effect of the addition of different amino acids to restore the inhibition ability of the Antarctic strain. Amino acids were selected as nutrient additives as they represent the *P. haloplanktis* TAC125 preferred carbon and nitrogen sources [14]. Interestingly, nine amino acids are able to restore the *P. haloplanktis* TAC125 antimicrobial activity when added to the GG medium (Table 2). Hence, it is possible that different carbon and/or nitrogen sources will activate different *P. haloplanktis* TAC125 metabolic pathways that, in turn, may end up in the production of different VOCs endowed with anti-Bcc activity. The different extent of growth inhibition displayed on the two Bcc target strains and the diverse effect of different amino acid addition on *P. haloplanktis* TAC125 inhibition ability on Bcc strains (Table 2) may be due to respective different sensitivity to a specific volatile compound, and/or to the production of different VOCs in these experimental conditions. It is indeed worth of mentioning that the efficiency of marine Antarctic bacteria to inhibit almost all Bcc strains so far tested may be related to the synergistic effect of multiple VOCs produced when the cells are grown in complex media.

In this paper, we further investigated on the VOCs produced by *P. haloplanktis* TAC125 when grown in GG medium containing L-methionine. This choice relies on two considerations: previously reported results suggested that at least some of the anti-Bcc VOCs may be sulphur containing compounds [10] and L-methionine is known to play a pivotal role in sulphur metabolism of most organisms [24]. Moreover, our experiments demonstrated that *P. haloplanktis* TAC125 is able to grow in GG+ L-methionine in automatic fermenter and clearly indicated that L-methionine is actually a growth substrate.

The addition of L-methionine to the growth medium resulted in the production of some VOCs (data not shown), amongst which methylamine. This simple amine may be the product of several microbial metabolic reactions, and therefore we explored the metabolic routes used by *P. haloplanktis* TAC125 to produce methylamine when growing on GG+L-methionine medium. The genome of *P. haloplanktis* TAC125 was *in silico* analyzed looking for the intracellular L-methionine destiny (data not shown), and this analysis revealed the absence of the genes encoding some key enzymes involved in previously reported L-methionine degradation pathways [25,26]. The above considerations suggest that L-methionine catabolism of the Antarctic bacterium offers several aspects of novelty thus supporting the idea that *P. haloplanktis* TAC125 evolved unknown metabolic routes for the use of this amino acid, some of which may end up with the production of methylamine. It is interesting to note that almost 11% of the protein encoding genes identified in *P. haloplanktis* TAC125 genome have still no homologous in any other organism [14].

Even though methylamine was never identified amongst the VOCs released by the Antarctic bacterium when grown in complex media [14], we focused our attention on it, since the antimicrobial activity of this amine was never reported. Our results demonstrated that this molecule is able to inhibit the growth of several Bcc strains at different concentrations and that its mode of action does not consist in a nonspecific pH increase. For all tested Bcc strains methylamine MVIC resulted to be in an mM concentration range, making however unrealistic its use as canonical/ classical antibiotic agent.

Although the identification of methylamine cellular target(s) in *B. cepacia* complex strains is out the scope of this study and will be object of future investigations, this is

the first paper where the anti-Bcc activity of a single volatile compound produced by an Antarctic marine bacterium was demonstrated.

### **Acknowledgements**

This work was supported by the EU-KBBE 2012-2016 project PharmaSea, grant N° 312184, by the Italian Cystic Fibrosis Research foundation (Grant FFC#12/2011), and PNRA (Programma Nazionale di Ricerche in Antartide) grant (PNRA 2013 AZ1.04).

### **References:**

- [1] Berdy J. Thoughts and facts about antibiotics: Where we are now and where we are heading. *J Antibiot* 2012; 65:385-395.
- [2] French GL. The continuing crisis in antibiotic resistance. *Int j antimicrob ag* 2010; 36:S3-S7.
- [3] Piddock LJ. The crisis of no new antibiotics-what is the way forward? *Lancet infect dis* 2012; 12:249-253.
- [4] Bologa CG, Ursu O, Oprea TI, Melancon CE, Tegos GP. Emerging trends in the discovery of natural product antibacterials. *Curr opin pharmacol* 2013; 13:678-687.
- [5] Newman DJ, Cragg GM. Natural products as sources of new drugs over the 30 years from 1981 to 2010. *J nat prod* 2012; 75:311-335.
- [6] Korpi A, Jarnberg J, Pasanen AL. Microbial volatile organic compounds. *Crit rev toxicol* 2009; 39:139-193.
- [7] Audrain B, Farag MA, Ryu CM, Ghigo JM. Role of bacterial volatile compounds in bacterial biology. *FEMS Microbiol Rev* 2015; 39:222-233.
- [8] Kai M, Effmert U, Berg G, Piechulla B. Volatiles of bacterial antagonists inhibit mycelial growth of the plant pathogen *Rhizoctonia solani*. *Arch microbial* 2007; 187:351-360.
- [9] Papaleo MC, Fondi M, Maida I, Perrin E, Lo Giudice A, Michaud L, Mangano S, Bartolucci G, Romoli R, Fani R. Sponge-associated microbial antarctic communities exhibiting antimicrobial activity against *Burkholderia cepacia* complex bacteria. *Biotechnol Adv* 2012; 30:272-293.
- [10] Romoli R, Papaleo MC, de Pascale D, Tutino ML, Michaud L, Lo Giudice A, Fani R, Bartolucci G. Characterization of the volatile profile of Antarctic bacteria by using solid-phase microextraction-gas chromatography-mass spectrometry. *J Mass Spectrom.* 2011; 46:1051-1060.
- [11] Papaleo MC, Romoli, R, Bartolucci G, Maida I, Perrin E, Fondi M, Orlandini V, Mengoni A, Emiliani G, Tutino ML, Parrilli E, de Pascale D, Michaud L, Lo Giudice A, Fani R. Bioactive volatile organic compounds from Antarctic (sponges) bacteria. *N Biotechnol* 2013; 30:824-838.

- [12]** Romoli R, Papaleo M, de Pascale D, Tutino ML, Michaud L, LoGiudice A, Fani R, Bartolucci G. GC–MS volatolomic approach to study the antimicrobial activity of the Antarctic bacterium *Pseudoalteromonas* sp. TB41. *Metabolomics* 2014; 10:42-59
- [13]** Maida I, Fondi M, Papaleo MC, Perrin E, Orlandini V, Emiliani G, de Pascale D, Parrilli E, Tutino ML, Michaud L, Lo Giudice A, Romoli R, Bartolucci G, Fani R. Phenotypic and genomic characterization of the Antarctic bacterium *Gillisia* sp. CAL575, a producer of antimicrobial compounds. *Extremophiles* 2014; 18:35-49.
- [14]** Medigue C, Krin E, Pascal G, Barbe V, Bernsel A, Bertin PN, Cheung F, Cruveiller S, D'Amico S, Duilio A, Fang G, Feller G, Ho C, Mangenot S, Marino G, Nilsson J, Parrilli E, Rocha EP, Rouy Z, Sekowska A, Tutino ML, Vallenet D, von Heijne G, Danchin A. Coping with cold: the genome of the versatile marine Antarctica bacterium *Pseudoalteromonas haloplanktis* TAC125. *Genome Res* 2005; 15:1325-1335.
- [15]** Giuliani M, Parrilli E, Pezzella C, Rippa V, Duilio A, Marino G, Tutino ML . A novel strategy for the construction of genomic mutants of the Antarctic bacterium *Pseudoalteromonas haloplanktis* TAC125. *Methods Mol Biol* 2012; 33:824-219.
- [16]** Parrilli E, Duilio A, Tutino ML. Heterologous protein expression in psychrophilic hosts. In Margesin R, Schinner F, Marx JC, Gerday C, editors. *Psychrophiles: from Biodiversity to Biotechnology*, Berlin Heidelberg: Springer-Verlag; 2008, p. 365-379.
- [17]** Rippa V, Papa R, Giuliani M, Pezzella C, Parrilli E, Tutino ML, Marino G, Duilio A. Regulated recombinant protein production in the Antarctic bacterium *Pseudoalteromonas haloplanktis* TAC125. *Methods Mol Biol* 2012; 824:203-218.
- [18]** Giuliani M, Parrilli E, Ferrer P, Baumann K, Marino G, Tutino ML. Process optimization for recombinant protein production in the psychrophilic bacterium *Pseudoalteromonas haloplanktis*. *Process Biochem* 2011; 46:953-959.
- [19]** Giuliani M, Parrilli E, Sannino F, Apuzzo GA, Marino G, Tutino ML. Recombinant production of a single-chain antibody fragment in *Pseudoalteromonas haloplanktis* TAC125. *Appl Microbiol Biot* 2014; 98:4887-4895.
- [20]** Fondi M, Maida I, Perrin E, Mellera A, Mocali S, Parrilli E, Tutino ML, Liò P, Fani R. Genome-scale metabolic reconstruction and constraint-based modelling of the Antarctic bacterium *Pseudoalteromonas haloplanktis* TAC125. *Environ Microbiol* 2015; 17:751-66.
- [21]** Papa R, Parrilli E, Sannino F, Barbato G, Tutino ML, Artini M, Selan L. Anti-biofilm activity of the antarctic marine bacterium *pseudoalteromonas haloplanktis* TAC125. *Res Microbiol* 2013; 164:450-456.
- [22]** Parrilli E, Papa R, Carillo S, Tilotta M, Casillo A, Sannino F, Cellini A, Artini M, Selan L, Corsaro MM, Tutino ML. Anti-biofilm activity of *Pseudoalteromonas haloplanktis* TAC125 against *Staphylococcus epidermidis* biofilm: Evidence of a signal molecule involvement? *Int J Immunopathol Pharmacol* 2015; 28:104-13.

- [23]** Zou CS, Mo MH, Gu YQ, Zhou JP, Zhang KQ. Possible contributions of volatile-producing bacteria to soil fungistasis. *Soil Biol Biochem* 2007; 39:2371–2379.
- [24]** Auger S, Danchin A, Verstraete IM. Global Expression Profile of *Bacillus subtilis* Grown in the Presence of Sulfate or Methionine. *J Bacteriol* 2002; 184:5179–5186.
- [25]** Parveen N, Cornell KA. Methylthioadenosine/S-adenosylhomocysteine nucleosidase, a critical enzyme for bacterial metabolism. *Mol Microbiol* 2011; 79:7-20.
- [26]** Duerre JA, Walker RD. *The Biochemistry of Adenosylmethionine*. New York: Columbia University Press; 1977

## SUPPLEMENTARY MATHIERIAL

**Fig. 3: *P. haloplanktis* TAC125 growth curves in automatic fermenter.** Comparison of *P. haloplanktis* TAC125 growth curves when the bacterium is grown at 20°C in batch in automatic fermenter in GG medium without (grey line) or with (black line) the addition of L-methionine at 40 mM final concentration. Each experiment was carried out in triplicate and error bar represents the standard deviation of each measurements. The inset table shows the values of main growth parameters ( $\mu$ , specific growth rate;  $X_{\max}$ , maximum biomass concentration).

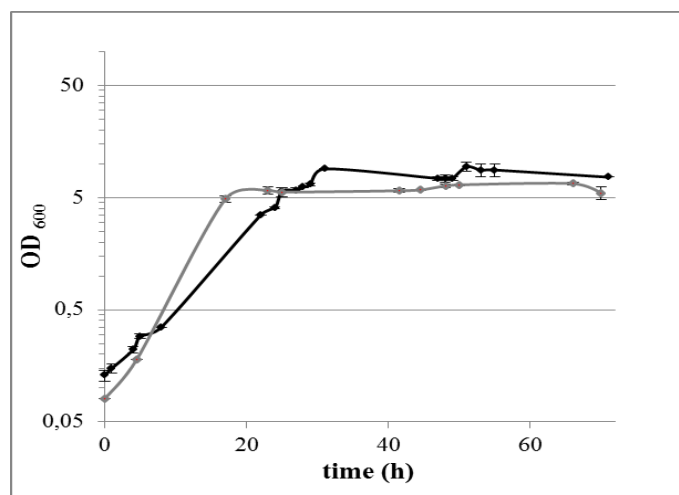
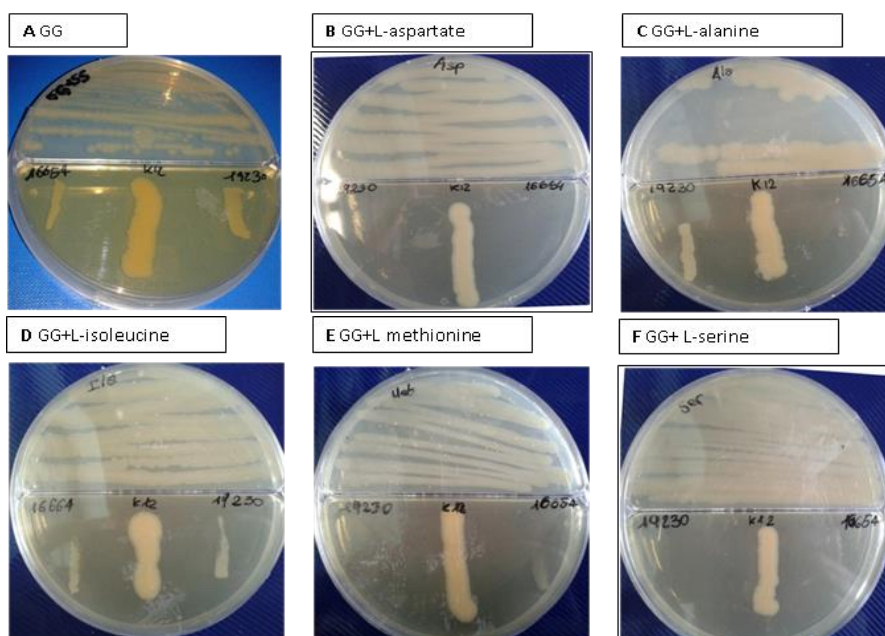
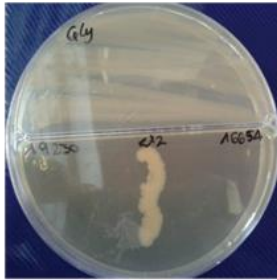


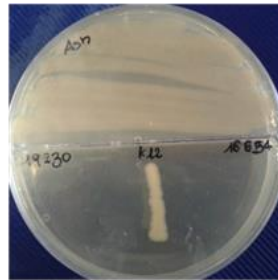
**Fig. 1S: The inhibition ability of the Antarctic bacterium when grown on GG agar medium and on GG+AA.** Cross-streaking experiments were carried out as previously described (Papaleo et al 2012) by using Petri dishes with a septum, target stains and the tester strain were grown on different media without any physical contact. The target strains (Bcc LMG 19230 and LMG 16654 and *Escherichia coli* K12) were grown on TYP the tester strain (*P. haloplanktis* TAC125) was grown on different media:



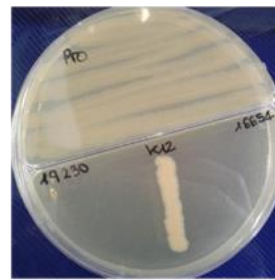
**G** GG+ Glycine



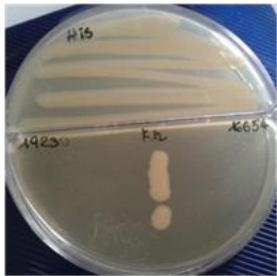
**H** GG+ L-asparagine



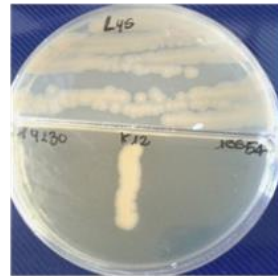
**I** GG+ L-proline



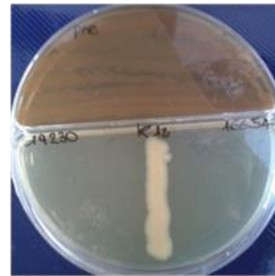
**L** GG+ L-histidine



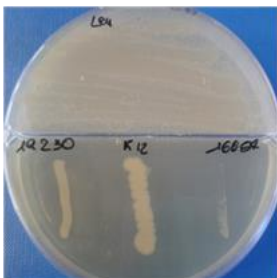
**M** GG+ L-lysine



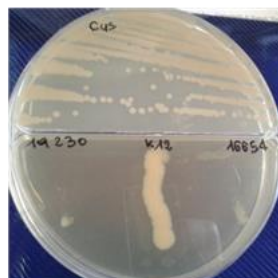
**N** GG+ L-phenylalanine



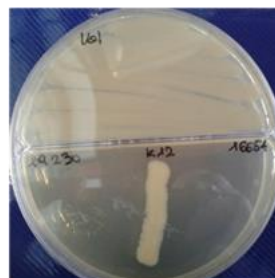
**O** GG+ L-leucine



**P** GG+ L-cysteine



**Q** GG+ L-valine







## **CHAPTER II**

### **Anti-biofilm molecules**



## Topic II: Identification of anti-biofilm molecules against *Staphylococcus epidermidis*

Biofilm is a multicellular community composed of prokaryotic and/or eukaryotic cells embedded in a matrix composed, at least partially, of material synthesized by the sessile cells in the community [45]. Biofilms were also estimated to be responsible in humans for a large proportion of persistent infections, such those derived from orthopaedic implants or indwelling catheters [46]. Indeed, pathogens embedded in biofilm matrix appear to be more resistant to many physical or chemical treatments, therefore even a well-designed antibiocidal cure often results in the selection of persistent pathogens cells, which are responsible for recurrent infections. However, issues derived from biofilm formation are not only relevant in medicine but in a wide range of sectors such as food industry [47], marine and industrial equipment [48].

Staphylococci are recognized as the most frequent causes of biofilm associated human infections. This exceptional status among biofilm associated pathogens is due to the fact that staphylococci are frequent commensal bacteria on the human skin and mucous surfaces. Indeed, staphylococci are among the most likely bacteria to infect any medical devices that penetrates those surfaces, such as when being inserted during surgery [49]. *Staphylococcus epidermidis* (*S. epidermidis*) contributes to making infections chronic and particularly difficult to eradicate.

The interest in the development of new approaches for the prevention and treatment of adhesion and biofilm formation capabilities has increased. A viable approach should target adhesive properties without affecting bacterial vitality in order to avoid the rapid appearance of escape mutants. Molecules implicated in active biofilm dispersal include glycosidases and proteases. There is a notable effort towards finding small available molecules that should “break up” the “tangled matrix” of the biofilm.

Previous results [24] show that the cell-free supernatant of *P. haloplanktis* TAC125 grown in static condition strongly inhibited the biofilm of *S. epidermidis*.

In particular, in the second part of my Ph.D. thesis you will find three papers:

- The first paper reports the definition of the best experimental condition in which *P. haloplanktis* TAC125 produces the anti-biofilm molecule. In particular, several process parameters were evaluated such as mode of bacterial growth, temperature and composition of medium. As often observed in many other bacterial biofilms, also *P. haloplanktis* TAC125 biofilm kinetic is characterized by an alternation of attachment and detachment phases. In order to assess the biofilm kinetic, the production of biofilm was evaluated daily (in the range 1-5 days). The supernatant of each condition was recovered and its effect on *S. epidermidis* strain O-47 was analyzed. A purification procedure was set up and the analysis of an enriched fraction demonstrated that the anti-biofilm activity is not due to a polysaccharide molecule but that it is due to small hydrophobic molecules that likely work as signal.
- In the second paper the set-up of biofilm cultivation of *P. haloplanktis* TAC125 in automatic bioreactor was proposed. The development of an efficient biofilm cultivation scheme in automatic fermenter is necessary to obtain a large amount of cell-free supernatant necessary for the anti-biofilm molecule/s purification; and the recovery of *P. haloplanktis* TAC125 cells grown in biofilm for physiologic studies. A fluidized-bed reactor fermentation in which selected floating polystyrene supports were homogeneously mixed and properly

exposed at the air-liquid interface was set up. The production of the anti-biofilm molecules from *P.haloplanktis* TAC125 in this condition was evaluated. This strategy allowed a larger-scale production of anti-biofilm molecule/s and paved the way to study of differences between *P. haloplanktis* TAC125 cells grown in biofilm and in planktonic conditions. In particular, the modifications occurring in the lipopolysaccharide of cells grown in biofilm were investigated.

- In the third paper the anti-biofilm activity of supernatants derived from cultures of cold-adapted bacteria belonging to *Pseudoalteromonas*, *Psychrobacter*, and *Psychromonas* genera was evaluated. In particular, supernatants were obtained from bacterial cultures made both in sessile and planktonic conditions. The potential anti-biofilm activity was tested on bacterial cultures of *P. aeruginosa* PAO1, three different strains of *S. aureus* and three different strains belonging *S. epidermidis* species. A preliminary physico-chemical characterization of supernatants was also performed, and these analyses highlighted the presence of molecules of different nature that act by inhibiting biofilm formation. Some of them are also able to impair the initial attachment of the bacterial cells to the surface, thus likely containing molecules acting as anti-biofilm surfactant molecules.

## Anti-biofilm activity of *pseudoalteromonas haloplanktis* tac125 against *staphylococcus epidermidis* biofilm: Evidence of a signal molecule involvement?

International Journal of  
Immunopathology and Pharmacology  
2015, Vol. 28(1) 104–113  
© The Author(s) 2015  
Reprints and permissions:  
sagepub.co.uk/journalsPermissions.nav  
DOI: 10.1177/0394632015572751  
iji.sagepub.com  
**SAGE**

E Parrilli,<sup>1</sup> R Papa,<sup>2</sup> S Carillo,<sup>1</sup> M Tilotta,<sup>2</sup> A Casillo,<sup>1</sup> F Sannino,<sup>1,3</sup>  
A Cellini,<sup>2</sup> M Artini,<sup>2</sup> L Selan,<sup>2</sup> MM Corsaro<sup>1</sup> and ML Tutino<sup>1</sup>

### Abstract

*Staphylococcus epidermidis* is recognized as cause of biofilm-associated infections and interest in the development of new approaches for *S. epidermidis* biofilm treatment has increased. In a previous paper we reported that the supernatant of Antarctic bacterium *Pseudoalteromonas haloplanktis* TAC125 presents an anti-biofilm activity against *S. epidermidis* and preliminary physico-chemical characterization of the supernatant suggested that this activity is due to a polysaccharide. In this work we further investigated the chemical nature of the anti-biofilm *P. haloplanktis* TAC125 molecule. The production of the molecule was evaluated in different conditions, and reported data demonstrated that it is produced in all *P. haloplanktis* TAC125 biofilm growth stages, also in minimal medium and at different temperatures. By using a surface coating assay, the surfactant nature of the anti-biofilm compound was excluded. Moreover, a purification procedure was set up and the analysis of an enriched fraction demonstrated that the anti-biofilm activity is not due to a polysaccharide molecule but that it is due to small hydrophobic molecules that likely work as signal. The enriched fraction was also used to evaluate the effect on *S. epidermidis* biofilm formation in dynamic condition by BioFlux system.

### Keywords

antibiofilm, Bioflux, dynamic biofilm assay, *P. haloplanktis* TAC125, *S. epidermidis* biofilm

Received 16 September 2014; accepted 15 December 2014

*Staphylococcus epidermidis* (*S. epidermidis*) is now being recognized as an important opportunistic pathogen that can cause significant problems when breaching the epithelial barrier, especially during biofilm-associated infection of indwelling medical devices.<sup>1,2</sup> Most diseases caused by *S. epidermidis* are of a chronic character and occur as device-related infections (such as intravascular catheter or prosthetic joint infections) and/or their complications.<sup>2</sup> The ability of this bacterium to adhere on both eukaryotic cells and abiotic surfaces and to form biofilm is an essential virulence factor. This capacity contributes to making *S. epidermidis* infections chronic and particularly difficult to eradicate.

Biofilms are sticky, surface-attached agglomerations of bacteria that are embedded in an extracellular

matrix and provide protection from antibiotics and mechanisms of host defense.<sup>3</sup> Considering the impact of *S. epidermidis* bacterial biofilms on human health, coagulase-negative staphylococci bloodstream infections originating from intravascular catheter infections are estimated to reach 250,000 cases per year in the USA with a mortality rate of 1–25%.<sup>4</sup> Interest in the development of innovative approaches for the

<sup>1</sup>Department of Chemical Sciences, Federico II University, Naples, Italy

<sup>2</sup>Department of Public Health and Infectious Diseases, Sapienza University, Rome, Italy

<sup>3</sup>Institute of Protein Biochemistry, CNR, Naples, Italy

### Corresponding author:

Ermenegilda Parrilli, Department of Chemistry, Federico II University, Complesso Universitario Monte Sant'Angelo, Via Cinthia 4, 80126 Naples, Italy.  
Email: erparril@unina.it

prevention and treatment of staphylococcal adhesion and biofilm formation capabilities has increased. A viable approach should target staphylococcal adhesive properties without affecting bacterial vitality in order to avoid the rapid appearance of escape mutants.

From another point of view, the biofilm could be considered as a source of novel drugs. Indeed, the specific environmental conditions prevailing within biofilms may induce profound genetic and metabolic rewiring of the biofilm-dwelling bacteria and therefore can allow the production of metabolites different from those obtained in planktonic condition. Furthermore, many bacterial biofilms secrete molecules such as quorum sensing signals,<sup>5</sup> surfactants,<sup>6</sup> enzymes,<sup>7</sup> and polysaccharides<sup>8,9</sup> that act by regulating biofilm architecture or mediating the release of cells from biofilms during the dispersal stage of the biofilm life cycle.<sup>7</sup> Also, the production of extracellular molecules that degrade adhesive components in the biofilm matrix is a basic mechanism used in the biological competition between phylogenetically different bacteria.<sup>10–12</sup>

Marine bacteria belonging to the genus *Pseudoalteromonas* produce compounds of biotechnological interest, including anti-biofilm molecules.<sup>13</sup> Marine bacteria from Antarctica represent an untapped reservoir of biodiversity; indeed, Antarctic microorganisms can synthesize a broad range of potentially valuable bioactive compounds.<sup>14–16</sup>

The present authors previously reported that *P. haloplanktis* TAC125 strain holds an anti-biofilm activity;<sup>15</sup> this bacterium had been isolated from Antarctic sea water near Terre Adelie.<sup>17</sup> The anti-biofilm activity of cell-free supernatant of *P. haloplanktis* grown in static and in planktonic condition was tested on different staphylococci. The results obtained demonstrated that only supernatant of *P. haloplanktis* grown in static condition inhibits biofilm of *S. epidermidis* but it was not effective on *S. aureus* biofilm. This anti-biofilm activity impairs biofilm development and disaggregates the mature biofilm of *S. epidermidis* without affecting bacterial viability, showing that its action is specifically directed against biofilm. A preliminary chemical characterization of the biofilm-inhibiting compound suggests that the biologically active component could be a polysaccharide.<sup>15</sup> The aim of the present work is to further investigate the chemical nature of *P. haloplanktis* TAC125 anti-biofilm

molecules to understand the mode of action of active molecules.

## Materials and methods

### Bacterial strains and culture conditions

The bacterial strains used in this work were: *S. epidermidis* O-47 isolated from clinical septic arthritis and kindly provided by Professor Gotz; *P. haloplanktis* TAC125 (17) was collected in 1992 from seawater near the French Antarctic Station Dumont d'Urville (60°40'; 40°01'E). Bacteria were grown in Brain Heart Infusion broth (BHI, Oxoid, UK) and synthetic medium GG (10 g/L D-Gluconic acid sodium, 10g/L glutamic acid, SCHATZ salt mixture). Biofilm formation was assessed in static condition while planktonic cultures were performed under vigorous agitation (180 rpm). All strains were maintained at –80°C in cryovials with 15% of glycerol.

### Biofilm formation of *P. haloplanktis* TAC125

**Static biofilm assay.** Quantification of *in vitro* biofilm production was based on the method described by Christensen with slight modifications.<sup>18</sup> Briefly, the wells of a sterile 24-well flat-bottomed polystyrene plate were filled with 1 mL of BHI, and an suitable dilution of Antarctic bacterial culture in exponential growth phase (about 0.1 OD 600 nm) was added into each well. The sterile 24-well flat-bottomed polystyrene plates were incubated for different times (24 h, 48 h, 72 h, 96 h, and 120 h) at 4°C. After rinsing with PBS, adhered cells were stained with 0.1% crystal violet, rinsed twice with double-distilled water, and thoroughly dried. The dye bound to adherent cells was solubilized with 20% (v/v) acetone and 80% (v/v) ethanol. The OD of each well was measured at 590 nm. Each data point is composed of four independent samples.

### Preparation of *P. haloplanktis* TAC125 supernatants

SN is the supernatant of a liquid culture of *P. haloplanktis* TAC125 grown without shaking in BHI at different temperatures (4°C, 15°C, 20°C). The wells of a sterile 24-well flat-bottomed polystyrene plate were filled with 900 mL of appropriate medium (BHI or GG) and 100 mL of overnight *P.*

*haloplanktis* TAC125 bacterial culture was added into each well. The plates were incubated at different temperatures as already reported for different times (24 h, 48 h, 72 h, 96 h, and 120 h). *P. haloplanktis* TAC125 biofilm formation was monitored each 24 h. Supernatants were recovered and separated from cells by centrifugation at 13,000 rpm. Then, they were sterilized by filtration through membranes with a pore diameter of 0.22  $\mu\text{m}$ , and stored at 4°C until use.

#### Biofilm formation of staphylococci

**Static biofilm assay.** Quantification of *in vitro* biofilm production was based on the method described by Christensen with slight modifications.<sup>18</sup> Briefly, the wells of a sterile 48-well flat-bottomed polystyrene plate were filled with 400  $\mu\text{L}$  of BHI medium; 1/100 dilution of overnight bacterial cultures was added to each well. The first row contained the untreated bacteria, while each of the remaining rows contained serial dilutions of supernatant (SN) starting from 1:2. The plates were incubated aerobically for 24 h at 37°C. After rinsing with PBS, adhered cells were stained with 0.1% crystal violet, rinsed twice with double distilled water, and thoroughly dried. The dye bound to adherent cells was resolubilized with 20% (v/v) acetone and 80% (v/v) ethanol. The OD of each well was measured at 590 nm. Each data point was composed of four independent samples.

**Dynamic biofilm assay.** To continuously monitor biofilm development in dynamic condition, we utilized a BioFlux 2000 microfluidic system (Fluxion Biosciences Inc., San Francisco, CA, USA), which allows the acquisition of microscopic images over time using the experimental protocol reported by Papa and co-workers.<sup>19</sup> Each flow channel connects to an input well (inlet) and an output well (outlet) on the plate. To grow biofilm in the BioFlux system, the channels were first primed. We filled the outlet with 100  $\mu\text{L}$  of sterile distilled water with flow at a shear setting of 1 dyne/cm<sup>2</sup> for 2 min. Coating with 100  $\mu\text{L}$  of 10  $\mu\text{g}/\text{mL}$  fibronectin was carried out for 2 min at 1 dyne/cm<sup>2</sup>. The fibronectin binding was performed for 30 min without flow. After priming, fibronectin was aspirated from the output wells and replaced with 100  $\mu\text{L}$  of fresh overnight cultures diluted to an OD 600 of 0.8. The channels were seeded by pumping from

the output wells to the input wells at 2.0 dyne/cm<sup>2</sup> for 4 s. Bacterial adhesion was performed for 30 min at 37°C without flow. A total of 2.0 mL of BHI was added to the input well and pumped at 1 dyne/cm<sup>2</sup> for 12 h. We used two inlet wells; in the first well we added F fraction at a concentration of 1 mg/mL. In the second well we added only BHI. Bright-field images were taken at 40X magnification at 1-min intervals for a total of 720 time points.

**SN treatment with NaIO<sub>4</sub>.** For NaIO<sub>4</sub> treatment, it was added at a final concentration of 20 mM to sample for 12 h at 37°C. As control, the same treatment was performed on BHI broth to exclude an anti-biofilm effect due to the NaIO<sub>4</sub> itself. After treatment, samples were sterilized by filtration through membranes with a pore diameter of 0.22  $\mu\text{m}$ , and stored at 4°C until use.

**Surface coating assay.** A volume of 25 mL of *P. haloplanktis* cell-free supernatant, or 25 mL of saline and BHI as controls, were transferred to the center of a well of a 24-well tissue-culture-treated polystyrene microtiter plate. The plate was incubated at room temperature to allow complete evaporation of the liquid. The wells were then filled with 1 mL of broth containing a 1/100 dilution of *S. epidermidis* overnight bacterial cultures and incubated at 37°C in static condition. After 18 h, the wells were rinsed with water and stained with 1 mL of 0.1% crystal violet. Stained biofilms were rinsed with water and dried, and the wells were photographed.

**Anti-biofilm molecule purification.** The first step was a dialysis against MilliQ water of *P. haloplanktis* TAC125 supernatant deriving sessile growth at 4°C. In this procedure a semipermeable membrane with a cutoff of 3,500 Da was used. The dialysate water was subjected to a gel-filtration liquid chromatography on a Biogel P-2 column (Bio-Rad, molecular mass separation range 100–1800 Da, 60  $\times$  0.75 cm, flow rate 15 mL/h, eluent water, fraction volume 1 mL).

The fraction resulting as active was further fractionated by high-performance liquid chromatography on a C18 column (Kinetex, Phenomenex, 150  $\times$  4.6 mm) eluting with the following program: 1% of B for 10 min (A: H<sub>2</sub>O, B: AcCN), 1 to 95% of B in 10 min, 95% of B for 10 min, flow rate 1 mL/min).



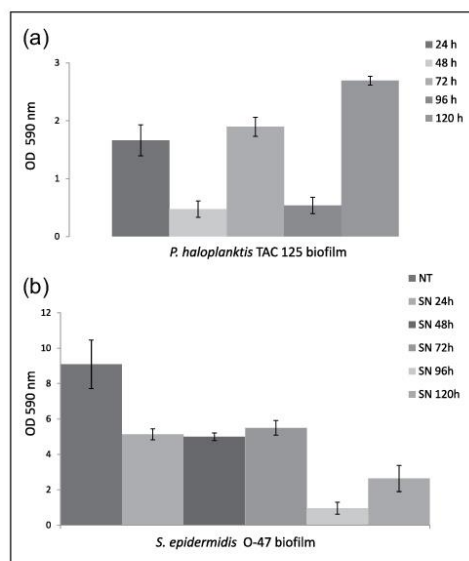


**Figure 1.** Kinetic biofilm development in *P. haloplanktis* TAC125 and production of anti-biofilm activity against *S. epidermidis* O-47. (a) Evaluation of *P. haloplanktis* biofilm formation at different times. (b) Biofilm formation of *S. epidermidis* strain O-47 treated with *P. haloplanktis* TAC125 supernatants deriving from sessile cultures obtained at different times.

## Results

### Optimization of *P. haloplanktis* TAC125 anti-biofilm molecule production conditions

**Study of the effect of bacterial biofilm kinetics on *P. haloplanktis* TAC125 anti-biofilm molecule production.** Previously reported results demonstrated that the production of the *P. haloplanktis* TAC125 anti-biofilm compounds was dependent on bacterial growth modality,<sup>15</sup> indeed the production of anti-biofilm compounds only occurs if Antarctic cells were grown in static condition. In order to assess whether the anti-biofilm was produced in all phases of biofilm development cycle, its formation over a 120-h period in BHI at 4°C was evaluated (Figure 1a). As shown in Figure 1a, *P. haloplanktis* TAC125 biofilm kinetics is characterized by phases of biofilm development (24 h, 72 h, 120 h) and phases of cells detachment (at 48 h, 96 h). Supernatants (SN) collected at different stages were tested to assess their effect on *S. epidermidis* strain O-47 biofilm formation (Figure 1B). In detail, supernatants of *P. haloplanktis* TAC125 cultures grown in sessile

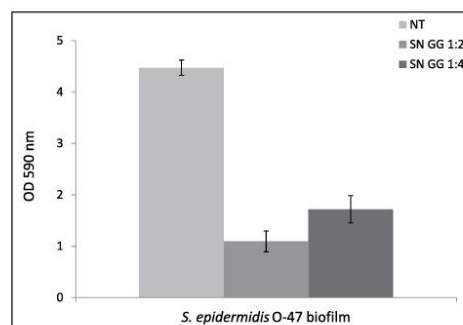


**Figure 2.** Biofilm formation of *S. epidermidis* O-47 in minimal medium GG in the presence and in the absence of scalar dilutions of *P. haloplanktis* supernatant. *P. haloplanktis* was grown in GG minimal medium in sessile condition.

condition at the different times (SN 24 h, SN 48 h, SN 72 h, SN 96 h, SN 120 h) were recovered and their effects on *S. epidermidis* strain O-47 biofilm were analyzed (Figure 1B). Reported data demonstrated that the anti-biofilm molecule is produced in all *P. haloplanktis* TAC125 biofilm stages although the best production is obtained at 96 h (Figure 1b); in fact, the supernatant collected at 96 h is able to decrease the biofilm formation of *S. epidermidis* strain O-47 about of 91%. Study of the effect of different culture media on *P. haloplanktis* TAC125 anti-biofilm compound production to evaluate whether the culture medium composition has influence on bioactive compound production, *P. haloplanktis* TAC125 was grown in a synthetic medium (based on gluconate and glutamate (GG)) in sessile condition at 4°C for a 96-h period. Then the effect of the obtained supernatant (SN-GG) on *S. epidermidis* strain O-47 biofilm was evaluated (Figure 2). In this experiment, *S. epidermidis* strain O-47 was grown in GG medium to avoid interference from the medium composition. As shown in Figure 2, the biofilm formation of *S. epidermidis* strain O-47 in the GG medium was lower than the BHI culture medium (Figure 1b), furthermore the SN-GG inhibitory effect is evident and dose-dependent. The treatment with SN-GG at a dilution of 1:2 induced a decrease in biofilm formation of *S. epidermidis* strain O-47 of approximately 85%.

**Study of the effect of different growth temperatures on *P. haloplanktis* TAC125 anti-biofilm compound production.** In order to assess whether growth temperature

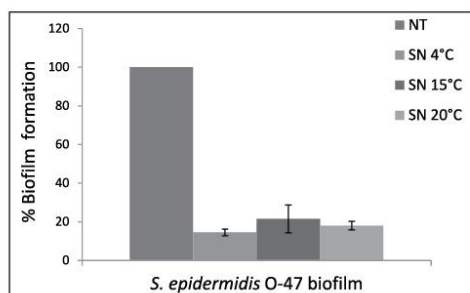


**Figure 3.** Biofilm formation of *S. epidermidis* O-47 in the presence and in the absence of *P. haloplanktis* supernatant deriving from sessile cultures performed at different temperatures. Data are reported as percentage of residual biofilm after the treatment.

has influence on anti-biofilm compound production, the Antarctic bacterium was grown in sessile condition at different temperatures (4°C, 15°C, 20°C). Corresponding supernatants were recovered for each condition after 96 h at 4°C, 96 h at 15°C, and 48 h at 20°C, and their effect on *S. epidermidis* strain O-47 biofilm was evaluated (Figure 3). As shown in Figure 3 the anti-biofilm compound was produced at all tested temperatures (4–20°C), demonstrating that anti-biofilm production is not temperature-dependent.

#### *P. haloplanktis* TAC125 anti-biofilm molecule is not a polysaccharide

Previous reported results suggested that *P. haloplanktis* TAC125 anti-biofilm activity could be due to a polysaccharide molecule.<sup>15</sup> Many anti-biofilm polysaccharides act as a surfactant molecule that modifies the physical characteristics of bacterial cells and abiotic surfaces. Therefore it was tested whether *P. haloplanktis* TAC125 supernatant could modify the surface properties of an abiotic substrate. To do this, evaporation coating was used to deposit the supernatant onto the surface of polystyrene wells, and then the ability of the coated surfaces to impair biofilm formation by *S. epidermidis* was tested. The supernatant deriving from sessile growth of *P. haloplanktis* at 4°C for 96 h was collected and used. When SN was applied to the polystyrene surfaces, the coated surfaces was not able to repel *S. epidermidis* biofilm formation in the area where the extract was deposited (data not

shown), indicating that SN did not act as a surfactant.

To further investigate the anti-biofilm nature, we started a preliminary purification of bioactive molecules from 96-h culture supernatant. Usually, a polysaccharide molecule can be separated from culture medium using a dialysis membrane with a 3,500 Da cutoff: in these conditions the polysaccharide is retained inside the dialysis tube. *P. haloplanktis* TAC125 supernatant deriving from sessile growth at 4°C was subjected to dialysis treatment and the sample retained inside the dialysis tube was subjected to size-exclusion chromatography (Sephacryl S-200). The retained sample and each chromatographic collected fraction were assayed in order to assess their anti-biofilm activity against *S. epidermidis* strain O-47 (data not shown). Results obtained demonstrated that none of the tested samples showed anti-biofilm activity (data not shown). Therefore, the anti-biofilm activity of dialysis permeate was evaluated and resulted to be active (data not shown). Consequently the bioactive molecules possessed a molecular mass lower than 3,500 Da, a molecular size not compatible with a polysaccharide.

It has been shown that NaIO<sub>4</sub> is able to oxidize the carbons bearing vicinal hydroxyl groups and to cleave the C-C bonds; this oxidizing activity was demonstrated also against polysaccharides.<sup>20</sup> The permeate was treated with NaIO<sub>4</sub>, for the above tests, the anti-biofilm activities of treated and untreated permeate were compared. The result of this experiment showed that NaIO<sub>4</sub> did not have effect on permeate anti-biofilm activity (data not shown). These data demonstrate that the reported anti-biofilm activity is not due to a polysaccharide molecule.

#### Partial purification of *P. haloplanktis* TAC125 anti-biofilm compounds

*P. haloplanktis* TAC125 supernatant deriving from sessile growth at 4°C was subject to dialysis treatment using a semipermeable membrane with a cutoff of 3500 Da. Both the retained and the permeate from the dialysis tube were tested for anti-biofilm activity and only the second one was shown to be active. The presence of a complex mixture in the permeate was shown by 1H NMR spectrum of the sample (data not shown). Consequently, a liquid chromatography on a

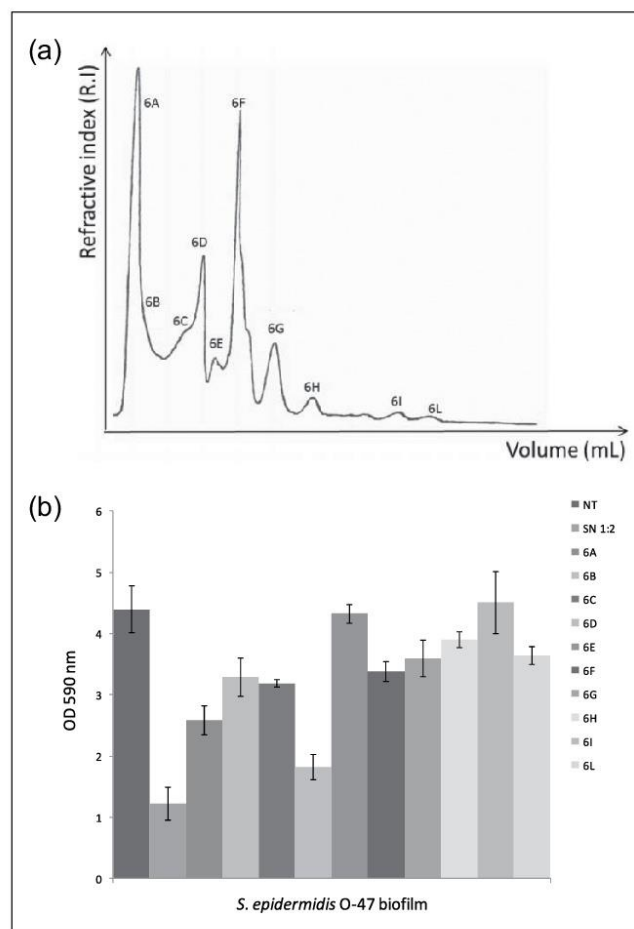


**Figure 4.** Purification of active compound from *P. haloplanktis* supernatant. (a) LC chromatographic profile of *P. haloplanktis* supernatant. (b) Biofilm formation by *S. epidermidis* O-47 in the presence and in the absence of exclusion chromatography fractions.

Biogel P-2 column was performed to fractionate the dialysate sample (Figure 4a) and the biological activity of each fraction was evaluated (Figure 4b). The obtained results indicated for the fraction 6D the best anti-biofilm activity, but once again  $^1\text{H}$  NMR spectrum revealed the presence of a complex mixture (data not shown). Reverse-phase HPLC on a C18 column was used to further purify 6D fraction and, the sub-fractions derived from this procedure were tested to evaluate the

anti-biofilm activity on *S. epidermidis* O-47 biofilm. The results (Figure 5) clearly showed that the treatment with F fraction induces a decrease of the biofilm formation of *S. epidermidis* strain O-47 about of 90%.

$^1\text{H}$  NMR spectrum suggested that the fraction F still is a mixture. However, proton NMR spectra obtained during the purification steps gave further confirmation that the molecule of interest is not a carbohydrate.



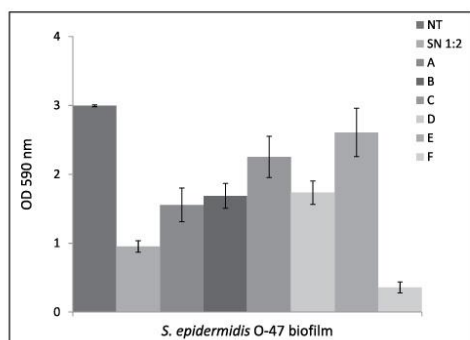


**Figure 5.** Biofilm formation by *S. epidermidis* O-47 in the presence and in the absence of HPLC chromatography fractions.

#### Effect of partially purified active compound(s) on *S. epidermidis* O-47 dynamic biofilm formation

Effect of F fraction treatment on *S. epidermidis* O-47 biofilm formation was also evaluated on BioFlux system.<sup>21</sup> The BioFlux system is a microfluidic device that precisely controls the flow of growth medium between two interconnected wells of a microtiter plate. By positioning the channel connecting the two wells over a window accessible for viewing by microscopy, biofilm growth can be monitored in a time-course assay in which images are collected at 1-min intervals. We collected 720 frames for each experiment, assembled in a time-lapse video. Selected images reported in Figure 6 show the biofilm development of *S. epidermidis* O-47 at different times, in the absence and in the presence of F fraction (bottom and top lanes of each panel, respectively).

Bacteria were seeded in both channels visible in each frame. After 30 min the flow was applied. In the top channel F fraction was added to the medium, while the bottom one contained only medium. Data obtained show an initial rapid growth of the bacteria, resulting in a confluent 'lawn' of cells that was followed by a period of detachment. F fraction clearly impaired the biofilm formation confirming results obtained in static system.

#### Discussion

In a previous paper<sup>15</sup> we demonstrated that the cell-free supernatant of Antarctic bacterium *P. haloplanktis* TAC125 was effective on *S. epidermidis*

biofilm even on the mature form. Moreover, the *P. haloplanktis* TAC125 supernatant resulted to have no antibacterial activity against free-living bacteria, and results to be species-specific.<sup>15</sup> Interestingly *P. haloplanktis* TAC125 produces this activity only when it is grown in sessile condition. This latter result could be explained in consideration that specific environmental conditions prevailing within biofilms may induce profound genetic and metabolic rewiring of the biofilm-dwelling bacteria,<sup>22</sup> which could lead to production of biofilm-specific metabolites. These peculiar features could be compatible with the action of different anti-biofilm molecules, such as polysaccharides,<sup>9</sup> biosurfactants,<sup>22</sup> quorum sensing inhibitors,<sup>23,24</sup> or signaling molecule that modulates the gene expression of recipient bacteria.<sup>25</sup>

In this work we aimed to assess which kind of anti-biofilm molecules are produced by the Antarctic bacterium. To collect information on anti-biofilm compound characteristics we explored the dependence of bioactive molecule production to growth conditions. Reported results demonstrated that the anti-biofilm compound is produced during all phases of *P. haloplanktis* TAC125 biofilm development with the best production of the molecules corresponding to biofilm detachment steps, and that the production is independent from the specific carbon and nitrogen source and is not temperature-dependent.

Previously reported data suggested that *P. haloplanktis* TAC 125 anti-biofilm compound is not a surfactant molecule because its action on mature biofilm is not immediate but requires a prolonged time.<sup>15</sup> In this paper we confirmed this hypothesis by surface coating assay, the reported result demonstrated that *P. haloplanktis* TAC125 supernatant did not modify the surface properties of abiotic substrate.

Preliminary physico-chemical characterization of supernatant of *P. haloplanktis* TAC125 suggested the hypothesis that the anti-biofilm molecule has a polysaccharidic nature,<sup>15</sup> in which case the data presented in the present paper disavow this hypothesis.

The setting up of a purification protocol allowed us to obtain a fraction (F fraction), that does not contain polysaccharides, enriched in anti-biofilm compound. The proposed purification protocol has to be optimized since its purification yield is very low, but it is interesting to note that F fraction,

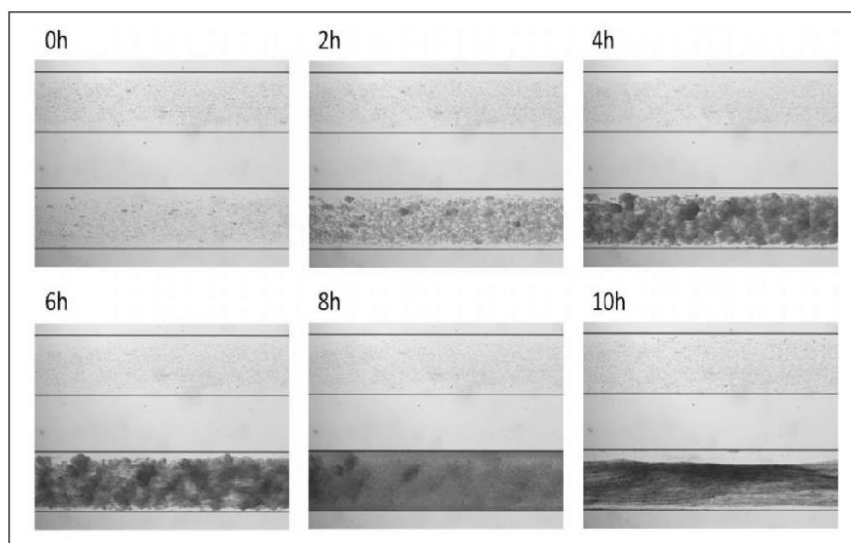


**Figure 6.** Biofilm formation of *S. epidermidis* O-47 in a BioFlux system. Each image contains two channels: top channel was SN-treated sample and bottom channel was the control one. Bright-field microscopic images were collected at 1-min intervals. The images presented were taken from the complete set of 720 images (see supplementary video bioflux for a video compilation of these images) taken at 40 X magnification.

which is still a mixture of several compounds, results as being active at a concentration lower than 1 mg/mL, suggesting that anti-biofilm molecule resulted as being endowed with a strong biological activity. Moreover, the molecules contained in the F fraction have a molecular weight smaller than 3,500 Da and display a hydrophobic character as indicated by F fraction elution time in reverse-phase chromatography. Therefore, reported results demonstrate that the *P. haloplanktis* TAC125 anti-biofilm activity is due to a small hydrophobic molecule, able to affect *S. epidermidis* biofilm formation and stability.

The *P. haloplanktis* TAC125 anti-biofilm molecule is active against several *S. epidermidis* strains, among others it is effective on the clinical isolate O-47, which is a naturally occurring *agr* mutant,<sup>26</sup> but it is inactive on *S. epidermidis* XX-17 *ica* mutant<sup>27</sup> (data not shown). The *ica* operon encodes enzymes responsible for production of polysaccharide intercellular adhesin (PIA or PNAG), which is the main component of polysaccharide matrix of staphylococcus biofilm.<sup>28</sup> These data could indicate in the *ica* genes the possible target of anti-biofilm molecules. *ica* genes regulation in *S.*

*epidermidis* is under the control of LuxS quorum sensing system.<sup>28</sup> It was reported that deletion of *luxS* gene in *S. epidermidis* enhances biofilm formation, this effect being due to an increase over four-fold of *ica* expression and resulting increase of PIA synthesis.<sup>29</sup>

Therefore, the LuxS communication system could be involved in bacterial intra-species communication between *S. epidermidis* and *P. haloplanktis* TAC125. The Antarctic bacterium genome analysis revealed that it is devoid of the *luxS* gene,<sup>17</sup> therefore the anti-biofilm effects of *P. haloplanktis* exoproducts could be due to a novel molecule, or to the synergistic actions of different molecules, that could work as an AI-2 agonist or as a ligand able to target the AI-2 receptor inducing an AI-2 signaling response. Only the full structural characterization of the active molecule will address the detailed mode of action of anti-biofilm molecules. However, regardless of the chemical nature of the anti-biofilm molecule, its efficacy was confirmed on *S. epidermidis* biofilm formation in dynamic condition using the BioFlux system.

BioFlux is an accurate representation of environmental or physiological conditions by precisely

controlling shear flow and can bridge the gap between *in vitro* and *in vivo* assays. Under these conditions, the bacteria progress through a series of developmental steps, ultimately forming a multicellular structure containing differentiated cell populations. The observation of the biofilm at various time-points throughout this process provides a glimpse of the temporal changes that occur.

Flow biofilm is closer to natural biofilms and can differ from static biofilms, evidently due to hydrodynamic influences on cell signaling. The reported results demonstrate that the *P. haloplanktis* TAC125 anti-biofilm is effective against *S. epidermidis* biofilm formation in dynamic condition; this conclusion is very promising with regard to its use in *in vivo* systems. Therefore the use of *P. haloplanktis* TAC125 anti-biofilm molecules during persistent infection sustained by staphylococci in combination therapy with antibiotics could be proposed.

#### Declaration of conflicting interests

The author(s) declared no potential conflicts of interest with respect to the research, authorship, and/or publication of this article.

#### Funding

This work was supported by Programma Nazionale di Ricerche in Antartide 2013/B1.04 Tutino.

#### References

- Dohar JE, Roland P, Wall GM et al. (2009) Differences in bacteriologic treatment failures in acute otitis externa between ciprofloxacin/dexamethasone and neomycin/polymyxin B/hydrocortisone: Results of a combined analysis. *Current Medical Research and Opinion* 25: 287–291.
- Rogers KL, Fey PD and Rupp ME (2009) Coagulase-negative staphylococcal infections. *Infectious Disease Clinics of North America* 23: 73–98.
- Costerton JW, Stewart PS and Greenberg EP (1999) Bacterial biofilms: A common cause of persistent infections. *Science* 284: 1318–1322.
- Otto M (2012) Molecular basis of *Staphylococcus epidermidis* infections. *Seminars in Immunopathology* 34: 201–214.
- Ni N, Li M, Wang J et al. (2009) Inhibitors and antagonists of bacterial quorum sensing. *Medicinal Research Reviews* 29: 65–124.
- Kiran GS, Sabarathnam B and Selvin J (2010) Biofilm disruption potential of a glycolipid biosurfactant from marine *Brevibacterium casei*. *FEMS Immunology and Medical Microbiology* 59: 432–438.
- Kaplan JB (2010) Biofilm dispersal: Mechanisms, clinical implications, and potential therapeutic uses. *Journal of Dental Research* 89: 205–218.
- Qin Z, Yang L, Qu D et al. (2009) *Pseudomonas aeruginosa* extracellular products inhibit staphylococcal growth, and disrupt established biofilms produced by *Staphylococcus epidermidis*. *Microbiology* 155: 2148–2156.
- Valle J, Da Re S, Henry N et al. (2006) Broad-spectrum biofilm inhibition by a secreted bacterial polysaccharide. *Proceedings of the National Academies of Science of the United States of America* 103: 12558–12563.
- Brook I (1999) Bacterial interference. *Critical Reviews in Microbiology* 25: 155–172.
- Wang CZ, Li M, Dong D et al. (2007) Role of ClpP in biofilm formation and virulence of *Staphylococcus epidermidis*. *Microbes and Infection* 9: 1376–1383.
- Wang CZ, Fan JJ, Niu C et al. (2010) Role of spx in biofilm formation of *Staphylococcus epidermidis*. *FEMS Immunology and Medical Microbiology* 59: 152–160.
- Klein GL, Soum-Souter E, Guede Z et al. (2011) The anti-biofilm activity secreted by a marine *Pseudoalteromonas* strain. *Biofouling* 27: 931–940.
- Jayatilake GS, Thornton MP, Leonard AC et al. (1996) Metabolites from an Antarctic sponge-associated bacterium, *Pseudomonas aeruginosa*. *Journal of Natural Products* 59: 293–296.
- Papa R, Parrilli E, Sannino F et al. (2013) Anti-biofilm activity of the Antarctic marine bacterium *Pseudoalteromonas haloplanktis* TAC125. *Research in Microbiology* 164: 450–456.
- Papaleo MC, Romoli R, Bartolucci G, et al. (2013) Bioactive volatile organic compounds from Antarctic (sponges) bacteria. *New Biotechnology* 30: 824–838.
- Medigue C, Krin E, Pascal G, et al. (2005) Coping with cold: The genome of the versatile marine Antarctica bacterium *Pseudoalteromonas haloplanktis* TAC125. *Genome Research* 15: 1325–1335.
- Artini M, Romano C, Manzoli L et al. (2011) Staphylococcal IgM enzyme-linked immunosorbent assay for diagnosis of periprosthetic joint infections. *Journal of Clinical Microbiology* 49: 423–425.
- Papa R, Artini M, Cellini A et al. (2013) A new anti-infective strategy to reduce the spreading of antibiotic resistance by the action on adhesion-mediated virulence factors in *Staphylococcus aureus*. *Microbial Pathogenesis* 63: 44–53.
- Bendaoud M, Vinogradov E, Balashova NV et al. (2011) Broad-spectrum biofilm inhibition by *Kingella kingae* exopolysaccharide. *Journal of Bacteriology* 193: 3879–3886.
- Benoit MR, Conant CG, Ionescu-Zanetti C et al. (2010) New device for high-throughput viability screening of

- flow biofilms. *Applied and Environmental Microbiology* 76: 4136–4142.
22. Beloin C, Michaelis K, Lindner K et al. (2006) The transcriptional antiterminator RfaH represses biofilm formation in *Escherichia coli*. *Journal of Bacteriology* 188: 1316–1331.
  23. Das P, Mukherjee S and Sen R (2009) Antiadhesive action of a marine microbial surfactant. *Colloids and Surfaces B: Biointerfaces* 71: 183–186.
  24. Rasmussen TB and Givskov M (2006) Quorum-sensing inhibitors as anti-pathogenic drugs. *International Journal of Medical Microbiology* 296: 149–161.
  25. Estrela AB, Heck MG and Abraham WR (2009) Novel approaches to control biofilm infections. *Current Medicinal Chemistry* 16: 1512–1530.
  26. Kim HS, Kim SM, Lee HJ et al. (2009) Expression of the *cpdA* gene, encoding a 3',5'-cyclic AMP (cAMP) phosphodiesterase, is positively regulated by the cAMP-cAMP receptor protein complex. *Journal of Bacteriology* 191: 922–930.
  27. Vuong C, Gerke C, Somerville GA et al. (2003) Quorum-sensing control of biofilm factors in *Staphylococcus epidermidis*. *Journal of Infectious Diseases* 188: 706–718.
  28. Xu L, Li HL, Vuong C et al. (2006) Role of the *luxS* quorum-sensing system in biofilm formation and virulence of *Staphylococcus epidermidis*. *Infection and Immunity* 74: 488–496.
  29. Cue D, Lei MG and Lee CY (2012) Genetic regulation of the intercellular adhesion locus in staphylococci. *Frontiers in Cellular and Infection Microbiology* 2: 38.
  30. Doherty N, Holden MT, Qazi SN et al. (2006) Functional analysis of *luxS* in *Staphylococcus aureus* reveals a role in metabolism but not quorum sensing. *Journal of Bacteriology* 188: 2885–2897.
  31. Cluzel ME, Zanella-Cleon I, Cozzzone AJ et al. (2010) The *Staphylococcus aureus* autoinducer-2 synthase *LuxS* is regulated by Ser/Thr phosphorylation. *Journal of Bacteriology* 192: 6295–6301.
  32. Nichols JD, Johnson MR, Chou CJ et al. (2009) Temperature, not *LuxS*, mediates AI-2 formation in hydrothermal habitats. *FEMS Microbiology Ecology* 68: 173–181.
  33. Tavender TJ, Halliday NM, Hardie KR et al. (2008) *LuxS*-independent formation of AI-2 from ribulose-5-phosphate. *BMC Microbiology* 8: 98.



## Large-scale biofilm cultivation of Antarctic bacterium *Pseudoalteromonas haloplanktis* TAC125 for physiologic studies and drug discovery

Ermenegilda Parrilli<sup>1</sup> · Annarita Ricciardelli<sup>1</sup> · Angela Casillo<sup>1</sup> ·  
Filomena Sannino<sup>1</sup> · Rosanna Papa<sup>2</sup> · Marco Tilotta<sup>2</sup> · Marco Artini<sup>2</sup> · Laura Selan<sup>2</sup> ·  
Maria Michela Corsaro<sup>1</sup> · Maria Luisa Tutino<sup>1</sup>

Received: 12 November 2015 / Accepted: 20 January 2016  
© Springer Japan 2016

**Abstract** Microbial biofilms are mainly studied due to detrimental effects on human health but they are also well established in industrial biotechnology for the production of chemicals. Moreover, biofilm can be considered as a source of novel drugs since the conditions prevailing within biofilm can allow the production of specific metabolites. Antarctic bacterium *Pseudoalteromonas haloplanktis* TAC125 when grown in biofilm condition produces an anti-biofilm molecule able to inhibit the biofilm of the opportunistic pathogen *Staphylococcus epidermidis*. In this paper we set up a *P. haloplanktis* TAC125 biofilm cultivation methodology in automatic bioreactor. The biofilm cultivation was designated to obtain two goals: (1) the scale up of cell-free supernatant production in an amount necessary for the anti-biofilm molecule/s purification; (2) the recovery of *P. haloplanktis* TAC125 cells grown in biofilm for physiological studies. We set up a fluidized-bed reactor fermentation in which floating polystyrene supports were homogeneously mixed, exposing an optimal air–liquid interface to let bacterium biofilm formation. The proposed methodology allowed a large-scale production of

anti-biofilm molecule and paved the way to study differences between *P. haloplanktis* TAC125 cells grown in biofilm and in planktonic conditions. In particular, the modifications occurring in the lipopolysaccharide of cells grown in biofilm were investigated.

**Keywords** Biofilm cultivation · *Pseudoalteromonas haloplanktis* TAC125 · Anti-biofilm · Bacterial biofilm phenotype

### Introduction

Biofilm is a structured aggregation of microorganisms associated with a surface and it is the predominant mode of growth for bacteria in most environments. The transition from the planktonic state to biofilm growth occurs as a consequence of environmental changes that trigger the activation of multiple regulatory networks (Hall-Stoodley et al. 2004; de la Fuente-Núñez et al. 2013). Thus, upon sensing a proper signal, free-living (planktonic) cells will initiate attachment to a surface, which will lead to the formation of a biofilm that has a greater ability to withstand environmental challenges. Bacteria possess a biofilm genetic program that could be triggered by stressful conditions, aiming at the adaptation to transiently hostile environments (de la Fuente-Núñez et al. 2013). This program involves the switch on of regulatory circuits that cause transient genetic alterations rather than permanent. Proteomic and transcriptomic studies have shown a global shift in metabolism when growth switches from planktonic to biofilm (de la Fuente-Núñez et al. 2013).

Although bacterial biofilm has drawn increasing attention due to many detrimental effects on human health (Percival et al. 2015), it can be used in many biotechnological

Communicated by H. Atomi.


**Electronic supplementary material** The online version of this article (doi:10.1007/s00792-016-0813-2) contains supplementary material, which is available to authorized users.

✉ Ermenegilda Parrilli  
erparril@unina.it

<sup>1</sup> Department of Chemical Sciences, Federico II University, Complesso Universitario Monte Sant'Angelo, Via Cintia 4, 80126 Naples, Italy

<sup>2</sup> Department of Public Health and Infectious Diseases, Sapienza University, Piazzale Aldo Moro 5, 00185 Rome, Italy

Published online: 05 February 2016

 Springer



applications (Rosche et al. 2009). Indeed, the specific environmental conditions prevailing within biofilms induce profound genetic and metabolic rewiring of the biofilm-dwelling bacteria that can allow the production of metabolites different from those obtained in planktonic condition. From this point of view, the biofilm could be considered as a source of novel drugs. Furthermore, many bacterial biofilms secrete molecules such as quorum sensing signals, surfactants, enzymes, and polysaccharides that act by regulating biofilm architecture or mediating the release of cells from biofilms during the dispersal stage of the biofilm life cycle (Valle et al. 2006; Qin et al. 2009; Ni et al. 2009; Kiran et al. 2010; Papa et al. 2015). While understanding of these aspects of biofilms has increased, further work is needed, especially in the field of in vitro systems development for growing and studying microbial biofilms.

Two major biofilm models are studied in the laboratory, biofilms grown without a continuous flow of fresh medium and biofilms grown with a continuous flow of fresh medium. These systems generally provide a surface that can be removed and examined once it is colonized to assess biofilm formation. Along with the development of these systems for biofilm physiology studies at small scale, the biotechnological applications of microbial biofilm, such as water purification and wastewater treatment and enhanced production of added-value fermentation products (Pongtharangku and Demirci 2007; Cheng et al. 2010) fostered the set-up of biofilm reactors for large-scale industrial production. Biofilm reactors have been proven quite effective in enhancing productions of added-value products, such as bioethanol, organic acids, enzymes, antibiotics, and polysaccharides as they can generate increased volumetric productivity rates by maintaining high biomass concentration in the bioreactors (Cheng et al. 2010).

In general, biofilm reactors can be categorized into two groups: fixed-bed and expanded-bed reactors. Fixed-bed reactors include all processes in which the biofilm develops on static media (Cheng et al. 2010; Szilágyi et al. 2013). Expanded-bed reactors include biofilm with continuously moving media driven by high air or liquid velocity, or by mechanical stirring (Cheng et al. 2010). A great variety of solid supports have been developed and designed to increase the specific surface area per volume of reactor to obtain higher efficiency and compactness (Cheng et al. 2010).

We previously (Papa et al. 2013b; Parrilli et al. 2015) demonstrated that the cell-free supernatant of Antarctic bacterium *Pseudoalteromonas haloplanktis* TAC125 (*P. haloplanktis* TAC125) inhibits *Staphylococcus epidermidis* (*S. epidermidis*) biofilm formation. Interestingly *P. haloplanktis* TAC125 shows this activity only when it is grown in sessile condition (Papa et al. 2013b). Recent investigation (Parrilli et al. 2015) on chemical nature of *P. haloplanktis* TAC125 anti-biofilm molecule demonstrated that

the anti-biofilm activity is due to small hydrophobic molecule that likely works as signal. These results are highly suggestive of actual differences in *P. haloplanktis* TAC125 cells physiology when sessile rather than planktonic lifestyle is adopted, and pave the way to several open questions about the biofilm-specific pathway involved in the anti-biofilm molecule synthesis. To answer these questions it is necessary to have a methodology to investigate the characteristics of *P. haloplanktis* TAC125 cell grown in biofilm. Moreover, the previously proposed purification protocol (Parrilli et al. 2015), even if it allowed to obtain an active fraction enriched in anti-biofilm compound, is characterized by a poor purification yield. Therefore, the purification and characterization of the anti-biofilm molecule requires a larger scale production.

In this paper, we set up a biofilm cultivation methodology of *P. haloplanktis* TAC125 in automatic bioreactor. The Gram-negative psychrotolerant marine bacterium *P. haloplanktis* TAC125 is one of the best-studied cultivable representatives of the marine bacterioplankton and it is considered a model organism of bacterial cold-adaptation (Medigue et al. 2005). Indeed, in the last few years the increasing interest in *P. haloplanktis* TAC125 has led to the accumulation of different data types, including its complete genome sequence (Medigue et al. 2005), its intracellular and extracellular proteome (Piette et al. 2010, 2011; Papa et al. 2006), detailed growth phenotypes (Wilmes et al. 2010; Giuliani et al. 2011), and a genome-scale metabolic model (Fondi et al. 2015). A fermentation scheme to up-scale *P. haloplanktis* TAC125 growth in automatic bioreactors, at a laboratory scale, was developed and used for batch (Giuliani et al. 2011), chemostat cultivation (Giuliani et al. 2011) and fed-batch fermentation (Wilmes et al. 2010). However, no strategy was established to obtain a biofilm cultivation of *P. haloplanktis* TAC125 in bioreactor.

In this paper, we proposed a biofilm cultivation of *P. haloplanktis* TAC125 in automatic bioreactor aimed at a larger scale production of *P. haloplanktis* TAC125 supernatant grown in biofilm condition, indispensable for the purification of the molecule active against *S. epidermidis* biofilm. The set up process also allowed a consistent enhancement of the recovery yield of *P. haloplanktis* TAC125 biomass, making now possible to carry out comparative physiologic studies of Antarctic bacterial cells grown in biofilm and in planktonic conditions.

## Materials and methods

### Bacterial strains and culture conditions

Bacterial strains used in this work were: *S. epidermidis* O-47 isolated from clinical septic arthritis and kindly

provided by Prof. Gotz (Heilmann et al. 1996); *P. haloplanktis* TAC125 (Medigue et al. 2005) collected in 1992 from seawater near French Antarctic Station Dumont d'Urville. Bacteria were grown in Brain Heart Infusion broth (BHI, Oxoid, UK). Biofilm formation was assessed in static condition while planktonic cultures were performed under vigorous agitation (180 rpm). All strains were maintained at  $-80^{\circ}\text{C}$  in cryovials with 15 % of glycerol.

#### Biofilm formation of *P. haloplanktis* TAC125 on supports in flask

Polystyrene supports were hand made using pieces of expanded polystyrene with two different shapes. The mean length of the outer side is 2 cm, the mean thickness is 1 cm and the mean surface exposed area is  $12\text{ cm}^2$  in case of support A. Type B are characterized by a mean thickness of 1 cm, a mean diameter of 0.5 cm and a mean surface exposed area of  $2.1\text{ cm}^2$ .

The supports were placed in water and sterilized in autoclave at  $121^{\circ}\text{C}$  for 20 min. After sterilization, the polystyrene supports were added to cell cultures. In detail, 250 ml glass wide-neck flasks were filled with 25 ml of BHI medium and an appropriate dilution of Antarctic bacterial culture in exponential growth phase (about 0.1 OD 600 nm) was added into each flask. Several replicates of autoclaved polystyrene supports were separately placed onto the surface of the broth with a sterile forceps to allow a homogeneous soaking of the surfaces and to enable biofilm formation at air-liquid interface. In detail, four replicates of support A (Fig. 1) and 24 replicates of support B (Fig. 1) were added in each flask, respectively. *P. haloplanktis* TAC125 cultures were incubated at 15 and at  $4^{\circ}\text{C}$  for 96 h in static condition. After incubation, supernatants were separated from polystyrene supports and sterilized by filtration through membranes with a pore diameter of  $0.22\text{ }\mu\text{m}$ ,

and stored at  $4^{\circ}\text{C}$  until use. Supports were recovered and rinsed twice with 40 ml of PBS. Then adhered cells on supports were stained with 0.1 % crystal violet, rinsed twice with double-distilled water, and thoroughly dried. The dye bound to adherent cells on supports was solubilized with 20 ml of 20 % (v/v) glacial acetic acid and 80 % (v/v) ethanol and the absorbance at 590 nm was measured.

#### Recovery of attached cells by sonication

250 ml glass wide-neck flasks were filled with 25 ml of BHI medium and an appropriate dilution of Antarctic bacterial culture in exponential growth phase (about 0.1 OD 600 nm) was added into each flask. Then four replicates of support A and 24 replicates of support B were added in each flask, respectively. *P. haloplanktis* TAC125 cultures were incubated at  $4^{\circ}\text{C}$  for 96 h in static condition, after incubation supports were transferred with a sterile forceps to a 50 ml Falcon tube filled with 10 ml of BHI broth, with the supports completely immersed into the broth. In detail, one single support A and six supports B in each Falcon tube were transferred, respectively. Samples were sonicated at three different exposure times (5, 10 and 15 min). Sonication was performed by using an ultrasound bath (Elmasonic S 30/H) at a constant ultrasound frequency of 37 kHz. The supports floated to the top of the liquid level while the detached biomass settled. Sonication fluid obtained after three different exposure times was transferred to 10 ml Falcon tubes, respectively. Samples were centrifuged at 13,000 rpm, supernatant was discarded and cell pellets were resuspended in a small volume of fresh broth. Cell suspensions were transferred in 2 ml microcentrifuge tubes and centrifuged at 13,000 rpm. Then supernatant was discarded and cell pellets were dried in an oven at  $55^{\circ}\text{C}$  for 24 h. Dry weight of recovered cell pellets was measured by using an analytical balance.

#### Anti-biofilm compound/s production in automatic bioreactor

*P. haloplanktis* TAC125 bacterial culture was grown in BHI medium in a Stirred Tank Reactor 3 L fermenter (Applikon) connected to an ADI-1030 Bio Controller (Applikon) with a working volume of 1 L. The bioreactor was equipped with the standard pH-,  $\text{pO}_2$ -, level- and temperature sensors for the bioprocess monitoring. To allow the biofilm formation, autoclaved solid polystyrene supports A were added into the bioreactor (33 supports in 1 L). The culture was carried out at  $15^{\circ}\text{C}$  for 48 h, or at  $4^{\circ}\text{C}$  for 96 h, in aerobic conditions using an airflow of  $6\text{ L h}^{-1}$ , without stirring. Supernatant was recovered and separated from supports and cells by a centrifugation at 13,000 rpm. Then, it was sterilized by filtration through membranes with a pore

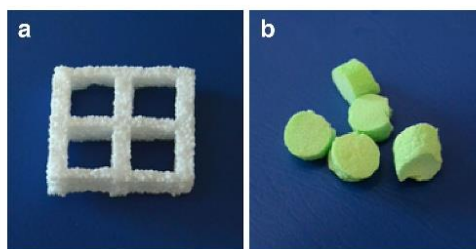


**Fig. 1** Autoclaved polystyrene supports. **a** Support A: the mean length of the outer side is 2 cm, the mean thickness is 1 cm and the mean surface exposed area is  $12\text{ cm}^2$ . **b** Support B: the mean thickness is 1 cm, the mean diameter is 0.5 cm and the mean surface exposed area is  $2.1\text{ cm}^2$



diameter of 0.22  $\mu\text{m}$ , and stored at 4 °C until use. Supports were recovered and subjected to biofilm detachment procedure previously described.

### Biofilm formation of staphylococci

Quantification of in vitro biofilm production was based on the method described by Christensen with slight modifications (Papa et al. 2013a; Artini et al. 2013). Briefly, the wells of a sterile 48-well flat-bottomed polystyrene plate were filled with 400  $\mu\text{L}$  of BHI medium. 1/100 Dilution of overnight bacterial cultures was added into each well (about 5.0 OD 600 nm). The first row contained the untreated bacteria, while each of the remaining rows contained serial dilutions of supernatant (SN) starting from 1:2. The plates were incubated aerobically for 24 h at 37 °C.

Biofilm formation was measured using crystal violet staining. After treatment, planktonic cells were gently removed; each well was washed three times with PBS and patted dry with a piece of paper towel in an inverted position. To quantify biofilm formation, each well was stained with 0.1 % crystal violet and incubated for 15 min at room temperature, rinsed twice with double-distilled water, and thoroughly dried. The dye bound to adherent cells was solubilized with 20 % (v/v) glacial acetic acid and 80 % (v/v) ethanol. After 30 min of incubation at room temperature, OD 590 nm was measured to quantify the total biomass of biofilm formed in each well. Each data point is composed of three independent experiments each performed at least in 3-replicates.

### LPS extraction and characterization

*P. haloplanktis* TAC125 cells were grown in planktonic and in biofilm conditions at 15 and 4 °C, respectively. Then the cells were extracted by phenol/chloroform/light petroleum ether (PCP) method to isolate the lipopolysaccharide (LPS) fractions (Galanos et al. 1969) and visualized by electrophoresis. For the extraction of LPS from *P. haloplanktis* TAC125 grown in planktonic conditions, bacterial cells were treated as already reported (Corsaro et al. 2001). PAGE was performed using the system of Laemmli et al. (1970) with sodium deoxycholate (DOC) as detergent. The separating gel contained final concentrations of 16 % acrylamide, 0.1 % DOC, and 375 mM Tris/HCl pH 8.8; the stacking gel contained 4 % acrylamide, 0.1 % DOC, and 125 mM Tris/HCl pH 6.8. LOS samples were prepared at a concentration of 0.05 % in the sample buffer (2 % DOC and 60 mM Tris/HCl pH 6.8 25 % glycerol, 14.4 mM 2-mercaptoethanol, and 0.1 % bromophenol blue). All concentrations are expressed as mass/volume percentage. The electrode buffer was composed of SDS (1 g L<sup>-1</sup>), glycine (14.4 g L<sup>-1</sup>), and Tris (3.0 g L<sup>-1</sup>). Electrophoresis was

performed at constant amperage of 30 mA. Gels were fixed in an aqueous solution of 40 % ethanol and 5 % acetic acid. LOS bands were visualized by silver staining (Tsai and Frasch 1982).

Monosaccharides were analyzed as acetylated methyl glycosides. The LPS samples (1 mg) were treated with HCl/CH<sub>3</sub>OH (1.25 M, 1 mL) and the methanolysis was performed as reported (Carillo et al. 2015). After acetylation the samples were analyzed on an Agilent Technologies gas chromatograph 6850A equipped with a mass selective detector 5973 N and a Zebron ZB-5 capillary column (Phenomenex, 30 m  $\times$  0.25 mm i.d., flow rate 1 mL min<sup>-1</sup>, He as carrier gas), accordingly with the following temperature program: 140 °C for 3 min, 140 °C  $\rightarrow$  240 °C at 3 °C min<sup>-1</sup>.

## Results and discussion

### Polystyrene supports selection

As previously reported (Papa et al. 2013b; Parrilli et al. 2015), *P. haloplanktis* TAC125 can be efficiently grown in biofilm condition using sterile 24-well flat-bottomed polystyrene plates. Therefore, the first step to assess a proper strategy to scale up the biofilm growth condition was the identification of suitable polystyrene supports for biofilm formation. *P. haloplanktis* TAC125 biofilm formation mostly occurs at air–liquid interface (Medigue et al. 2005), therefore we selected supports able to float and characterized by a large surface area per volume unit to promote microorganism adhesion. Two types of polystyrene supports were tested (Fig. 1).

To assess the ability of *P. haloplanktis* TAC125 to form biofilm on selected polystyrene supports, Antarctic bacterium was grown in BHI medium using glass wide-neck flasks in the presence of the supports A or B, at 15 and 4 °C in static condition for 96 h. *P. haloplanktis* TAC125 resulted to be able to form biofilm on both types of polystyrene supports and a qualitative measurement of formed biofilm was performed as described in “Materials and methods”. The amount of biofilm formed on 5 type A supports or on 30 type B supports resulted to be almost the same (data not shown). This result is not surprising as type A supports have a mean exposed surface area of 12 cm<sup>2</sup>, about six times higher than that of type B supports (mean exposed surface area 2.1 cm<sup>2</sup>).

Moreover, supernatants of *P. haloplanktis* TAC125 grown in the presence of tested supports were found to be able to inhibit *S. epidermidis* O-47 biofilm formation (data not shown).

In view of a possible characterization of cells in biofilm, supports were treated with ultrasounds for three different exposure times (5, 10 and 15 min) to allow biofilm

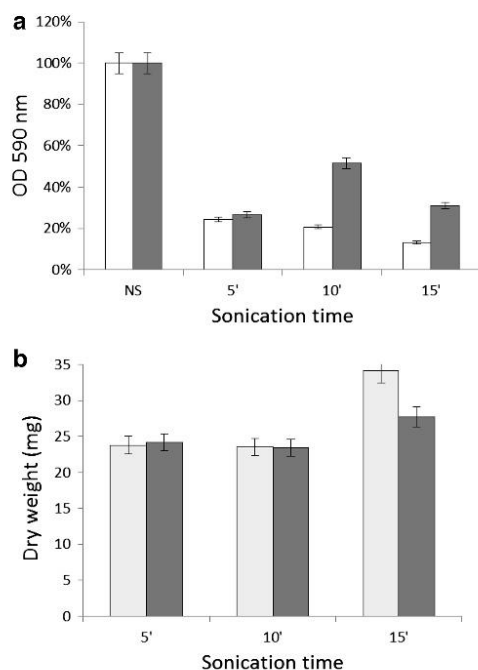


**Fig. 2** Evaluation of *P. haloplanktis* TAC125 biofilm removal from polystyrene supports by sonication. Data reported are referred to treatment of five supports A (white bar) and 30 supports B (gray bar). **a** Crystal violet staining: supports A and B stained before (NS) and after sonication for biofilm mass evaluation. **b** Dry weight of cell pellets recovered from supports A and B after sonication

detaching and biomass recovery. Sonication was performed using an ultrasound bath at a constant ultrasound frequency of 37 kHz. After treatments, a qualitative analysis of residual biofilm biomass was determined using crystal violet staining (Fig. 2a).

For a quantitative evaluation, the dry weight of cell pellets recovered after sonication of the supports was determined (Fig. 2b). As shown in Fig. 2, both supports were suitable for biofilm formation, but support A allowed a better biofilm detachment and cell recovery after sonication. Therefore, we selected the support A for the set-up of biofilm cultivation of Antarctic bacterium in automatic bioreactor.

#### Set up of *P. haloplanktis* TAC125 biofilm cultivation in automatic bioreactor

To develop a scalable process for *P. haloplanktis* TAC125 growth in biofilm, Antarctic bacterium was grown in

bioreactor in the presence of supports A, without stirring and keeping a low air inflow (see “Materials and methods”). The experimental conditions were chosen to obtain a sort of fluidized-bed reactor, in which the supports were homogeneously mixed and properly exposed to air–liquid interface, where *P. haloplanktis* TAC125 biofilm formation mostly occurs. Moreover, all parameter were selected to avoid the shearing detachment of biofilm. To attain these aims, several airflow conditions and ratios between medium volume and number of added supports were tested (data not shown). The best results were obtained using 33 supports A in 1 L of BHI medium using an airflow of 6 L h<sup>-1</sup> without stirring.

To evaluate the molecule/s anti-biofilm production in the selected conditions, Antarctic bacterium was grown in BHI in a 3L-stirred tank reactor (Applikon ADI 1030) at two different temperatures (4 and 15 °C) in the presence of supports A. Corresponding supernatants were recovered for each condition after 24, 48, 72 and 96 h at 4 °C and after 24, 48 and 72 h at 15 °C, respectively, and their effect on *S. epidermidis* strain O-47 biofilm was evaluated (Fig. 3). Anti-biofilm effect is reported as percentage of residual biofilm after treatment in comparison with biofilm formation by untreated bacteria. As shown in Fig. 3, the anti-biofilm compound was produced at both tested temperatures and in all tested conditions. In particular, at 15 °C the greatest production occurs at 72 h of cultivation, while at lower temperature (4 °C) 96 h of incubation are needed to achieve the best anti-biofilm compound production (Fig. 3). This result is in perfect agreement with previously reported production conditions (Parrilli et al. 2015) where sterile 24-well flat-bottomed polystyrene devices were used. Therefore the proposed *P. haloplanktis* TAC125 biofilm cultivation is suitable for a larger scale production of anti-biofilm molecule and it allows to obtain an amount of cell-free supernatant sufficient for the future purification.

#### Comparison between *P. haloplanktis* TAC125 lipopolysaccharide extracted from planktonic and biofilm associated cells

It is widely accepted that the choice of biofilm lifestyle imposes profound physiological, metabolic, and morphological changes to planktonic growing bacteria. It is very likely that also Antarctic marine bacteria do not escape this general rule. However, only very limited information, essentially coming from the study of *P. haloplanktis* TAC125, are available on cold-adapted bacteria grown in sessile conditions. Therefore, the second—but not less important—aim of this work was to demonstrate that the optimized fermentation process allowed the easy recovery of *P. haloplanktis* TAC125 biomass grown in biofilm, ready to be used in comparative structural analyses with respect to

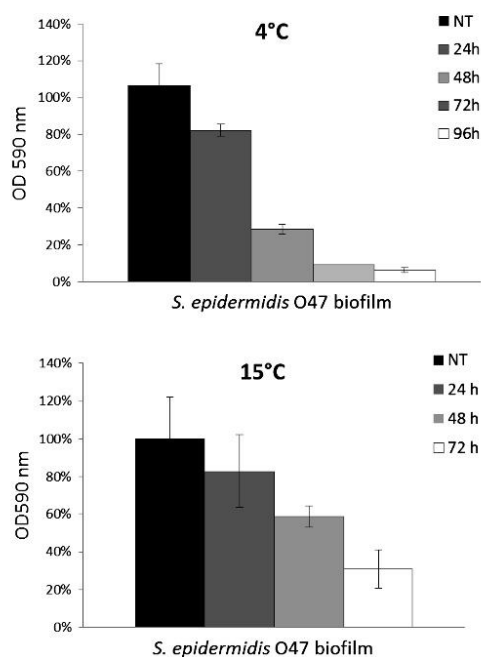


**Fig. 3** *S. epidermidis* biofilm formation in the presence of *P. haloplanktis* TAC125 cell-free supernatants. *P. haloplanktis* TAC125 was grown in an automatic bioreactors in the presence of supports A at 4 °C and at 15 °C. Corresponding supernatants recovered at different times were tested. Data are reported as percentage of residual biofilm after the treatment. Each data point represents the mean  $\pm$  SD of three independent experiments each performed at least in 3-replicates of three independent samples

cells grown in planktonic conditions. Amongst the cellular components that were structurally characterized in planktonic *P. haloplanktis* TAC125 cells, LPS was the object of the comparative analysis. LPS is the major constituent of all Gram-negative outer membranes, and although their structure varies in response to certain environmental stimuli (Raetz and Whitfield 2002), few studies have investigated changes in structure of LPSs extracted from cells grown in biofilms (Hansen et al. 2007; Ciornei et al. 2010; Chalabaev et al. 2014). In particular, reversible loss of lipopolysaccharide O-antigen and alteration of lipid A have been observed in some *Pseudomonas aeruginosa* strains when grown in biofilm (Ciomei et al. 2010). Recently, Chalabaev and coworkers demonstrated that *Escherichia coli* LPS displays some modifications, in particular occurring in the lipid A moiety, when the molecules extracted from the two growth conditions were compared (Chalabaev et al. 2014). Here, we compared *P. haloplanktis* TAC125 LPS obtained

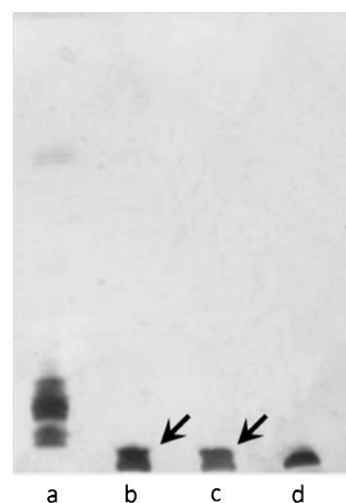


**Fig. 4** 16 % DOC-PAGE analysis of *Escherichia coli* O55:B5 LPS used as standard (a), *P. haloplanktis* TAC125, LPSb4 (b), LPSb15 (c), and *P. haloplanktis* TAC125 LSP15 (d). The arrows indicate the LPS bands extracted from cells grown in biofilm

during biofilm growth at 15 °C (LPSb15) and 4 °C (LPSb4) with previously characterized LPS extracted by planktonic bacteria grown at 15 °C (LSP15) (Corsaro et al. 2001). Dried cells embedded in the biofilm were extracted by PCP procedure to isolate the crude LPS. The purified samples were analyzed by DOC-PAGE electrophoresis and visualized with silver nitrate staining (Fig. 4).

Electrophoresis analysis revealed that all the samples contain bands at low molecular masses indicating the rough nature of LPS. This latter revealed that *P. haloplanktis* TAC125, grown in static condition, produced a lipopolysaccharide with the same nature of the LPS previously described for planktonic condition (Corsaro et al. 2001). Nevertheless, a difference was observed between the samples grown in sessile (Fig. 4, lanes b and c) and planktonic conditions (Fig. 4, lane d). Indeed, while the planktonic LPS showed only one band, two bands were clearly detectable for LPS molecules extracted from cells grown in biofilm. A glycosyl analysis was then performed on the three different LPS samples (LPSb15, LPSb4 and LSP15) to assess if this difference could be due to a modification in the sugar composition.

The analysis was carried out by GC-MS of the acetylated methyl glycosides and revealed for all the samples the presence of galactose (Gal), 2-amino-2-deoxymannose (ManN), 2-amino-2-deoxyglucose (GlcN) and heptose (Fig. S1-S3). Since all these monosaccharides were already



described to be the components of *P. haloplanktis* TAC125 LPS (Corsaro et al. 2001), it can be deduced that the glycosyl composition of LPSb15 and LPSb4 is the same of LPSp15 (Fig. S1–S3). Then, the detection of an additional band in LPS molecules extracted from cells grown in biofilm conditions suggests that the modification could be present in the lipid A moiety (Ciornei et al. 2010; Chalabaev et al. 2014). Further characterization of LPS from *P. haloplanktis* TAC125 biofilm cells by NMR and mass spectrometry will help in the identification of the punctual differences with respect to planktonic bacteria.

## Conclusions

Cold-adapted marine bacteria represent an untapped reservoir of biodiversity endowed with an interesting chemical repertoire. A preliminary characterization of molecules isolated from cold-adapted bacteria revealed that these compounds display antimicrobial, anti-fouling and various pharmaceutically relevant activities (Bowman et al. 2005). *P. haloplanktis* TAC125 is considered to be one of the model organisms of cold-adapted bacteria and it resulted to be a source of bioactive metabolites of biotechnological relevance, such as anti-biofilm molecules (Papa et al. 2013b, Parrilli et al. 2015). In particular *P. haloplanktis* TAC125 produces this activity only when it is grown in sessile condition (Papa et al. 2013b), confirming that the study of biofilm lifestyle allows to analyze a different associated chemical diversity. The proposed strategy for a biofilm cultivation of the Antarctic bacterium in automatic bioreactor makes also possible the isolation of bioactive compounds produced at very low amount. Beside this “drug discovery” aspect, this paper reports for the first time the possibility to recover Antarctic bacteria biomass grown in biofilm, paving the way to study the features of a cold-adapted biofilm.

**Acknowledgments** This work was supported by Programma Nazionale di Ricerca in Antartide 2013/B1.04 Tutino and Programma Operativo Nazionale Ricerca e Competitività 2007–2013 (D. D. Prot. n. 01/Ric. del 18.1.2010)-PON01\_01802.

## References

- Artini M, Papa R, Scoarughi GL, Galano E, Barbato G, Pucci P, Selan L (2013) Comparison of the action of different proteases on virulence properties related to the staphylococcal surface. *J Appl Microbiol* 114:266–277
- Bowman JP, McCammon SA, Dann AL (2005) Biogeographic and quantitative analyses of abundant uncultivated gamma-proteobacterial clades from marine sediment. *Microb Ecol* 49:451–460
- Carillo S, Casillo A, Pieretti G, Parrilli E, Sannino F, Bayer-Giraldi M, Cosconati S, Novellino E, Ewert M, Deming JW, Lanzetta R, Marino G, Parrilli M, Randazzo A, Tutino ML, Corsaro MM (2015) Unique capsular polysaccharide structure from the Psychrophilic Marine Bacterium *Colwellia psychrerythraea* 34H. *J Am Chem Soc* 137:179–189
- Chalabaev S, Chauhan A, Novikov A, Iyer P, Szczesny M, Beloin C, Caroff M, Ghigo JM (2014) Biofilms formed by gram-negative bacteria undergo increased lipid A palmitoylation, enhancing in vivo survival. *MBio* 19(5):e01116–e01214
- Cheng KC, Demirci A, Catchmark JM (2010) Advances in biofilm reactors for production of value-added products. *Appl Microbiol Biotechnol* 87:445–456
- Ciornei CD, Novikov A, Beloin C, Fitting C, Caroff M, Ghigo JM, Cavaillon JM, Adib-Conquy M (2010) Biofilm-forming *Pseudomonas aeruginosa* bacteria undergo lipopolysaccharide structural modifications and induce enhanced inflammatory cytokine response in human monocytes. *Innate Immun* 16:288–301
- Corsaro MM, Lanzetta R, Parrilli E, Parrilli M, Tutino ML (2001) Structural investigation on the lipooligosaccharide fraction of psychrophilic *Pseudoalteromonas haloplanktis* TAC 125 bacterium. *Eur J Biochem* 268:5092–5097
- de la Fuente-Núñez C, Reffuveille F, Fernández L, Hancock RE (2013) Bacterial biofilm development as a multicellular adaptation: antibiotic resistance and new therapeutic strategies. *Curr Opin Microbiol* 16:580–589
- Fondi M, Maida I, Perrin E, Mellera A, Mocali S, Parrilli E, Tutino ML, Liò P, Fani R (2015) Genome-scale metabolic reconstruction and constraint-based modelling of the Antarctic bacterium *Pseudoalteromonas haloplanktis* TAC125. *Environ Microb* 17:751–766
- Galanos C, Lüderitz O, Westphal O (1969) New method for the extraction of R Lipopolysaccharides. *Eur J Biochem* 9:245–249
- Giuliani M, Parrilli E, Ferrer P, Baumann K, Marino G, Tutino ML (2011) Process optimization for recombinant protein production in the psychrophilic bacterium *Pseudoalteromonas haloplanktis*. *Process Biochem* 46:953–959
- Hall-Stoodley L, Costerton JW, Stoodley P (2004) Bacterial biofilms: from the natural environment to infectious diseases. *Nat Rev Microbiol* 2:95–108
- Hansen SK, Rainey PB, Haagensen JA, Molin S (2007) Evolution of species interactions in a biofilm community. *Nature* 445:533–536
- Heilmann C, Gerke C, Perdreau-Remington F, Götz F (1996) Characterization of Tn917 insertion mutants of *Staphylococcus epidermidis* affected in biofilm formation. *Infect Immun* 64:277–282
- Kiran GS, Sabarathnam B, Selvin J (2010) Biofilm disruption potential of a glycolipid biosurfactant from marine *Brevibacterium casei*. *FEMS immunol med microbial* 59:432–438
- Laemmli UK (1970) Cleavage of structural proteins during the assembly of the head of bacteriophage T4. *Nature* 227:680–685
- Medigue C, Krin E, Pascal G et al (2005) Coping with cold: the genome of the versatile marine Antarctica bacterium *Pseudoalteromonas haloplanktis* TAC125. *Genome Res* 15:1325–1335
- Ni N, Li M, Wang J, Wang B (2009) Inhibitors and antagonists of bacterial quorum sensing. *Med Res Rev* 29:65–124
- Papa R, Glagla S, Danchin A, Schweder T, Marino G, Duilio A (2006) Proteomic identification of a two-component regulatory system in *Pseudoalteromonas haloplanktis* TAC125. *Extremophiles* 10:483–491
- Papa R, Artini M, Cellini A, Tilotta M, Galano E, Pucci P, Amoresano A, Selan L (2013a) A new anti-infective strategy to reduce the spreading of antibiotic resistance by the action on adhesion-mediated virulence factors in *Staphylococcus aureus*. *Microb Pathog* 63:44–53
- Papa R, Parrilli E, Sannino F, Barbato G, Tutino ML, Artini M, Selan L (2013b) Anti-biofilm activity of the Antarctic marine bacterium *Pseudoalteromonas haloplanktis* TAC125. *Res Microbiol* 164(5):450–456
- Papa R, Selan L, Parrilli E, Tilotta M, Sannino F, Feller G, Tutino ML, Artini M (2015) Anti-biofilm activities from marine cold

- adapted bacteria against staphylococci and *Pseudomonas aeruginosa*. Microbiol. Front. doi:10.3389/fmicb.2015.01333
- Parrilli E, Papa R, Carillo S, Tilotta M, Casillo A, Sannino F, Cellini A, Artini M, Selan L, Corsaro MM, Tutino ML (2015) Anti-biofilm activity of *Pseudoalteromonas haloplanktis* TAC125 against *Staphylococcus epidermidis* biofilm: evidence of a signal molecule involvement? Int J Immunopathol Pharmacol 28:104–113
- Percival SL, Suleman L, Vuotto C, Donelli G (2015) Healthcare-associated infections, medical devices and biofilms: risk, tolerance and control. J Med Microbiol 64:323–334
- Piette F, D'Amico S, Struvay C, Mazzucchelli G, Renaut J, Tutino ML, Danchin A, Leprince P, Feller G (2010) Proteomics of life at low temperatures: trigger factor is the primary chaperone in the Antarctic bacterium *Pseudoalteromonas haloplanktis* TAC125. Mol Microbiol 76:120–132
- Piette F, D'Amico S, Mazzucchelli G, Danchin A, Leprince P, Feller G (2011) Life in the cold: a proteomic study of cold-repressed proteins in the antarctic bacterium *Pseudoalteromonas haloplanktis* TAC125. Appl Environ Microbiol 77:3881–3883
- Pongtharangku T, Demirci A (2007) Online recovery of nisin during fermentation and its effect on nisin production in biofilm reactor. Appl Microbiol Biotechnol 74:555–662
- Qin Z, Yang L, Qu D, Molin S, Tolker-Nielsen T (2009) *Pseudomonas aeruginosa* extracellular products inhibit staphylococcal growth, and disrupt established biofilms produced by *Staphylococcus epidermidis*. Microbiology 155:2148–2156
- Raetz CR, Whitfield C (2002) Lipopolysaccharide endotoxins. Annu Rev Biochem 71:635–700
- Rosche B, Li XZ, Hauer B, Schmid A, Buehler K (2009) Microbial biofilms: a concept for industrial catalysis? Trends Biotechnol 27:636–643
- Szilágyi N, Kovács R, Kenyeres I, Csikó Z (2013) Biofilm development in fixed bed biofilm reactors: experiments and simple models for engineering design purposes. Water Sci Technol 68:1391–1399
- Tsai CM, Frasch CE (1982) Staining of lipopolysaccharide in SDS polyacrylamide gels using silver staining method. Anal Biochem 119:115–119
- Valle J, Da Re S, Henry N, Fontaine T, Balestrino D, Latour-Lambert P, Ghigo JM (2006) Broad-spectrum biofilm inhibition by a secreted bacterial polysaccharide. Proc Natl Acad Sci USA 103:12558–12563
- Wilmes B, Hartung A, Lalk M, Liebeke M, Schweder T, Neubauer P (2010) Fed-batch process for the psychrotolerant marine bacterium *Pseudoalteromonas haloplanktis*. Microb Cell Fact 9:72



# Anti-Biofilm Activities from Marine Cold Adapted Bacteria Against Staphylococci and *Pseudomonas aeruginosa*

Rosanna Papa<sup>1</sup>, Laura Selan<sup>1</sup>, Ermenegilda Parrilli<sup>2</sup>, Marco Tilotta<sup>1</sup>, Filomena Sannino<sup>2</sup>, Georges Feller<sup>3</sup>, Maria L. Tutino<sup>2</sup> and Marco Artini<sup>1\*</sup>

<sup>1</sup> Department of Public Health and Infectious Diseases, Sapienza University, Rome, Italy, <sup>2</sup> Department of Chemical Sciences, University of Naples Federico II, Naples, Italy, <sup>3</sup> Laboratory of Biochemistry, Centre for Protein Engineering, University of Liège, Liège, Belgium

## OPEN ACCESS

### Edited by:

Márcia Vanusa Da Silva,  
Universidade Federal  
de Pernambuco, Brazil

### Reviewed by:

Robert J. C. McLean,  
Texas State University, USA  
Joanna S. Brooke,  
DePaul University, USA

### \*Correspondence:

Marco Artini  
marco.artini@uniroma1.it

### Specialty section:

This article was submitted to  
Antimicrobials, Resistance  
and Chemotherapy,  
a section of the journal  
Frontiers in Microbiology

**Received:** 11 August 2015

**Accepted:** 13 November 2015

**Published:** 14 December 2015

### Citation:

Papa R, Selan L, Parrilli E, Tilotta M,  
Sannino F, Feller G, Tutino ML  
and Artini M (2015) Anti-Biofilm  
Activities from Marine Cold Adapted  
Bacteria Against Staphylococci  
and *Pseudomonas aeruginosa*.  
Front. Microbiol. 6:1333.  
doi: 10.3389/fmicb.2015.01333

Microbial biofilms have great negative impacts on the world's economy and pose serious problems to industry, public health and medicine. The interest in the development of new approaches for the prevention and treatment of bacterial adhesion and biofilm formation has increased. Since, bacterial pathogens living in biofilm induce persistent chronic infections due to the resistance to antibiotics and host immune system. A viable approach should target adhesive properties without affecting bacterial vitality in order to avoid the appearance of resistant mutants. Many bacteria secrete anti-biofilm molecules that function in regulating biofilm architecture or mediating the release of cells from it during the dispersal stage of biofilm life cycle. Cold-adapted marine bacteria represent an untapped reservoir of biodiversity able to synthesize a broad range of bioactive compounds, including anti-biofilm molecules. The anti-biofilm activity of cell-free supernatants derived from sessile and planktonic cultures of cold-adapted bacteria belonging to *Pseudoalteromonas*, *Psychrobacter*, and *Psychromonas* species were tested against *Staphylococcus aureus*, *Staphylococcus epidermidis*, and *Pseudomonas aeruginosa* strains. Reported results demonstrate that we have selected supernatants, from cold-adapted marine bacteria, containing non-biocidal agents able to destabilize biofilm matrix of all tested pathogens without killing cells. A preliminary physico-chemical characterization of supernatants was also performed, and these analyses highlighted the presence of molecules of different nature that act by inhibiting biofilm formation. Some of them are also able to impair the initial attachment of the bacterial cells to the surface, thus likely containing molecules acting as anti-biofilm surfactant molecules. The described ability of cold-adapted bacteria to produce effective anti-biofilm molecules paves the way to further characterization of the most promising molecules and to test their use in combination with conventional antibiotics.

**Keywords:** Polar bacteria, anti-virulence, anti-biofilm molecules, anti-adhesive, non-biocidal agents



## INTRODUCTION

The great ability of bacteria to colonize new environments can be linked, in most cases, to their capacity to develop a protective architecture called biofilm. The biofilm lifestyle is associated with a high tolerance to exogenous stress, and treatment of biofilms with antibiotics or other biocides is usually ineffective at eradicating them (Hall-Stoodley and Stoodley, 2009). Biofilm formation is therefore a major problem in many fields, ranging from the food industry to medicine (López et al., 2010; Høiby et al., 2011). It is worth mentioning that, in medical settings, biofilms are the cause of persistent infections implicated in 80% or more of all microbial cases-releasing harmful toxins and even obstructing indwelling catheters (Epstein et al., 2012).

*Staphylococci* are recognized as the most frequent causes of biofilm-associated infections (Otto, 2008). *Staphylococcus aureus* (*S. aureus*) is an opportunistic dangerous pathogen that can cause serious diseases in humans, ranging from skin and soft tissue infections to invasive infections of the bloodstream, heart, lungs and other organs. A statistical study showed that 30% of U.S. population was colonized by *S. aureus* (Nicholson et al., 2013). In addition, 1.5% of U.S. population was found to be a carrier of methicillin-resistant *S. aureus* (MRSA) that is a major cause of healthcare-related infections, responsible for significant proportion of nosocomial infections worldwide. Recently in the U.S., deaths from MRSA infections have surpassed those from many other infectious diseases, including HIV/AIDS (Nicholson et al., 2013).

*Staphylococcus epidermidis*, conventionally considered as a commensal bacterium of human skin, it can cause significant problems when breaching the epithelial barrier, especially during biofilm-associated infection of indwelling medical devices (Dohar et al., 2009; Rogers et al., 2009). Most diseases caused by *S. epidermidis* are of a chronic character and occur as device-related infections (such as intravascular catheter or prosthetic joint infections) and/or their complications (Rogers et al., 2009).

*Pseudomonas aeruginosa* (*P. aeruginosa*) is an important pathogen responsible for infections in patients who suffer from respiratory diseases (Saxena et al., 2014) like cystic fibrosis (CF). Recurrent and chronic respiratory tract infections in CF patients result in progressive lung damage and represent the primary cause of morbidity and mortality. *P. aeruginosa* can cause hard to treat life threatening infections due to its high resistance to antibiotics and to the ability to form antibiotic tolerant biofilms.

The development of anti-biofilm strategies is therefore of major interest and currently constitutes an important field of investigation in which non-biocidal molecules are highly valuable to avoid the rapid appearance of escape mutants.

From another point of view, the biofilm could be considered as a source of novel drugs and holds great potential due to the specific physical and chemical conditions of its ecosystem. For example, the production of extracellular molecules that degrade adhesive components in the biofilm matrix is a basic mechanism used in the biological competition between phylogenetically different bacteria (Brook, 1999; Wang et al., 2007, 2010). These compounds often exhibit broad-spectrum biofilm-inhibiting or

biofilm-detaching activity when tested *in vitro* and their use in a combination therapy with antibiotics could be of interest.

Marine bacteria are a resource of biologically active products (Debbab et al., 2010). Cold-adapted marine bacteria represent an untapped reservoir of biodiversity endowed with an interesting chemical repertoire. A preliminary characterization of molecules isolated from cold-adapted bacteria revealed that these compounds display antimicrobial, anti-fouling and various pharmaceutically relevant activities (Bowman, 2007). The ability of Polar marine bacteria, belonging to different genera/species, to synthesize bioactive molecules might represent the results of the selective pressure to which these bacteria are subjected. One of the developed survival strategies may be represented by the production of metabolites with anti-biofilm activity, which might be exploited to fight the biological competition of other bacteria.

Recently, we observed that Antarctic marine bacterium *Pseudoalteromonas haloplanktis* TAC125 produces and secretes several compounds of biotechnological interest (Papaleo et al., 2013), including molecules inhibiting the biofilm of the human pathogen *S. epidermidis* (Papa et al., 2013b; Parrilli et al., 2015). This activity impairs biofilm development and disaggregates the mature biofilm without affecting bacterial viability, showing that its action is specifically directed against biofilm (Papa et al., 2013b; Parrilli et al., 2015).

In this work we evaluated the anti-biofilm activity of supernatants derived from cultures of cold-adapted bacteria belonging to *Pseudoalteromonas*, *Psychrobacter*, and *Psychromonas* genera. Supernatants were obtained from bacterial cultures made both in sessile and planktonic conditions. The potential anti-biofilm activity was tested on bacterial cultures of *P. aeruginosa* PAO1, three different strains of *S. aureus* and three different strains belonging *S. epidermidis* species. The results obtained highlighted that several supernatants show anti-biofilm activity against most species analyzed. Preliminary evaluations on the physico-chemical nature of the molecules responsible for anti-biofilm activity emphasized their different nature.

## MATERIALS AND METHODS

### Bacterial Strains and Culture Conditions

Bacterial strains used in this work are listed in Table 1. Bacteria were grown in Brain Heart Infusion broth (BHI, Oxoid, UK). Biofilm formation was assessed in static conditions. Planktonic cultures were grown in flasks under vigorous agitation (180 rpm). Cold-adapted bacteria were grown at 15°C, while staphylococci and *P. aeruginosa* were grown at 37°C.

### Biofilm Formation of Polar Bacteria

Biofilm formation of cold-adapted bacteria was obtained at 15°C in BHI (Oxoid, UK). The wells of a sterile 24-well flat-bottomed polystyrene plate were filled with 1 ml of BHI, and an opportune dilution of bacterial culture in exponential growth phase (about 0.1 OD 600 nm) was added into each well. The plates were aerobically incubated up to 96 h at 15°C in static condition, measuring biofilm formation each 24 h. After the removal of spent medium and of not adhered cells and rinsing with PBS,

TABLE 1 | Strains used in this study.

Strain	Origin	Reference and/or source
<i>Pseudoalteromonas haloplanktis</i> TAA207	Antarctic sea water <sup>a</sup> (marine sediment)	Liège collection
<i>Pseudoalteromonas haloplanktis</i> TAE56	Antarctic sea water <sup>a</sup> (algae necrosed suspended in sea water)	Liège collection
<i>Pseudoalteromonas haloplanktis</i> TAE57	Antarctic sea water <sup>a</sup> (algae necrosed suspended in sea water)	Liège collection
<i>Pseudoalteromonas haloplanktis</i> TAE79	Antarctic sea water <sup>a</sup> (algae necrosed suspended in sea water)	Liège collection
<i>Pseudoalteromonas haloplanktis</i> TAE80	Antarctic sea water <sup>a</sup> (algae necrosed suspended in sea water)	Liège collection
<i>Psychrobacter</i> sp.TAD1	Antarctic sea water <sup>a</sup>	Liège collection
<i>Psychrobacter</i> sp.TAD18	Antarctic sea water <sup>a</sup> (frozen algae)	Liège collection
<i>Pseudoalteromonas haloplanktis</i> TAB87	Antarctic sea water <sup>a</sup>	Liège collection
<i>Psychrobacter arcticus</i> 273-4	Siberian permafrost sediment cores	Bakermans et al., 2006
<i>Psychromonas arctica</i>	Arctic seawater (Svalbard islands, Arctic)	Groudieva et al., 2003
<i>Staphylococcus aureus</i> 6538P	Clinical isolate	ATCC collection
<i>Staphylococcus aureus</i> 25923	Clinical isolate	ATCC collection
<i>Staphylococcus aureus</i> 20372	Clinical isolate from septic arthritis	ATCC collection
<i>Staphylococcus epidermidis</i> RP62A	Reference strain isolated from infected catheter	ATCC collection
<i>Staphylococcus epidermidis</i> O-47	Clinical isolate from septic arthritis	Heilmann et al., 1996
<i>Staphylococcus epidermidis</i> XX-17	Clinical isolate from infected catheter	Our collection
<i>Pseudomonas aeruginosa</i> PAO1	Clinical isolate from wound	ATCC collection

<sup>a</sup>Isolated from Antarctic coastal sea water sample collected in the vicinity of the French Antarctic station Dumont d'Urville, Terre Adélie (66°40' S; 140° 01' E).

adhered cells were stained with 0.1% crystal violet, rinsed twice with double-distilled water, and thoroughly dried as previously described (Papa et al., 2013a). The dye bound to adherent cells was solubilized with 20% (v/v) glacial acetic acid and 80% (v/v) ethanol. The absorbance of each well was measured at 590 nm. Each data point is composed of four independent experiments performed in triplicate.

### Preparation of Cell-free Supernatants from Cold-adapted Bacteria

The cell-free supernatants of a liquid culture of cold-adapted strains grown in sessile condition were designated as SNB, while the cell-free supernatants of a liquid culture of psychrophilic strains grown in planktonic condition were designated as SNP.

For the preparation of SNB, wells of a sterile 24-well flat-bottomed polystyrene plate were filled with 900  $\mu$ l of BHI and

100  $\mu$ l of each overnight bacterial culture was added into each well. The plates were incubated at 15°C monitoring biofilm formation each 24 h. After 96 h, supernatants were recovered and centrifuged at 13000 rpm at 4°C for 30 min. Supernatants were sterilized by filtration through membranes with a pore diameter of 0.22  $\mu$ m, and stored at 4°C until use.

For the preparation of SNP bacterial cultures were grown in planktonic conditions at 15°C under vigorous agitation (180 rpm) for 24 h. Supernatants were recovered by centrifugation at 13000 rpm at 4°C and processed as described above.

### Biofilm Formation of *Staphylococci* and *Pseudomonas*

Biofilm formation of *Staphylococcus* and *Pseudomonas* species was evaluated in the presence of SNB and SNP supernatants, respectively. Quantification of *in vitro* biofilm production was based on method previously reported (Artini et al., 2015). Briefly, the wells of a sterile 96-well flat-bottomed polystyrene plate were filled with 100  $\mu$ l of the appropriate medium. 1/100 dilution of overnight bacterial cultures was added into each well (about 5.0 OD 600 nm). Each well was filled with 50  $\mu$ l of BHI and 50  $\mu$ l of each supernatant, respectively. In this way each supernatant was used diluted 1:2 with a final concentration of 50%. As control, the first row contained bacteria grown only in 100  $\mu$ l of BHI (untreated bacteria). The plates were incubated aerobically for 24 h at 37°C.

Biofilm formation was measured using crystal violet staining. After treatment, planktonic cells were gently removed; each well was washed three times with PBS and patted dry with a piece of paper towel in an inverted position. To quantify biofilm formation, each well was stained with 0.1% crystal violet and incubated for 15 min at room temperature, rinsed twice with double-distilled water, and thoroughly dried. The dye bound to adherent cells was solubilized with 20% (v/v) glacial acetic acid and 80% (v/v) ethanol. After 30 min of incubation at room temperature, OD<sub>590</sub> was measured to quantify the total biomass of biofilm formed in each well. Each data point is composed of three independent experiments each performed at least in eight-replicates.

### Surface Coating Assay

A volume of 25  $\mu$ l of cell-free supernatant (SNB or SNP), or 25  $\mu$ l of saline as control, was deposited to the center of a well of a 24-well tissue-culture-treated polystyrene microtiter plate. The plate was incubated at 37°C for 1 h to allow complete evaporation of the liquid. The wells were then filled with 1 ml of broth containing 10<sup>4</sup>–10<sup>5</sup> CFU/ml of *S. epidermidis* O-47 and incubated at 37°C. After 18 h, wells were rinsed with water and stained with 1 ml of 0.1% crystal violet. Stained biofilms were rinsed with water and dried, and the wells were photographed.

### Physico-chemical Characterization of Anti-biofilm Compounds

The heat sensitivity of anti-biofilm compounds were evaluated by incubating the culture supernatants (SNB or SNP), for 1 h



in a water bath at 50°C and cooled on ice. For the protease treatment, proteinase K (Sigma Aldrich, St Louis, MO, USA) was added to aliquots of supernatants at a final concentration of 1 mg/ml and the reactions were incubated for 1 h at 37°C. As controls, supernatants were incubated for 1 h at 37°C without proteinase K, a treatment which did not impair the anti-biofilm activities. For each of the above tests, the anti-biofilm activities of treated and untreated culture supernatants were compared using the microtiter plate assay against staphylococci and *P. aeruginosa* PAO1, respectively. Each data point is composed of three independent experiments performed in six-replicates.

### Statistics and Reproducibility of Results

Data reported were statistically validated using Student's *t*-test comparing mean absorbance of treated and untreated samples. The significance of differences between mean absorbance values was calculated using a two-tailed Student's *t*-test. A *p*-value of <0.05 was considered significant.

## RESULTS

### Cold-adapted Bacteria Biofilm Formation

Biofilm formation of Polar bacteria was evaluated at 15°C in BHI at different times as described in material and methods section. Bacteria were grown in static condition in the same medium used for staphylococci and *P. aeruginosa* cultures to avoid interference in the following experiments due to the medium composition. The biofilm-forming ability of Polar bacterial strains was tested by a quantitative assay. The best production of biofilm was obtained by incubating the cells in static condition for 96 h at 15°C (data not shown). Almost all studied bacteria are able to form biofilm with different capabilities (Table 2). For example, in the tested condition, *Pseudoalteromonas haloplanktis* TAE80 and *Psychrobacter arcticus* 273-4 seemed to be unable to produce biofilm, while *Psychromonas arctica* was found to be a strong biofilm producer, as already reported (Vishnivetskaya et al., 2000; Groudieva et al., 2003).

### Effect of Exoproducts Derived from Cold-adapted Cultures on Biofilm Formation of Different Pathogen

The anti-biofilm effects of cold-adapted bacterial culture supernatants grown at 15°C either in planktonic or sessile conditions were examined on different pathogens: *P. aeruginosa* PAO1, three strains belonging to *S. epidermidis* species, and three strains belonging to *S. aureus* species (Table 1).

The specific environmental conditions prevailing within biofilms induce profound genetic and metabolic rewiring of the biofilm-dwelling bacteria and can allow the production of metabolites different from those obtained in planktonic condition. Therefore, supernatants deriving from sessile growths were designated as B letter, while supernatants deriving from planktonic cultures under vigorous agitation were designated as P letter, respectively.

TABLE 2 | Biofilm formation of the investigated bacterial strains.

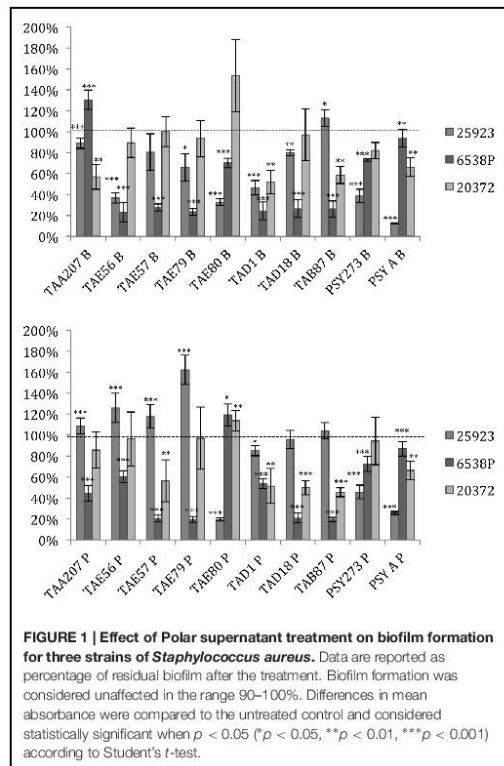
Strain	Biofilm (OD 590 nm)
TAA207	0.41 ± 0.09
<i>Pseudoalteromonas haloplanktis</i> TAE56	0.15 ± 0.06
<i>Pseudoalteromonas haloplanktis</i> TAE57	0.20 ± 0.10
<i>Pseudoalteromonas haloplanktis</i> TAE79	0.90 ± 0.20
<i>Pseudoalteromonas haloplanktis</i> TAE80	0.03 ± 0.02
<i>Psychrobacter</i> sp.TAD1	0.60 ± 0.20
<i>Psychrobacter</i> sp.TAD18	0.90 ± 0.20
<i>Pseudoalteromonas haloplanktis</i> TAB87	0.90 ± 0.20
<i>Psychrobacter arcticus</i> 273-4	0.09 ± 0.07
<i>Psychromonas arctica</i>	11.00 ± 1.00
<i>Staphylococcus aureus</i> 6538P	1.10 ± 0.10
<i>Staphylococcus aureus</i> 25923	1.90 ± 0.30
<i>Staphylococcus aureus</i> 20372	0.80 ± 0.20
<i>Staphylococcus epidermidis</i> RP62A	1.10 ± 0.10
<i>Staphylococcus epidermidis</i> O-47	2.10 ± 0.20
<i>Staphylococcus epidermidis</i> XX-17	0.69 ± 0.06
<i>Psychrobacter aeruginosa</i> PAO1	2.40 ± 0.50

Each data point is composed of four independent experiments performed in triplicate. Standard errors are reported.

In order to exclude that the tested Polar supernatants contain molecules affecting bacterial viability, the 20 cell-free supernatants were analyzed also for antimicrobial activity. An opportune dilution (10<sup>6</sup> cfu/ml) were used as reported by National Committee for Clinical Laboratory Standards (NCCLS, 2004) of each bacterial culture of *S. aureus* and *P. aeruginosa* in exponential phase was seeded on TSA plates. Each plate was spotted with Polar cell free supernatant separately and incubated at 37°C for 20 h. No antimicrobial activity on *S. aureus* and *P. aeruginosa* strains was highlighted for all tested supernatants (data not shown).

Anti-biofilm effect is reported as percentage of residual biofilm after treatment in comparison with untreated bacteria. In some cases an increase of biofilm formation was highlighted after the treatment.

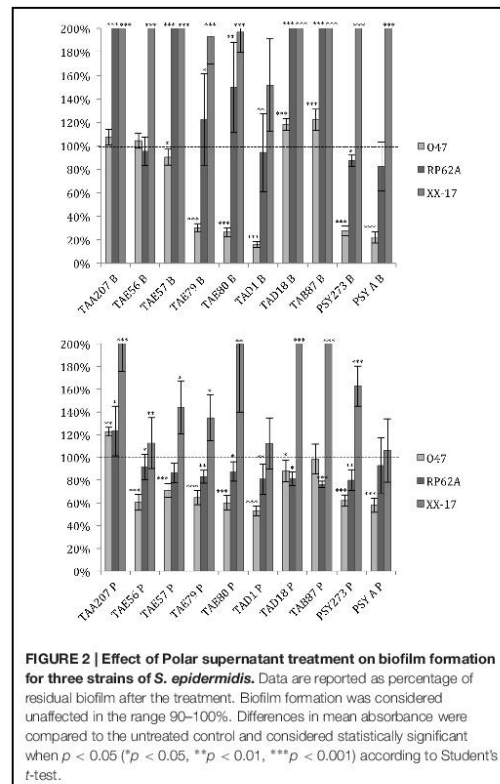
Several supernatants of Polar bacteria have anti-biofilm activity against all *S. aureus* tested strains (Figure 1, Supplementary Table S1). *S. aureus* 6538P showed a reduction in biofilm formation when treated with cold-adapted bacteria supernatants except in the case of TAA207 B and TAE80 P supernatants. TAE80 and PSYA supernatants deriving from both sessile and planktonic growth conditions showed a good anti-biofilm effect on *S. aureus* 25923, a reference strain for CF infections (Alhanout et al., 2011) (Figure 1). Three supernatants (TAD1 B, TAD18 P, TAB87 P) allowed a reduction of *S. aureus* 20372 biofilm higher than 50% (Figure 1). As shown in Figure 1, supernatants derived from sessile and planktonic cultures showed differences in their ability to prevent *S. aureus* biofilm formation and the effect of each supernatant is strictly strain-specific. Indeed, in such cases, the same supernatant is able to impair biofilm formation of one strain rather than others belonging to the same bacterial species; for example, TAD18 P is able to inhibit the biofilm formation of *S. aureus* 6538P and *S. aureus* 20372 but it is of not effective on *S. aureus*



25923. It is interesting to note that supernatants derived from sessile and planktonic cultures of the same Polar bacterium showed differences in their ability to prevent *S. aureus* biofilm formation, for example TAE80 B supernatant is able to impair biofilm of *S. aureus* 6538P while TAE80 P induces a significant increase in the biofilm formation. In addition TAE79 B, but not TAE79 P, produces an anti-biofilm molecule able to inhibit the biofilm formation of *S. aureus* 25923. On the contrary TAE79 P treatment increases the biofilm production of 25923 strain. It is worth mentioning that one supernatant, i.e., TAD1 B, is quite effective in interfering with biofilm formation of all tested *S. aureus* strains.

As far as *S. epidermidis* is concerned (Figure 2), in most cases the treatments induced an increase in biofilm formation, except for *S. epidermidis* O-47 strain treated with TAE79, TAE80, TAD1 P, PSY273 and PSYA supernatants derived from planktonic and sessile cultures where a strong reduction was evidenced (Figure 2).

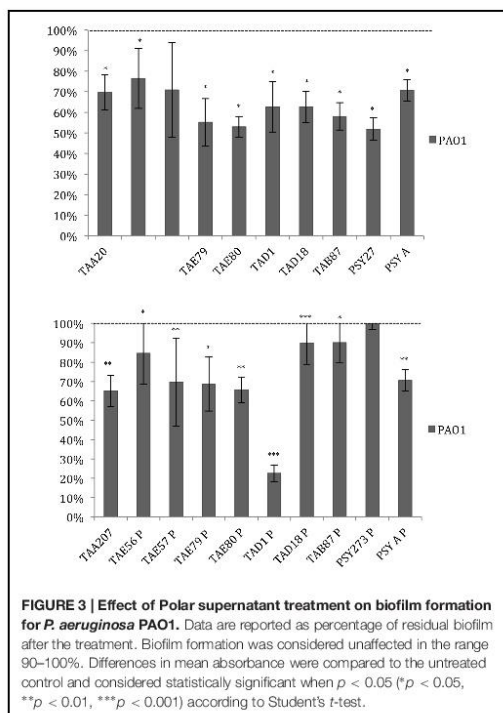
Also in the case of *S. epidermidis*, supernatants derived from sessile and planktonic cultures of the same Polar bacterium showed differences in their ability to prevent biofilm formation. Cell free supernatant of TAE56P is able to inhibit the biofilm of



*S. epidermidis* O-47 while TAE56B has no effect, indicating that the anti-biofilm molecule is produced only when the cells are grown in planktonic condition.

Data reported in Figure 3 demonstrated that the ability of *P. aeruginosa* PAO1 to form biofilm is affected by all cold-adapted supernatants deriving from sessile cultures with a rate of reduction between 30 and 50%. Only TAD1 P is able to reduce the *P. aeruginosa* PAO1 biofilm more than 70%. An additional control experiment was performed for *P. aeruginosa* in order to exclude a dilution effect on the bacterial growth after the supplementation with each supernatant due to diverse nutrient concentration between the untreated bacteria and the treated ones. In particular, as growth medium was also used BHI 2X concentrated. This experiment was performed in addition to the standard condition because we noted an inhibitory effect on biofilm formation when *P. aeruginosa* was treated with all supernatants. Data obtained with BHI twofold concentrated were nearly superimposable excluding an effect due to the diverse nutrient concentration between the treated and untreated bacteria (data not shown).





### Physico-chemical Characterization of Anti-biofilm Compounds from Polar Bacteria

To determine a preliminary chemical characterization of biofilm-inhibiting compounds, cell free supernatants of cold-adapted bacteria were dispensed in several aliquots, and submitted to chemical (proteinase K) and physical (thermal) treatments. Percentage of biofilm inhibition of each treated aliquot was determined on *S. epidermidis* O-47, *S. aureus* 6538P and *P. aeruginosa* PAO1 biofilms (Table 3). Data are reported as the percentage of anti-biofilm activity remaining after each treatment compared to the effect of the same untreated supernatant. As shown in Table 3, the proteinase K treatment reduced the anti-biofilm activity of tested supernatants on *S. epidermidis* O-47 and *S. aureus* 6538P biofilms, while this treatment did not interfere with their anti-biofilm ability on *P. aeruginosa* PAO1 except for TAD18 B, indeed the proteinase K treatment reduced its anti-biofilm activity at value less than 10%.

Furthermore, thermal treatment at 50°C significantly reduced the anti-biofilm effect of almost all supernatants on *S. aureus* but did not impair their activity on *P. aeruginosa* and *S. epidermidis*. This latter suggests that each supernatant contains different molecules with anti-biofilm activity that works selectively and independently on different bacterial species.

### Anti-biofilm Surfactant Activity of Polar Compounds

To assess the ability of cell free Polar bacteria supernatants to modify the surface properties of an abiotic substrate, a surface coating assay was performed. Evaporation coating was used to deposit each supernatant onto the surface of polystyrene wells, and then the ability of the coated surfaces to repel biofilm formation by *S. epidermidis* O-47 was tested. This latter pathogen was selected for this assay as it is the strongest biofilm producer amongst the bacteria used in this work and because it is able to preferentially form biofilm on the surface while *P. aeruginosa* typically forms biofilm at the liquid/air interface.

As clearly visible in Figure 4, TAE80 supernatants derived from both planktonic and sessile cultures and TAD1 supernatant derived from only sessile growth, were able to repel biofilm formation specifically only in the area where the supernatants were deposited, indicating that they contain molecules acting as anti-biofilm surfactants.

### DISCUSSION

In this paper the attention was focused on anti-biofilm molecules produced by cold-adapted marine bacteria since they represent an untapped reservoir of biodiversity and a potential source of molecules able to inhibit pathogens biofilm formation. The target pathogens chosen were *P. aeruginosa*, *S. aureus*, and *S. epidermidis*.

Biofilm is a key element in *S. epidermidis*, *S. aureus*, and *P. aeruginosa* infectious processes, but the matrix composition and molecules involved in attachment, development and detachment phases in these three bacterial species, are very different (Joo and Otto, 2012). Further, pathways and regulation of quorum sensing systems in these three strains are deeply different (Solano et al., 2014).

In staphylococci biofilm formation depends on a complex interplay of several elements such as adhesins, extracellular matrix binding proteins, biofilm associated proteins, proteins involved in PIA synthesis (*icaADBC*), autolysins (Alt), etc. *Staphylococcus* strains used in this work were chosen on the basis of different characteristics. In particular, *S. aureus* ATCC 6538P is a reference strain for antimicrobial testing; *S. aureus* ATCC 25923 and ATCC 20372 are clinical isolates. As for their ability to form biofilm, *S. aureus* strains were classified as reported: ATCC 25923 is a strong biofilm producer, ATCC 6538P is a medium/strong biofilm producer and ATCC 20372 is a medium/weak biofilm producer according to Cafiso et al. (2007).

Several cold adapted bacteria produce molecules able to interfere with *S. aureus* biofilm formation. These molecules display a different efficiency on different *S. aureus* tested strains and in all strains the anti-biofilm molecules seems to be proteinaceous. On the contrary only few Polar strains produce anti-biofilm molecules active on *S. epidermidis* O-47 and RP62A biofilms, and none are able to interfere with *S. epidermidis* XX-17 biofilm formation. It is important to underline that XX-17 strain produces a biofilm characterized by a polysaccharide *ica*-independent poorly characterized so far.

**TABLE 3 |** Effect of physico-chemical treatments on the anti-biofilm activity of cold-adapted bacteria supernatants on *S. epidermidis* O-47, *S. aureus* 6538P and *P. aeruginosa* PAO1, respectively.

	Proteinase K treatment			Heat treatment		
	<i>S. epidermidis</i>	<i>S. aureus</i>	<i>P. aeruginosa</i>	<i>S. epidermidis</i>	<i>S. aureus</i>	<i>P. aeruginosa</i>
TAA207 P	ND	<10%	100%	ND	<10%	100%
TAE56 P	<10%	<10%	ND	90% <sup>NS</sup>	<10%	ND
TAE57 P	<10%	<10%	80%**	100%	<10%	100%
TAE79 P	<10%	<10%	85%***	100%	<10%	100%
TAE80 P	<10%	ND	70%***	100%	ND	100%
TAD1 P	<10%	<10%	85%**	80%	<10%	100%
TAD18 P	ND	<10%	ND	ND	<10%	ND
TAB87 P	ND	<10%	ND	ND	<10%	ND
PSY273 P	<10%	<10%	ND	90% <sup>NS</sup>	<10%	ND
PSYA P	<10%	ND	100%	90% <sup>NS</sup>	ND	100%
TAA207 B	ND	ND	100%	ND	ND	90% <sup>NS</sup>
TAE56 B	ND	<10%	100%	ND	40%	100%
TAE57 B	ND	<10%	70%	ND	<10%	100%
TAE79 B	<10%	<10%	80%	80%*	<10%	100%
TAE80 B	<10%	<10%	100%	90% <sup>NS</sup>	<10%	100%
TAD1 B	<10%	<10%	100%	60%**	<10%	100%
TAD18 B	ND	<10%	<10%	ND	50%	100%
TAB87 B	ND	<10%	80% <sup>NS</sup>	ND	<10%	100%
PSY273 B	<10%	<10%	70%**	100%	<10%	100%
PSYA B	<10%	ND	100%	100%	ND	100%

With P letter was designated the cell-free supernatants of cold-adapted strains grown in planktonic condition; with B letter was designated the cell-free supernatants of cold-adapted strains grown in sessile condition. Data are reported as percentage of residual activity compared with each untreated supernatant. Differences in mean absorbance were compared to the untreated control and considered significant when  $p < 0.05$  (\* $p < 0.05$ , \*\* $p < 0.01$ , \*\*\* $p < 0.001$ ; NS, Not Significant) according to Student's t-test. ND, not determined.

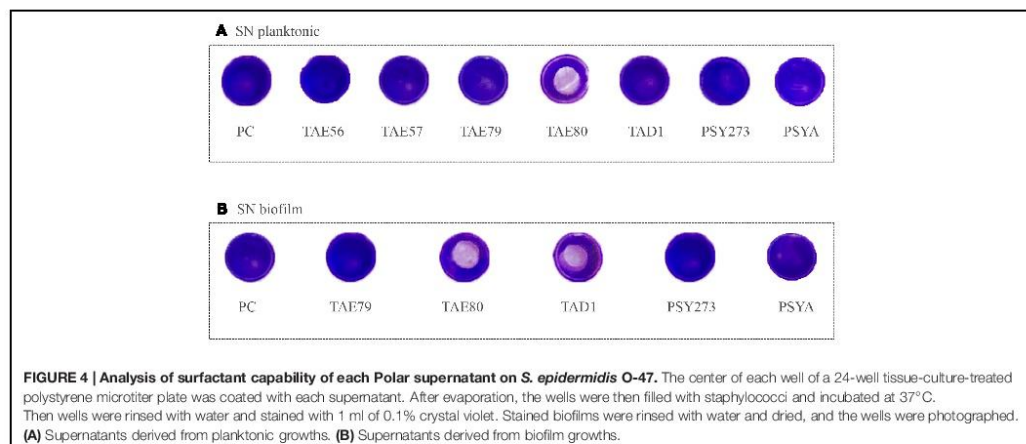


**FIGURE 4 |** Analysis of surfactant capability of each Polar supernatant on *S. epidermidis* O-47. The center of each well of a 24-well tissue-culture-treated polystyrene microtiter plate was coated with each supernatant. After evaporation, the wells were then filled with staphylococci and incubated at 37°C. Then wells were rinsed with water and stained with 1 ml of 0.1% crystal violet. Stained biofilms were rinsed with water and dried, and the wells were photographed. (A) Supernatants derived from planktonic growths. (B) Supernatants derived from biofilm growths.

*Staphylococcus epidermidis* RP62A is a reference strain isolated from infected catheter; *S. epidermidis* XX-17 and O-47 are clinical isolates. The clinical isolate O-47 is a naturally occurring non-functional *agr* mutant characterized by a frameshift mutation within *agrC* (Vuong et al., 2003) while the *S. epidermidis* XX-17 is an *ica* defective mutant (Artini et al., 2013). Determination

of *S. epidermidis* biofilm formation showed a strong production for the O-47 strain, medium/strong production for the reference strain RP62A and a medium/weak biofilm formation for the XX-17 strain defined according to the literature (Cafiso et al., 2004). Moreover, the six staphylococcal strains considered here were previously investigated to assess the presence of genes coding

for various proteins involved in adhesion and biofilm formation (Artini et al., 2013).

In *P. aeruginosa* the biofilm matrix is totally different, because the bacterium produces three exopolysaccharides, the glucose-rich Pel polysaccharide (Friedman and Kolter, 2004), the mannose-rich Psl polysaccharide (Friedman and Kolter, 2004), and alginate (Govan and Deretic, 1996). In particular, for *P. aeruginosa* we used the reference strain PAO1 since the biofilm characterization of this strain was previously reported (Yang et al., 2005).

The reported differences in biofilm features of the three pathogens could explain the different ability of cold adapted bacteria supernatants to impair their biofilm formation. It is interesting to note that, in all reported cases, the supernatants proved to be non-biocidal and specifically directed against biofilm.

All studied Polar strains are able to produce anti-biofilm molecules against *P. aeruginosa* biofilm. Furthermore in all cases the anti-biofilm molecules seems to have the same chemical-physical features (were not heat-labile and seem to have a non-protein nature), except in case of TAD18 B. These results could suggest that the molecule responsible for the anti-biofilm activity is the same for all cold-adapted strains. In particular, Polar anti-biofilm molecules involved in the inhibition of *P. aeruginosa* biofilm could be polysaccharides or a small molecule acting as quorum sensing inhibitors. Several studies have identified different bacterial polysaccharides and signaling molecules that inhibit biofilm formation by wide spectrum of bacteria including *P. aeruginosa* (Valle et al., 2006; Wittschier et al., 2007; Kim et al., 2009).

The increase of biofilm production following the treatment with such supernatants is an interesting result. This latter strengthens the hypothesis regarding the production of bacterial molecules able to regulate the biofilm formation inter- and intra- species in different environmental niches. The regulatory pathways of this phenotype could be linked to competition dynamics of extreme habitats (i.e., Polar niches). The identification of the molecules responsible for these mechanisms could be interesting and also open new perspectives for the control of bacterial biofilm formation. It is worth to note that “row” supernatants that we used represent a complex pool of chemical cues that could be characterized by different capabilities either responsible for impair biofilm formation and increase it.

Data reported in this paper demonstrate that anti-biofilm activity of cold-adapted bacteria supernatants deriving from planktonic and sessile cell cultures display several differences in terms of specificity and efficiency. Some biofilm-specific metabolites previously reported (Gjersing et al., 2007; Booth et al., 2011; Yeom et al., 2013) may exhibit an antagonist effect against competing microorganisms. Indeed, several studies showed that bacterial biofilm constitute untapped sources of natural bioactive molecules antagonizing adhesion or biofilm formation of other bacteria (Papa et al., 2013b; Rendueles et al., 2013). Furthermore, differences between activity of supernatants, derived from sessile and planktonic cultures, could be linked to a different concentration of active molecules produced in these two

growth conditions. This latter could be particularly relevant if the active molecules are involved in quorum sensing signaling.

Moreover, in this paper we report that several cold-adapted strains (TAD1, TAE79, TAE80, PSY273 and PSYA), belonging to different genera, are able to produce different anti-biofilm molecules active against *S. epidermidis*, *S. aureus* and *P. aeruginosa* biofilms.

The preliminary chemical characterization of the anti-biofilm molecules indicates that the same bacterium produces different molecules active against different targets. For example, TAD1 produces a thermo-stable protein active against *S. epidermidis* biofilm, a thermo-labile protein active against *S. aureus* biofilm, and a non-proteinaceous molecule able to impair *P. aeruginosa* biofilm. Furthermore the supernatants of TAD1 deriving from biofilm and planktonic growth showed also a different behavior in surface coating assay, suggesting the production of an anti-biofilm surfactant molecule only when TAD1 is grown in sessile form. Also for the supernatants deriving from TAE80 growths were evidenced the presence of different anti-biofilm molecules that are able to specifically act against the different bacterial species tested. In particular, we analyzed the dose dependent profile of TAE80 supernatants deriving from planktonic and biofilm growths tested against strongest biofilm producers belonging the three different species (Supplementary Figure S1). Both TAE80 supernatants (TAE80B and TAE80P) showed an anti-biofilm activity clearly dose-dependent against *S. aureus* 25923 and *S. epidermidis* O-47 while their activity against *P. aeruginosa* does not seem to be dose-dependent.

The ability of cold-adapted marine bacteria to produce several anti-biofilm molecules could suggest that the capacity to avoid the biofilm and colonization of competitor bacteria is a selective advantage in this extreme environment. Besides their ecological meaning, the anti-biofilm molecules from cold-adapted bacteria may have interesting biomedical applications combined with conventional antibiotics in order to eradicate biofilm infection.

## FUNDING

This work was supported by Programma Nazionale di Ricerche in Antartide 2013/B1.04 Tutino. This work was supported by Programma Operativo Nazionale Ricerca e Competitività 2007–2013 (D. D. Prot. n. 01/Ric. del 18.1.2010) – PON01\_01802.

## SUPPLEMENTARY MATERIAL

The Supplementary Material for this article can be found online at: <http://journal.frontiersin.org/article/10.3389/fmicb.2015.01333>

**FIGURE S1 | A dose-dependent effect on biofilm formation of *S. aureus* 25923 (A), *S. epidermidis* O-47 (B), *P. aeruginosa* PaO1 (C) in the presence of scalar concentration of TAE80 B and TAE80 P, respectively (starting from 50%).** Results are representative of three independent experiments. UN, untreated samples.



## REFERENCES

- Alhanout, K., Brunel, J. M., Dubus, J. C., Rolain, J. M., and Andrieu, V. (2011). Suitability of a new antimicrobial aminosterol formulation for aerosol delivery in cystic fibrosis. *J. Antimicrob. Chemother.* 66, 2797–2800. doi: 10.1093/jac/dkr380
- Artini, M., Cellini, A., Scoarughi, G. L., Papa, R., Tilotta, M., Palma, S., et al. (2015). Evaluation of contact lens multipurpose solutions on bacterial biofilm development. *Eye Contact Lens* 41, 177–182.
- Artini, M., Papa, R., Scoarughi, G. L., Galano, E., Barbato, G., Pucci, P., et al. (2013). Comparison of the action of different proteases on virulence properties related to the staphylococcal surface. *J. Appl. Microbiol.* 114, 266–277. doi: 10.1111/jam.12038
- Bakermans, C., Ayala-del-Río, H. L., Ponder, M. A., Vishnivetskaya, T., Gilichinsky, D. A., Thomashow, M. F., et al. (2006). *Psychrobacter cryohalolentis* sp. nov. and *Psychrobacter arcticus* sp. nov., isolated from Siberian permafrost. *Int. J. Syst. Evol. Microbiol.* 56, 1285–1291. doi: 10.1099/ijls.0.64043-0
- Booth, S. C., Workentine, M. L., Wen, J., Shaykhtudinov, R., Vogel, H. J., Ceri, H., et al. (2011). Differences in metabolism between the biofilm and planktonic response to metal stress. *J. Proteome Res.* 10, 3190–3199. doi: 10.1021/pr2002353
- Bowman, J. P. (2007). Bioactive compound synthetic capacity and ecological significance of marine bacterial genus *Pseudoalteromonas*. *Mar. Drugs* 5, 220–241. doi: 10.3390/md504220
- Brook, I. (1999). Bacterial interference. *Crit. Rev. Microbiol.* 25, 155–172. doi: 10.1080/10408419991299211
- Cafiso, V., Bertuccio, T., Santagati, M., Campanile, F., Amicosante, G., and Perilli, M. G. (2004). Presence of the *ica* operon in clinical isolates of *Staphylococcus epidermidis* and its role in biofilm production. *Clin. Microbiol. Infect.* 10, 1081–1088. doi: 10.1111/j.1469-0691.2004.01024.x
- Cafiso, V., Bertuccio, T., Santagati, M., Demelio, V., Spina, D., Nicoletti, G., et al. (2007). Agr-Genotyping and transcriptional analysis of biofilm-producing *Staphylococcus aureus*. *FEMS Immunol. Med. Microbiol.* 51, 220–227. doi: 10.1111/j.1574-695X.2007.00298.x
- Debbab, A., Aly, A. H., Lin, W. H., and Proksch, P. (2010). Bioactive compounds from marine bacteria and fungi. *Microb. Biotechnol.* 3, 544–563. doi: 10.1111/j.1751-7915.2010.00179.x
- Dohar, J. E., Hebda, P. A., Veeh, R., Awad, M., Costerton, J. W., Hayes, J., et al. (2009). Mucosal biofilm formation on middle-ear mucosa in a nonhuman primate model of chronic suppurative otitis media. *Laryngoscope* 115, 1469–1472. doi: 10.1097/01.mlg.0000172036.62897.d4
- Epstein, A. K., Wong, T. S., Belisle, R. A., Boggs, E. M., and Aizenberg, J. (2012). Liquid-infused structured surfaces with exceptional anti-biofouling performance. *Proc. Natl. Acad. Sci. USA* 109, 13182–13187. doi: 10.1073/pnas.1201973109
- Friedman, L., and Kolter, R. (2004). Two genetic loci produce distinct carbohydrate-rich structural components of the *Pseudomonas aeruginosa* biofilm matrix. *J. Bacteriol.* 186, 4457–4465. doi: 10.1128/JB.186.14.4457-4465.2004
- Gjersing, E. L., Herberg, J. L., Horn, J., Schaldach, C. M., and Maxwell, R. S. (2007). NMR metabolomics of planktonic and biofilm modes of growth in *Pseudomonas aeruginosa*. *Anal. Chem.* 79, 8037–8045. doi: 10.1021/ac070800t
- Govan, J. R., and Deretic, V. (1996). Microbial pathogenesis in cystic fibrosis: mucoid *Pseudomonas aeruginosa* and *Burkholderia cepacia*. *Microbiol. Rev.* 60, 539–574.
- Groudieva, T., Grote, R., and Antranikian, G. (2003). *Psychromonas arctica* sp. nov., a novel psychrotolerant, biofilm-forming bacterium isolated from Spitzbergen. *Int. J. Syst. Evol. Microbiol.* 53, 539–545. doi: 10.1099/ijls.0.02182-0
- Hall-Stoodley, L., and Stoodley, P. (2009). Evolving concepts in biofilm infections. *Cell. Microbiol.* 11, 1034–1043. doi: 10.1111/j.1462-5822.2009.01323.x
- Heilmann, C., Gerke, C., Perdreau-Remington, F., and Götz, F. (1996). Characterization of Tn917 insertion mutants of *Staphylococcus epidermidis* affected in biofilm formation. *Infect. Immun.* 64, 277–282.
- Høiby, N., Ciofu, O., Johansen, H. K., Song, Z. J., Moser, C., Jensen, P. O., et al. (2011). The clinical impact of bacterial biofilms. *Int. J. Oral. Sci.* 3, 55–65. doi: 10.4248/IJOS11026
- Joo, H. S., and Otto, M. (2012). Molecular basis of in vivo biofilm formation by bacterial pathogens. *Chem. Biol.* 19, 1503–1513. doi: 10.1016/j.chembiol.2012.10.022
- Kim, H. S., Kim, S. M., Lee, H. J., Park, S. J., and Lee, K. H. (2009). Expression of the *cpdA* gene, encoding a 3',5'-cyclic AMP (cAMP) phosphodiesterase, is positively regulated by the cAMP-cAMP receptor protein complex. *J. Bacteriol.* 191, 922–930. doi: 10.1128/JB.01350-08
- López, D., Vlamakis, H., and Kolter, R. (2010). Biofilms. *Cold Spring Harb. Perspect. Biol.* 2:a000398. doi: 10.1101/cshperspect.a000398
- Nicholson, T. L., Shore, S. M., Smith, T. C., and Frana, T. S. (2013). Livestock-associated methicillin-resistant *Staphylococcus aureus* (la-mrsa) isolates of swine origin form robust biofilms. *PLoS ONE* 8:e73376. doi: 10.1371/journal.pone.0073376
- Otto, M. (2008). Staphylococcal biofilms. *Curr. Top. Microb. Immunol.* 322, 207–228.
- Papa, R., Artini, M., Cellini, A., Tilotta, M., Galano, E., Pucci, P., et al. (2013a). A new anti-infective strategy to reduce the spreading of antibiotic resistance by the action on adhesion-mediated virulence factors in *Staphylococcus aureus*. *Microb. Pathog.* 63, 44–53. doi: 10.1016/j.micpath.2013.05.003
- Papa, R., Parrilli, E., Sannino, F., Barbato, G., Tutino, M. L., Artini, M., et al. (2013b). Anti-biofilm activity of the Antarctic marine bacterium *Pseudoalteromonas haloplanktis* TAC125. *Res. Microbiol.* 164, 450–456. doi: 10.1016/j.resmic.2013.01.010
- Papaleo, M. C., Romoli, R., Bartolucci, G., Maida, I., Perrin, E., Fondi, M., et al. (2013). Bioactive volatile organic compounds from Antarctic (sponges) bacteria. *Nat. Biotechnol.* 30, 824–838. doi: 10.1016/j.nbt.2013.03.011
- Parrilli, E., Papa, R., Carillo, S., Tilotta, M., Casillo, A., Sannino, F., et al. (2015). Anti-biofilm activity of *Pseudoalteromonas haloplanktis* TAC125 against *Staphylococcus epidermidis* biofilm: evidence of a signal molecule involvement? *Int. J. Immunopathol. Pharmacol.* 28, 104–113. doi: 10.1177/0394632015572751
- Renduelo, O., Kaplan, J. B., and Ghigo, J. M. (2013). Antibiofilm polysaccharides. *Environ. Microbiol.* 15, 334–346. doi: 10.1111/j.1462-2920.2012.02810.x
- Rogers, K. L., Fey, P. D., and Rupp, M. E. (2009). Coagulase-negative staphylococcal infections. *Infect. Dis. Clin. North. Am.* 23, 73–98. doi: 10.1016/j.idc.2008.10.001
- Saxena, S., Banerjee, G., Garg, R., and Singh, M. (2014). Comparative study of biofilm formation in *Pseudomonas aeruginosa* isolates from patients of lower respiratory tract infection. *J. Clin. Diagn. Res.* 8, DC09–DC11. doi: 10.7860/JCDR/2014/7808.4330
- Solano, C., Echeverez, M., and Lasa, I. (2014). Biofilm dispersion and quorum sensing. *Curr. Opin. Microbiol.* 18, 96–104. doi: 10.1016/j.mib.2014.02.008
- Valle, J., Da Re, S., Henry, N., Fontaine, T., Balestrino, D., Latour-Lambert, P., et al. (2006). Broad-spectrum biofilm inhibition by a secreted bacterial polysaccharide. *Proc. Natl. Acad. Sci. U.S.A.* 103, 12558–12563. doi: 10.1073/pnas.0605399103
- Vishnivetskaya, T., Kathariou, S., McGrath, J., Gilichinsky, D., and Tiedje, J. M. (2000). Low-temperature recovery strategies for the isolation of bacteria from ancient permafrost sediments. *Extremophiles* 4, 165–173. doi: 10.1007/s007920070031
- Vuong, C., Gerke, C., Somerville, G. A., Fischer, E. R., and Otto, M. (2003). Quorum-sensing control of biofilm factors in *Staphylococcus epidermidis*. *J. Infect. Dis.* 188, 706–718. doi: 10.1086/377239
- Wang, C., Fan, J., Niu, C., Wang, C., Villaruz, A. E., Otto, M., et al. (2010). Role of *spx* in biofilm formation of *Staphylococcus epidermidis*. *FEMS Immunol. Med. Microbiol.* 59, 152–160. doi: 10.1111/j.1574-695X.2010.00673.x
- Wang, C., Li, M., Dong, D., Wang, J., Ren, J., Otto, M., et al. (2007). Role of ClpP in biofilm formation and virulence of *Staphylococcus epidermidis*. *Microbes Infect.* 9, 1376–1383. doi: 10.1016/j.micinf.2007.06.012
- Wittschier, N., Lengsfeld, C., Vorthems, S., Stratmann, U., Ernst, J. F., Verspohl, E. J., et al. (2007). Large molecules as anti-adhesive compounds against pathogens. *J. Pharm. Pharmacol.* 59, 777–786. doi: 10.1211/jpp.59.6.0004
- Yang, W., Shi, L., Jia, W. X., Yin, X., Su, J. Y., Kou, Y., et al. (2005). Evaluation of the biofilm-forming ability and genetic typing for clinical isolates of *Pseudomonas aeruginosa* by enterobacterial repetitive intergenic consensus-based PCR. *Microbiol. Immunol.* 49, 1057–1061. doi: 10.1111/j.1348-0421.2005.tb03702.x



Yeom, J., Shin, J. H., Yang, J. Y., Kim, J., and Hwang, G. S. (2013). (1)H NMR-based metabolite profiling of planktonic and biofilm cells in *Acinetobacter baumannii* 1656-2. *PLoS ONE* 8:e57730. doi: 10.1371/journal.pone.0057730

**Conflict of Interest Statement:** The authors declare that the research was conducted in the absence of any commercial or financial relationships that could be construed as a potential conflict of interest.

Copyright © 2015 Papa, Selan, Parrilli, Tilotta, Sannino, Feller, Tutino and Artini. This is an open-access article distributed under the terms of the Creative Commons Attribution License (CC BY). The use, distribution or reproduction in other forums is permitted, provided the original author(s) or licensor are credited and that the original publication in this journal is cited, in accordance with accepted academic practice. No use, distribution or reproduction is permitted which does not comply with these terms.

## **CHAPTER III**

### **Cryoprotectants**

### Topic III: Study of “cryoprotectant” molecules for biotechnological application

The application of cryopreservation to living cells and tissues has revolutionized many Biotechnology areas, such as plant and animal breeding programs, and modern medicine.

Freeze-thaw cycles are quite common in the cold Polar Regions. Cold-adapted microorganisms are accustomed to being frozen within their habitats. Such organisms are also expected to have evolved adaptations to survive repeated freezing and thawing cycles, as these processes tend to damage living cells and attenuate cell viability. Cold-adapted bacterium *Colwellia psychrerythraea* strain 34H (*C. psychrerythraea* 34H), whose genome was sequenced [38], has attracted particular attention because it was reported to produce cryoprotectants [50] as a survival strategy [40]. In particular, *C. psychrerythraea* 34H cells are surrounded by a polysaccharidic capsule. Amongst all molecules to show cryoprotectant activity, the importance of sugars as CPA was clearly recognized by Maximov in the early 1900's [51].

In this part of my thesis the chemical analysis of purified capsular material from *C. psychrerythraea* 34H cells revealed the occurrence of a novel structure amongst bacterial polysaccharides: a linear tetrasaccharide repeating unit containing two amino sugars and two uronic acid, of which one is amidated by a threonine. The presence of amminoacid is quite uncommon in marine bacteria. The decoration of the polysaccharide with Thr is particularly intriguing, as glycosylated Thr residues are essential for the interaction of anti-freeze glycoproteins (AFGPs) with ice crystals [52]. In line with this indirect observation, in vitro assays demonstrated that the *C. psychrerythraea* 34H capsular polysaccharide is endowed with ice re-crystallization inhibition activity.

## A Unique Capsular Polysaccharide Structure from the Psychrophilic Marine Bacterium *Colwellia psychrerythraea* 34H That Mimics Antifreeze (Glyco)proteins

Sara Carillo,<sup>†,∇</sup> Angela Casillo,<sup>†,∇</sup> Giuseppina Pieretti,<sup>†</sup> Ermenegilda Parrilli,<sup>†</sup> Filomena Sannino,<sup>†,‡</sup> Maddalena Bayer-Giraldi,<sup>‡</sup> Sandro Cosconati,<sup>#</sup> Ettore Novellino,<sup>||</sup> Marcela Ewert,<sup>§</sup> Jody W. Deming,<sup>§</sup> Rosa Lanzetta,<sup>†</sup> Gennaro Marino,<sup>†</sup> Michelangelo Parrilli,<sup>†</sup> Antonio Randazzo,<sup>||</sup> Maria L. Tutino,<sup>\*,†</sup> and M. Michela Corsaro<sup>\*,†</sup>

<sup>†</sup>Department of Chemical Sciences, University of Naples Federico II, Complesso Universitario Monte S. Angelo, Via Cintia 4, 80126 Naples, Italy

<sup>‡</sup>Institute of Protein Biochemistry, CNR, Via Pietro Castellino 111, 80131 Naples, Italy

<sup>§</sup>School of Oceanography, University of Washington, Box 357940, Seattle, Washington 98195, United States

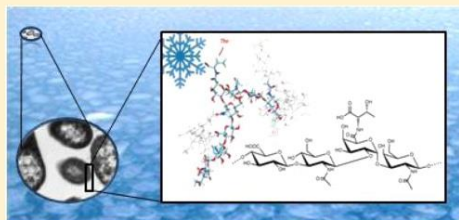
<sup>||</sup>Helmholtz-Zentrum für Polar- und Meeresforschung, Alfred-Wegener-Institut, Am Alten Hafen 26, 27568 Bremerhaven, Germany

<sup>||</sup>Department of Pharmacy, University of Naples Federico II, Via D. Montesano, 49, 80131 Naples, Italy

<sup>#</sup>DiSTABiF, Seconda Università di Napoli, Via Vivaldi 43, 81100 Caserta, Italy

### Supporting Information

**ABSTRACT:** The low temperatures of polar regions and high-altitude environments, especially icy habitats, present challenges for many microorganisms. Their ability to live under subfreezing conditions implies the production of compounds conferring cryotolerance. *Colwellia psychrerythraea* 34H, a  $\gamma$ -proteobacterium isolated from subzero Arctic marine sediments, provides a model for the study of life in cold environments. We report here the identification and detailed molecular primary and secondary structures of capsular polysaccharide from *C. psychrerythraea* 34H cells. The polymer was isolated in the water layer when cells were extracted by phenol/water and characterized by one- and two-dimensional NMR spectroscopy together with chemical analysis. Molecular mechanics and dynamics calculations were also performed. The polysaccharide consists of a tetrasaccharidic repeating unit containing two amino sugars and two uronic acids bearing threonine as substituent. The structural features of this unique polysaccharide resemble those present in antifreeze proteins and glycoproteins. These results suggest a possible correlation between the capsule structure and the ability of *C. psychrerythraea* to colonize subfreezing marine environments.



### INTRODUCTION

Cold-adapted bacteria are microorganisms able to thrive in habitats where the average temperatures are permanently or transiently below 15 °C, and often well below that value. They have successfully colonized all cold environments, including alpine and polar settings, the deep ocean, caves, terrestrial and ocean subsurface, and the upper atmosphere. Besides a general interest in understanding mechanisms underlying their ability to survive and grow at temperatures near or below the freezing point of water, in recent years cold-adapted microorganisms have received extra consideration due to the potential biotechnological applications of their enzymes.<sup>1–3</sup>

Because microorganisms are at thermal equilibrium with their environment, it is reasonable to assume that structural and functional components in psychrophiles (optimal growth at

≤15 °C) have adapted, to some degree, to the requirements of a low temperature existence,<sup>4</sup> including the possible presence of ice crystals in their immediate surroundings.

The reported mechanisms of bacterial adaptation to low temperature include the overexpression of cold-shock and heat-shock proteins, the presence of unsaturated and branched fatty acids that maintain membrane fluidity,<sup>5</sup> the different phosphorylation of membrane proteins and lipopolysaccharides,<sup>6–11</sup> and the production of cold-active enzymes,<sup>12</sup> antifreeze proteins (AFPs), and cryoprotectants.<sup>13</sup> The latter are chemical substances that generally include small molecules, such as glycine betaine, some amino acids, sugars (glucose, fructose),

Received: July 25, 2014

Published: December 19, 2014

and sugar alcohols (mannitol, glycerol). However, in the past decade, the high molecular mass extracellular exudates of psychrophiles have reached a prominent position among the cryoprotectants.<sup>14,15</sup> These exudates, which are a rich source of carbohydrate-containing compounds, influence the physico-chemical environment of bacterial cells and are believed to contribute to numerous processes involved in microbial cold-adaptation.

The potential roles of extracellular polysaccharide substances (EPS) in the cold-adapted bacterial lifestyle have been investigated from both environmental and organismal perspectives.<sup>16–18</sup> Initial chemical characterizations of EPS produced and secreted by cold-adapted bacteria in culture have revealed complex mixtures composed primarily of large sugar compounds, with lesser fractions of protein, lipid, and various small molecules. Nichols and coauthors demonstrated that exopolysaccharides produced by Antarctic bacteria were very diverse and that most of the EPS contained charged uronic acid residues; several also contained sulfate groups and some strains produced large polymers.<sup>19</sup> The presence of EPS can also alter interactions between the cell and the environment because EPS coatings determine the surface chemistry reactivity of cells by increasing the type and number of functional groups available for interaction, as demonstrated for the cold-adapted organism *Hymenobacter aerophilus*.<sup>20</sup>

Despite their important roles in cryoprotection and environmental interactions, few exopolysaccharide structures from cold-adapted bacteria have been accurately elucidated.<sup>7,19,21</sup> In addition, an increased understanding of the structural characteristics of these polymers is a prerequisite to potential biotechnological exploitation of cold-adapted bacterial EPS.

*Colwellia psychrerythraea* 34H is a Gram-negative bacterium belonging to the phylum  $\gamma$ -proteobacteria. Enriched from Arctic marine sediments at  $-1\text{ }^{\circ}\text{C}$ , it proved to be strictly psychrophilic.<sup>18</sup> *C. psychrerythraea* 34H produces extracellular polysaccharides<sup>12,22</sup> with cryoprotectant function and apparent ice-affinity,<sup>23,24</sup> yet its structural characteristics are not well known. In this study, we demonstrated that under the applied growth conditions *C. psychrerythraea* 34H cells are characterized by the presence of a capsule, which was purified as capsular polysaccharide (CPS) and subjected to complete structural determination. We further investigated the three-dimensional structure of the macromolecule by molecular mechanics and dynamics calculations. The results revealed an intriguing model, where the apparent “zigzag” structure exhibits on the edge putative ice-interaction sites.

## MATERIALS AND METHODS

**Cell Growth.** *C. psychrerythraea* 34H<sup>12,22</sup> was grown aerobically at  $4\text{ }^{\circ}\text{C}$  in Marine Broth medium (DIFCO 2216). When the liquid culture reached late exponential phase ( $\text{OD}_{600} = 2$ ), cells were harvested by centrifugation for 20 min at 5000 rpm and  $4\text{ }^{\circ}\text{C}$ . Cells used for transmission electron microscopy (TEM) were grown at  $4\text{ }^{\circ}\text{C}$  as colonies on a 15% agar-containing Marine Broth plate.

**Transmission Electron Microscopy.** TEM analysis was performed by the Interdepartmental Centre for Electron Microscopy Service, University of Naples Federico II. The samples were prepared for TEM observations as detailed in Basile et al.<sup>25</sup> Briefly, specimens were fixed with 3% glutaraldehyde, post-fixed with 1% osmium tetroxide, dehydrated with ethanol up to propylene oxide, and embedded in Spurr's epoxy medium. Ultrathin sections (60 nm thick) were collected on copper grids and stained with uranyl acetate and lead citrate. A FEI EM 208S transmission electron microscope, with an accelerating voltage of 80 kV, was used for observations.

**Capsular Polysaccharide Isolation and Purification.** Dried cells (4.8 g) were extracted first with phenol/chloroform/light petroleum (PCP) method to recover lipooligosaccharide (LOS) for core oligosaccharide structural characterization<sup>26</sup> and then by hot phenol/water method as reported previously.<sup>27,28</sup> A 300 mg amount of water extract was dialyzed and then digested with proteases, DNases, and RNases to remove contaminating proteins and nucleic acids. The water extract was hydrolyzed with 1% aqueous  $\text{CH}_3\text{COOH}$  (9 mL,  $100\text{ }^{\circ}\text{C}$ , 5 h). The resulting suspension was then centrifuged (10000g,  $4\text{ }^{\circ}\text{C}$ , 30 min). The pellet was washed twice with water, and the supernatant layers were combined and lyophilized (80 mg). The supernatant portion was then fractionated on a Biogel P-10 column (Biorad,  $1.5 \times 110\text{ cm}$ , flow rate 17 mL/h, fraction volume 2.5 mL), eluted with water buffered (pH 5.0) with 0.05 M pyridine, and 0.05 M acetic acid, obtaining two fractions. The first, eluted with the void volume, contained a polysaccharidic material (25 mg), while the second was constituted by oligosaccharides (48 mg). The polysaccharidic material was further purified on a Sephacryl S-400HR (Sigma,  $1 \times 110\text{ cm}$ , flow rate 15.6 mL/h, fraction volume 2.5 mL) eluted with 0.05 M ammonium hydrogen carbonate, providing a major fraction containing a fairly pure polysaccharide (CPS, 6 mg).

**DOC–PAGE Analysis.** PAGE was performed using the system of Laemmli<sup>29</sup> with sodium deoxycholate (DOC) as detergent. The separating gel contained final concentrations of 14% acrylamide, 0.1% DOC, and 375 mM Tris/HCl (pH 8.8); the stacking gel contained 4% acrylamide, 0.1% DOC, and 125 mM Tris/HCl (pH 6.8). CPS samples were prepared at a concentration of 0.05% in the sample buffer (2% DOC and 60 mM Tris/HCl [pH 6.8], 25% glycerol, 14.4 mM 2-mercaptoethanol, and 0.1% bromophenol blue). All concentrations are expressed as mass/vol percentage. The electrode buffer was composed of SDS (1 g/L), glycine (14.4 g/L), and Tris (3.0 g/L). Electrophoresis was performed at a constant amperage of 30 mA. Gels were fixed in an aqueous solution of 40% ethanol and 5% acetic acid. LOS and CPS bands were visualized by both silver staining and Alcian blue as described previously.<sup>30,31</sup>

**Static Light Scattering (SLS).** SLS measurements were performed as reported.<sup>32</sup> A homemade instrument composed by a Photocor compact goniometer, a SMD 6000 Laser Quantum 50 mW light source operating at 5325 Å, a photomultiplier (PMT-120-OP/B), and a correlator (Flex02-01D) from Correlator.com was used. All measurements were performed at  $(25.00 \pm 0.05)\text{ }^{\circ}\text{C}$  with temperature controlled through the use of a thermostat bath. The mass-average molecular weight,  $M_w$ , was obtained from the equation  $K_{1S}C_1/R_0 = 1/M_w + 2BC_1$  at two different concentrations of  $C_1$  (1 and 0.5 mg/mL), where  $C_1$  is the CPS mass concentration,  $B$  is the second virial concentration, and  $K_{1S} = 4\pi^2 n_0^2 (dn/dc_1)^2 / N_A \lambda^4$ , where  $n_0 = 1.33$  is the refractive index of water,  $dn/dc_1$  is the refractive index of CPS, and  $\lambda$  is the laser wavelength. The excess Rayleigh ratio was measured at two different angles ( $\theta = 90^\circ$  and  $40^\circ$ ). The values of  $R_0$  were calculated by using toluene as reference. From the extrapolation of the scattering intensity of the two solutions at 0 concentration and the 0 angle (Zimm plot), the molecular weight was evaluated.

**Sugar and Amino Acid Analysis.** Monosaccharides were analyzed as acetylated methyl glycosides. Methanolysis was performed in 1.25 M HCl/MeOH (0.5 mL,  $80\text{ }^{\circ}\text{C}$ , 20 h), and the sample was extracted twice with hexane. The organic layer containing the fatty acids methyl esters was directly analyzed, while the methanol layer was dried and acetylated with  $\text{Ac}_2\text{O}$  and pyridine (50  $\mu\text{L}$ ,  $100\text{ }^{\circ}\text{C}$ , 30 min). Methylation was performed with  $\text{CH}_3\text{I}$  in DMSO and NaOH (20 h).<sup>33,34</sup> The product was carboxymethyl reduced with NaBD<sub>4</sub>, hydrolyzed with 2 M TFA (120  $^{\circ}\text{C}$ , 2 h), reduced with NaBD<sub>4</sub>, and finally acetylated with  $\text{Ac}_2\text{O}$  and pyridine (50  $\mu\text{L}$  each,  $100\text{ }^{\circ}\text{C}$ , 30 min). The absolute configuration of the sugars was determined by gas-chromatography analysis of their acetylated (S)-2-octyl glycosides, while the absolute configuration of the amino acid residue was inferred by analyzing its butyl ester derivative.<sup>35</sup> All the samples were analyzed on an Agilent Technologies 6850A gas chromatograph equipped with a 5973N mass-selective detector and a Zebron ZB-5 capillary column (Phenomenex, 30 m  $\times$  0.25 mm i.d., flow rate 1 mL/min, He as carrier gas). Acetylated methyl glycosides were analyzed accordingly with the



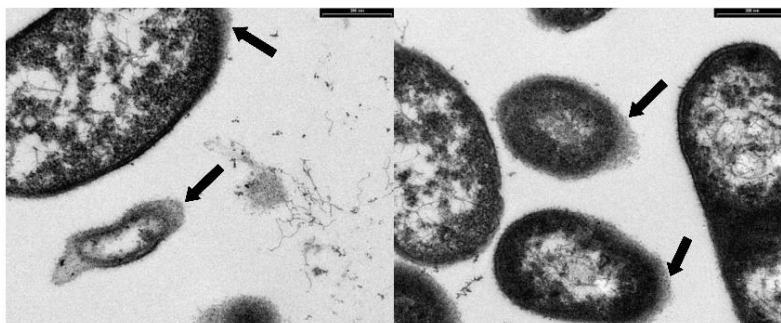


**Figure 1.** Transmission electron microscopy images of thin sections of *Colwellia psychrerythraea* 34H. The black arrows indicate the bacterial capsule.

following temperature program: 150 °C for 3 min, 150 °C → 240 °C at 3 °C/min. For partially methylated alditol acetates the temperature program was 90 °C for 1 min, 90 °C → 140 °C at 25 °C/min, 140 °C → 200 °C at 5 °C/min, 200 °C → 280 °C at 10 °C/min, and 280 °C for 10 min. Analysis of acetylated octyl glycosides was performed at 150 °C for 5 min, then 150 °C → 240 °C at 6 °C/min, and 240 °C for 5 min, while analysis of acetylated butyl ester of the amino acid was performed at 100 °C for 2 min, 100 °C → 180 °C at 3 °C/min, then 180 °C → 300 °C at 15 °C/min.

**NMR Spectroscopy.**  $^1\text{H}$  and  $^{13}\text{C}$  NMR spectra were recorded using a Bruker Avance 600 MHz spectrometer equipped with a cryoprobe. All two-dimensional homo- and heteronuclear experiments (double quantum-filtered correlation spectroscopy, DQF-COSY; total correlation spectroscopy TOCSY; rotating-frame nuclear Overhauser enhancement spectroscopy, ROESY; nuclear Overhauser effect spectroscopy, NOESY; distortionless enhancement by polarization transfer–heteronuclear single quantum coherence,  $^1\text{H}$ – $^{13}\text{C}$  DEPT-HSQC; heteronuclear multiple bond correlation,  $^1\text{H}$ – $^{13}\text{C}$  HMBC; and 2D F2-coupled HSQC) were performed using standard pulse sequences available in the Bruker software. The mixing time for TOCSY and ROESY experiments was 100 ms. NOESY experiments were performed at mixing times of 70, 100, 150, and 200 ms, in order to identify genuine NOEs effects. Chemical shifts were measured at 298 K in  $\text{D}_2\text{O}$ . TOCSY (mixing time 100 ms) and NOESY (mixing time 200 ms) experiments were also performed in  $\text{H}_2\text{O}/\text{D}_2\text{O}$  9:1.

**Structure Calculations.** A simplified model of the polysaccharide having about five repetitions of the tetra-saccharide A-B-C-D (**M1**, see Figure 5a) was constructed through the carbohydrate builder within the Glycam web server,<sup>36</sup> while the Thr residue attached to the  $\alpha$ -galactopyranuronic acid was constructed employing the builder module in the Maestro package of the Schroedinger Suite 2014. Restrained simulated annealing (SA) calculations were performed on **M1** using the AMBER 14.0 package<sup>37</sup> with sugars described by the latest GLYCAM06 force field (GLYCAM\_06j-1);<sup>38</sup> parameters for Thr residue were retrieved from the ff14sb force field within the AMBER 14.0 package as well as missing bond parameters. For annealing simulations, the General Born solvation (igb = 2) with monovalent salt concentration corresponding to 0.1 M was used. The complex was heated to 600 K in the first 5 ps, cooled to 100 K for the next 13 ps, and then cooled to 0 K for the last 2 ps. The temperature of the system was maintained with a varying time constant: 0.4 ps during heating, 4 ps during cooling to 100 K, 1 ps for the final cooling stage, and then reduced from 0.1–0.05 for the last picosecond. The force constants for NOE constraints were increased from 3 to 30 kcal  $\text{mol}^{-1} \text{\AA}^{-2}$  during the first 5 ps and then maintained constant for the rest of the simulation. These force constants were applied in the form of a parabolic, flat-well energy term, where  $r$  is the model distance or torsion angle and  $k$  is the respective force constant.

$$E_{\text{constraint}} = \begin{cases} k(r_2 - r)^2 & r_1 \leq r < r_2 \\ 0 & r_2 \leq r \leq r_3 \\ k(r_3 - r)^2 & r_3 \leq r < r_4 \end{cases}$$

The values for  $r_1$  and  $r_4$  represent upper and lower distance bounds, defining the energetic penalty before and after the flat-well energy term. The upper distance bounds were retrieved by NOE cross-peak volume integrations performed with the iNMR (www.inmr.net), using the NOESY experiment collected at mixing time of 100 ms. The NOE volumes were then converted to distance restraints after they were calibrated using the known fixed distance ( $\text{H6}_\text{D}/\text{H6}_\text{D}$ ) (Tables S1 and S2).

An unrestrained energy minimization step completed the SA run. This SA/energy minimization procedure was repeated 200 times. SA simulations were then analyzed by clustering the resulting **M1** conformations through the average linkage method and a cluster member cutoff of 1.25 Å root-mean-squared difference (rmsd) calculated on the sugars rings atoms within the central 2 repetitions of the tetramer A-B-C-D. This clustering allowed selecting 33 different conformational clusters for which the most populate one had a frequency of occurrence of 51/200 conformations. Moreover, conformations of this latter cluster feature the lowest overall potential energy and NMR restraint violations. Thus, the representative structure (i.e., the closest to the centroid of the cluster) of this cluster was considered for subsequent molecular dynamics (MD) simulations. After charge neutralization by the addition of 11  $\text{Na}^+$  ions, the complex was solvated with 10277 water molecules in a truncated octahedral box of pre-equilibrated TIP3P water.<sup>39</sup> Several equilibration steps were performed comprising minimization of the solvent molecules with the polysaccharide **M1** fixed, minimization of the whole system, and slow heating to 300 K with weak positional restraints on **M1** atoms under constant-volume conditions. The following 20 ns production runs were applied in the NPT ensemble. The particle mesh Ewald method<sup>40</sup> was used to evaluate the electrostatic interactions with a direct space sum cutoff of 10 Å. With the bond lengths involving hydrogen atoms kept fixed with the SHAKE algorithm, a time step of 2 fs was employed.<sup>41</sup> Related conformational substates populated during the MD simulation were analyzed with the AMBER's PTRAJ module.<sup>42</sup> For the production run trajectory, the first frame configuration was taken as a reference for subsequent mass-weighted rmsd calculations considering all atoms excluding hydrogens. Illustrations of the structures were generated using Chimera.<sup>43</sup>

**Ice Recrystallization Inhibition Assay.** Ice recrystallization was measured using an Optical Recrystallometer (Otogo Osmometers, New Zealand) as reported elsewhere.<sup>44,45</sup> The solutions were prepared in ultrapure Milli-Q water with 9‰ NaCl. We measured the CPS sample (10 mg/mL = 6.6  $\mu\text{M}$ ) and positive and negative controls. As a positive control we used a recombinant AFP from the sea-ice diatom *Fragilariopsis cylindrus*. The protein was provided by M. Bayer-Giraldi

and produced recombinantly in *E. coli* as described previously.<sup>44</sup> As a negative control we used chondroitin, a CPS produced by an engineered *E. coli* K4.<sup>46</sup> All particle solutions (CPS, AFP, and chondroitin) were measured at the same concentration of 6.6  $\mu$ M. Furthermore, we measured a particle-free solution of Milli-Q water with 9 % NaCl. We injected 200  $\mu$ L solution in a cold, thin glass sample tube and shock-froze the sample at  $-80^{\circ}\text{C}$ . Ice was annealed in the Optical Recrystallometer for 1.5 h at  $-4^{\circ}\text{C}$ . The device was cooled by a refrigerated circulating fluid and connected to a dry air (nitrogen gas) source to avoid condensation on the sample tube surface. The intensity of the light transmitted through the sample was recorded over time, where its increase is a measure for recrystallization. The increase was reported as  $I_t - I_0$ , where  $I_t$  is the intensity at a moment  $t$  and  $I_0$  is the initial intensity. The procedure was repeated three times for each sample.

## RESULTS

**Cell Growth and TEM.** The presence of capsular structures around cells of *C. psychrerythraea* 34H grown at  $4^{\circ}\text{C}$  was first highlighted by classic Indian ink staining<sup>47</sup> (data not shown) and then confirmed by TEM analysis. TEM images (Figure 1) revealed details of the cell envelope, including the presence of a capsular structure surrounding most of the observed cells.

**CPS Extraction, Purification, and Characterization.** The extraction protocol used on dried *C. psychrerythraea* 34H yielded 95 mg of LOS extract. The purified sample was visualized by 14% DOC-PAGE using either silver nitrate or Alcian blue staining methods (Figure 2). The silver nitrate



**Figure 2.** Analysis of the CPS fraction from *C. psychrerythraea* 34H by 14% DOC-PAGE. The gel was stained with silver nitrate (a) and Alcian blue dye (b).

showed the presence of only one band at low molecular masses, corresponding to LOS, which has been characterized elsewhere.<sup>26</sup> Instead, the Alcian blue staining method, which is sensitive to polyanionic substances, allowed us to visualize bands at higher molecular masses, too. Sugar and fatty acid analysis of the sample showed the presence mainly of galacturonic acid (GalA), glucuronic acid (GlcA), 2-amino-2-deoxy-glucose (GlcN), and 2-amino-2-deoxy-galactose (GalN), together with 3,6-dideoxyhexose, mannose, and 3-hydroxylated dodecanoic acid, which belong to the LOS, confirming its presence in the aqueous extract. The molecular masses of CPS and LOS species were expected to be very different on the basis of the DOC-PAGE analysis. Nevertheless, the well-known ability of the LOS to form micellar aggregates in aqueous

solution did not allow the separation of the two molecular species by size exclusion chromatography. As an alternative, the sample was hydrolyzed under mild acidic conditions to cleave the glycosidic linkage between the lipid A and the saccharidic region of the LOS. After centrifugation, the supernatant containing the CPS and the core oligosaccharidic portion of the LOS was separated from a precipitate constituted by the lipid A. The supernatant mixture was separated on a Biogel P-10 chromatography column, using pyridinium acetate buffer as eluent. Two fractions were obtained: the first one, eluted in the void volume, contained the higher molecular mass material; the second one (OS) contained species with lower molecular mass, corresponding to the core oligosaccharide of the LOS. A further purification of the higher molecular mass material on a Sephacryl S-400HR chromatography column, using ammonium hydrogen carbonate as eluent, resulted in obtaining a major fraction containing the CPS under study. The evaluation of the molecular mass of CPS was obtained through the SLS technique. The analysis indicated an average molecular weight of 1500 kDa and revealed the presence of a single distribution around 100 nm (Figure S1). The large size of the scattering object suggests that probably the CPS self-assemble in a single aggregate.

To determine monosaccharide composition a methanolysis reaction followed by an acetylation was performed on the CPS, and the obtained acetylated methyl glycosides were injected into the GC-MS. This analysis revealed the presence of GalA, GlcA, GlcN, and GalN, besides a signal attributed to a threonine residue on the basis of the comparison with an authentic standard. The absence of fatty acids in the GC-MS chromatogram indicated that the LOS was definitively removed. A D-configuration was identified for all the monosaccharides, whereas L-configuration was found for threonine. Finally, the methylation analysis revealed the presence of 4-substituted GlcA, 3-substituted GlcN, and 3-substituted GalN. No indications about the GalA substitution were found.

CPS polysaccharide was then analyzed by one- and two-dimensional NMR (DQF-COSY, TOCSY, ROESY, NOESY,  $^1\text{H}$ - $^{13}\text{C}$  DEPT-HSQC,  $^1\text{H}$ - $^{13}\text{C}$  HMBC, 2D F2-coupled HSQC). The 2D NMR analyses allowed the complete characterization of all of the spin systems. The anomeric configurations have been deduced from the  $^1J_{\text{C1,H1}}$  coupling constants and, *inter alia*, by  $^3J_{\text{H1,H2}}$  and chemical shifts values.

The  $^1\text{H}$ - $^{13}\text{C}$  DEPT-HSQC NMR spectrum (Figure 3, Table 1) displayed the presence of four anomeric cross-peaks at  $\delta$  5.31/98.3 (A), 4.50/104.7 (B), 4.35/104.5 (C), and 4.36/102.3 ppm (D). The correlations present in the COSY, TOCSY, and HMBC spectrum (Table 1, Figures S2–S4) indicated a *gluco*-configuration to residues B and C and a *galacto*-configuration to residues A and D. In particular, for residue B, starting from H1 signal in the COSY and TOCSY experiments, H2 up to H5 signals were rapidly identified, due to large  $^3J_{\text{H,H}}$  ring coupling constants. Then, the identification of H6 protons was obtained from HMBC spectrum, based on the correlations between C4 carbon atom at  $\delta$  69.8 ppm and the two H6 protons at  $\delta$  3.78/3.61 ppm. As for residue C, we observed a coincidence of the chemical shift value of its proton anomeric signal with that of D. Therefore, after identification of H2 of C at  $\delta$  3.23 ppm in the COSY spectrum, the glucuronic acid was recognized, due to the cross-peaks from this proton up to H5 in the TOCSY experiment. This last was in turn connected in the HMBC spectrum with a carboxyl signal at  $\delta$  175.4 ppm. The



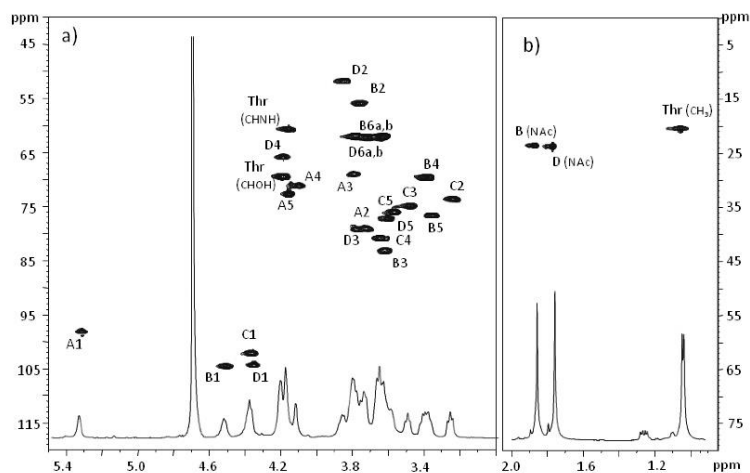


**Figure 3.** Carbinolic anomeric (a) and aliphatic (b) regions of  $^1\text{H}$ ,  $^{13}\text{C}$  DEPT-HSQC spectrum of CPS from *C. psychrerythraea* 34H. The spectrum was recorded in  $\text{D}_2\text{O}$  at 298 K at 600 MHz. The letters refer to residues as described in Table 1.

**Table 1.**  $^1\text{H}$  and  $^{13}\text{C}$  NMR Assignments of CPS<sup>a</sup>

residue	H1 C1	H2 C2	H3 C3	H4 C4	H5 C5	H6a,b C6
A, 2- $\alpha$ -D-GalpA6L/Thr	5.31 98.3	3.72 79.2	3.79 69.2	4.09 71.2	4.16 72.9	— 171.5
B, 3- $\beta$ -D-GlcpNAc	4.50 104.7	3.75 56.0	3.62 83.3	3.38 69.8	3.35 76.8	3.78–3.61 62.1
C, 4- $\beta$ -D-GlcpA	4.35 104.5	3.23 73.9	3.48 74.9	3.65 81.0	3.59 77.3	— 175.4
D, 3- $\beta$ -D-GalpNAc	4.36 102.3	3.84 52.0	3.76 79.3	4.19 66.1	3.56 76.1	3.71–3.64 62.3

<sup>a</sup>Spectra were recorded in  $\text{D}_2\text{O}$  at 298 K. Signals at  $\delta$  5.31/98.3 ppm, previously assigned respect to acetone as internal standard ( $\delta$  H 2.225 ppm and  $\delta$  C 31.45 ppm), were used as reference. Additional chemical shifts: NAc at  $\delta$  1.86/23.7 ppm ( $\text{CH}_3$ ), 176.4 ppm (CO), 1.77/23.8 ppm ( $\text{CH}_3$ ), 176.0 ppm (CO); Thr at  $\delta$  1.05/20.5 ppm ( $\text{CH}_3$ ), 4.18/69.8 ppm (CHOH), 4.15/60.8 ppm (CHNH), 177.2 ppm (COOH).

correlations in the TOCSY experiment of H2 of D with only H3 and H4 indicated an interruption of magnetization transfer between H4 and H5, due to the small  $^3J_{\text{H4,H5}}$  coupling constant value, according to a *galacto*-configuration. The H5 was therefore identified in the NOESY and ROESY spectra (Figures S5 and S6) by NOE contacts between H5 and H1/H3. The galacturonic acid residue A was recognized on the basis of the presence of cross-peaks from H1 up to H4 in the TOCSY spectrum. Then, in the same experiment, starting from H4 at  $\delta$  4.09 ppm the H5 resonance was easily identified at  $\delta$  4.16 ppm.

An additional spin system of a threonine residue was present. In fact, three resonances at 1.05/20.5, 4.18/69.8, and 4.15/60.8 ppm, attributed to  $\text{CH}_3$ , CHOH, and CHNH groups respectively were found. Finally, threonine carboxyl group ( $\delta$  177.2 ppm) was revealed by the long-range scalar coupling present in the HMBC experiment (Table 1, Figure S4). An integration of all anomeric signals in the  $^1\text{H}$  NMR spectrum showed a ratio of 1:1:2 (Figure S7), thus indicating a tetrasaccharide repeating unit. The stoichiometric substitution

of threonine was deduced from the integration of its methyl signal at  $\delta$  1.05 ppm with that of H2 of C at  $\delta$  3.23 ppm, as indicated from the ratio of 3:1 (Figure S7).

Residue A was assigned to a 2-substituted galactopyranuronic acid as its C2 resonance was shifted downfield ( $\delta$  79.2 ppm) with respect to that of an unsubstituted galacturonic acid unit,<sup>48</sup> and its  $\alpha$  configuration was deduced from the  $^1J_{\text{C1,H1}}$  coupling constant value (181 Hz). Moreover its H5 proton showed a long-range scalar connectivity with its C6 carbon atom at 171.5 ppm. This last value was shifted upfield with respect to the reference value,<sup>48</sup> thus indicating that the carboxyl group is involved in an amide linkage.<sup>49</sup> This fact indicated that threonine substitutes the position C6 of residue A, according to NOESY spectrum in  $\text{H}_2\text{O}/\text{D}_2\text{O}$  (see below). Residue C was assigned to a 4-substituted glucuronic acid, as its C4 resonance was shifted downfield ( $\delta$  81.0 ppm) with respect to the reference value,<sup>50</sup> and its  $\beta$  configuration was inferred from the  $^1J_{\text{C1,H1}}$  (169 Hz). In addition, both its H4 and H5 protons



showed a correlation in the HMBC spectrum with a carboxyl signal at  $\delta$  175.4 ppm (Figure S4).

Residues B and D were identified as a 3-substituted  $\beta$ -glucosamine and  $\beta$ -galactosamine, respectively, on the basis of  $^1J_{\text{C,H1}}$  values (169 Hz for both) and the correlations of their H2 protons at  $\delta$  3.75 and  $\delta$  3.84 ppm, with the nitrogen-bearing carbons at  $\delta$  56.0 and 52.0 ppm, respectively. Moreover, both residues showed downfield chemical shifts for their C3 carbons ( $\delta$  83.3 and 79.3 ppm, respectively). Both H2 protons were also shifted downfield indicating the presence of acyl substituents on the amino groups, which are acetyl groups. In fact, both methyl signals at  $\delta$  1.86 and 1.77 ppm displayed in the HMBC experiment long-range scalar couplings with signals at  $\delta$  56.0/176.4 and 52.0/176.0 ppm, respectively (Figure S4).

The sequence of residues and the confirmation of the attachment points of glycosidic linkages were obtained by an in depth analysis of the HMBC, NOESY, and ROESY spectra (Figures S4–S6). Long range scalar correlations were observed in the HMBC spectrum for C1 of D (C1D) and H4 of C (H4C), H1C and C3B, and H1B and C2A. The substitution of residue D by the residue A was deduced from the ROESY and NOESY experiments, as both spectra showed inter-residue dipolar couplings between H1A and H3D and H4D. Inter-residue dipolar couplings were also observed between H1D and H4C, H1C and H3B, and H1B and H2A.

Finally, the amide linkage between threonine and C6 of galacturonic acid was confirmed by a NOE contact between the amino acid NH ( $\delta$  7.60 ppm), identified in the TOCSY experiment (Figure S8), and H5 of residue A ( $\delta$  4.16 ppm), measured in a NOESY experiment in  $\text{H}_2\text{O}/\text{D}_2\text{O}$  (Figure S9).

All the above data allowed us to attribute a linear structure to the repeating unit of the CPS from *C. psychrerythraea* 34H, as illustrated in Figure 4.

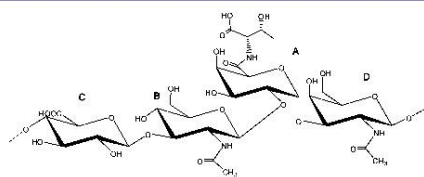


**Figure 4.** Primary repeating tetrasaccharide structure of the capsular polysaccharide isolated from *C. psychrerythraea* 34H.

**Three-Dimensional Structure Characterization.** In order to determine the three-dimensional structure of the CPS, an in-depth analysis of all NMR experiments was performed. The large proton–proton coupling constants observed in residues B and C suggested that all the protons are in axial positions. Then, the large coupling between H2 and H3 in residues A and D also suggested a trans-diaxial arrangement of these hydrogens. These data, along with NOE connectivities in the NOESY spectra between 1,3-diaxial protons, unambiguously indicated that all four sugar moieties assume the classical  $^4C_1$  chair conformation. Therefore, dihedral angle constraints were used to keep the sugar in this conformation during structure calculations. NOESY spectra also showed NOEs between H2A and H1B, and between H1A/H1B–H3B–H3D–H4D, H3B/H1C, H4B/H1C–H2C, and H5B/H1C, indicating the relative spatial orientation of the sugars. Interestingly, NOEs between H1B/H4D and H4B/H1D clearly

indicated that the sugar moieties B and D were spatially close to each other. In order to build a three-dimensional model taking into account all of the experimental data, restrained molecular mechanics and dynamics calculations were performed. Considering that the molecular weight of the polysaccharide is approximately 1500 kDa, and that performing reliable structure calculations at atomic level on a such high molecular mass structure is not possible (especially considering the lack of long-range distance restraints), we opted to create a simplified model (M1, Figure 5a), taking into account about five repetitions of the tetramer A-B-C-D. Using the approach described in Materials and Methods, a total of 200 structures were generated. The calculations provided a mixture of isoenergetic conformers characterized by no NOE violations  $>0.4$  Å (Table S3).

However, the central repeat, having a more realistic environment, could be clustered in a well-defined family having a good superimposition with rmsd values of 0.77 Å calculated on all heavy atoms of the sugar rings (Figure 6, Figure S10). Thus, the representative structure (i.e., the closest to the centroid of the cluster) of this cluster was subjected to MD simulations to probe its thermodynamic stability and to further refine this model in explicit solvent.

**Ice Recrystallization Inhibition Assay.** In order to determine if CPS actively interacts with ice, we tested its effect as ice recrystallization inhibitor. Ice grains recrystallize over time, as large crystals develop at the expense of smaller ones. Some molecules able to attach to ice, for example AFPs, inhibit recrystallization.<sup>44,51</sup> Due to light refraction at ice grain boundaries, light transmittance through ice is directly proportional to the size of crystals in the sample. Large ice crystals result in high light transmittance, while small crystals result in low transmittance. Therefore, the recrystallization of ice crystals can be followed recording the change of light intensity over the time. Chondroitin, an anionic polysaccharide constituted by alternating *N*-acetyl galactosamine and glucuronic acid residues, was used as negative control due to the similarity of its structure with that of CPS.

The ice recrystallization assay (Figure 7) showed that the presence of CPS inhibits recrystallization. Indeed, the light intensity change of the CPS-sample was smaller than the increase recorded for both negative controls. The chondroitin had no statistically relevant effect on ice recrystallization.

## DISCUSSION

Cold-adapted bacteria colonize a large portion of Earth's biosphere. They survive and thrive in alpine, polar, and other cold regions via numerous molecular adaptations.<sup>4</sup> Many of the adaptive mechanisms have been deduced from genomic and proteomic data, but extracellular strategies that may contribute to surviving in extreme environments are less well investigated by such approaches. The extracellular exudates, composed primarily of exopolysaccharides, that are produced by psychrophilic and ice-dwelling microorganisms have reached a prominent position among the cryoprotectants.<sup>14–18,21</sup> The term exopolysaccharide includes either cell-membrane associated or totally cell-free macromolecules. When the exopolysaccharide is firmly associated with the bacterial cell surface, the microorganism presents a capsule that can be recognized by either light or electron microscopy.<sup>52</sup> The aim of this study was to characterize the primary and the three-dimensional structures of the capsular material produced by the stenopsychrophilic bacterium *C. psychrerythraea* 34H. Further-

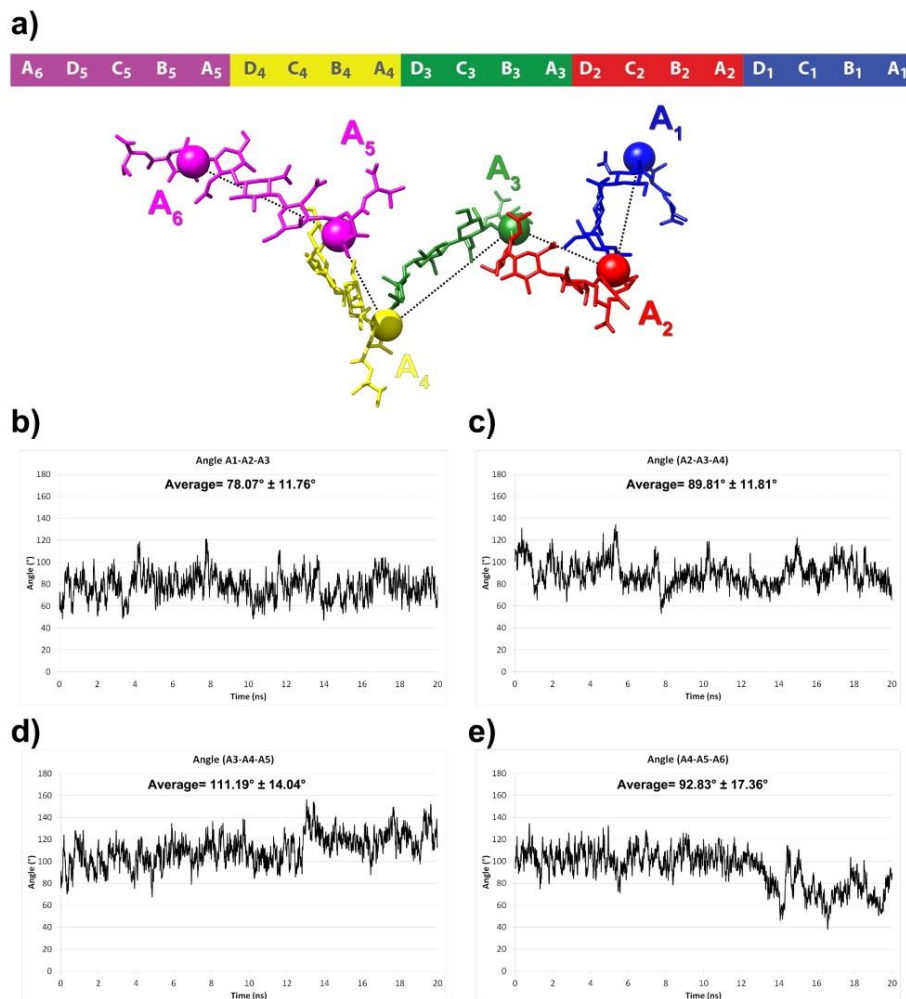


**Figure 5.** (a) Front view of the average M1 structure deriving from the 20 ns MD production run together with a pictorial representation of its sugar residue sequence. Repetitions 1, 2, 3, 4, and 5 are represented as blue, red, green, yellow, and magenta sticks, respectively. The C2 atoms of the A1–A6 sugar residues, used to calculate the hinge angles are represented as spheres. Plots of the hinge angle values (deg) formed by the C2 atoms of the A1–A2–A3, A2–A3–A4, A3–A4–A5, and A4–A5–A6 are represented in (b), (c), (d), and (e), respectively. The degree of flexibility for each hinge angle is calculated as the standard deviation from the values obtained from the last 20 ns of simulation.

more, we tested whether CPS interacts with ice by assessing its ice-recrystallization inhibition activity.

*C. psychrerythraea* 34H has been considered a model for the study of bacterial growth and survival strategies in cold marine environments.<sup>22</sup> The synthesis of extracellular polysaccharides appears to be important to cold-adaptation of this strain, especially in subfreezing environments.<sup>12,17,23,24</sup> Data reported here unravel the structure of a CPS surrounding individual cells of *C. psychrerythraea* 34H (Figure 1), which in turn defines the organism's interface with its environment.

The results of chemical and spectroscopic analyses of the purified capsular material revealed a structure new among bacterial polysaccharides: a linear tetrasaccharide repeating unit containing two amino sugars and two uronic acids, of which one is amidated by a threonine (Figure 4).

Even though the glycosyl composition may be comparable to that of EPS produced by many marine bacteria, the presence of amino acids is quite uncommon.<sup>50,53,54</sup> Sulfates or organic acids have generally been found as substituents on the sugar

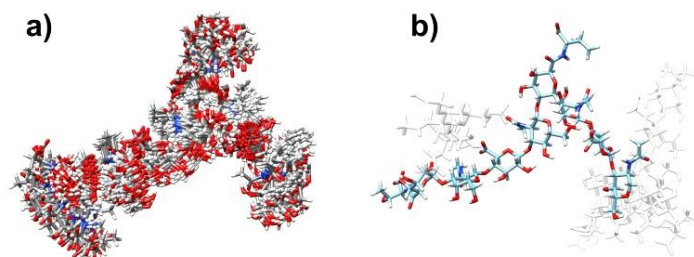


**Figure 6.** (a) Superimposition of the 51 conformations of M1 belonging to the most populated cluster as calculated through annealing simulations. For clarity reasons, only the central 2 repetitions of the tetramer A-B-C-D, on which the clustering was attained, are represented. (b) Representative M1 conformation of the most populated cluster. The central 2 repetitions of the tetramer A-B-C-D are represented as cyan sticks, while the remaining repetitions are displayed as transparent white sticks.

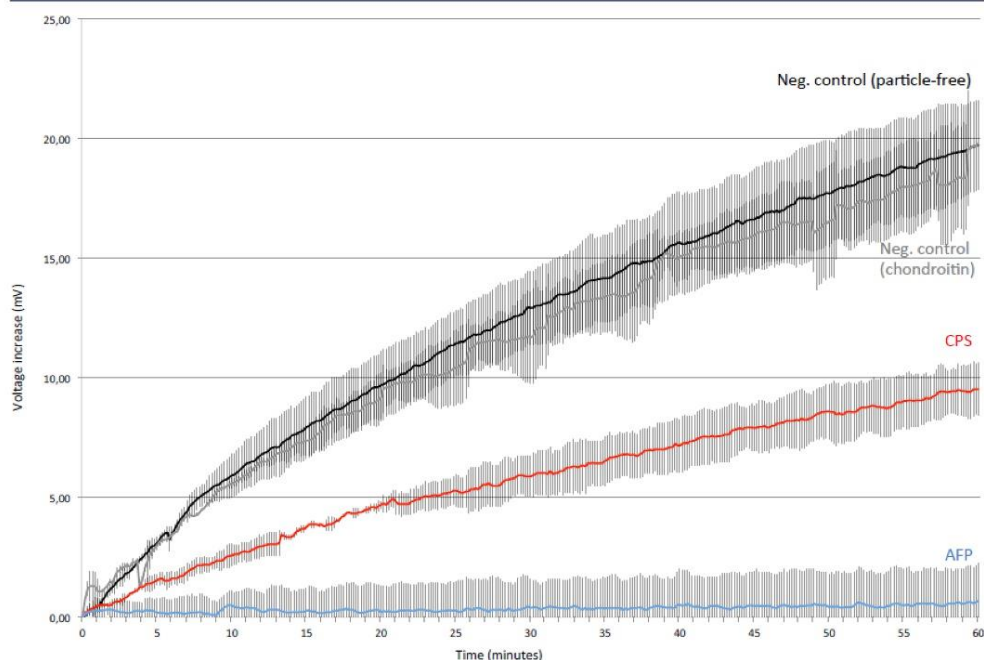


**Figure 7.** Recrystallization of frozen samples as assayed in the Optical Recrystallometer. The light intensity increase as a function of time is indicative of the recrystallization processes of ice crystals. Measurements were performed for 1 h at 4 °C. We measured a solution with CPS (red), a positive control with AFP from *F. cylindrus* (blue), a negative control with chondroitin (gray), and a particle-free positive control (black). The solutions were prepared in ultrapure Milli-Q water with 9‰ NaCl, particle concentration was adjusted to 6.6  $\mu\text{M}$ . The curves are an average of three samples; error bars show standard deviation.

backbone;<sup>55</sup> protein has been detected in some bacterial EPS but their relation with the sugar backbone is unknown.<sup>56,57</sup>

The decoration of the polysaccharide with Thr is particularly intriguing to consider. In fact, amino acid motifs are common, and crucial for the interaction with ice, in several different kinds of AFPs.<sup>55–57</sup> For example, antifreeze glycoproteins (AFGPs) isolated from fish blood plasma consist of a regular tripeptide sequence of Ala-Ala-Thr with a disaccharide fragment ( $\beta$ -D-

galactosyl-(1–3)- $\alpha$ -D-galactosamine) linked to the threonine residue.<sup>58–61</sup>

It is noteworthy that the polysaccharide described here displays a structural feature very close to that present in AFGPs. Actually, a  $\beta$ -N-acetyl-galactosamine is substituted by an  $\alpha$ -galacturonosyl residue bearing an amide-linked threonine.

AFP are known to control ice growth by attaching to ice crystals by their ice-binding-site. The spacing between relevant



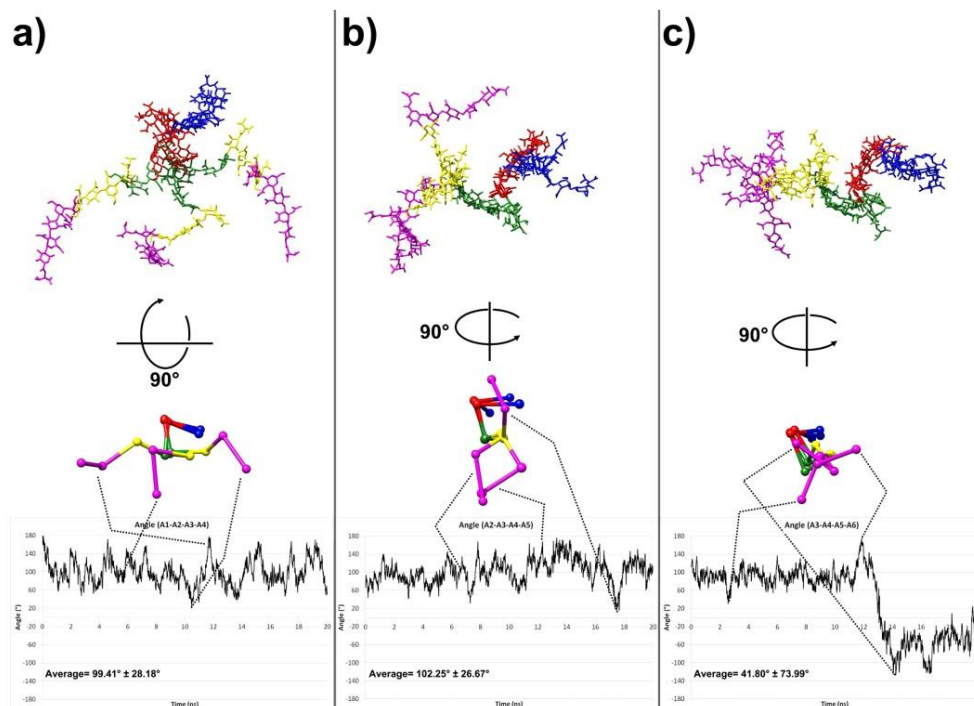


**Figure 8.** Three representative conformations of **M1** describing the pseudodihedral angles during the last 20 ns of the MD simulation formed by the C2 sugar atoms of the A residues, (a) A1-A2-A3-A4, (b) A2-A3-A4-A5, and (c) A3-A4-A5-A6. The top of the picture depicts the three superimposed conformations describing the lowest, average, and highest values of the three pseudodihedral angles. These are also depicted as pictorial representations (stick and balls) in the middle of the picture in a 90° rotated view to better show the changes in the dihedral angles. In the bottom of the picture the plots describing the three pseudodihedral angles during the 20 ns simulation are reported.

amino acids on the ice-binding sites often resembles the atomic distances typical for the ice lattice. Several times, the amino acids show a repetitive pattern or periodic folding, thus showing regularly spaced OH groups.<sup>62–65</sup> The periodic folding of this kind of structure is of particular interest, along with the composition of the polysaccharide, which is composed of repetitive tetrasaccharide units. In order to determine a possible spatial arrangement of the CPS, all the NMR experiments were analyzed and molecular mechanics and dynamics calculations were performed. We focused our attention on a simplified model (**M1**) of the capsule comprising basically five repeats of the tetrasaccharide base unit. A number of isoenergetic conformations were obtained; only information about the local conformation adopted by the polysaccharide could be retrieved. Interesting structural features characterized the obtained models. First of all, the chains of the sugars A-B-C-D were fairly linear. Furthermore, the orientation of sugars B and D, linked to equatorial position O2 and axial position O1 of sugar A, conferred a “hairpin-like” disposition to the chains. This portion of the polysaccharide seems to be repeated in the space forming an overall “zigzag” structure, where threonines of sugars A are placed at the very corner of the polysaccharide. The analysis of the 20 ns MD trajectories gave an idea of the

flexibility of the computed structure. In particular, plotting of the angle formed by the C2 atoms of each A sugar residues (Figure 5a) allowed monitoring the hinge motions experienced by **M1** during the dynamic calculations. The angles ranged roughly from 80° to 110°, and the angle formed by the residues A4-A5-A6 turned out to be the most flexible one ( $92.83^\circ \pm 17.36$ , Figure 5e). This result was expected considering that this angle is formed by the terminal repetitions of the molecule. Furthermore, the flexibility of the model was also monitored by plotting of three pseudodihedral angles formed by the C2 sugar atoms of the A residues: A1-A2-A3-A4, A2-A3-A4-A5, and A3-A4-A5-A6 (Figure 8). As depicted in Figure 8a,b, the A1-A2-A3-A4 and A2-A3-A4-A5 pseudodihedral angles range from a minimum of  $\approx 20^\circ$  to a maximum of  $\approx 180^\circ$ . Nevertheless, calculating the averages and the standard deviations for the aforementioned angles makes clear that the most frequent variation from the average is  $\pm 20^\circ$  (see the bottom plots of Figure 8a,b). On the other hand, plotting the A3-A4-A5-A6 pseudodihedral angle values demonstrated that after about 13 ns of dynamic the terminal repetition (formed by A6-D5-C5-B5-A5 residues) rotates from the remaining part of the polysaccharide of about  $320^\circ$ . In this case, calculation of the standard deviation (see the bottom plots of Figure 8c) suggests

that this terminal end of the polysaccharide is indeed very flexible. Altogether these data suggest that the computed model, although maintaining an overall "zigzag" arrangement, is very flexible and that the overall structure can be imagined like a spatial repetition of an hairpin-like substructure, where the threonines are placed externally and available to interact with the ice.

These results, the resemblance of our CPS structure to that of AFGPs, and the lack of sequence coding for a known AFP in the genome of *C. psychrerythraea* 34H<sup>65</sup> prompted us to assay for ice recrystallization inhibition activity of the *Colwellia* CPS-purified extract. Our analyses of ice recrystallization activity suggest that CPS interacts with ice in a way resembling AFPs, further supporting structural CPS observations. Results showed that CPS has an effect on recrystallization, whereas other particles like chondroitin in our negative particle control have no statistically relevant effect. It is therefore conceivable that CPS binds to ice, pinning and immobilizing ice grain boundaries with an effect similar to that reported for AFPs. The results showed an effect less marked with respect to that displayed by a recombinant AFP from the sea-ice diatom, which is a strong inhibitor of recrystallization compared to other AFPs.<sup>44</sup> However, the comparison between two very different molecules, such as a polysaccharide and a protein, may not be appropriate or rigorous. Besides ice-binding patterns, the size, composition, and conformation of the molecules also play roles in modulating the effect on ice. Furthermore, it should be considered that the natural concentrations of both CPS and AFP, and therefore the effective magnitude of ice activity under relevant environmental or physiological conditions remains unknown.

The only other example of a polysaccharide reported to have properties resembling AFP activity was extracted from a freeze-tolerant beetle, *Upis ceramoides*.<sup>66</sup> The fact that the polysaccharide examined also contained lipid leaves unresolved whether the polysaccharide or the lipid component was responsible for the activity.<sup>66</sup>

This study has demonstrated for the first time the existence of a capsular polysaccharide that in its purified form is endowed with ice recrystallization inhibition activity. Its unique structure, in contrast to that isolated from the beetle *U. ceramoides*, is strongly related to that of AFGPs, both for the presence of a Thr residue and for the Gal-Gal disaccharide motif.

## ■ ASSOCIATED CONTENT

### Supporting Information

NOE data; hydrodynamic radius distribution of the aggregates in a CPS solution; COSY, TOCSY, HMBC, NOESY, ROESY, and <sup>1</sup>H NMR spectra; and superimposition of the S1 conformations of M1 belonging to the most populated cluster as calculated through annealing simulations. This material is available free of charge via the Internet at <http://pubs.acs.org>.

## ■ AUTHOR INFORMATION

### Corresponding Authors

tutino@unina.it  
corsaro@unina.it

### Author Contributions

<sup>†</sup>S.C. and A.C. contributed equally.

### Notes

The authors declare no competing financial interest.

## ■ ACKNOWLEDGMENTS

Dedicated to the memory of Prof. Alessandro Ballio (1921–2014). We thank Prof. Luigi Paduano of Chemical Sciences Department, University of Naples Federico II, for molecular mass determination and Prof. Alba Silipo for the valuable discussion about NMR spectra. The authors thank the Centro Interdipartimentale Metodologie Chimico Fisiche, University of Naples Federico II, and BioTekNet for the use of the 600 MHz NMR spectrometer. This work was supported by Programma Nazionale di Ricerca in Antartide 2010 (grant PNRA 2010/A1.05) and 2013 (grant PNRA 2013/B1.03), and the Walters Endowed Professorship (to J.W.D.).

## ■ REFERENCES

- (1) Cavicchioli, R. *Nat. Rev. Microbiol.* **2006**, *4*, 331–43.
- (2) Cavicchioli, R.; Siddiqui, K. S.; Andrews, D.; Sowers, K. R. *Curr. Opin. Biotechnol.* **2002**, *13*, 253–261.
- (3) D'Amico, S.; Collins, T.; Marx, J. C.; Feller, G.; Gerday, C. *EMBO Rep.* **2006**, *7*, 385–389.
- (4) Casanueva, A.; Tuffin, M.; Cary, C.; Cowan, D. A. *Trends Microbiol.* **2010**, *18*, 374–381.
- (5) Chattopadhyay, M. K. J. *Biosci.* **2006**, *31*, 157–165.
- (6) Ummarino, S.; Corsaro, M. M.; Lanzetta, R.; Parrilli, M.; Peter-Katalinić, J. *Rapid Commun. Mass Spectrom.* **2003**, *17*, 2226–2232.
- (7) Corsaro, M. M.; Lanzetta, R.; Parrilli, E.; Parrilli, M.; Tutino, M. L.; Ummarino, S. *J. Bacteriol.* **2004**, *186*, 29–34.
- (8) Corsaro, M. M.; Pieretti, G.; Lindner, B.; Lanzetta, R.; Parrilli, E.; Tutino, M. L.; Parrilli, M. *Chemistry* **2008**, *14*, 9368–9376.
- (9) Carillo, S.; Pieretti, G.; Parrilli, E.; Tutino, M. L.; Gemma, S.; Molteni, M.; Lanzetta, R.; Parrilli, M.; Corsaro, M. M. *Chemistry* **2011**, *17*, 7053–7060.
- (10) Ray, M. K.; Kumar, G. S.; Shivaji, S. *Microbiology* **1994**, *140*, 3217–3223.
- (11) Ray, M. K.; Kumar, G. S.; Shivaji, S. *J. Bacteriol.* **1994**, *176*, 4243–4249.
- (12) Huston, A. L.; Methé, B. A.; Deming, J. W. *Appl. Environ. Microbiol.* **2004**, *70*, 3321–3328.
- (13) Deming, J. W. *Extremophiles: cold environments*. In *Encyclopedia of microbiology*, 3rd ed.; Lederberg, J., Schaechter, M., Eds.; Elsevier: Oxford, 2009.
- (14) Krembs, C.; Deming, J. W.; Junge, K.; Eicken, H. *Deep Sea Res. Part I, Oceanogr. Res. Pap.* **2002**, *49*, 2163–2181.
- (15) Krembs, C.; Deming, J. W. The role of exopolymers in microbial adaptation to sea ice. In *Psychrophiles: from biodiversity to biotechnology*; Margesin, R., Schinner, F., Marx, J.-C., Gerday, C., Eds.; Springer-Verlag: Berlin, 2008; pp 247–264.
- (16) Guézennec, J. J. *Ind. Microbiol. Biotech.* **2002**, *29*, 204–208.
- (17) Krembs, C.; Eicken, H.; Deming, J. W. *Proc. Natl. Acad. Sci. U.S.A.* **2011**, *108*, 3653–3658.
- (18) Ewert, M.; Deming, J. W. *Biology* **2013**, *2*, 603–628.
- (19) Nichols, C. M.; Lardière, S. G.; Bowman, J. P.; Nichols, P. D.; Gibson, J. A. E.; Guézennec, J. *Microb. Ecol.* **2005**, *49*, S78–S89.
- (20) Baker, M. G.; Lalonde, S. V.; Konhauser, K. O.; Foght, J. M. *Appl. Environ. Microbiol.* **2010**, *76*, 102–109.
- (21) Sheng-Bo, L.; Xiu-Lan, C.; Hai-Lun, H.; Xi-Ying, Z.; Bin-Bin, X.; Yong, Y.; Bo, C.; Bai-Cheng, Z.; Yu-Zhong, Z. *Appl. Environ. Microbiol.* **2013**, *79*, 224.
- (22) Methé, B. A.; Nelson, K. E.; Deming, J. W.; Momen, B.; Melamud, E.; Zhang, X.; Moul, J.; Madupu, R.; Nelson, W. C.; Dodson, R. J.; Brinkac, L. M.; Daugherty, S. C.; Durkin, A. S.; DeBoy, R. T.; Kolonay, J. F.; Sullivan, S. A.; Zhou, L.; Davidsen, T. M.; Wu, M.; Huston, A. L.; Lewis, M.; Weaver, B.; Weidman, J. F.; Khouiri, H.; Utterback, T. R.; Feldblyum, T. V.; Fraser, C. M. *Proc. Natl. Acad. Sci. U.S.A.* **2005**, *102*, 10913–10918.
- (23) Marx, J. G.; Carpenter, S. D.; Deming, J. W. *Can. J. Microbiol.* **2009**, *55*, 63–72.
- (24) Ewert, M.; Deming, J. W. *Ann. Glaciol.* **2011**, *52*, 111–117.



- (25) Basile, A.; Cañero, G.; Spagnuolo, V.; Castaldo Cobiánchi, R. *J. Biol.* **1994**, *18*, 69–81.
- (26) Carillo, S.; Pieretti, G.; Lindner, B.; Parrilli, E.; Sannino, F.; Tutino, M. L.; Lanzetta, R.; Parrilli, M.; Corsaro, M. M. *Eur. J. Org. Chem.* **2013**, 3771–3779.
- (27) Galanos, C.; Lüderitz, O.; Westphal, O. *Eur. J. Biochem.* **1969**, *9*, 245–249.
- (28) Westphal, O.; Jann, K. *Methods Carbohydr. Chem.* **1965**, *5*, 83–91.
- (29) Laemmli, U. K. *Nature* **1970**, *227*, 680–685.
- (30) Tsai, C. M.; Frasch, C. E. *Anal. Biochem.* **1982**, *119*, 115–119.
- (31) Al-Hakim, A.; Linhardt, R. J. *Electrophoresis* **1990**, *11*, 23–28.
- (32) Simeone, L.; Mangiapia, G.; Vitiello, G.; Irace, C.; Colonna, A.; Ortona, O.; Montesarchio, D.; Paduano, L. *Bioconjugate Chem.* **2012**, *23*, 758–770.
- (33) Ciucanu, I.; Kerek, F. *Carbohydr. Res.* **1984**, *131*, 209–217.
- (34) Forsberg, L. S.; Ramadas Bhat, U.; Carlson, R. W. *J. Biol. Chem.* **2000**, *275*, 18851–18863.
- (35) Leontin, K.; Lindberg, B.; Lönngren, J. *Carbohydr. Res.* **1978**, *62*, 359–362.
- (36) Woods Group GLYCAM Web; Complex Carbohydrate Research Center, University of Georgia, Athens, GA, 2005–2014; <http://www.glycam.com>.
- (37) Case, D. A.; Babin, V.; Berryman, J. T.; Betz, R. M.; Cai, Q.; Cerutti, D. S.; Cheatham, T. E. III; Darden, T. A.; Duke, R. E.; Gohlke, H.; Goetz, A. W.; Gusarov, S.; Homeyer, N.; Janowski, P.; Kaus, J.; Kolossváry, I.; Kovalenko, A.; Lee, T. S.; LeGrand, S.; Luchko, T.; Luo, R.; Madej, B.; Merz, K. M.; Paesani, F.; Roe, D. R.; Roitberg, A.; Sagui, C.; Salomon-Ferrer, R.; Seabra, G.; Simmerling, C. L.; Smith, W.; Swails, J.; Walker, R. C.; Wang, J.; Wolf, R. M.; Wu, X.; Kollman, P. A. *AMBER*, 14th ed.; University of California, San Francisco, 2014.
- (38) Kirschner, K. N.; Yongye, A. B.; Tschampel, S. M.; Daniels, C. R.; Foley, B. L.; Woods, R. J. *J. Comput. Chem.* **2008**, *29*, 622–655.
- (39) Jorgensen, W. L.; Chandrasekhar, J.; Madura, J. D.; Impey, R. W.; Klein, M. L. *J. Chem. Phys.* **1983**, *79*, 926–935.
- (40) (a) Darden, T.; York, D.; Pedersen, L. *J. Chem. Phys.* **1993**, *98*, 10089–10092. (b) Essmann, U.; Perera, L.; Berkowitz, M. L.; Darden, T.; Lee, H.; Pedersen, L. G. *J. Chem. Phys.* **1995**, *103*, 8577–8593.
- (41) van Gunsteren, W. F.; Berendsen, H. J. C. *Mol. Phys.* **1977**, *34*, 1311–1327.
- (42) Shao, J.; Tanner, S. W.; Thompson, N.; Cheatham, T. E., III. *J. Chem. Theory Comput.* **2007**, *3*, 2312–2334.
- (43) Pettersen, E. F.; Goddard, T. D.; Huang, C. C.; Couch, G. S.; Greenblatt, D. M.; Meng, E. C.; Ferrin, T. E. *J. Comput. Chem.* **2004**, *25*, 1605–1612.
- (44) Bayer-Giraldi, M.; Weikusat, I.; Besir, H.; Dieckmann, G. *Cryobiology* **2011**, *63*, 210–219.
- (45) Bayer-Giraldi, M.; Jin, E. S.; Wilson, P. W. Characterization of Ice Binding Proteins from Sea Ice Algae. In *Plant Cold Acclimation*; Hincha, D. K., Zuther, E., Eds.; Methods in Molecular Biology; Springer: New York, 2014; 1166.
- (46) Cimini, D.; De Rosa, M.; Carlino, E.; Ruggiero, A.; Schiraldi, C. *Microb. Cell. Fact.* **2013**, *12*, 46–57.
- (47) Taylor, W. H.; Juni, E. *J. Bacteriol.* **1960**, *81*, 688.
- (48) Ramos, M. L. D.; Caldeira, M. M. M.; Gil, V. M. S. *Carbohydr. Res.* **1996**, *286*, 1–15.
- (49) Sidorczyk, Z.; Swierko, A.; Knirel, Y. A.; Vinogradov, E. V.; Chernyak, A. Y.; Kononov, L. O.; Cedzynski, M.; Rozalski, A.; Kaca, W.; Shashkov, A. S.; Kochetkov, N. K. *Eur. J. Biochem.* **1995**, *230*, 713–721.
- (50) Bock, K.; Pedersen, C. *Adv. Carbohydr. Chem. Biochem.* **1983**, *41*, 27–66.
- (51) Knight, C. A.; Duman, J. A. *Cryobiology* **1986**, *23*, 256–262.
- (52) Sutherland, I. W. Biotechnology of microbial exopolysaccharides. In *Cambridge Studies in Biotechnology*; Baddiley, J., Carey, N. H., Higgins, I. J., Potter, W. G., Eds.; Cambridge University Press: Cambridge, 1990; pp 1–11.
- (53) Komandrova, N. A.; Isakov, V. V.; Tomshich, S. V.; Romanenko, L. A.; Perepelov, A. V.; Shashkov, A. S. *Biochemistry (Moscow)* **2010**, *75*, 623–628.
- (54) Palusiak, A. *Carbohydr. Res.* **2013**, *380*, 16–22.
- (55) Nichols, C. M.; Guézennec, J.; Bowman, J. P. *Mar. Biotechnol.* **2005**, *7*, 253–271.
- (56) Mancuso Nichols, C.; Lardière, S. G.; Bowman, J. P.; Nichols, P. D.; Gibson, J. A.; Guézennec, J. *Microb. Ecol.* **2005**, *49*, 578–589.
- (57) Daley, M. E.; Sykes, B. D. *Protein Sci.* **2003**, *12*, 1323–1331.
- (58) Ben, N. R. *ChemBioChem* **2001**, *2*, 161–166.
- (59) Harding, M. M.; Anderberg, P. I.; Haymet, A. D. J. *Eur. J. Biochem.* **2003**, *270*, 1381–1392.
- (60) Lin, F.; Davies, P. L.; Graham, L. A. *Biochemistry* **2011**, *50*, 4467–4478.
- (61) Graether, S. P.; Kuiper, M. J.; Gagné, S. M.; Walker, V. K.; Jia, Z.; Sykes, B. D.; Davies, P. L. *Nature* **2000**, *406*, 325–328.
- (62) Jia, Z.; Davies, P. L. *Trends Biochem. Sci.* **2002**, *27*, 101–110.
- (63) Scotter, A. J.; Marshall, C. B.; Graham, L. A.; Gilbert, J. A.; Granham, C. P.; Davies, P. L. *Cryobiology* **2006**, *53*, 229–239.
- (64) Pertaya, N.; Marshall, C. B.; Celik, Y.; Davies, P. L.; Braslavsky, I. *Biophys. J.* **2008**, *95*, 333–341.
- (65) Raymond, J. A.; Fritsen, C.; Shen, K. *FEMS Microbiol. Ecol.* **2007**, *61*, 214–221.
- (66) Walters, K. R.; Serianni, A. S.; Sformo, T.; Barnes, B. M.; Duman, J. G. *Proc. Natl. Acad. Sci. U.S.A.* **2009**, *106*, 20210–20215.

## REFERENCES

- [1] **Whitman W.B., Coleman D.C., Wiebe W.J.** Prokaryotes: The unseen majority. *Proc. Natl. Acad. Sci. USA* 1998, 95:6578–6583.
- [2] **Bhatnagar I., Kim S.K.** Immense essence of excellence: Marine microbial bioactive compounds. *Mar. Drugs* 2010, 8:2673–2701. doi: 10.3390/md8102673.
- [3] **Houssen W., Jaspars M.** Isolation of marine natural products. In *Natural Products Isolation: Methods and Protocols*, 3rd ed.; Sarker, S.D., Nahar, L., Eds.; Humana Press: Clifton, NJ, USA, 2012; 864:367–392. doi: 10.1007/978-1-61779-624-1\_14.
- [4] **Sipkema D., Franssen M.R., Osinga R., Tramper J., Wijffels R.** Marine sponges as pharmacy. *Mar. Biotechnol.* 2005, 7:142–162. doi: 10.1007/s10126-004-0405-5.
- [5] **Blunt J.W., Copp B.R., Keyzers R.A., Munro M.H.G., Prinsep M.R.** Marine natural products. *Nat. Prod. Rep.* 2012, 29:144–222. doi: 10.1039/c2np00090c.
- [6] **Mayer A.M., Glaser K.B., Cuevas C., Jacobs R.S., Kem W., Little R.D., McIntosh J.M., Newman D.J., Potts B.C., Shuster D.E.** The odyssey of marine pharmaceuticals: a current pipeline perspective. *Trends Pharmacol. Sci.* 2010; 31: 255-265. doi: 10.1016/j.tips.2010.02.005.
- [7] **Blunt J.W., Copp B.R., Keyzers R.A., Munro M.H., Prinsep M.R.** Marine Natural products. *Nat. Prod. Rep.* 2014, 31:160-258. doi: 10.1039/c3np70117d.
- [8] **Kornprobst J.M.** Encyclopedia of marine natural products, Volume 1. Weinheim: Wiley-Blackwell; 2010, 43:169-447. ISBN 10:3527327037.
- [9] **Thomas T.R.A., Kavlekar D.P., LokaBharathi P.A.** Marine drugs from sponge microbe association. A review. *Mar. Drugs* 2010, 8: 1417-1468. doi:10.3390/md8041417.
- [10] **Felczykowska A., Bloch S.K., Nejman-Faleńczyk B., Barańska S.** Metagenomic approach in the investigation of new bioactive compounds in the marine environment. *Acta Biochim. Pol.* 2012, 59: 501-505.
- [11] **Mahajan G., Thomas B., Parab R., Patel Z.E., Kuldharan S., Yemparala V., Mishra P.D., Ranadive P., D'Souza L., Pari K., Girish H.S.** In vitro and in vivo activities of antibiotic PM181104. *Antimicrob. Agents Chemother.* 2013, 57:5315-5319. doi: 10.1128/AAC.01059-13.
- [12] **Debbab A., Amal H. Aly, Wen H. Lin, Proksch P.** Bioactive Compounds from Marine Bacteria and Fungi. *Microbial Biotechnology* 2010, 3(5):544–563. doi: 10.1111/j.1751-7915.2010.00179.
- [13] **Matthew D. Lebar, Jaime L. Heimbegner, J. Baker B.** Cold-water marine natural products. *Nat. Prod. Rep.* 2007, 24:774–797. doi: 10.1039/B516240.



- [14] Marx J.C., Collins T., D'Amico S., Feller G., Gerday C. Cold-adapted enzymes from marine Antarctic microorganisms. *Mar. Biotechnol.* 2007, 9:293-304. doi: 10.1007/s10126-006-6103-8.
- [15] Margesin R., Schinner F., Marx J-C, Gerday C. In: Psychrophiles: from Biodiversity to Biotechnology (eds.), 2008. Springer-Verlag Berlin Heidelberg.
- [16] Feller G., Gerday C. Psychrophilic enzymes: hot topics in cold adaptation. 2003 doi:10.1038/nrmicro773.
- [17] Carillo S., Pieretti G., Lindner B., Parrilli E., Sannino F., Tutino M.L., Lanzetta R., Parrilli M., Corsaro M.M. Structural Characterization of the Core Oligosaccharide Isolated from the Lipo-polysaccharide of the Psychrophilic Bacterium *Colwellia psychrerythraea* Strain 34H. *Eur. J. Org. Chem.* 2013, 3771–3779. doi: 10.1002/ejoc.201300005.
- [18] Gilbert J.A., Davies P.L., Laybourn-Parry J. A hyperactive, Ca<sup>2+</sup>-dependent antifreeze protein in an Antarctic bacterium. *FEMS Microbiol. Lett.* 2005, 245:67. doi: 10.1016/j.femsle.2005.02.022.
- [19] Corsaro M.M., Lanzetta R., Parrilli E., Parrilli M., Tutino M.L., Ummarino S. Influence of Growth Temperature on Lipid and Phosphate Contents of Surface Polysaccharides from the Antarctic Bacterium *Pseudoalteromonas haloplanktis* TAC 125. *J. Bacteriol.*, 2004, 1:29-34. doi: 10.1128/JB.186.1.29-34.2004.
- [20] De Santi C., Tutino M.L., Mandrich L., Giuliani M., Parrilli E., Del Vecchio P., de Pascale D. The hormone-sensitive lipase from *Psychrobacter* sp. TA144: New insight in the structural/functional characterization. *Biochimie*, 2010, 92:949–957. doi: 10.1016/j.biochi.2010.04.001.
- [21] Feller George. Molecular adaptations to cold in psychrophilic enzymes. *Cell. Mol. Life Sci.*, 2003, 60:648. doi: 10.1007/s00018-003-2155-3.
- [22] Marsh A.G., Maxson R., Manahan D.T. High Macromolecular Synthesis with Low Metabolic Cost in Antarctic Sea Urchin Embryos. *Science*, 2001, 291:1950. doi: 10.1126/science.1056341.
- [23] Papaleo M.C., Fondi M., Maida I., Perrin E., Lo Giudice A., Michaud L., Mangano S., Bartolucci G., Romoli R., Fani R. Sponge-associated microbial antarctic communities exhibiting antimicrobial activity against *Burkholderia cepacia* complex bacteria. *Biotechnol. Adv.* 2012, 30:272-293. doi: 10.1016/j.biotechadv.2011.06.011.
- [24] Papa R., Parrilli E., Sannino F., Barbato G., Tutino M.L., Artini M., Selan L. Anti-biofilm activity of the Antarctic marine bacterium *Pseudoalteromonas haloplanktis* TAC125. *Research in Microbiology*, 2013, 164:450-456. doi: 10.1016/j.resmic.2013.01.010.
- [25] Medigue C., Krin E., Pascal G., Barbe V., Bernsel A., Bertin P.N., Cheung F., Cruveiller S., D'Amico S., Duilio A., Fang G., Feller G., Ho C., Mangenot S.,

**Marino G., Nilsson J., Parrilli E., Rocha E.P., Rouy Z., Sekowska A., Tutino M.L., Vallenet D., von Heijne G., Danchin A.** Coping with cold: the genome of the versatile marine Antarctica bacterium *Pseudoalteromonas haloplanktis* TAC125. *Genome Res.*, 2005, 15:1325-1335. doi: 10.1101/gr.4126905.

**[26] Fondi M., Maida I., Perrin E., Meller A., Mocali S., Parrilli E., Tutino M.L., Liò P., Fani R.** Genome-scale metabolic reconstruction and constraint-based modelling of the Antarctic bacterium *Pseudoalteromonas haloplanktis* TAC125. *Environ. Microbiol.*, 2015, 17:751–766. doi:10.1111/1462-2920.12513.

**[27] Duilio A., Tutino M.L., and Marino G.** Recombinant protein production in Antarctic Gram-negative bacteria. *Methods Mol. Biol.*, 2004, 267:225–237.

**[28] Rippa V., Papa R., Giuliani M., Pezzella C., Parrilli E., Tutino M.L., Marino G., Duilio A.** Regulated recombinant protein production in the Antarctic bacterium *Pseudoalteromonas haloplanktis* TAC125. *Methods Mol. Biol.*, 2012, 824:203-218. doi: 10.1007/978-1-61779-433-9\_10.

**[29] Wilmes B., Hartung A., Lalk M., Liebeke M., Schweder T., Neubauer P.** Fed-batch process for the psychrotolerant marine bacterium *Pseudoalteromonas haloplanktis*. *Microb. Cell Fact.*, 2010, 9:72. doi: 10.1186/1475-2859-9-72.

**[30] Corchero J.L., Gasser B., Resina D., Smith W., Parrilli E., Vazquez F., Abasolo I., Giuliani M., Jantti J., Ferrer P., Saloheimo M., Mattanovich D., Schwartz S. Jr, Tutino M.L., Villaverde A.** Unconventional microbial systems for the cost-efficient production of high-quality protein therapeutics. *Biotechnol. Adv.*, 2013, 31:140–153. doi: 10.1016/j.biotechadv.2012.09.001.

**[31] Parrilli E., Giuliani M., Giordano D., Russo R., Marino G., Verde C., Tutino M.L.** The role of a 2-on-2 haemoglobin in oxidative and nitrosative stress resistance of Antarctic *Pseudoalteromonas haloplanktis* TAC125. *Biochimie* 2010, 92:1003–1009. doi: 10.1016/j.biochi.2010.04.018.

**[32] Giuliani M., Parrilli E., Ferrer P., Baumann K., Marino G., Tutino M.L.** Process optimization for recombinant protein production in the psychrophilic bacterium *Pseudoalteromonas haloplanktis*. *Process. Biochem.* 2011, 46:953–959. doi: 10.1016/j.procbio.2011.01.011.

**[33] Dragosits M., Frascotti G., Bernard-Granger L., Vazquez F., Giuliani M., Baumann K., Rodriguez-Carmona E., Tokkanen J., Parrilli E., Wiebe M.G., Kunert R., Maurer M., Gasser B., Sauer M., Branduardi P., Pakula T., Saloheimo M., Penttilä M., Ferrer P., Tutino M.L., Villaverde A., Porro D., Mattanovich D.** Influence of growth temperature on the production of antibody Fab fragments in different microbes: a host comparative analysis. *Biotechnol. Prog.*, 2011, 27:38–46. doi: 10.1002/btpr.524.

**[34] Gasser B., Saloheimo M., Rinas U., Dragosits M., Rodriguez Carmona E., Baumann K., Giuliani M., Parrilli E., Branduardi P., Lang C., Porro D., Ferrer P., Tutino M.L., Mattanovich D., Villaverde A.** Protein folding and conformational

stress in microbial cells producing recombinant proteins: a host comparative overview. *Microb. Cell Fact.*, 2008, 7:11. doi: 10.1186/1475-2859-7-11.

**[35] Piette F., D'Amico S., Struvay C., Mazzucchelli G., Renaut J., Tutino M.L., Danchin A., Leprince P., Feller G.** Proteomics of life at low temperatures: trigger factor is the primary chaperone in the Antarctic bacterium *Pseudoalteromonas haloplanktis* TAC125. *Mol. Microbiol.*, 2010, 76:120-132. doi: 10.1111/j.1365-2958.2010.07084.x.

**[36] Piette F., D'Amico S., Mazzucchelli G., Danchin A., Leprince P., Feller G.** Life in the Cold: a Proteomic Study of Cold-Repressed Proteins in the Antarctic Bacterium *Pseudoalteromonas haloplanktis* TAC125. *Appl. Environ. Microbiol.*, 2011, 11:3881-3883. doi: 10.1128/AEM.02757-10.

**[37] Papaleo M.C., Romoli R., Bartolucci G., Maida I., Perrin E., Fondi M., Orlandini V., Mengoni A., Emiliani G., Tutino M.L., Parrilli E., de Pascale D., Michaud L., Lo Giudice A., Fani R.** Bioactive volatile organic compounds from Antarctic (sponges) bacteria. *N. Biotechnol.*, 2013, 30:824-838. doi: 10.1016/j.nbt.2013.03.011.

**[38] Methé B., Nelson K.E., Deming J.W., Momen B., Melamud E., Zhang X., Moulton J., Madupu R., Nelson W.C., Dodson R.J., Brinkac L.M., Daugherty S.C., Durkin A.S., DeBoy R.T., Kolonay J.F., Sullivan S.A., Zhou L., Daviden T.M., Martin W., Huston A.L., Lewis M., Weaver B., Weidman J.F., Khouri H., Utterback T.R., Feldblyum T.V., Fraser C.M.** The psychrophilic lifestyle as revealed by the genome sequence of *Colwellia psychrerythraea* 34H through genomic and proteomic analyses. *P. Natl. Acad. Sci. USA*, 2005, 102:10913–10918. doi: 10.1073/pnas.0504766102.

**[39] Huston A.L., Methe B., Deming J.W.** Purification, Characterization, and Sequencing of an Extracellular Cold-Active Aminopeptidase Produced by Marine Psychrophile *Colwellia psychrerythraea* Strain 34H. *Appl. Environ. Microbiol.*, 2004, 3321-3328. doi: 10.1128/AEM.70.6.3321–3328.2004.

**[40] Joseph G.M., Carpenter S.D., Deming J.W.** Production of cryoprotectant extracellular polysaccharide substances (EPS) by the marine psychrophilic bacterium *Colwellia psychrerythraea* strain 34H under extreme conditions. *Can. J. Microbiol.*, 2009, 55: 63-72. doi:10.1139/W08-130.

**[41] Newman D.J., Cragg G.M.** Natural products as sources of new drugs over the 30 years from 1981 to 2010. *J nat prod.*, 2012, 75:311-335. doi: 10.1021/np200906s.

**[42] Waites M.J., Morgan N.L., Higon G., Rockey J.S.** Industrial Microbiology: An Introduction. Oxford, UK: Blackwell Science, 2001.

**[43] Janos Berdy.** Thoughts and facts about antibiotics: Where we are now and where we are heading. *The Journal of Antibiotics*, 2012; 65:385–395. doi: 10.1038/ja.2012.27.

- [44] **Minerdi D., Bossi S., Gullino M.L., Garibaldi A.** Volatile organic compounds: a potential direct long-distance mechanism for antagonistic action of *Fusarium oxysporum* strain MSA 35. *Environmental Microbiology* , 2009; 11:844–854. doi:10.1111/j.1462-2920.2008.01805.x.
- [45] **Costerton J.W.** The biofilm primer. Springer, 2007.
- [46] **Francolini I., Donelli G.** Prevention of biofilm-based medical-device related infections. *FEMS Immunol. Med. Microbiol.*, 2010, 59:227-238. doi: 10.1111/j.1574-695X.2010.00665.x.
- [47] **Lequette Y., Boels G., Clarisse M., Faille C.** Using enzymes to remove biofilms of bacterial isolates sampled in the food-industry. *Biofouling*, 2010; 26:421-431.doi: 10.1080/08927011003699535.
- [48] **Holmstrom C., Egan S., Franks A., Mc Cloy S., Kjelleberg S.** Antifouling activities by marine surface associated *Pseudoalteromonas* species. *FEMS Microbiol. Ecol.*, 2002, 41:47-58. doi: 10.1111/j.1574-6941.2002.tb00965.x.
- [49] **Otto, M.** Staphylococcal biofilm. *Curr. Top Microbiol. Immunol.* 2008, 322:207–228. doi: 10.1007/978-3-540-75418-3\_10.
- [50] **Walters Jr.K.R., Serianni A.S., Voituron Y., Sformo T., Barnes B.M., Duman J.G.** A thermal hysteresis-producing xylomannan glycolipid antifreeze associated with cold tolerance is found in diverse taxa. *J. Comp. Physiol. B.*, 2011, 181:631–640. Doi: 10.1007/s00360-011-0552-8.
- [51] **Barry J. Fuller.** Cryoprotectants: the essential antifreezes to protect life in the frozen state. *CryoLetters*, 2004, 25:375-388.
- [52] **Graether S.P., Kuiper M.J., Gagné S.M., Walker V.K., Jia Z., Sykes B.D., Davies P.L.** Beta-helix structure and ice-binding properties of a hyperactive antifreeze protein from an insect. *Nature*, 2000, 406:325-8.

## CONCLUSIONS

Cold marine regions have been underexplored, and indigenous microbiota may be endowed of a more interesting chemical repertoire. The microorganisms that thrive in these cold environments are referred to as psychrophiles or cold-adapted. A preliminary characterization of molecules isolated from these bacteria suggested that these compounds may find applications in many biotechnological fields.

In my PhD project I worked on three chemical classes of bioactive compound from marine microorganisms: antimicrobial Volatile Organic Compounds (VOCs), anti-biofilms molecules, and cryoprotectants.

I demonstrated that *Pseudoalteromonas haloplanktis* TAC125 is able to produce volatile bioactive molecules endowed with an inhibitory activity against human pathogens belonging to the *Burkholderia cepacia* complex (Bcc). Moreover one of these molecules, methylamine, was identified and I demonstrated that this molecule is able to inhibit the growth of several Bcc strains in dose-dependent way.

My work also proved that *Pseudoalteromonas haloplanktis* TAC125 is able to produce anti-biofilm molecule/s against the biofilm of one of the major human opportunistic pathogens, *Staphylococcus epidermidis*. Moreover, I demonstrated that cold-adapted bacteria belonging to *Pseudoalteromonas*, *Psychrobacter*, and *Psychromonas* genera are able to produce anti-biofilm compounds active against opportunistic pathogens such as *Staphylococcus aureus* and *Pseudomonas aeruginosa*.

As for cryoprotectant molecules, my attention was focused on the cold adapted bacterium *Colwellia psychrerythraea* 34H.

*Colwellia psychrerythraea* 34H resulted to have a capsula with a very peculiar structure. The particularity of this molecule is the presence of a threonine on a linear tetrasaccharide repeating unit, likely the presence of threonine is responsible of cryoprotectant activity of capsular material.

In conclusion, my PhD work clearly demonstrated that cold adapted bacteria are very promising source of biotechnologically relevant molecules.

## OTHER PAPERS PUBLISHED DURING THE PhD PROGRAMME AND NOT DESCRIBED IN THE DISSERTATION

1. Carillo S., Pieretti G., Lindner B., Parrilli E., **Sannino F.**, Tutino M.L., Lanzetta R., Parrilli M., Corsaro M.M.. *Structural characterization of the Core Oligosaccharide Isolated from the Lipopolysaccharide of the Psychrophilic Bacterium Colwellia psychrerythraea strain 34H*. *Eur. J. Org. Chem.*, 2013, 18:3771-3779. doi: 10.1002/ejoc.201300005.
2. Papa R., Parrilli E., **Sannino F.**, Barbato G., Tutino M.L., Artini M., Selan L.. *Anti-Biofilm activity of the antarctic marine bacterium Pseudoalteromonas haloplanktis TAC125*. *Res. Microbiol.*, 2013, 164(5):450-6. doi: 10.1016/j.resmic.2013.01.010.
3. Giuliani M., Parrilli E., **Sannino F.**, Apuzzo G., Marino G., Tutino M.L. *Recombinant Production of a single chain antibody fragment in Pseudoalteromonas haloplanktis TAC125*. *Appl. Microbiol. Biotechnol.*, 2014, 98(11):4887-95. doi: 10.1186/s12934-015-0320-7.
4. Unzueta U., Vázquez F., Accardi G., Mendoza R., Toledo-Rubio V., Giuliani M., **Sannino F.**, Parrilli E., Abasolo I., Schwartz Jr.S., Tutino M.L., Villaverde A., Corchero J.L., Ferrer-Miralles N. *Strategies for the production of difficult-to-express full-length eukaryotic proteins using microbial cell factories: production of human alpha-galactosidase A*. *Appl. Microbiol. Biotechnol.*, 2015, 99:5863–5874. doi: 10.1007/s00253-014-6328-9.
5. Casillo A., Parrilli E., **Sannino F.**, Lindner B., Lanzetta R., Parrilli M., Tutino M.L., Corsaro M.M. *Structural Investigation of the Oligosaccharide Portion Isolated from the Lipooligosaccharide of the Permafrost Psychrophile Psychrobacter arcticus 273-4*. *Mar. Drugs*, 2015, 13, 4539-4555. doi: 10.3390/md13074539.
6. Leone S., **Sannino F.**, Tutino M.L., Parrilli E. Picone D. *Acetate: Friend or foe? Efficient production of a sweet protein in Escherichia coli BL21 using acetate as a carbon source*. *Microb. Cell Fact.*, 2015, 14(1):106. doi: 10.1186/s12934-015-0299-0.
7. Giuliani M., Parrilli E., **Sannino F.**, Apuzzo G., Marino G., Tutino M.L. *Soluble Recombinant Protein Production in Pseudoalteromonas haloplanktis TAC125*. Elena García-Fruitós (ed.), *Insoluble Proteins: Methods and Protocols*, Methods in Molecular Biology, vol. 1258, Springer Science+Business Media New York 2015 .
8. Giuliani M., Parrilli E., **Sannino F.**, Apuzzo G.A., Tutino M.L., Marino G.. *La produzione di anticorpi ricombinanti nel batterio antartico Pseudoalteromonas haloplanktis TAC125* Rendiconti Accademia Nazionale delle Scienze detta dei XL. Memorie di Scienze Fisiche e Naturali ISBN 987-88-548-7171-7

## Poster communications:

- **18-21 May 2013. American Society for Microbiology 113<sup>th</sup> General Meeting. DENVER, COLORADO.** The Anti-Biofilm Activity Secreted by Antarctic *Pseudoalteromonas haloplanktis*. R. Papa, E. Parrilli, **F. Sannino**, S. Carillo, M. M. Corsaro, A. Servello, C. Genovese, M. L. Tutino, M. Artini, L. Selan.
- **EUROBIOFILMS 2013 meeting. Ghent (Belgium) from 9 to 12 September 2013.** Antibiofilm activity of the Antarctic *Pseudoalteromonas haloplanktis*. L. Selan, M. Artini, R. Papa, M. Tilotta, **F. Sannino**, S. Carillo, M. M. Corsaro, M. L. Tutino, E. Parrilli



- **30th Meeting of the Società Italiana di Microbiologia Generale e Biotecnologie Microbiche (SIMGBM). Ischia, September 18th-21st 2013.** Development of new synthetic media for recombinant protein production in Antarctic bacterium *P. haloplanktis* TAC125. **Filomena Sannino**, Ermenegila Parrilli, Umberto Salvatore, Gennaro Apuzzo, Gennaro Marino, and Maria Luisa Tutino.
- **30th Meeting of the Società Italiana di Microbiologia Generale e Biotecnologie Microbiche (SIMGBM). Ischia, September 18th-21st 2013.** Novel approach towards the identification of bioactive volatile molecules produced by the Antarctic marine bacterium *Pseudoalteromonas haloplanktis* TAC125. **Filomena Sannino**, Ermenegila Parrilli, Gennaro Apuzzo, Gennaro Marino, Donatella de Pascale, Isabel Maida, Maria Cristiana Papaleo, Marco Fondi, Elena Perrin, Renato Fani and Maria Luisa Tutino.
- **30th Meeting of the Società Italiana di Microbiologia Generale e Biotecnologie Microbiche (SIMGBM). Ischia, September 18th-21st 2013.** Looking for novel cold-adapted lipases within *Pseudoalteromonas* genus: from data mining to biotechnological application. Gennaro Antonio Apuzzo, **Filomena Sannino**, Ermenegilda Parrilli, Concetta De Santi, Pietro Tedesco, Marco Fondi, Isabel Maida, Renato Fani, Donatella de Pascale, Maria Luisa Tutino.
- **30th Meeting of the Società Italiana di Microbiologia Generale e Biotecnologie Microbiche (SIMGBM). Ischia, September 18th-21st 2013.** Antibiofilm activity of the Antarctic *Pseudoalteromonas haloplanktis* TAC125. E. Parrilli, R. Papa, M. Tilotta, M. Marino, S. Carillo, M. M. Corsaro, G. Pieretti, **F. Sannino**, L. Selan, M. Artini, M. L. Tutino
- **IFIB 2013 Italian Forum on Industrial Biotechnology and Bioeconomy & EEN-Biotech and Bioeconomy Partnering Event 22 and 23 October 2013-Naples, Castel dell'Ovo.** Polyhydroxyalkanoates from Psychrophilic bacteria. **Filomena Sannino**, Marco Vastano, Ermenegilda Parrilli, Maria Luisa Tutino, Cinzia Pezzella and Giovanni Sannia
- **15-17 Maggio 2014. "Cortona Procaroti 2014"** organizzato dalla SIMGBM Società italiana Microbiologia Generale e Biotecnologie Microbiche. Volatile organic compounds from a marine Antarctic bacterium: development of a novel capture and identification strategy. Filomena Sannino, Ermenegilda Parrilli, Gennaro Antonio Apuzzo, Donatella de Pascale, Pietro Tedesco, Isabel Maida, Elena Perrin, Marco Fondi, Renato Fani, Gennaro Marino and Maria Luisa Tutino
- **9-10 October 2014. Meeting of ESCMID Study Group for Biofilms.** The anti-biofilm activity secreted by the Antarctic bacterium *Pseudoalteromonas haloplanktis* TAB23. **Filomena Sannino**, Ermenegilda Parrilli, Rosanna Papa, Marco Tilotta, Marco Artini, Laura Selan, Maria Luisa Tutino

## RESEARCH ACTIVITY IN FOREIGN LABORATORIES

From 1 May 2015 to July 31st 2015 my research activity was carried out in Prof. Thomas O. Larsen's laboratory at the Center for Microbial Biotechnology, BioCentrum-DTU, Technical University of Denmark, Kgs. Lyngby, Denmark.

## Structural Characterization of the Core Oligosaccharide Isolated from the Lipopolysaccharide of the Psychrophilic Bacterium *Colwellia psychrerythraea* Strain 34H

Sara Carillo,<sup>[a]</sup> Giuseppina Pieretti,<sup>[a]</sup> Buko Lindner,<sup>[b]</sup> Ermenegilda Parrilli,<sup>[a]</sup> Sannino Filomena,<sup>[a]</sup> Maria Luisa Tutino,<sup>[a]</sup> Rosa Lanzetta,<sup>[a]</sup> Michelangelo Parrilli,<sup>[a]</sup> and Maria Michela Corsaro<sup>\*[a]</sup>

*Dedicated to the memory of Ernesto Fattorusso*

**Keywords:** Bacteria / Lipopolysaccharides / Carbohydrates / Oligosaccharides / Structure elucidation / NMR spectroscopy

Cold-adapted bacteria are microorganisms that thrive at very low temperatures in permanently cold environments (0–10 °C). Their ability to survive under these harsh conditions is the result of molecular evolution and adaptations, which include the structural modification of the phospholipid membrane. To give insight into the role of the membrane in the mechanisms of adaptation to low temperature, the characterization of other cell-wall components is necessary. Among these components, the lipopolysaccharides are complex amphiphilic macromolecules embedded in the outer leaflet of the external membrane, of which they are the major constitu-

ents. The cold-adapted *Colwellia psychrerythraea* 34H bacterium, living in deep sea and Arctic and Antarctic sea ice, was cultivated at 4 °C. The lipooligosaccharide (LOS) was isolated and analysed by means of chemical analysis. Then it was degraded either by mild hydrazinolysis (*O*-deacylation) or hot KOH (4 M; *N*-deacylation). Both products were investigated in detail by <sup>1</sup>H and <sup>13</sup>C NMR spectroscopy and by ESI FT-ICR mass spectrometry. The oligosaccharide portion consists of a unique and very short species with the following general structure:  $\alpha$ -L-Col-(1→2)- $\alpha$ -D-GalA-(1→2)- $\alpha$ -D-Man-[3-*P*-D-Gro]-(1→5)- $\alpha$ -D-Kdo-4-*P*-Lipid-A.

### Introduction

Microorganisms can thrive in what we call extreme environments on Earth. Macelroy named these lovers ("philos" to Greeks) of extreme environments "extremophiles".<sup>[1]</sup> They had to adapt to one or several extreme physicochemical parameters: thermophiles and hyperthermophiles live above 60 °C near geysers and hydrothermal vents; halophiles thrive in hyper-saline environments; alkaliphiles prefer high pH; and acidophiles thrive at low pH.<sup>[2]</sup> Cold-adapted microorganisms include both steno-psychrophilic (formerly "true psychrophile") and eury-psychrophilic (formerly "psychrotolerant" or "psychrotrophic") organisms. The former show an optimal growth temperature of 15 °C, and a maximum temperature for growth of 20 °C; the latter

have the ability to grow at temperatures below 15 °C, but have maximum growth rates at temperature optima above 18 °C.<sup>[3,4]</sup> To survive extremes of pH, temperature, and salinity, microorganisms have been found to develop unique defenses against their environment, leading to the biosynthesis of unusual molecules ranging from simple osmolytes to complex secondary metabolites. In addition, the cell envelope shows adaptive changes in the face of the extreme environmental conditions, particularly in its lipid composition.

Microorganisms that thrive in permanently or seasonally very cold habitats solve the "freezing risk" by adopting heterogeneous strategies, such as the maintenance of membrane fluidity by increasing the synthesis of unsaturated fatty acids, and by changing the chain length of the fatty acids,<sup>[5–7]</sup> and also the quality and quantity of phosphorylation.<sup>[8,9]</sup> The outer membrane of Gram-negative bacteria forms a barrier for the cell, and it is made up of phospholipids, outer-membrane proteins (OMP), and lipopolysaccharides (LPS). The lipopolysaccharides are complex amphiphilic macromolecules embedded in the outer leaflet of the external membrane of which they are the major constituents. Smooth-form lipopolysaccharides (S-LPS) consist of three covalently linked regions, the glycolipid lipid A,

[a] Dipartimento di Scienze Chimiche, Università degli Studi di Napoli Federico II, Complesso Universitario Monte S. Angelo, Via Cintia 4, 80126 Napoli, Italy  
Fax: +39-081-674393  
E-mail: corsaro@unina.it  
Homepage: <http://www.unina.it>

[b] Division of Immunochimistry, Research Center Borstel, Leibniz-Center for Medicine and Biosciences  
Parkallee 10, 23845 Borstel, Germany

Supporting information for this article is available on the WWW under <http://dx.doi.org/10.1002/ejoc.201300005>.

also known as the endotoxin for human pathogens, the oligosaccharide region (core region), and the O-specific polysaccharide (O-chain, O-antigen). Rough-form lipopolysaccharides (R-LPS), also named lipooligosaccharides (LOS), lack the polysaccharide portion.<sup>[10,11]</sup> In order to check whether a role is played by the lipopolysaccharides in the molecular mechanism of adaptation to low temperatures, the complete structural determination of these molecules must be undertaken.

*Colwellia psychrerythraea* strain 34H, a Gram-negative bacterium isolated from Arctic marine sediments, is an intensively investigated steno-psychrophilic bacterium.<sup>[12]</sup> It has cardinal growth temperatures (optimum of 8 °C, maximum of 19 °C, and extrapolated minimum of −14.5 °C)<sup>[12]</sup> that rank among the lowest of all characterized bacteria, which makes this bacterium an attractive model to study the adaptive strategies of the cellular envelope to a sub-zero lifestyle.

In this paper, we report the structural characterization of the carbohydrate backbone of the LOS of *Colwellia psychrerythraea* 34H. The lipooligosaccharide was degraded both by mild hydrazinolysis (O-deacylation) and hot KOH (4 M; N-deacylation). Both products were investigated by chemical analysis, by <sup>1</sup>H and <sup>13</sup>C NMR spectroscopy, and by electrospray-ionization Fourier transform ion cyclotron resonance mass spectrometry.

## Results and Discussion

### LPS Extraction and Preliminary Analysis

*Colwellia psychrerythraea* strain 34H cells were grown aerobically, and the recovered cell pellet was extracted using phenol/chloroform/light petroleum (PCP) to obtain the crude LPS.<sup>[13]</sup> When it was analysed by DOC-PAGE electrophoresis, the crude LPS showed positive silver staining. In particular, a rough LPS (LOS<sub>PCP</sub>) was revealed (Figure 1). Subsequent extraction by the phenol/water method<sup>[14]</sup> yielded only a low amount of the lipooligosaccharide (LOS<sub>W</sub>), the purity of which was lower than that of the LOS<sub>PCP</sub>. The sugar composition of the LOS<sub>PCP</sub> was obtained by GC–MS analysis of the acetylated methyl glycosides. Thus, the occurrence of D-galacturonic acid (GalA), 2-amino-2-deoxy-D-glucose (GlcN), D-mannose (Man), 3,6-dideoxy-L-xylo-hexose (colitose, Col), and 3-deoxy-D-manno-oct-2-ulopyranosonic acid (Kdo) was revealed. The latter residue was revealed only after dephosphorylation of the LOS<sub>PCP</sub>, which was achieved by HF treatment. This result suggested the presence of a phosphate group on this residue, which prevented the detection of Kdo by GC–MS.<sup>[15]</sup> Methylation analysis indicated the presence of terminal Col, 6-substituted GlcN, 2-substituted GalA, and 2,3-disubstituted Man. The methylation data also revealed that all the residues were in the pyranose form.

The absolute configurations of the sugar residues were determined by GC–MS analysis of the corresponding acetylated 2-octyl glycosides.<sup>[16]</sup>



Figure 1. 14% DOC-PAGE analysis of *Colwellia psychrerythraea* strain 34H LOS<sub>PCP</sub> (lane A) and *Escherichia coli* O55:B5 LPS used as standard (lane B).

GC–MS analysis of the fatty acid methyl esters revealed the presence of decanoic, dodecanoic, 3-hydroxydodecanoic, tetradecenoic, tetradecanoic, pentadecenoic, pentadecanoic, 3-hydroxytetradecenoic, esadecenoic, esadecanoic, octadecenoic, and octadecanoic acids.

### Mass Spectrometric Analysis of the O-Deacylated LOS<sub>PCP</sub>

The LOS<sub>PCP</sub> was O-deacylated with anhydrous hydrazine<sup>[17]</sup> and the product obtained (LOS-OH) was analysed by ESI FT-ICR MS. The charge-deconvoluted spectrum showed the presence of one main species (M) at 1844.607 Da. Other signals were attributed to potassium and sodium adducts (Figure 2). To obtain further structural information, the LOS-OH was subjected to capillary skimmer dissociation (CSD), which generated the Y and B fragments<sup>[18]</sup> resulting from the cleavage of the Kdo/lipid A linkage.<sup>[19]</sup>

The CSD spectrum (Figure 3) showed the presence of a fragment at 922.176 Da, which was assigned to the core oligosaccharide, and a second fragment at 922.423 Da, which was assigned to the lipidA-OH. In particular, the following composition was assigned to the core oligosaccharide: Gro-ColGalAManKdoP<sub>2</sub> (accurate mass 922.175 Da), where Gro represents a glycerol residue. To the lipid A-OH was assigned the following composition: GlcN<sub>2</sub>P<sub>2</sub>[C12:0(3-OH)][C14:1(3-OH)] (accurate mass 922.426 Da), in agreement with the information obtained by chemical analysis.

### NMR Spectroscopic Analysis of the Fully Deacylated LOS<sub>PCP</sub>

To characterize the core oligosaccharide, the LOS-OH was further N-deacylated by strong alkaline hydrolysis, and the resulting oligosaccharide (OS) was analysed by one- and two-dimensional NMR spectroscopy (Table 1, Figures 4, 5, 6, and S1).



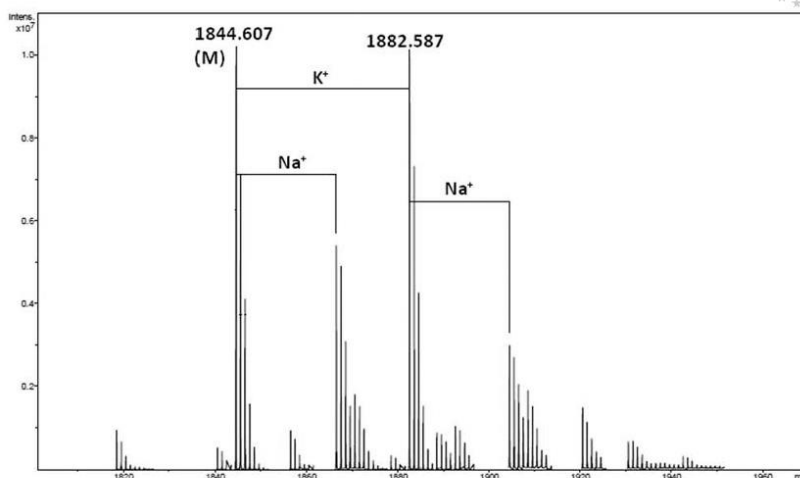


Figure 2. Charge-deconvoluted ESI FT-ICR mass spectrum of the LOS-OH isolated from *Colwellia psychrerythraea* strain 34H. The spectrum was acquired in negative-ion mode.

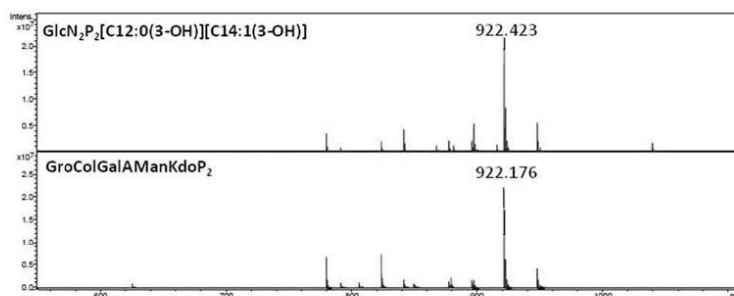


Figure 3. Charge-deconvoluted CSD mass spectrum of the LOS-OH isolated from *Colwellia psychrerythraea* strain 34H. The spectrum was acquired in negative-ion mode.

Table 1.  $^1\text{H}$  and  $^{13}\text{C}$  NMR assignments of the fully deacylated oligosaccharide of the LOS<sub>PCP</sub> from *Colwellia psychrerythraea* strain 34H. The values are referenced to acetone as internal standard ( $^1\text{H}$ :  $\delta = 2.225$  ppm;  $^{13}\text{C}$ :  $\delta = 31.45$  ppm). The spectra were recorded at 302 K.

Residue	1-H C-1	2-H C-2	3-H C-3	4-H C-4	5-H C-5	6a-H C-6	6b-H/7-H C-7	7b-H/8-H C-8
A	5.56	3.38	3.88	3.39	4.09	3.80	4.21	
$\alpha$ -GlcP <sub>N-1-P</sub>	92.8	55.3	70.6	71.1	73.9	70.3		
B	5.30	4.03	3.93	3.69	4.14	3.88	3.65	
2- $\alpha$ -Manp	100.2	80.8	71.5	68.6	73.6	62.4		
C	5.16	3.84	4.09	4.24	4.41	—		
2- $\alpha$ -GalpA	101.7	76.9	70.0	72.3	73.4	174.8		
D	4.97	3.95	1.93	3.81	4.13	1.13		
$\alpha$ -Colp	101.5	64.7	34.2	69.6	68.2	16.8		
E	4.82	3.07	3.81	3.81	3.70	3.46	3.69	
6- $\beta$ -GlcP <sub>N-4-P</sub>	99.9	56.8	72.9	75.5	75.3	63.7		
F	—	—	1.95–2.15	4.49	4.20	3.76	3.76	3.64–3.86
5- $\alpha$ -Kdop-4-P	174.2	101.0	35.5	71.2	74.1	72.8	70.4	64.9

In particular,  $^1\text{H}$ – $^1\text{H}$  DQF-COSY (double quantum-filtered correlation spectroscopy),  $^1\text{H}$ – $^1\text{H}$  TOCSY (total correlation spectroscopy),  $^1\text{H}$ – $^1\text{H}$  ROESY (rotating-frame nuclear Overhauser enhancement spectroscopy),  $^1\text{H}$ – $^{13}\text{C}$

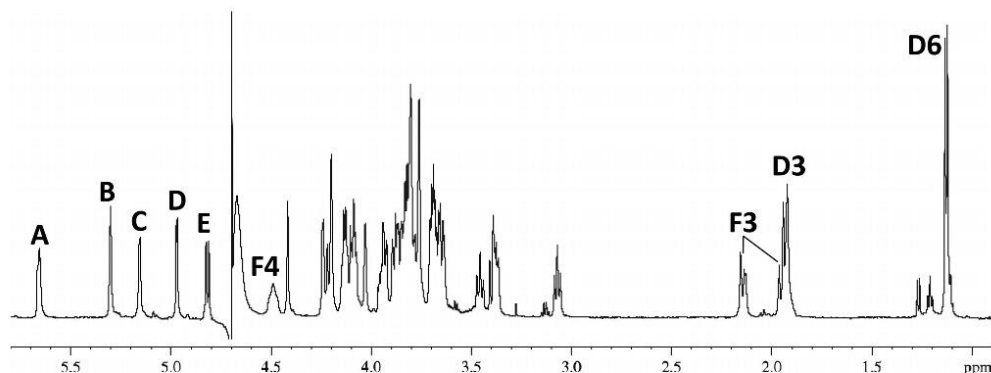


Figure 4.  $^1\text{H}$  NMR spectrum of the oligosaccharide (OS) obtained by strong alkaline hydrolysis of the  $\text{LOS}_{\text{PCP}}$ . The spectrum was recorded in  $\text{D}_2\text{O}$  at 302 K at 600 MHz. The letters refer to the residues as described in Table 1 and Scheme 1.

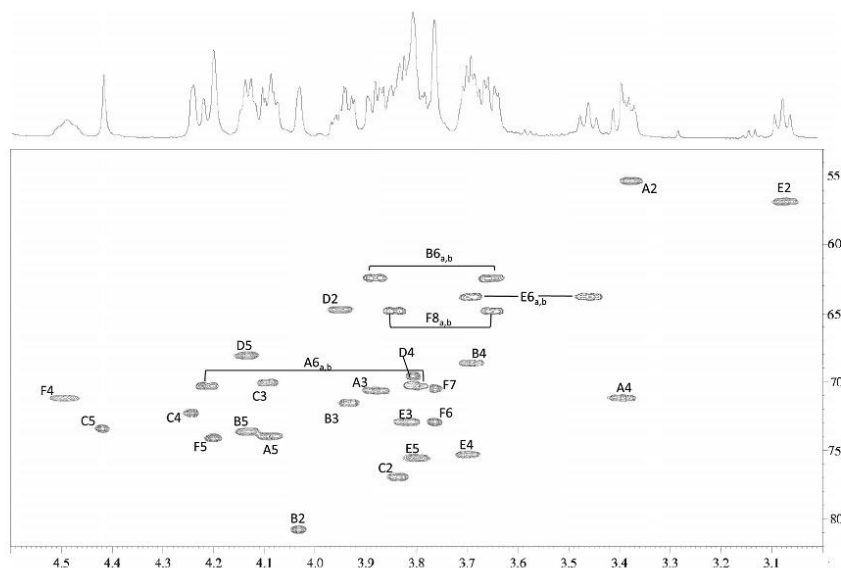


Figure 5. Alcohol signals region ( $\delta = 3.0\text{--}4.6$  ppm) of the  $^1\text{H}\text{--}^{13}\text{C}$  DEPT-HSQC spectrum of OS. The spectrum was recorded in  $\text{D}_2\text{O}$  at 302 K at 600 MHz using acetone as an internal standard ( $\delta_{\text{H}} = 2.225$  ppm and  $\delta_{\text{C}} = 31.45$  ppm). The letters refer to the residues as described in Table 1 and Scheme 1.

DEPT-HSQC (distortionless enhancement by polarization transfer-heteronuclear single quantum coherence),  $^1\text{H}\text{--}^{13}\text{C}$  HSQC-TOCSY,  $^1\text{H}\text{--}^{13}\text{C}$  HMBC (heteronuclear multiple bond correlation), 2D  $F_2$ -coupled HSQC, and  $^{31}\text{P}$  NMR spectroscopy were performed.

The  $^1\text{H}$  NMR spectrum (Figure 4) of the fully deacylated  $\text{LOS}_{\text{PCP}}$  showed the presence of five anomeric proton signals (A–E) between  $\delta = 4.7$  and 5.7 ppm. By taking into account all the 2D NMR experiments, the spin systems of all the monosaccharides were identified.

Residue A was assigned as the 6-substituted  $\alpha\text{-GlcP}N\text{-}1\text{-}P$  of lipid A on the basis of the multiplicity of the anomeric proton signal due to its phosphorylation ( $^3J_{\text{H,P}} = 6.1$  Hz). Moreover, the C-2 resonance occurred at  $\delta = 55.3$  ppm, which indicated a nitrogen-bearing carbon atom, and the C-6 resonance was shifted downfield by glycosylation to  $\delta = 70.3$  ppm.

Residue E, with C-1/1-H signals at  $\delta = 99.9/4.82$  ( $^1J_{\text{C-1,1-H}} = 166.3$  Hz), was assigned as the lipid A 6-substituted  $\beta\text{-GlcP}N\text{-}4\text{-}P$  residue, as a result of its C-2 chemical

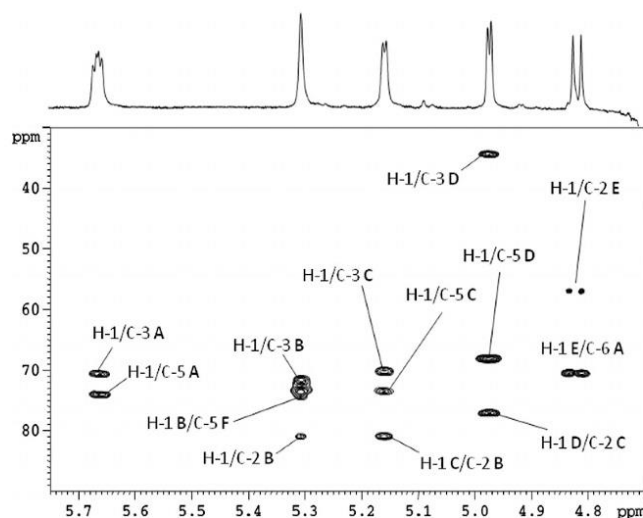


Figure 6. Anomeric region of the  $^1\text{H}$ - $^{13}\text{C}$  HMBC spectrum of OS. The spectrum was recorded in  $\text{D}_2\text{O}$  at 302 K at 600 MHz using acetone as an internal standard ( $\delta_{\text{H}} = 2.225$  ppm and  $\delta_{\text{C}} = 31.45$  ppm). The letters refer to the residues as described in Table 1 and Scheme 1.

shift at  $\delta = 56.8$  and its linkage to O-6 of residue A. In fact 1-H of residue E showed a long-range scalar coupling with C-6 of residue A in the HMBC spectrum. The  $\beta$ -anomeric configuration was corroborated by the intrareidue NOE correlations observed between 1-H and both 3-H and 5-H in the ROESY spectrum. Moreover, the downfield shifts of 4-H and C-4 are diagnostic for the presence of a phosphate group linked at O-4.<sup>[20]</sup>

The Kdo (residue F) proton and carbon chemical shifts were identified starting from the diastereotopic protons  $3_{\text{ax}}\text{-H}$  and  $3_{\text{eq}}\text{-H}$ . The chemical-shift difference between these protons depends on the configuration of the C-1 carbon atom, being different for the  $\alpha$  and  $\beta$  anomers. In this case, the difference of  $\Delta(3_{\text{ax}}\text{-H} - 3_{\text{eq}}\text{-H}) = 0.2$  ppm allowed us to assign an  $\alpha$  configuration to the residue.<sup>[21]</sup> Moreover, both protons showed a correlation in the DQF-COSY spectrum with a signal at  $\delta = 4.49$  ppm, assigned as Kdo 4-H, which was in turn correlated to a carbon atom with signal at  $\delta = 71.2$  ppm in the DEPT-HSQC spectrum. Both 4-H and C-4 resonances were shifted downfield relative to reference values,<sup>[22]</sup> and the observed chemical shifts were diagnostic for the presence of a phosphate in that position.<sup>[23]</sup> The Kdo 5-H proton was identified by vicinal scalar coupling with 4-H in the DQF-COSY spectrum, and the corresponding carbon atom was downfield shifted to  $\delta = 74.1$  ppm indicating glycosylation at this position. In addition, the Kdo anomeric carbon atom showed a long-range correlation with 6-H of residue E, thus confirming its linkage to the lipid A backbone.

Residue B was assigned as a 2-substituted  $\alpha$ -mannopyranose on the basis of the small  $J_{1\text{-H},2\text{-H}}$  and  $J_{2\text{-H},3\text{-H}}$  coupling-constant values. The glycosylation at the C-2 position was inferred by comparing the carbon chemical shift values

with standard values,<sup>[24]</sup> and the  $\alpha$ -anomeric configuration was established by the  $J_{\text{C-1},1\text{-H}}$  coupling-constant value, which was 176.4 Hz. The HMBC spectrum (Figure 6) showed the presence of a long-range scalar coupling between the 1-H proton of this residue and C-5 of Kdo, thus indicating that this position was substituted by residue B.

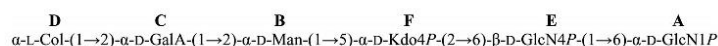
Residue C, with 1-H/C-1 signals at  $\delta = 5.16/101.7$  ppm, was identified as a 2-substituted  $\alpha$ -galactopyranuronic acid, since its C-6 signal occurred at  $\delta = 174.8$  ppm, and its C-2 signal was shifted downfield to  $\delta = 76.9$  ppm. The  $\alpha$ -anomeric configuration was inferred from its  $J_{\text{C-1},1\text{-H}}$  coupling-constant value of 176.3 Hz. This residue was linked to residue B at the O-2 position, as shown by the presence of a correlation between 1-H of residue C and C-2 of residue B in the HMBC spectrum (Figure 6).

The last residue (D) of the core oligosaccharidic chain was identified as a terminal  $\alpha$ -colitose, since its 3-H/C-3 and 6-H/C-6 signals occurred at  $\delta = 1.93/34.2$  and  $1.13/16.8$  ppm, respectively. The  $\alpha$ -anomeric configuration was inferred from its  $J_{\text{C-1},1\text{-H}}$  value of 173.9 Hz. Its 1-H showed an interresidue NOE correlation with 2-H of residue C in the ROESY spectrum, and a long-range scalar coupling with the signal at  $\delta = 101.7$  ppm of a carbon atom in the HMBC spectrum (Figure 6). Thus, it was shown to be linked to residue C at the O-2 position.

To sum up, the above data allowed the identification of the main carbohydrate backbone of the lipopolysaccharide from *Colwellia psychrerythraea*, as shown in Scheme 1.

The  $^{31}\text{P}$  NMR spectrum of OS confirmed the presence of only three phosphomonoester signals (Kdo-4-*P* at  $\delta = 3.9$  ppm, GlcN-4-*P* at  $\delta = 3.5$  ppm, and GlcN-1-*P* at  $\delta = 2.6$  ppm), in contrast with the results obtained from the analysis of the LOS-OH mass spectra, which indicated the





Scheme 1.

presence of four phosphate groups. This, together with the lack of the glycerol residue in the OS structure, suggested that these groups did not withstand the alkaline treatment, which is consistent with the lability of diesters under these hydrolysis conditions.<sup>[25]</sup> In addition, the finding of a 2,3-disubstituted mannose in the methylation analysis did not fit with the above reported structure.

#### NMR Spectroscopic Analysis of the LOS-OH

To establish the structure of the core oligosaccharide including the labile groups lost during the harsh alkaline treatment, the LOS-OH was analysed by NMR spectroscopy (Figures 7, S2 and S3). In particular <sup>1</sup>H–<sup>1</sup>H DQF-COSY, <sup>1</sup>H–<sup>1</sup>H TOCSY, <sup>1</sup>H–<sup>1</sup>H ROESY, and <sup>1</sup>H–<sup>13</sup>C

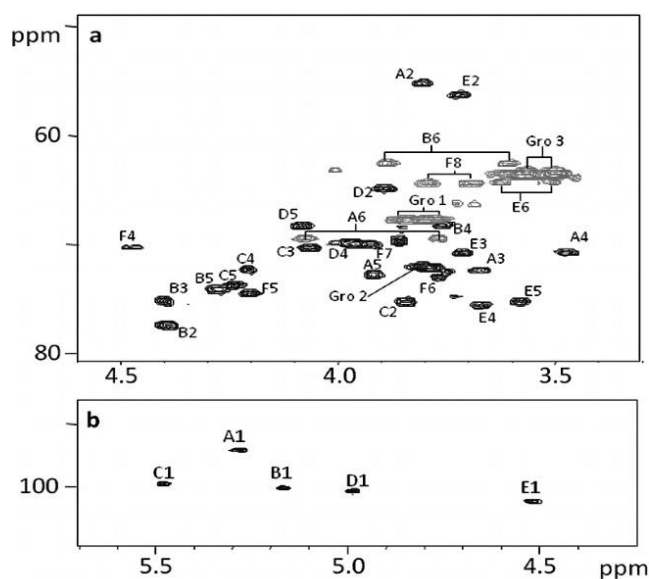
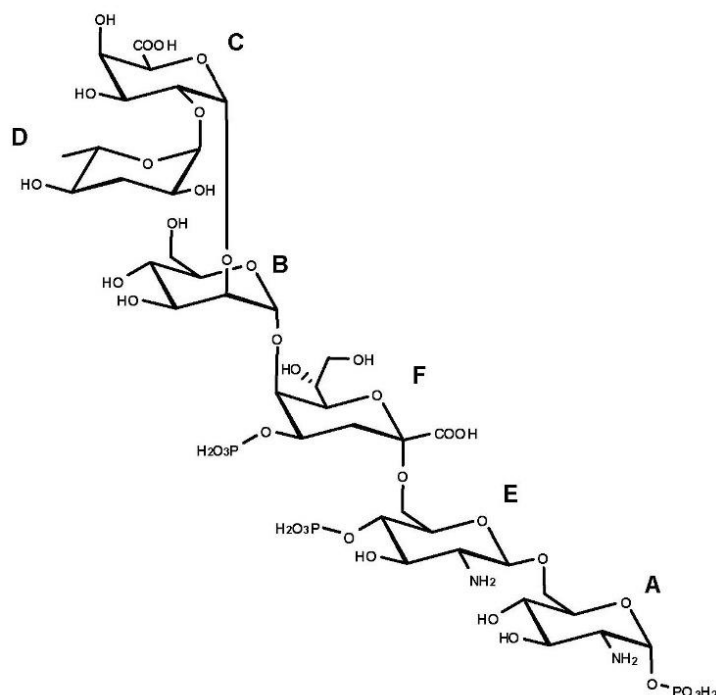


Figure 7. Carbinol (a) and anomeric (b) regions of the <sup>1</sup>H–<sup>13</sup>C DEPT-HSQC spectrum of LOS-OH from *Colwellia psychrerythraea* strain 34H. The spectrum was recorded in D<sub>2</sub>O at 298 K at 600 MHz using acetone as an internal standard ( $\delta_{\text{H}} = 2.225$  ppm and  $\delta_{\text{C}} = 31.45$  ppm). The letters refer to the residues as described in Table 2 and Scheme 2.

Table 2. <sup>1</sup>H and <sup>13</sup>C NMR assignments of the LOS-OH from *Colwellia psychrerythraea* strain 34H. All the values are referenced to acetone as internal standard (<sup>1</sup>H:  $\delta = 2.225$  ppm; <sup>13</sup>C:  $\delta = 31.45$  ppm). The spectra were recorded at 298 K.

Residue	1-H C-1	2-H C-2	3-H C-3	4-H C-4	5-H C-5	6a-H C-6	6b-H/7-H C-7	7b-H/8-H C-8
A	5.27	3.80	3.67	3.47	3.91	3.76	4.06	
$\alpha$ -GlcN-1-P	94.1	55.1	72.4	70.7	72.7	69.4		
B	5.16	4.40	4.40	3.75	4.27	3.87	3.61	
2- $\alpha$ -Manp-3-P	100.2	77.3	75.1	68.1	74.1	62.4		
C	5.47	3.85	4.06	4.20	4.42	–		
2- $\alpha$ -GalpA	99.7	75.1	70.0	72.2	73.4	nd		
D	4.98	3.87	1.88–1.98	3.97	4.07	1.13		
$\alpha$ -Colp	100.3	64.9	34.3	69.7	68.2	17.1		
E	4.51	3.71	3.67	3.67	3.57	3.49	3.62	
6- $\beta$ -GlcN-4-P	102.5	56.2	72.4	75.5	75.1	64.2		
F	–	–	1.89–2.16	4.47	4.19	3.76	3.91	3.68–3.78
5- $\alpha$ -Kdop-4-P	nd	nd	35.5	70.1	74.5	72.9	69.8	64.3
<i>r</i> -Gro-1-P	3.79–3.83	3.77	3.49–3.56					
	67.7	71.9	63.4					



Scheme 2.

DEPT-HSQC spectra were acquired. Analysis of all the spectra (Table 2) confirmed that the main carbohydrate backbone was that shown in Scheme 1, but that additional signals due to the glycerol residue were present.

In more detail, the signal of C-1 of the Gro residue occurred at  $\delta = 67.7$  ppm in the  $^1\text{H}$ - $^{13}\text{C}$  DEPT-HSQC spectrum (Figure 7), thus indicating its phosphorylation at C-1. Furthermore, the signals of 3-H and C-3 of residue B were shifted downfield to  $\delta = 4.40/75.1$  ppm, thus indicating that Gro was linked to the mannose residue at position O-3 by a phosphodiester linkage, consistent with the presence of the 2,3-disubstituted mannose in the GC-MS methylation analysis. To determine the relative configuration of the Gro residue, it was oxidized to glyceric acid. The product was hydrolysed, the free glyceric acid was esterified with chiral 2-octanol, and the resulting octyl ester derivative was analysed by GC-MS.<sup>[26]</sup> By comparison of its retention time with that of a standard sample, it was found to be D-configured.

In conclusion, the complete structure of the core lipid A saccharidic backbone of the LPS from *Colwellia psychrerythraea* strain 34H is as shown in Scheme 2.

## Conclusions

In this paper, we reported the complete structure of the sugar backbone of the lipopolysaccharide fraction from

*Colwellia psychrerythraea* strain 34H, a strictly psychrophilic marine bacterium isolated from deep sea and Arctic and Antarctic sea ice.<sup>[12]</sup> The molecules were extracted by the PCP method, and they had a lipooligosaccharide fraction. The complete structural determination was achieved by chemical analysis, NMR spectroscopy, and ESI mass spectrometry. It is worth noting the lack of heptose residues in the inner core of *C. psychrerythraea*. Actually, in their place, an  $\alpha$ -mannose residue is linked to the Kdo. This structural feature is commonly found in the *Rhizobiaceae* family, but has never before been found in extremophiles. Moreover, colitose and glycerol are present in the *Colwellia* LOS. Both these residues have been already found in several O-polysaccharides and K-antigens from Gram-negative bacteria, but to the best of our knowledge, this is the first time that they have been found in a core oligosaccharide. Until now, only a few structures of LPSs from other cold-adapted microorganisms have been characterised. By comparing the *C. psychrerythraea* 34H LOS structure with those obtained from *P. haloplanktis* TAC125<sup>[27,28]</sup> and TAB23,<sup>[29]</sup> and from *P. arctica*,<sup>[15]</sup> it turned out that they have in common the lack of an O-chain and the presence of a high charge density in the core region due to the presence of acidic monosaccharides and phosphate groups. In addition, the core regions have been found to be made up of only a few sugar units. These structural features seem to be com-

mon to cold-adapted microorganisms. Recently, O-chain polysaccharides were found in LPS from *Psychrobacter muricolla* and *cryohalensis*. Although the latter microorganisms had been isolated at  $-9^{\circ}\text{C}$ , the LPS was extracted from bacterial cells grown at  $24^{\circ}\text{C}$ .<sup>[30,31]</sup> It would be worth investigating the LPS produced at a lower growth temperature.

## Experimental Section

**Bacteria Growth and LOS Isolation:** *Colwellia psychrerythraea* 34H was grown aerobically at  $4^{\circ}\text{C}$  in marine broth medium (DIFCO™ 2216). When the liquid culture reached the late exponential phase ( $\text{OD}_{600} = 2$ ), cells were harvested by centrifugation at  $3000\text{ g}$  at  $4^{\circ}\text{C}$  for 20 min. Dried bacteria cells (4.8 g) were extracted by the PCP method<sup>[13]</sup> to give  $\text{LOS}_{\text{PCP}}$  (52 mg, yield 1.1% w/w of dried cells).

**Sugar and Fatty Acids Analysis:** A sample of  $\text{LOS}_{\text{PCP}}$  (0.5 mg) was treated first with HF (48% aq.; 100  $\mu\text{L}$ ); then methanolysis was performed. The monosaccharides obtained were acetylated and analysed by GC–MS as described previously,<sup>[15]</sup> while the fatty acids were analysed as methyl esters. The sugars were identified by comparison with standard samples. In particular, the colitose standard was obtained from *Escherichia coli* O55:B5 LPS (Sigma). The absolute configurations of the sugars were determined by gas chromatography of the acetylated (S)-2-octyl glycosides.<sup>[16]</sup> The absolute configuration of Gro was determined by GC–MS analysis of its 2-octyl ester derivative. Briefly, it was oxidized using 2,2,6,6-tetramethylpiperidine-1-oxyl (TEMPO), then hydrolysed with TFA (trifluoroacetic acid; 2 M), and esterified with chiral 2-octanol.<sup>[26]</sup> All the sugar derivatives were analysed with an Agilent Technologies 6850A gas chromatography apparatus equipped with a mass-selective detector 5973N and a Zebron ZB-5 capillary column (Phenomenex,  $30\text{ m} \times 0.25\text{ mm i.d.}$ , flow rate  $1\text{ mL min}^{-1}$ , He as carrier gas). Acetylated methyl glycosides were analysed using the following temperature program:  $150^{\circ}\text{C}$  for 3 min,  $150 \rightarrow 240^{\circ}\text{C}$  at  $3^{\circ}\text{C min}^{-1}$ . Fatty acids were analysed as follows:  $140^{\circ}\text{C}$  for 3 min,  $140 \rightarrow 280^{\circ}\text{C}$  at  $10^{\circ}\text{C min}^{-1}$ ,  $280^{\circ}\text{C}$  for 20 min. The analysis of acetylated octyl glycosides was performed as follows:  $150^{\circ}\text{C}$  for 5 min, then  $150 \rightarrow 240^{\circ}\text{C}$  at  $6^{\circ}\text{C min}^{-1}$ ,  $240^{\circ}\text{C}$  for 5 min. The glyceric acid octyl ester derivatives were analysed with the following temperature program:  $80^{\circ}\text{C}$  for 5 min,  $80 \rightarrow 200^{\circ}\text{C}$  at  $5^{\circ}\text{C min}^{-1}$ ,  $200 \rightarrow 300^{\circ}\text{C}$  at  $10^{\circ}\text{C min}^{-1}$ .

**Linkage Analysis:** The linkage positions of the monosaccharides were determined by GC–MS analysis of the partially methylated alditol acetates. Briefly, the  $\text{LOS}_{\text{PCP}}$  (1 mg) was methylated with  $\text{CH}_3\text{I}$  (300  $\mu\text{L}$ ) and NaOH powder in DMSO (1.0 mL) for 20 h.<sup>[32]</sup> The product was treated with  $\text{NaBD}_4$  to reduce the uronate groups, then totally hydrolysed with TFA (2 M) at  $120^{\circ}\text{C}$  for 2 h, reduced again with  $\text{NaBD}_4$ , acetylated with  $\text{Ac}_2\text{O}$  and pyridine (50  $\mu\text{L}$  each,  $100^{\circ}\text{C}$ , 30 min), and the resulting product mixture was analysed by GC–MS. The temperature program used was:  $90^{\circ}\text{C}$  for 1 min,  $90 \rightarrow 140^{\circ}\text{C}$  at  $25^{\circ}\text{C min}^{-1}$ ,  $140 \rightarrow 200^{\circ}\text{C}$  at  $5^{\circ}\text{C min}^{-1}$ ,  $200 \rightarrow 280^{\circ}\text{C}$  at  $10^{\circ}\text{C min}^{-1}$ ,  $280^{\circ}\text{C}$  for 10 min.

**Deacylation of the LOS:** The  $\text{LOS}_{\text{PCP}}$  (20 mg) was first dried under vacuum over phosphoric anhydride and then incubated with hydrazine (1.0 mL,  $37^{\circ}\text{C}$ , 1.5 h). To precipitate the LOS-OH, cold acetone was added. The pellet was recovered after centrifugation ( $4^{\circ}\text{C}$ , 10000 g, 30 min), washed three times with acetone, and finally suspended in water and lyophilized (14 mg).<sup>[17]</sup> The LOS-OH (8 mg) was dissolved in KOH (4 M aq.; 1.0 mL) and incubated at

$120^{\circ}\text{C}$  for 16 h. The KOH was neutralized with HCl (2 M aq.) until  $\text{pH} = 6$ , and the mixture was extracted three times with  $\text{CHCl}_3$ . The aqueous phase was recovered and desalted on a Sephadex G-10 column (Amersham Biosciences,  $2.5 \times 43\text{ cm}$ ,  $31\text{ mL h}^{-1}$ , fraction volume 2.5 mL, eluent  $\text{NH}_4\text{HCO}_3$  10 mM). The eluted oligosaccharide mixture was then lyophilized (3.5 mg, 44% w/w).

**NMR Spectroscopy:**  $^1\text{H}$  and  $^{13}\text{C}$  NMR spectra were recorded with a Bruker Avance 600 MHz spectrometer equipped with a cryoprobe. All two-dimensional homo- and heteronuclear experiments (COSY, TOCSY, ROESY, HSQC-DEPT, HSQC-TOCSY, 2D  $F_2$ -coupled HSQC, and HMBC) were performed by using standard pulse sequences available in the Bruker software. The mixing time for TOCSY, ROESY, and HSQC-TOCSY experiments was 100 ms. Chemical shifts were measured in  $\text{D}_2\text{O}$  at 302 K and 298 K for OS and LOS-OH, respectively, by using acetone as an internal standard ( $\delta_{\text{H}} = 2.225\text{ ppm}$  and  $\delta_{\text{C}} = 31.45\text{ ppm}$ ).

**Mass Spectrometry Analysis:** Electrospray-ionization Fourier transform ion cyclotron (ESI FT-ICR) mass spectrometry was performed in the negative-ion mode with an APEX QE (Bruker Daltonics) instrument equipped with a 7 T actively shielded magnet. The LOS-OH sample was dissolved at a concentration of ca.  $10\text{ ng mL}^{-1}$  and analysed as described previously.<sup>[33]</sup> Mass spectra were charge-deconvoluted, and the mass numbers given refer to the monoisotopic masses of the neutral molecules.

**Supporting Information** (see footnote on the first page of this article): The whole  $^1\text{H}$ - $^{13}\text{C}$  DEPT-HSQC spectra of OS and LOS-OH, as well as the proton spectra of LOS-OH are reported in this section. The main signals are described in the main text of the article. Moreover the elemental analysis of both the products are reported.

## Acknowledgments

The authors thank the Centro Interdipartimentale Metodologie Chimico Fisiche Università di Napoli and BioTekNet for the use of the 600 MHz NMR spectrometer. This work was supported by the Programma Nazionale di Ricerca in Antartide 2010 (grant PNRA 2010/A1.05).

- [1] R. D. Macelroy, *Biosystems* **1974**, *6*, 74–75.
- [2] L. J. Rothschild, R. L. Mancinelli, *Nature* **2001**, *409*, 1092–1101.
- [3] R. J. Morita, *Bacteriol. Rev.* **1975**, *39*, 144–167.
- [4] R. Cavicchioli, *Nat. Rev. Microbiol.* **2006**, *4*, 331–343.
- [5] S. D'Amico, T. Collins, J. C. Marx, G. Feller, C. Gerday, *EMBO Rep.* **2006**, *7*, 385–389.
- [6] N. Beales, *Comp. Rev. Food Sci. Food Safety* **2004**, *3*, 1–20.
- [7] M. K. Chattopadhyay, *J. Biosci.* **2006**, *31*, 157–165.
- [8] M. M. Corsaro, R. Lanzetta, E. Parrilli, M. Parrilli, M. L. Tutino, S. Ummanino, *J. Bacteriol.* **2004**, *186*, 29–34.
- [9] M. K. Ray, G. Seshu Kumar, S. Shivaji, *J. Bacteriol.* **1994**, *176*, 4243–4249.
- [10] C. Alexander, E. T. Rietschel, *J. Endotoxin Res.* **2001**, *7*, 167–202.
- [11] M. Caroff, D. Karibian, *Carbohydr. Res.* **2003**, *338*, 2431–2447.
- [12] B. A. Methé, K. E. Nelson, J. W. Deming, B. Momen, E. Melamud, X. Zhang, J. Moul, R. Madupu, W. C. Nelson, R. J. Dodson, L. M. Brinkac, S. C. Daugherty, A. S. Durkin, R. T. DeBoy, J. F. Kolonay, S. A. Sullivan, L. Zhou, T. M. Davidsen, M. Wu, A. L. Huston, M. Lewis, B. Weaver, J. F. Weidman, H. Khouri, T. R. Utterback, T. V. Feldblyum, C. M. Fraser, *Proc. Natl. Acad. Sci. USA* **2005**, *102*, 10913–10918.
- [13] C. Galanos, O. Lüderitz, O. Westphal, *Eur. J. Biochem.* **1969**, *9*, 245–249.



- [14] O. Westphal, K. Jann, *Methods Carbohydr. Chem.* **1965**, 5, 83–91.
- [15] M. M. Corsaro, G. Pieretti, B. Lindner, R. Lanzetta, E. Parrilli, M. L. Tutino, M. Parrilli, *Chem. Eur. J.* **2008**, 14, 9368–9376.
- [16] K. Leontein, B. Lindberg, J. Lönnngren, *Carbohydr. Res.* **1978**, 62, 359–362.
- [17] O. Holst, *Methods Mol. Biol.* **2000**, 145, 345–353.
- [18] B. Dörmann, C. Costello, *Glycoconjugate J.* **1988**, 5, 397–409.
- [19] A. Kondakova, B. Lindner, *Eur. J. Mass Spectrom.* **2005**, 11, 535–546.
- [20] O. Holst, S. Müller-Loennies, B. Lindner, H. Brade, *Eur. J. Biochem.* **1993**, 214, 695–701.
- [21] P. K. Agrawal, C. A. Bush, N. Qureshi, K. Takayama, *Adv. Biophys. Chem.* **1994**, 4, 179–236.
- [22] G. Pieretti, M. M. Corsaro, R. Lanzetta, M. Parrilli, S. Vilches, S. Merino, J. M. Tomás, *Eur. J. Org. Chem.* **2009**, 1365–1371.
- [23] S. Müller-Loennies, L. Brade, H. Brade, *Eur. J. Biochem.* **2002**, 269, 1237–1242.
- [24] K. Bock, C. Pedersen, *Adv. Carbohydr. Chem. Biochem.* **1983**, 41, 27–66.
- [25] K. Nummila, I. Kilpeläinen, U. Zähringer, M. Vaara, I. M. Helander, *Mol. Microbiol.* **1995**, 16, 271–278.
- [26] T. Rundlöf, G. Widmalm, *Anal. Biochem.* **1996**, 243, 228–233.
- [27] M. M. Corsaro, R. Lanzetta, E. Parrilli, M. Parrilli, M. L. Tutino, *Eur. J. Biochem.* **2001**, 268, 5092–5097.
- [28] S. Ummerino, M. M. Corsaro, R. Lanzetta, M. Parrilli, J. Peter-Katalinić, *Rapid Commun. Mass Spectrom.* **2003**, 17, 2226–2232.
- [29] S. Carillo, G. Pieretti, E. Parrilli, L. Tutino, S. Gemma, M. Molteni, R. Lanzetta, M. Parrilli, M. M. Corsaro, *Chem. Eur. J.* **2011**, 17, 7053–7060.
- [30] A. N. Kondakova, K. A. Novototskaya-Vlasova, N. P. Arbat-sky, M. S. Drutskaya, V. A. Shcherbakova, A. S. Shashkov, D. A. Gilichinsky, S. A. Nedospasov, Y. A. Knirel, *J. Nat. Prod.* **2012**, 75, 2236–2240.
- [31] A. N. Kondakova, K. A. Novototskaya-Vlasova, M. S. Drutskaya, S. N. Senchenkova, V. A. Shcherbakova, A. S. Shashkov, D. A. Gilichinsky, S. A. Nedospasov, Y. A. Knirel, *Carbohydr. Res.* **2012**, 349, 78–81.
- [32] I. Ciucanu, F. Kerek, *Carbohydr. Res.* **1984**, 131, 209–217.
- [33] G. Pieretti, S. Carillo, B. Lindner, K. K. Kim, K. C. Lee, J. S. Lee, R. Lanzetta, M. Parrilli, M. M. Corsaro, *Chem. Eur. J.* **2012**, 18, 3729–3735.

Received: January 7, 2013

Published Online: April 26, 2013

## Anti-biofilm activity of the Antarctic marine bacterium *Pseudoalteromonas haloplanktis* TAC125

Rosanna Papa<sup>a</sup>, Ermenegilda Parrilli<sup>b</sup>, Filomena Sannino<sup>b,c</sup>, Gaetano Barbato<sup>d</sup>,  
Maria Luisa Tutino<sup>b</sup>, Marco Artini<sup>a</sup>, Laura Selan<sup>a,\*</sup>

<sup>a</sup> Department of Public Health and Infectious Diseases, Sapienza University, Piazzale Aldo Moro 5, 00185 Rome, Italy

<sup>b</sup> Department of Chemical Sciences, Federico II University, Complesso Universitario Monte Sant'Angelo, Via Cinthia 4, 80126 Naples, Italy

<sup>c</sup> Institute of Protein Biochemistry, CNR, Via Pietro Castellino 111, 80131 Naples, Italy

<sup>d</sup> Department of Science and Chemical Technologies, University of Rome Tor Vergata, Via della Ricerca Scientifica 1, 00133 Rome, Italy

Received 24 September 2012; accepted 24 January 2013

Available online 11 February 2013

### Abstract

Considering the increasing impact of bacterial biofilms on human health, industrial and food-processing activities, the interest in the development of new approaches for the prevention and treatment of adhesion and biofilm formation capabilities has increased. A viable approach should target adhesive properties without affecting bacterial vitality in order to avoid the rapid appearance of escape mutants.

It is known that marine bacteria belonging to the genus *Pseudoalteromonas* produce compounds of biotechnological interest, including anti-biofilm molecules. *Pseudoalteromonas haloplanktis* TAC125 is the first Antarctic Gram-negative strain whose genome was sequenced. In this work the anti-biofilm activity of *P. haloplanktis* supernatant was examined on different staphylococci. Results obtained demonstrated that supernatant of *P. haloplanktis*, grown in static condition, inhibits biofilm of *Staphylococcus epidermidis*. In order to define the chemical nature of the biofilm-inhibiting compound, the supernatant was subject to various treatments. Data reported demonstrated that the biologically active component is sensible to treatment with sodium periodate suggesting its saccharidic nature.

© 2013 Institut Pasteur. Published by Elsevier Masson SAS. All rights reserved.

**Keywords:** Anti-biofilm; *Staphylococcus*; *Pseudoalteromonas*; Antarctic

### 1. Introduction

Biofilm is the predominant mode of growth for bacteria in most environments (Bendaoud et al., 2011) and particularly with respect to chronic infections (Dohar et al., 2009). They are relevant in a wide range of clinical domains including medicine and surgery (Francolini and Donelli, 2010) and food industry (Lequette et al., 2010). Biofilms also contaminate a wide variety of infrastructure elements such as water and air purification systems (Sublette et al., 2006), optical sensors

(Kerr et al., 1998), marine and industrial equipments (Holmstrom et al., 2002).

In medical settings, biofilms are the cause of persistent infections-implicated in 80% or more of all microbial cases-releasing harmful toxins and even obstructing indwelling catheters (Epstein et al., 2012) or causing orthopaedic implant infections (Drago et al., 2013). Staphylococci are recognized as the most frequent causes of biofilm-associated infections (Otto, 2008; Arciola et al., 2012). Taking into account the increasing impact of bacterial biofilms, the interest in the development of new approaches for the prevention and treatment of adhesion and biofilm formation capabilities has amplified. A viable approach should target adhesive properties without affecting bacterial vitality in order to avoid the rapid appearance of escape mutants. Many bacterial biofilms secrete molecules such as quorum sensing signals (Ni et al., 2009),

\* Corresponding author. Tel.: +39 0649694261; fax: +39 0649694298.

E-mail addresses: rosanna.papa@uniroma1.it (R. Papa), erparri1@uniroma1.it (E. Parrilli), mena.10@libero.it (F. Sannino), barbato.g@fastwebnet.it (G. Barbato), tutino@uniroma1.it (M.L. Tutino), marco.artini@uniroma1.it (M. Artini), laura.selan@uniroma1.it (L. Selan).

surfactants (Kiran et al., 2010), enzymes (Kaplan, 2010), and polysaccharides (Qin et al., 2009; Valle et al., 2006) that function regulating biofilm architecture or mediating the release of cells from biofilms during the dispersal stage of the biofilm life cycle (Kaplan, 2010).

These compounds often exhibit broad-spectrum biofilm-inhibiting or biofilm-detaching activity when tested against biofilms cultured *in vitro*. Such compounds may represent a novel source of anti-biofilm compounds for technological development.

Marine bacteria belonging to the genus *Pseudoalteromonas* produce compounds of biotechnological interest, including anti-biofilm molecules (Klein et al., 2011). Marine bacteria from Antarctica represent an untapped reservoir of biodiversity, indeed, Antarctic microorganisms can synthesize a broad range of potentially valuable bioactive compounds (Jayatilake et al., 1996).

*Pseudoalteromonas haloplanktis* TAC125 is the first Antarctic Gram-negative strain whose genome was sequenced (Medigue et al., 2005). Genomic and metabolic features of this strain, accounting for its remarkable versatility, were discovered by combining genome sequencing and further *in silico* and *in vivo* analyses. *P. haloplanktis* TAC125 was also the first Antarctic bacterium in which an efficient gene-expression technology was set up allowing the production of homologous and heterologous recombinant proteins (Rippa et al., 2012; Corchero et al., 2012). The host versatility was recently widened by the development of an efficient genetic scheme for the construction of genome targeted insertion/deletion mutants, which allows a deeper understanding of *P. haloplanktis* TAC125 physiology (Giuliani et al., 2012; Parrilli et al., 2010).

In this work we examined the anti-biofilm activity of *P. haloplanktis* culture supernatant, grown in static or in dynamic condition, on different *Staphylococcus epidermidis* and *Staphylococcus aureus* strains. *P. haloplanktis* TAC125 secreted an anti-biofilm activity which impaired biofilm development of *S. epidermidis*. Results obtained demonstrated that the cell-free supernatants of *P. haloplanktis* grown in static condition strongly inhibited bacterial adhesion. In particular, *S. epidermidis* showed the highest susceptibility to the treatment. This strong inhibitory effect was also observed on the mature biofilm of *S. epidermidis*. Interestingly, the *P. haloplanktis* supernatant was devoid of antibacterial activity against free-

living bacteria, showing that its activity was specifically directed against biofilm. The chemical nature of the biofilm-inhibiting compound was preliminarily determined using various treatments. Treatment with sodium periodate impaired *P. haloplanktis* supernatant capacity to inhibit biofilm formation suggesting that the biologically active component could be a polysaccharide.

## 2. Materials and methods

### 2.1. Bacterial strains and culture conditions

Bacterial strains used in this work are listed in Table 1. Bacteria were grown in Brain Heart Infusion broth (BHI, Oxoid, UK). Biofilm formation was assessed in static assay and planktonic cultures were performed under vigorous agitation (180 rpm). *P. haloplanktis* TAC125 was grown at 4 °C while staphylococci were grown at 37 °C.

### 2.2. Biofilm formation of *P. haloplanktis* TAC125

Biofilm formation of *P. haloplanktis* TAC125 was obtained at 4 °C in Brain Heart Infusion broth (BHI, Oxoid, UK). The wells of a sterile 24-well flat-bottomed polystyrene plate were filled with 1 ml of BHI, and an opportune dilution of Antarctic bacterial culture in exponential growth phase (about 0.1 OD 600 nm) was added into each well. The plates were aerobically incubated for 96 h at 4 °C. After rinsing with PBS, adhered cells were stained with 0.1% crystal violet, rinsed twice with double-distilled water, and thoroughly dried as previously described (Christensen et al., 1985). The dye bound to adherent cells was resuspended with 20% (v/v) glacial acetic acid and 80% (v/v) ethanol per well. The OD of each well was measured at 590 nm. Each data point is composed of three independent samples.

### 2.3. Preparation of *P. haloplanktis* TAC125 supernatants

SN4B is the supernatant of a liquid culture of *P. haloplanktis* TAC125 grown without shaking (biofilm) and SN4A is the supernatant of a liquid culture of *P. haloplanktis* TAC125 grown with shaking (planktonic growth), respectively.

Table 1  
Strains used in this study.

Strain	Origin	Reference and/or source
<i>P. haloplanktis</i> TAC125	Antarctic sea water <sup>a</sup>	Medigue et al., 2005
<i>S. aureus</i> 6538P	Clinical isolate	ATCC collection
<i>S. aureus</i> 25923	Clinical isolate	ATCC collection
<i>S. aureus</i> 20372	Clinical isolate from septic arthritis	ATCC collection
<i>S. aureus</i> 1511	Clinical isolate from infected catheter	Our collection
<i>S. epidermidis</i> RP62A	Reference strain isolated from infected catheter	ATCC collection
<i>S. epidermidis</i> O-47	Clinical isolate from septic arthritis	Heilmann et al., 1996
<i>S. epidermidis</i> XX-17	Clinical isolate from infected catheter	Our collection
<i>S. epidermidis</i> 1521	Clinical isolate from infected catheter	Our collection

<sup>a</sup> Isolated from Antarctic coastal sea water sample collected in the vicinity of the French Antarctic station Dumont d'Urville, Terre Adélie (66°40' S; 140° 01' E).



### 2.3.1. Preparation of SN4B

The wells of a sterile 24-well flat-bottomed polystyrene plate were filled with 900  $\mu$ l of BHI and 100  $\mu$ l of overnight *P. haloplanktis* TAC125 bacterial culture was added into each well. The plates were incubated at 4 °C monitoring biofilm formation each 24 h. After 96 h, supernatant was recovered and centrifuged at 13,000 rpm. Supernatant was then transferred into a Centricon tube (Millipore, Billerica, MA, USA) with 10 kDa MWCO. It was 10-fold concentrated by centrifugation at 4000 rpm, 4 °C. Supernatant was sterilized by filtration through membranes with a pore diameter of 0.22  $\mu$ m, and stored at 4 °C until use.

### 2.3.2. Preparation of SN4A

*P. haloplanktis* TAC125 bacterial culture was grown in planktonic form at 4 °C under vigorous agitation (180 rpm). Supernatant was recovered by centrifugation at 13,000 rpm at 4 °C and processed as above described.

### 2.4. Biofilm formation of staphylococci

Biofilm formation of staphylococcal species was evaluated in the presence of SN4A and SN4B supernatants. Quantification of *in vitro* biofilm production was based on method previously reported (Artini et al., 2011). Briefly, the wells of a sterile 48-well flat-bottomed polystyrene plate were filled with 400  $\mu$ l of the appropriate medium. 1/100 dilution of overnight bacterial cultures was added into each well. The first row contained the untreated bacteria, while each of the remaining rows contained serial dilutions of SN4A and SN4B starting from 1:2. The plates were incubated aerobically for 24 h at 37 °C. After rinsing with PBS, adhered cells were stained with 0.1% crystal violet, rinsed twice with double-distilled water, and thoroughly dried as previously described (Christensen et al., 1985). The dye bound to adherent cells was resuspended with 20% (v/v) glacial acetic acid and 80% (v/v) ethanol per well. The OD of each well was measured at 590 nm. Each data point is composed of three independent samples.

Assay on preformed biofilm was also performed. The wells of a sterile 48-well flat-bottomed polystyrene plate were filled with 400  $\mu$ l of 1/100 diluted overnight bacterial cultures grown in BHI. The plates were aerobically incubated for 24 h at 37 °C. After 24 h the content of the plates was poured off and the wells washed with sterile distilled water to remove the unattached bacteria. The remaining attached bacteria were treated with 400  $\mu$ l of the appropriate medium containing serial dilution of SN4A and SN4B (starting from 100%) aerobically incubated for 2, 4, 8 and 24 h at 37 °C. After each time-point the plates were treated as previously described. Each data point is composed of four independent samples.

### 2.5. Initial attachment assay

The attachment assay was carried out as previously reported with slight modifications (Nithya and Pandian, 2010). Overnight cultures were diluted 1/100 in BHI and grown at 37 °C up

to reaching 0.5 OD ml<sup>-1</sup>. The wells of a sterile 48-well flat-bottomed polystyrene plate were filled with 100  $\mu$ l of bacterial cultures and 300  $\mu$ l of the appropriate medium containing serial dilution of SN4B. The assay was carried out for 1 h at 37 °C to allow the cells to adhere to the surface. After incubation, the plates were processed as previously described. Each data point is composed of four independent samples.

### 2.6. Physico-chemical characterization of SN4B anti-biofilm compound

To examine the heat sensitivity, the culture supernatants were incubated for 1 h in a water bath at 50 °C and cooled on ice. For the protease treatment, proteinase K (Sigma Aldrich, St Louis, MO) was added to SN4B at a final concentration of 1 mg ml<sup>-1</sup> and the reactions were incubated for 1 h at 37 °C. As controls, SN4B was incubated for 1 h at 37 °C without proteinase K, which did not impair the anti-biofilm activities. For the polysaccharide treatment, NaIO<sub>4</sub> at a final concentration of 20 mM was added to supernatant for 12 h at 37 °C. As controls the same treatment was performed on BHI broth to exclude an anti-biofilm effect due to the NaIO<sub>4</sub>. For each of the above tests, the anti-biofilm activities of treated and untreated culture supernatants were compared using the microtiter plate assay against *S. epidermidis* O-47. Each data point is composed of four independent samples.

## 3. Results

### 3.1. Effect of *P. haloplanktis* TAC125 exoproducts on biofilm formation of staphylococci

Biofilm formation of *P. haloplanktis* TAC125 was evaluated at 4 °C in BHI with over a 96 h period. *P. haloplanktis* TAC125 was grown in the same medium used for staphylococci cultures to avoid interference due to the medium composition. The best production (more than about 2.5 OD 590 nm) of *P. haloplanktis* TAC125 biofilm was obtained incubating the cells in static for 96 h at 4 °C (data not shown).

The effects of filter sterilized supernatants of *P. haloplanktis* TAC125 cultures grown in planktonic and sessile form at 4 °C on different *S. epidermidis* and *S. aureus* strains (Table 1) were examined. SN4B was defined the supernatant of *P. haloplanktis* deriving from static growth and SN4A the supernatant of *P. haloplanktis* liquid culture grown in dynamic condition, respectively. Preliminary experiments were carried out to assess the effect of supernatants on the growth rate of *S. epidermidis* and *S. aureus*. Bacterial cultures were separately treated with SN4B and SN4A supernatants at a concentration of 50% and growths were monitored over 24 h. In Fig. 1A the growth curves of *S. epidermidis* O-47 in the presence and in the absence of above described supernatants were reported. As shown, SN4B and SN4A did not affect *S. epidermidis* duplication rate. Bacterial growth curves were found to be nearly superimposable both in the presence and in the absence of supernatants. Same results were obtained evaluating the effect

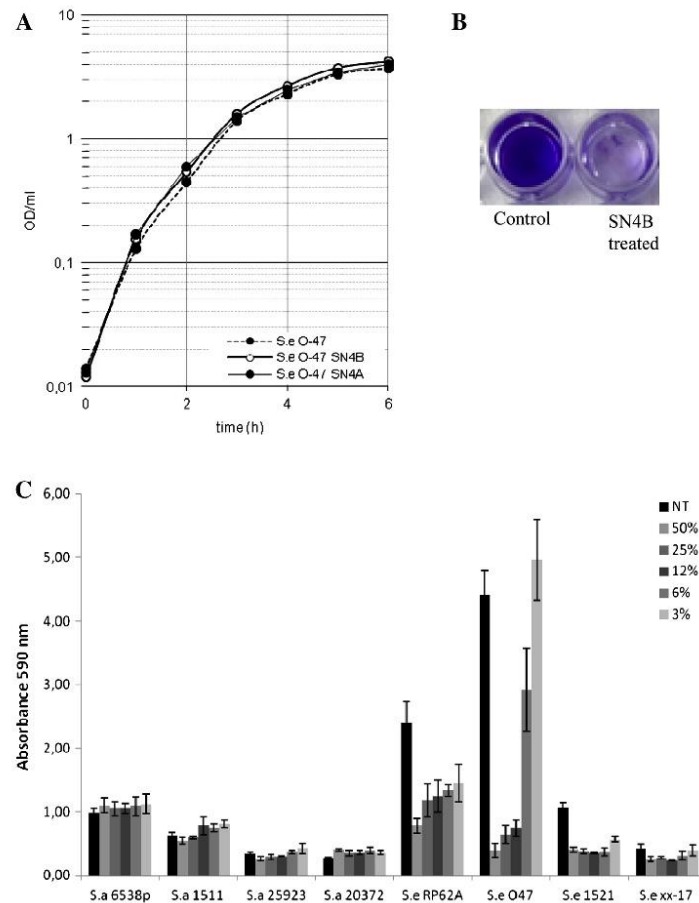


Fig. 1. Inhibition of *S. aureus* and *S. epidermidis* biofilm formation by *P. haloplanktis* TAC125 SN4B supernatant. (A) Growth curves of *S. epidermidis* O-47 in the presence and in the absence of 50% SN4B or SN4A supernatant. Growth was monitored by measuring the absorbance of the cultures at 600 nm. (B) Biofilm formation by *S. epidermidis* O-47 in 48-well microtiter plate wells in the presence and in the absence of 50% SN4B supernatant. (C) Effect of SN4B treatment on biofilm formation for each staphylococcal strain. SN4B supernatant was tested using serial dilutions starting from 1:2 (50%). Each data point represents the mean  $\pm$  SD of three independent experiments. *S. a.*, *S. aureus* species; *S. e.*, *S. epidermidis* species.

of SN4B and SN4A supernatants on the *S. aureus* growth rate (data not shown).

SN4A and SN4B supernatants effect on biofilm production of staphylococci was evaluated and the SN4B supernatant showed to have a good anti-biofilm effect on *S. epidermidis* species (Fig. 1B) while it did not have effect on *S. aureus* species (Fig. 1C). By contrast SN4A did not show any inhibitory effect on tested strains (data not shown). SN4B had a similar effect on all *S. epidermidis* strains tested showing a species-specific effect. The inhibitory effect is clearly dose-dependent with an efficacy higher than 50% already at 1:8 dilution (17% residual biofilm for *S. epidermidis* O-47).

Attachment behaviour of *S. epidermidis* biofilm formation, in the presence and in the absence of SN4B culture

supernatant was investigated. Initial attachment of the bacteria to a solid surface is the first step in biofilm formation. As reported in Fig. 2 SN4B culture supernatant at a concentration of 50% decreased the attachment of *S. epidermidis* and this effect was more pronounced on strongest biofilm former strain O-47 (biofilm reduction of about 40%).

### 3.2. *P. haloplanktis* TAC125 exoproducts impair mature biofilm of *S. epidermidis*

The effect of SN4B on *S. epidermidis* mature biofilm was also tested. Single-species mature biofilm of *S. epidermidis* RP62A and *S. epidermidis* O-47 was separately treated with serial dilutions of SN4B starting from a concentration of 100%.

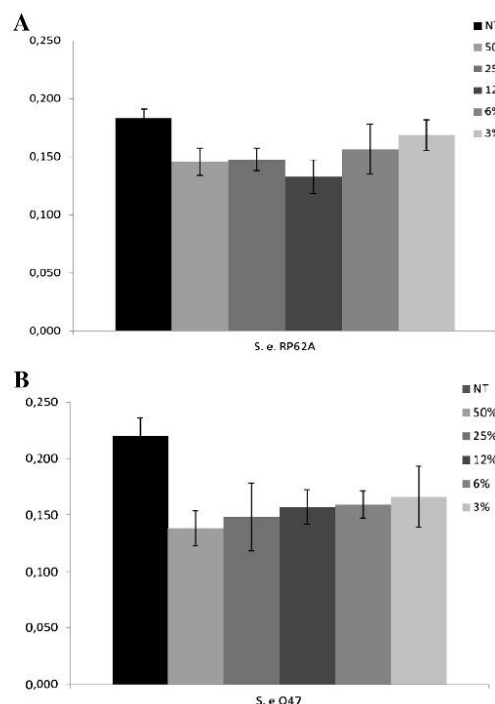


Fig. 2. Effect of SN4B supernatant on initial attachment of *S. epidermidis* species. Bacteria were treated with serial dilution of SN4B starting from 50%. Each data point is composed of four independent samples.

The effect on preformed biofilm was evaluated at different treatment time, SN4B supernatant didn't disaggregate the *S. epidermidis* mature biofilm after 2, 4, and 8 h (data not shown) but it was able to impair mature biofilm of *S. epidermidis* after 24 h of treatment (Fig. 3). Indeed, the results showed a significant reduction in the absorbance of the treated samples, demonstrating that SN4B was also extremely effective in the dispersal of *S. epidermidis* preformed biofilm (*S. epidermidis* O-47 untreated bacteria OD 590 nm =  $1.863 \pm 0.219$ ; SN4B-treated bacteria OD 590 nm =  $0.457 \pm 0.122$ ) (Fig. 3). This result suggested that the supernatant action was not restricted to initial bacterial attachment on abiotic surface but was also effective on mature biofilm.

### 3.3. Physico-chemical characterization of *P. haloplanktis* TAC125 anti-biofilm compounds

To have information about the chemical nature of the biofilm-inhibiting compound, SN4B supernatant was dispensed in several aliquots, each submitted to different chemical and physical treatments. Percentage of inhibition of each treated aliquot of SN4B was determined against *S. epidermidis* O-47 (Table 2). Neither proteinase K treatment nor heat

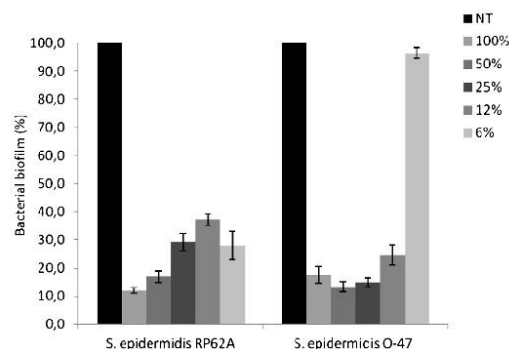


Fig. 3. Effect of SN4B supernatant on 24 h biofilm of *S. epidermidis* species. Data are reported as percentage of residual biofilm. The mature biofilm was treated with serial dilution of SN4B starting from 100%. Each data point is composed of four independent samples.

treatment affected the biofilm-inhibiting activity of SN4B (Table 2). The biofilm-inhibiting material was heat stable, in fact it retained about 91.5% of its inhibitory activity after 1 h at 50 °C. Treatment of SN4B supernatant sodium metaperiodate significantly reduced its biofilm-inhibiting activity (about 5% of residual activity). It has been shown that  $\text{NaIO}_4$  is able to hydrolyse compounds by oxidizing the carbons bearing vicinal hydroxyl groups and cleaving the C–C bonds, this hydrolytic activity was demonstrated also against polysaccharides (Bendaoud et al., 2011). These data suggested that the biologically active component could be a polysaccharide.

## 4. Discussion

Disrupting the multicellular structure of bacterial biofilm was proposed as the most promising strategy for increasing the sensitivity of pathogens in biofilm to antibiotics and host immune systems (Costerton and Stewart, 2001). The rationale of this work is to look for new compounds inhibiting virulence rather than bacterial growth; in fact this choice may impose a weaker selective pressure for the development of antibiotic resistance relative to current antibiotics. Moreover, even in this era of combinatorial chemistry, compounds from natural origin still provide a high number of interesting structures.

Marine bacteria produce several compounds which may be of potential biotechnological interest, and in particular culture supernatants derived from most of them have been shown to

Table 2  
Effect of various treatments on the anti-biofilm activity of SN4B.

Treatment	Percentage of residual biofilm <sup>a</sup>
None	0 ± 5.2
50 °C, 1 h	8.5 ± 0.7
Proteinase K, 1 h at 37 °C	24.3 ± 2.2
$\text{NaIO}_4$ , 12 h at 37 °C	94.7 ± 9.6

<sup>a</sup> Inhibition of SN4B was determined against *S. epidermidis* O-47 using the microtiter plate assay and was reported as percentage of residual biofilm after the treatment. The values were calculated from four replicates.



exhibit anti-biofilm activity against both Gram positive and Gram negative bacteria, including *Acinetobacter*, *S. aureus*, *Salmonella typhimurium*, *Shigella sonnei*, *Listeria monocytogenes* and several *Bacillus* species (Rendueles et al., 2013).

Antarctic marine bacterium *P. haloplanktis* TAC125 has several genes and operons that may play an important role in colonization of both biotic and abiotic surfaces (Medigue et al., 2005) and in the experimental conditions here used a strong biofilm formation on polystyrene plates was observed. In this work we examined the anti-biofilm activity of cell-free supernatant of *P. haloplanktis* grown in sessile and in planktonic condition on different staphylococci. Results obtained demonstrated that only supernatant of *P. haloplanktis* grown in static condition (SN4B) inhibits biofilm of *S. epidermidis*. This latter result could be explained in consideration that specific environmental conditions prevailing within biofilms may induce profound genetic and metabolic rewiring of the biofilm-dwelling bacteria (Beloin and Ghigo, 2005). This could lead to production of biofilm-specific metabolites or polymers, some of which may also exhibit an antagonist effect over competing microorganisms. Consistent with this hypothesis, several anti-biofilm molecules have been identified in cell-free extracts isolated directly from mature *in vitro* cultured biofilms (Rendueles et al., 2013). Although it has been considered that SN4B supernatant derived from a static growth where could coexist both planktonic and biofilm phenotypes. Thus the active compounds could be produced by the planktonic cells stimulated by the oxygen limitation since bacteria are grown without shaking.

It is interesting to note that previously characterized anti-biofilm compounds have often a broad-spectrum biofilm inhibition activity (Bendaoud et al., 2011; Klein et al., 2011; Rendueles et al., 2013) while the *P. haloplanktis* TAC125 anti-biofilm molecule seemed to be species-specific. *P. haloplanktis* TAC125 supernatant is, in fact, inactive against biofilm of *S. aureus* and *Pseudomonas aeruginosa* (data not shown).

Most of the known anti-biofilm molecules are also antibacterial (bactericidal or bacteriostatic). By contrast, *P. haloplanktis* TAC125 supernatant lacks of antibacterial activity against free-living bacteria, making its activity specifically directed against biofilms. Very few natural molecules were reported to display anti-biofilm activity without being also antibacterial. Such molecules could be polysaccharides (Valle et al., 2006), biosurfactants (Das et al., 2009), or quorum sensing inhibitors (Rasmussen and Givskov, 2006; Estrela et al., 2009).

Since the *P. haloplanktis* TAC125 anti-biofilm molecule has been shown to exhibit no bacteriostatic nor bactericidal activity, its anti-biofilm activity is likely to be mediated by mechanisms other than growth inhibition. There are three hypothetical non-antibacterial modes of action.

The first hypothesis is that the anti-biofilm molecule could act as a surfactant molecule that modifies the physical characteristics of bacterial cells and abiotic surfaces. Another possible mode of action is competitive inhibition of multivalent carbohydrate–protein interactions (Wittschier et al., 2007). Thus, the anti-biofilm compound might block lectins or sugar binding proteins present on the surface of bacteria, or block tip adhesins of fimbriae and pili (Zinger-Yosovich and Gilboa-Garber,

2009). The third hypothesis is that the *P. haloplanktis* TAC125 anti-biofilm compound might act as a signalling molecule that modulates the gene expression of recipient bacteria (Kim et al., 2009). Indeed, bacterial communication is one of the regulatory mechanisms suggested to be involved in biofilm formation (Parsek and Greenberg, 2005).

The results of the initial attachment assay indicate that the culture supernatant SN4B inhibited the biofilm formation by contrasting the initial attachment of bacterial cells to the surface.

Moreover the results here obtained demonstrated that the *P. haloplanktis* TAC125 anti-biofilm action is effective on mature biofilm, it is interesting to note that the action on mature biofilm is not immediate but requires a prolonged time. This latter result suggests that the anti-biofilm compound could act as a signal that downregulated the adhesive properties of the cell surface or the biofilm matrix rather than a surfactant that rapidly carries its action.

There are different bacterial communication systems, both strict intraspecific and interspecific systems. One system suggested to serve as a bacterial intra- and interspecies communication system uses the autoinducer-2 (AI-2) produced by *luxS* gene, as a signalling molecule (Federle and Bassler, 2003; Yoshida et al., 2005). *LuxS* has also been identified in *S. epidermidis* (Xu et al., 2006; Li et al., 2008), but *P. haloplanktis* TAC125 genome analysis revealed that the Antarctic bacterium is devoid of *luxS* gene (Medigue et al., 2005) suggesting the anti-biofilm activity could be due to a not identified signalling molecule.

The anti-biofilm effects of *P. haloplanktis* exoproducts could be due to a novel molecule or the synergistic actions of different molecules. A preliminary physico-chemical characterization of SN4B supports the hypothesis of a compound of polysaccharide nature because treatment with periodate impaired its capacity to inhibit biofilm formation.

It is well known that bacterial exopolysaccharides exhibit highly variable structures and it is likely that they also perform additional functions besides their implied function in matrix stabilization and energy storage (Rendueles et al., 2013). In fact, several studies showed that certain bacterial mutants deficient in capsular polysaccharide production exhibit increased biofilm formation (Valle et al., 2006; Flahaut et al., 2008). These observations suggest that some bacterial exopolysaccharides can perform functions that inhibit or destabilize the biofilm. Understanding the mode of action of SN4B will require identification of the active molecules.

Since *S. epidermidis* is the main microorganism responsible for most of the chronic graft infections, medical applications could be proposed. The present study was intended at obtaining new molecules with anti-adhesive properties whose use could be proposed during persistent infection sustained by staphylococci in combination therapy with antibiotics.

#### Acknowledgements

This work was supported by P.N.R.A. (Programma Nazionale di Ricerche in Antartide 2009–2011) and by Pharmasea PF7 2012–16.

## References

- Arciola, C.R., Hänsch, G.M., Visai, L., Testoni, F., Maurer, S., Campoccia, D., Selan, L., Montanaro, L., 2012. Interactions of staphylococci with osteoblasts and phagocytes in the pathogenesis of implant-associated osteomyelitis. *Int. J. Artif. Organs* 35, 713–726.
- Artini, M., Scoarughi, G.L., Papa, R., Cellini, A., Carpentieri, A., Pucci, P., Amoresano, A., Gazzola, S., Cocconcelli, P.S., Selan, L., 2011. A new anti-infective strategy to reduce adhesion-mediated virulence in *Staphylococcus aureus* affecting surface proteins. *Int. J. Immunopathol. Pharmacol.* 24, 661–672.
- Beloin, C., Ghigo, J.M., 2005. Finding gene-expression patterns in bacterial biofilms. *Trends Microbiol.* 13, 16–19.
- Bendaoud, M., Vinogradov, E., Balashova, N.V., Kadouri, D.E., Kachlany, S.C., Kaplan, J.B., 2011. Broad-spectrum biofilm inhibition by *Kingella kingae* exopolysaccharide. *J. Bacteriol.* 193, 3879–3886.
- Christensen, G.D., Simpson, W.A., Younger, J.J., Baddour, L.M., Barrett, F.F., Melton, D.M., Beachey, E.H., 1985. Adherence of coagulase-negative staphylococci to plastic tissue culture plates: a quantitative model for the adherence of staphylococci to medical devices. *J. Clin. Microbiol.* 22, 996–1006.
- Corchero, J.L., Gasser, B., Resina, D., Smith, W., Parrilli, E., Vázquez, F., Abasolo, I., Giuliani, M., Jäntti, J., Ferrer, P., Saloheimo, M., Mattanovich, D., Schwartz Jr., S., Tutino, L., Villaverde, A., 2012. Unconventional microbial systems for the cost-efficient production of high-quality protein therapeutics. *Biotechnol. Adv.* <http://dx.doi.org/10.1016/j.biotechadv.2012.09.001>
- Costerton, J.W., Stewart, P.S., 2001. Battling biofilms—the war is against bacterial colonies that cause some of the most tenacious infections known. The weapon is knowledge of the enemy's communication system. *Sci. Am.* 285, 74–81.
- Das, P., Mukherjee, S., Sen, R., 2009. Antiadhesive action of a marine microbial surfactant. *Colloids Surf. B. Biointerfaces* 71, 183–186.
- Dohar, J.E., Hebda, P.A., Veeh, R., Awad, M., Costerton, J.W., Hayes, J., Ehrlich, G.D., 2009. Mucosal biofilm formation on middle-ear mucosa in a nonhuman primate model of chronic suppurative otitis media. *The Laryngoscope* 115, 1469–1472.
- Drago, L., Vecchi, E.D., Mattina, R., Romanò, C.L., 2013. Activity of N-acetyl-L-cysteine against biofilm of *Staphylococcus aureus* and *Pseudomonas aeruginosa* on orthopedic prosthetic materials. *Int. J. Artif. Organs* (Epub ahead of print).
- Epstein, A.K., Wong, T.S., Belisle, R.A., Boggs, E.M., Aizenberg, J., 2012. Liquid-infused structured surfaces with exceptional anti-biofouling performance. *Proc. Natl. Acad. Sci. U.S.A.* 109, 13182–13187.
- Estrela, A.B., Heck, M.G., Abraham, W.R., 2009. Novel approaches to control biofilm infections. *Curr. Med. Chem.* 16, 1512–1530.
- Federle, M.J., Bassler, B.L., 2003. Interspecies communication in bacteria. *J. Clin. Invest.* 112, 1291–1299.
- Flahaut, S., Vinogradov, E., Kelley, K.A., Brennan, S., Hiramoto, K., Lee, J.C., 2008. Structural and biological characterization of a capsular polysaccharide produced by *Staphylococcus haemolyticus*. *J. Bacteriol.* 190, 1649–1657.
- Francolini, I., Donelli, G., 2010. Prevention of biofilm-based medical-device-related infections. *FEMS Immunol. Med. Microbiol.* 59, 227–238.
- Giuliani, M., Parrilli, E., Pezzella, C., Rippa, V., Duilio, A., Marino, G., Tutino, M.L., 2012. A novel strategy for the construction of genomic mutants of the Antarctic bacterium *Pseudoalteromonas haloplanktis* TAC125. *Methods Mol. Biol.* 824, 219–233.
- Heilmann, C., Gerke, C., Perdreau-Remington, F., Götz, F., 1996. Characterization of Tn917 insertion mutants of *Staphylococcus epidermidis* affected in biofilm formation. *Infect. Immun.* 64, 277–282.
- Holmstrom, C., Egan, S., Franks, A., McCloy, S., Kjelleberg, S., 2002. Antifouling activities by marine surface associated *Pseudoalteromonas* species. *FEMS Microbiol. Ecol.* 41, 47–58.
- Jayatilake, G.S., Thornton, M.P., Leonard, A.C., Grimwade, J.E., Baker, B.J., 1996. Mar. Metabolites from an Antarctic sponge-associated bacterium, *Pseudomonas aeruginosa*. *J. Nat. Prod.* 59 (3), 293–296. PubMed PMID: 8882433.
- Kaplan, J.B., 2010. Biofilm dispersal: mechanisms, clinical implications and potential therapeutic uses. *J. Dent. Res.* 89, 205–218.
- Kerr, A., Cowling, M.J., Beveridge, C.M., Smith, M.J., Parr, A.C.S., 1998. The early stages of marine biofouling and its effect on two types of optical sensors. *Environ. Int.* 24, 331–343.
- Kim, H.S., Kim, S.M., Lee, H.J., Park, S.J., Lee, K.H., 2009. Expression of the *cpdA* gene, encoding a 3',5'-cyclic AMP (cAMP) phosphodiesterase, is positively regulated by the cAMP-cAMP receptor protein complex. *J. Bacteriol.* 191, 922–930.
- Kiran, G.S., Sabarathnam, B., Selvin, J., 2010. Biofilm disruption potential of a glycolipid biosurfactant from marine *Brevibacterium casei*. *FEMS Immunol. Med. Microbiol.* 59, 432–438.
- Klein, G.L., Soum-Soutéra, E., Guede, Z., Bazire, A., Compère, C., Dufour, A., 2011. The anti-biofilm activity secreted by a marine *Pseudoalteromonas* strain. *Biofouling* 27, 931–940.
- Lequette, Y., Boels, G., Clarisse, M., Faille, C., 2010. Using enzymes to remove biofilms of bacterial isolates sampled in the food-industry. *Biofouling* 26, 421–431.
- Li, M., Villaruz, A.E., Vadyvaloo, V., Sturdevant, D.E., Otto, M., 2008. AI-2-dependent gene regulation in *Staphylococcus epidermidis*. *BMC Microbiol.* 8, 4.
- Médigue, C., Krin, E., Pascal, G., Barbe, V., Bernsel, A., Bertin, P.N., Cheung, F., Cruveiller, S., D'Amico, S., Duilio, A., Fang, G., Feller, G., Ho, C., Mangelot, S., Marino, G., Nilsson, J., Parrilli, E., Rocha, E.P., Rouy, Z., Sekowska, A., Tutino, M.L., Vallenet, D., von Heijne, G., Danchin, A., 2005. Coping with cold: the genome of the versatile marine Antarctica bacterium *Pseudoalteromonas haloplanktis* TAC125. *Genome Res.* 15, 1325–1335.
- Ni, N., Li, M., Wang, J., Wang, B., 2009. Inhibitors and antagonists of bacterial quorum sensing. *Med. Res. Rev.* 29, 65–124.
- Nithya, C., Pandian, S.K., 2010. The in vitro activity of selected marine bacterial culture supernatants against *Vibrio* spp. *Arch. Microbiol.* 192, 843–854.
- Otto, M., 2008. Staphylococcal biofilm. *Curr. Top. Microbiol. Immunol.* 322, 207–228.
- Parrilli, E., Giuliani, M., Giordano, D., Russo, R., Marino, G., Verde, C., Tutino, M.L., 2010. The role of a 2-on-2 haemoglobin in oxidative and nitrosative stress resistance of Antarctic *Pseudoalteromonas haloplanktis* TAC125. *Biochimie* 92, 1003–1009.
- Parsek, M.R., Greenberg, E.P., 2005. Sociomicrobiology: the connections between quorum sensing and biofilms. *Trends Microbiol.* 13, 27–33.
- Qin, Z., Yang, L., Qu, D., Molin, S., Tolker-Nielsen, T., 2009. *Pseudomonas aeruginosa* extracellular products inhibit staphylococcal growth, and disrupt established biofilms produced by *Staphylococcus epidermidis*. *Microbiology* 155, 2148–2156.
- Rasmussen, T.B., Givskov, M., 2006. Quorum-sensing inhibitors as anti-pathogenic drugs. *Int. J. Med. Microbiol.* 296, 149–161.
- Rendueles, O., Kaplan, J.B., Ghigo, J.M., 2013. Antibiofilm polysaccharides. *Environ. Microbiol.* 15, 334–346.
- Rippa, V., Papa, R., Giuliani, M., Pezzella, C., Parrilli, E., Tutino, M.L., Marino, G., Duilio, A., 2012. Regulated recombinant protein production in the Antarctic bacterium *Pseudoalteromonas haloplanktis* TAC125. *Methods Mol. Biol.* 824, 203–218.
- Sublette, K., Peacock, A., White, D., Davis, G., Ogles, D., Cook, D., Kolhatkar, R., Beckmann, D., Yang, X., 2006. Monitoring subsurface microbial ecology in a sulfate-amended, gasoline-contaminated aquifer. *Ground Water Monit. R* 26, 70–78.
- Valle, J., Da Re, S., Henry, N., Fontaine, T., Balestrino, D., Latour-Lambert, P., Ghigo, J.M., 2006. Broad-spectrum biofilm inhibition by a secreted bacterial polysaccharide. *Proc. Natl. Acad. Sci. U.S.A.* 103, 12558–12563.
- Wittschier, N., Lengsfeld, C., Vorthems, S., Stratmann, U., Ernst, J.F., Verspohl, E.J., Hensel, A., 2007. Large molecules as anti-adhesive compounds against pathogens. *J. Pharm. Pharmacol.* 59, 777–786.
- Xu, L., Li, H., Vuong, C., Vadyvaloo, V., Wang, J., Yao, Y., Otto, M., Gao, Q., 2006. Role of the luxS quorum-sensing system in biofilm formation and virulence of *Staphylococcus epidermidis*. *Infect. Immun.* 74, 488–496.
- Yoshida, A., Ansai, T., Takehara, T., Kuramitsu, H.K., 2005. LuxS-based signaling affects *Streptococcus mutans* biofilm formation. *Appl. Environ. Microbiol.* 71, 2372–2380.
- Zinger-Yosovich, K.D., Gilboa-Garber, N., 2009. Blocking of *Pseudomonas aeruginosa* and *Ralstonia solanacearum* lectins by plant and microbial branched polysaccharides used as food additives. *J. Agric. Food Chem.* 57, 6908–6913.



## Recombinant production of a single-chain antibody fragment in *Pseudoalteromonas haloplanktis* TAC125

Maria Giuliani · Ermenegilda Parrilli ·  
Filomena Sannino · Gennaro Antonio Apuzzo ·  
Gennaro Marino · Maria Luisa Tutino

Received: 22 November 2013 / Revised: 24 January 2014 / Accepted: 28 January 2014 / Published online: 18 February 2014  
© Springer-Verlag Berlin Heidelberg 2014

**Abstract** Recombinant protein production in cold-adapted bacteria has proved to be a valuable option to overcome solubility concerns often came up in conventional expression hosts. ScFvs are examples of “difficult proteins” due to their tendency to form inclusion bodies when expressed in *Escherichia coli*. In this paper, the recombinant production of a single-chain antibody (ScFvOx) in the psychrophilic bacterium *Pseudoalteromonas haloplanktis* TAC125 is reported. The expression vector for the ScFvOx production was designed to address the recombinant protein in the periplasmic space and to allow the formation of the antibody disulphide bonds. For periplasmic export, two different export mechanisms were evaluated. By combining the genetic tools available for recombinant protein expression in psychrophilic hosts with an ad hoc medium and fermentation modality and optimised expression conditions at low temperatures, we obtained the highest yield of soluble and epitope-binding ScFvOx reported so far by conventional prokaryotic

expression. The observed proficiency of the Antarctic bacterium to produce recombinant antibody fragments was related to the unusually high number of genes encoding peptidyl prolyl *cis-trans* isomerases found in *P. haloplanktis* TAC125 genome, making this bacterium the host of choice for the recombinant production of this protein class.

**Keywords** scFvOx · Single-chain antibody · *Pseudoalteromonas haloplanktis* TAC125 · Psychrophilic gene expression system

### Introduction

Protein-engineering technology led to the development of different formats of monoclonal antibody variable fragments that can effectively replace the corresponding whole molecule

**Electronic supplementary material** The online version of this article (doi:10.1007/s00253-014-5582-1) contains supplementary material, which is available to authorized users.

M. Giuliani · E. Parrilli · F. Sannino · G. A. Apuzzo · G. Marino ·  
M. L. Tutino  
Dipartimento di Scienze Chimiche, Università di Napoli “Federico  
II”, Via Cinthia, 4, 80126 Naples, Italy

M. Giuliani  
e-mail: maria.giuliani@gmail.com

E. Parrilli  
e-mail: erparril@unina.it

F. Sannino  
e-mail: filomena.sannino2@unina.it

G. A. Apuzzo  
e-mail: gen.apuzzo@gmail.com

G. Marino  
e-mail: gmarino@unina.it

F. Sannino  
Consiglio Nazionale delle Ricerche, Istituto di Biochimica delle  
Proteine, Via P. Castellino, 111, 80134 Naples, Italy

M. L. Tutino (✉)  
Dipartimento di Scienze Chimiche, Università di Napoli “Federico  
II”, Complesso universitario Monte Sant’Angelo, Via Cintia,  
80126 Naples, Italy  
e-mail: tutino@unina.it

**Present Address:**  
M. Giuliani  
Novartis Vaccines and Diagnostics, Via Fiorentina, 1, 53100 Siena,  
Italy



in many applications, but exhibiting a reduced structural complexity.

Single-chain variable fragment (scFv) is the minimal fragment (~30 kDa) that still retains the active antigen-binding unit of immunoglobulin molecules. Clinical applications require the availability of large amount of functional and cost-effective scFvs. However, the recombinant production in the conventional bacterial host *Escherichia coli* of this protein family exhibits several issues, due to scFvs tendency to form insoluble aggregates when overproduced in *E. coli* (Somerville et al. 1994). To overcome these issues, several approaches have been explored with some success, including their co-expression with molecular chaperones or folding catalysts (Levy et al. 2013), due to the notable observation that immunoglobulin folding kinetics may be slowed down by *cis-trans* isomerisation of Xaa-proline bond (Feige et al. 2010), or the lowering of expression temperature. This latter approach is often applied when the recombinant products accumulate into the inclusion bodies (IB) (Baneyx 1999), since low temperature minimise hydrophobic interactions (Yang et al. 1992), which are the drive force involved in IB formation (Carrio et al. 2005). However, *E. coli* cultivation at sub-optimal temperatures generally results in decrease in biomass productivity, due to the temperature downshift effect on the bacterial specific growth rate, and may induce the cold-shock response (Coleman et al. 2003). On the contrary, the use of naturally cold-adapted bacteria as host for recombinant protein production may represent an effective alternative to enhance conformational quality and solubility of pharmaceutical protein products.

In this context, the marine bacterium *Pseudoalteromonas haloplanktis* TAC125 is one of the few cold-adapted bacterial species under intense investigation. Some of its physiological and metabolic properties make this Antarctic Gram-negative microorganism a promising cold cell factory. As an example, it is one of the fastest growing psychrophiles so far characterized, able to duplicate in the range between 0 and 30 °C (Tutino et al. 2001). The determination of *P. haloplanktis* TAC125 genome (Medigue et al. 2005) revealed that the bacterial genome is characterized by a quite high number of rRNA and tRNA genes (106, sometimes organized in long runs of repeated sequences), which may account for its relevant capacity for translation and fast growth performances at low temperatures. Furthermore, the bacterium is remarkably well adapted to protection against reactive oxygen species (ROS) under cold condition, having evolved a novel anti-ROS and anti-RNS strategy which makes use of a two-on-two haemoglobin (Parrilli et al. 2010). Over the last decade, a reliable gene transfer/gene expression technology has been successfully achieved with the Antarctic bacterium *P. haloplanktis* TAC125 (Giuliani et al. 2012; Parrilli et al. 2008b; Rippa et al. 2012), which allow the addressing of recombinant proteins towards any specific cell compartment

or to the extra-cellular medium (Parrilli et al. 2008a). The host versatility was recently widened by the development of an efficient genetic scheme, allowing the construction of genome targeted insertion/deletion mutants and permitting to create genetically engineered strains with improved features regarding protein production (Giuliani et al. 2012; Parrilli et al. 2008a; Parrilli et al. 2010). In view of its application for industrial purposes, laboratory-scale fermentation processes have been developed, demonstrating the feasibility of *P. haloplanktis* TAC125 growth in batch (Parrilli et al. 2010), in a C-limited chemostat cultivation (Giuliani et al. 2011), and in fed-batch fermentations (Wilmes et al. 2010). The efficiency of cold-adapted expression systems was also validated by the successful production of difficult proteins and biopharmaceuticals (Corchero et al. 2013; Dragosits et al. 2011; Gasser et al. 2008; Giuliani et al. 2011).

To further test the performances of psychrophilic expression system in recombinant antibody fragments production, the anti-2-phenyl-5-oxazolone single-chain variable fragment (ScFvOx) was chosen as model (Fiedler and Conrad 1995). ScFvOx is a typical example of aggregation-prone scFv and it has been used for years as model for IB refolding protocol development (Patil et al. 2008). The recombinant production was addressed in the periplasmic space to allow the formation of the antibody disulphide bonds. Indeed, the gene fragments encoding the signal peptide of two secreted cold-adapted proteins were alternatively fused with the *scFvOx* gene, in particular the sequences encoding the leader peptide belonging to *P. haloplanktis* TAC125 DsbA (disulphide bond formation, DsbA) (Madonna et al. 2006), a periplasmic protein, and to *P. haloplanktis* TAB23 secreted  $\alpha$ -amylase (Feller et al. 1992). The production and the cellular localisation of the recombinant proteins have been investigated. By the use of a selected leader peptide a new expression system was developed for scFvOx production in lab-scale fermentation processes. The protein was entirely translocated in the periplasmic space and produced in soluble and active form.

## Materials and methods

### Bacterial strains, genetic manipulations and culture conditions

*E. coli* DH5 $\alpha$  [*supE44*,  $\Delta$ *lacU169* ( $\phi$ 80 *lacZAM15*) *hsdR17*, *recA1*, *endA1*, *gyrA96*, *thi-1*, *relA1*] (Hanahan 1983) was used as host for the gene cloning. *E. coli* strain S17-1( $\lambda$ *pir*) [*thi*, *pro*, *hsd* ( $r^-$   $m^+$ ) *recA*::RP4-2-TC<sup>r</sup>::Mu Km<sup>r</sup>::Tn7, Tp<sup>r</sup>, Sm<sup>r</sup>,  $\lambda$ *pir*] (Tascon et al. 1993) was used as donor in intergeneric conjugation experiments (Parrilli et al. 2008b). *E. coli* cells were routinely grown in LB broth containing 100  $\mu$ g/mL of ampicillin if transformed.

The Gram-negative Antarctic bacterial strain *P. haloplanktis* TAC125 is deposited and available at the Institut Pasteur

Collection (CIP 108707) (Birolo et al. 2000) was grown in different conditions when transformed by different gene expression systems. In particular, when transformed with constitutive ones, the recombinant psychrophilic cells were grown in shaken flasks at 15 °C in rich TYP medium (Parrilli et al. 2008b). When transformed with L-malate inducible gene expression system, recombinant *P. haloplanktis* TAC125 cells were grown in a stirred tank reactor 3 L fermenter (Applikon) connected to an ADI 1030 Bio Controller (Applikon) with a working volume of 1 L, in SCHATZ mineral medium (1 g KH<sub>2</sub>PO<sub>4</sub>, 1 g NH<sub>4</sub>NO<sub>3</sub>, 10 g NaCl, 0.2 g MgSO<sub>4</sub>·7H<sub>2</sub>O, 0.01 g FeSO<sub>4</sub>·7H<sub>2</sub>O, 0.01 g CaCl<sub>2</sub>·2H<sub>2</sub>O) supplemented with 0.5 % (w/v) L-leucine, 0.5 % (w/v) L-isoleucine and 1.0 % (w/v) L-valine (LIV medium), 100 µg mL<sup>-1</sup> ampicillin. Recombinant protein production was initiated by addition of 0.4 % (w/v) L-malate in early exponential phase (corresponding to about 0.6 OD<sub>600nm</sub>) (Giuliani et al. 2011). The culture was carried out at 15 °C in aerobic conditions (dissolved oxygen tension (DOT) ≥30 %), airflow of 20 L h<sup>-1</sup> and a stirring rate of 500 rpm. The culture pH was maintained at 7.0 by automatic addition of H<sub>2</sub>SO<sub>4</sub> 5 % (v/v). The cell biomass from a pre-inoculum, performed in shaken flask with the same medium and temperature used for the following experiment was used to inoculate batch culture. Chemostat cultivation was then started using a SCHATZ ( ) medium supplemented with 0.5 % (w/v) L-leucine and 0.4 % (w/v) L-malate as feeding at a dilution rate of  $D=0.05\text{ h}^{-1}$  (Giuliani et al. 2011). Cell growth was monitored by measuring the optical density (OD) at 600 nm using a UVIKON 922 spectrophotometer (Kontron).

For biomass determination, suitable sample volumes were washed in demineralised water, collected and dried on pre-weighed filter discs and dried at 110 °C until constant weight. The dry cell weight was correlated with OD at 600 nm throughout the following equation (Giuliani et al. 2011):

$$\text{Dry cell weight (g L}^{-1}\text{)} = 0.74 \times \text{OD}_{600\text{nm}}$$

#### Amplification of scFv-c-myc gene and construction of recombinant periplasmic expression vectors

DNA manipulation and analysis were performed according to standard methods (Sambrook and Russell 2001). Plasmidic DNA extraction and fragments purification was carried out with the QIAprep Spin Miniprep Kit and Qiaquick gel extraction kit from Qiagen, respectively. Restriction enzymes, T4 DNA ligase, alkaline phosphatase, Phusion High-Fidelity DNA Polymerase were supplied by Promega, Boehringer-Roche, Fermentas or Finnzyme.

The *scFvOx-c-myc* gene was PCR amplified according to standard methods (Sambrook and Russell 2001) from the source vector pScPelB, a derivative of the pSEX100-phOx

phagemid vector (GenBank: X82190.1), kindly provided by Dr B. Soehling, University of Halle (Germany), in order to introduce 5' *SmaI-SalI* and 3' *EcoRI* restriction sites by using primers Sc-SS-fw (5'-CAGCCCCGGGTCGACATGGCCG) and Sc-tagE respectively (5'-GCTTGTCGAATTCCTATGCCG GCCC). The amplification was performed in a mixture containing 60 ng of template, 50 pmol of each oligonucleotide primer, 10 µl of 5× Phusion HF Buffer, 200 µM dNTP, 0.02 U/µl of Phusion HF DNA Polymerase in a final volume of 50 µl. The mixture was incubated at 95 °C for 10 min followed by 25 cycles of amplification (consisting of 30" at 98 °C, 30" at 55 °C and 60" at 72 °C) and a cycle in which the extension reaction at 72 °C was prolonged for 15 min in order to complete DNA synthesis. The amplified fragment was cloned into pGEMTeasy (Promega) vector and its nucleotide sequence was checked by sequencing to rule out the occurrence of any mutation during synthesis.

The *scFvOx-c-myc* gene was double digested with *SalI/EcoRI* and inserted into the corresponding sites of the psychrophilic periplasmic vectors pPM13psD and pPM13psA (Vigentini et al. 2006), generating the pPM13psD-*scFvOx-c-myc* and pPM13psA-*scFvOx-c-myc* vectors used for the screening of signal peptide for periplasmic secretion.

For pUCRP-*scFv* expression vector construction the *psD-scFvOx-c-myc* gene was PCR amplified according to standard methods (Sambrook and Russell 2001) from the previously constructed pPM13psD-*scFvOx-c-myc* vector in order to introduce the 3' *XhoI* restriction sites and to remove the stop codon by using the primers PsD-N-fw (5'-CGGCGCATATGCTTAAAAAATTAAACTGAG) and the c-Myc-X-rv respectively (5'-ATATCTCGAGGGCCCTTTCGGCCCCATTC). The amplified fragment was cloned into pGEMTeasy (Promega) vector and its nucleotide sequence was determined to rule out the occurrence of mutations during synthesis. The gene fragment was then digested with *NdeI/XhoI* and cloned into a modified pUCRP vector (unpublished results from this laboratory) in-frame to a C-terminal 6xHis tag coding sequence.

#### Recombinant ScFvOx production and cellular localization

Aliquots of recombinant *P. haloplanktis* TAC125 cell pellet, corresponding to 50 mL culture volume, were resuspended in Na-phosphate buffer 50 mM pH 8.0, NaCl 300 mM, phenylmethanesulfonylfluoride (PMSF) 1 mM and subjected to 5 cycles of French Press (Sinstem, Limited Basic Z Model) at 1.8 kbar. The resulting suspension was subjected to ultracentrifugation (Beckman 50.2Ti) at 45,000 rpm for 2 h at 4 °C and the supernatant, corresponding to total soluble cell extract, used for further analysis. The pellet, corresponding to cell debris and insoluble matter, was dissolved in Laemmli Sample Buffer (Sambrook and Russell 2001) solution and stored as insoluble fraction for further analysis.



The periplasmic proteins preparation was carried out by resuspending bacterial pellets in 1/20 of culture volume of borate buffer ( $\text{Na}_2\text{B}_4\text{O}_7$  200 mM, NaCl 130 mM, ethylenediaminetetraacetic acid (EDTA) 5 mM, pH 8.0) and incubating the mixture 18 h at 4 °C. The suspension was centrifuged at 8,000 rpm for 15 min at 4 °C and the supernatant used for further analysis, while the recovered cell pellet was lysed as reported above, leading to the recovery of the soluble fraction, defined the cytoplasmic extract.

Protein samples (5 µg protein extracts and 500 ng pure proteins) were analysed by sodium dodecyl sulphate polyacrylamide gel electrophoresis (SDS-PAGE) (10 % acrylamide, w/v) according to standard methods (Sambrook and Russell 2001). For Western blotting analysis, 1 µg protein extracts were subjected to standard SDS-PAGE gel electrophoresis, and transferred to a polyvinylidene difluoride membrane (PVDF) (Immobilon PSQ, Millipore). After blocking the membrane 1 h at RT in blocking buffer (phosphate buffer saline (PBS), 5 % w/v skimmed milk, 0.05 % v/v Triton X-100) immunodetection was performed using anti c-Myc mAb (Calbiochem), which were diluted 1:5,000 in blocking buffer and incubated for 1 h at RT. Peroxidase conjugate antimouse IgG (Calbiochem) diluted 1:10,000 in blocking buffer was used as secondary antibody. Proteins were detected by chemiluminescence (Pierce).

Concentrations of active ScFvOx were determined by ELISA assay as previously described by Lange et al. (2005). Refolded purified ScFvOx IB produced in *E. coli* (Lange et al. 2005) was used as standard for the assay.

Protein concentration was determined with the Bio-Rad protein assay (Bradford 1976), using bovine serum albumin as standard.

The 6xHis tagged recombinant ScFvOx was affinity purified on  $\text{Ni}^{2+}$ -NTA resin in batch conditions. 200 µl of HIS-Select Nickel Affinity Gel resin (Sigma-Aldrich), pre-equilibrated with binding buffer (Na-phosphate buffer 50 mM pH 8.0, NaCl 300 mM) were incubated with about 25 mg of crude protein extracts for 16 h at 4 °C while shaking. Five washing steps were performed with washing buffer (Na-phosphate 50 mM pH 8.0, NaCl 300 mM, imidazole 30 mM). Protein elution was carried with 50 µl of elution buffer (Na-phosphate 50 mM pH 8, NaCl 300 mM, imidazole 250 mM). A second elution step was performed with 50 µl of the same elution buffer supplemented with 500 mM imidazole.

## Results

Choice of molecular signals for recombinant ScFvOx secretion

Antibody fragments, as well as all antibody molecules, contain disulphide bonds in their tertiary structure each in every

immunoglobulin domain. To achieve soluble and biologically competent production of recombinant antibody fragments in *P. haloplanktis* TAC125 a useful option is to address the recombinant proteins into the periplasmic compartment where the oxidising environment and the enzymatic repertoire allows disulphide bonds formation.

Two different psychrophilic signal peptides were tested for periplasmic secretion of recombinant ScFvOx in *P. haloplanktis* TAC125: one (PsA) isolated from a psychrophilic *P. haloplanktis* TAB23  $\alpha$ -amylase (Feller et al. 1992) and the other (PsD) from the endogenous periplasmic protein DsbA (disulphide bond oxidoreductase I) (Madonna et al. 2006). In order to assess the ability of the selected signal peptides to promote recombinant ScFvOx translocation across bacterial inner membrane, the *scFvOx* gene was fused to each leader peptide encoding sequence into the *P. haloplanktis* periplasmic gene expression vectors under the control of a strong constitutive psychrophilic promoter (Duilio et al. 2004). The resulting fusion proteins, PsA-ScFvOx, PsD-ScFvOx, contain the c-Myc tag at their C-terminal end to allow the product immunodetection.

Recombinant *P. haloplanktis* TAC125 strains were grown in TYP medium at 15 °C in shaken flasks. Protein patterns of the soluble and insoluble cell extracts were analysed by SDS-PAGE to evaluate the production of the ScFvOx by the psychrophilic expression host. Interestingly, the analysis revealed that no ScFvOx production (either in insoluble or soluble forms) is obtained when its periplasmic translocation is driven by the  $\alpha$ -amylase signal peptide PsA (data not shown). On the contrary, the periplasmic protein PsD-ScFvOx was produced in fully soluble form by *P. haloplanktis* TAC125 recombinant cells (Fig. 1 panel a), since no recombinant protein was found into the insoluble fraction (Fig. S1, lane B).

To assess the recombinant ScFvOx subcellular localisation, recombinant cells were subjected to cellular fractionation (cytoplasm and periplasm). Total cellular soluble extracts and corresponding periplasmic and cytoplasmic fractions of the recombinant *P. haloplanktis* TAC125 strains were analysed by Western blotting using specific anti c-Myc monoclonal antibodies. As shown in Fig. 1 panel b, a specific signal is present in total extract of recombinant cells showing an apparent molecular weight corresponding to the expected one for recombinant ScFvOx-c-Myc fusion protein (~35 kDa). The same specific signal is present in the recombinant periplasmic fraction and absent in the corresponding cytoplasm, thus suggesting that ScFvOx-c-Myc protein is totally translocated in the bacterial periplasmic space and produced in soluble form.

Construction of an inducible psychrophilic gene expression system and periplasmic ScFvOx recombinant production

Preliminary production trials by *P. haloplanktis* TAC125 (pPM13psD-scFvOx-c-myc) demonstrated that the amount

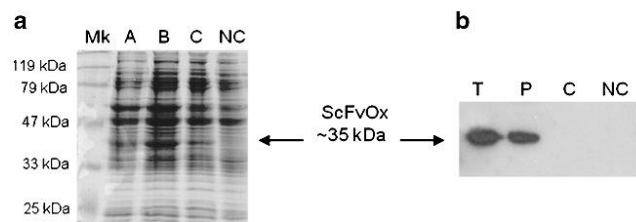


**Fig. 1** Panel **a**: SDS-PAGE analysis of ScFvOx production. *A*, *B* and *C* are total soluble protein extracts from recombinant *PhTAC125* (pPM13psD-scFvOx) strain at respectively 24, 36–48 h cultivation. *Mk* molecular weight protein ladder. Panel **b**: anti c-Myc Western blotting

analysis of ScFvOx cellular localization on total soluble proteins (*T*), periplasmic (*P*) and cytoplasmic fraction of recombinant *PhTAC125* (pPM13psD-scFvOx) cells. Total soluble protein extract of *P. haloplanktis* TAC125 wild-type strain was used as negative control (*NC*)

of recombinant protein produced was quite low, making difficult its functional characterization. Therefore, a novel gene expression system was constructed, *psD-scFvOx-c-myc* gene was PCR amplified to remove the stop codon and to add an in-frame C-terminal 6xHis tag coding sequence; the resulting gene was then cloned into pUCRP vector (Papa et al. 2007) under transcription regulation of a psychrophilic promoter inducible by L-malate addition, which production performances in a fully defined growth medium (LIV medium) were recently optimised (Giuliani et al. 2011).

The ScFvOx recombinant production was firstly carried out by L-malate induced batch cultivation in LIV medium at 15 °C, following experimental conditions described in (Giuliani et al. 2011). The production yield was evaluated by ELISA assays in presence of the hapten 2-phenyl-5-oxazolone on total soluble extracts from samples collected at different times of cultivation. As shown in Fig. 2 panel a, after an unusual lag phase (about 25 h long), *P. haloplanktis* TAC125(pUCRPscfvox) strain started to duplicate faster, and also ScFvOx production titre enhanced rapidly, reaching the highest observed yield after about 50 h incubation. A maximum yield of  $4.69 \pm 0.12 \text{ mg L}^{-1}$  of soluble and biologically active ScFvOx was obtained leading to a specific productivity of  $0.94 \pm 0.03 \text{ mg gX}^{-1}$ .

Cellular localisation of recombinant ScFvOx was also investigated by cellular fractionation and SDS-PAGE analysis of total soluble protein extracts, cytoplasmic and periplasmic fractions (Fig. 2 panel b). The analysis revealed that a band corresponding to recombinant ScFvOx-c-Myc-6xHis (about 35 kDa) is present only in total and periplasmic extracts of recombinant *P. haloplanktis* TAC125 cells. The latter observation demonstrates that ScFvOx antibody fragment is not only nicely produced in soluble and active form but it is also efficiently and totally translocated in the periplasmic compartment. The protein was never detected in insoluble cell debris (data not shown).

Recombinant ScFvOx was affinity purified from total cellular extracts collected after 48 h of batch cultivation in optimised conditions by using the C-terminal 6xHis tag (Fig. 3). The binding activity of purified ScFvOx was verified

by ELISA assay in the presence of the hapten 2-phenyl-5-oxazolone. The analysis revealed a yield of  $4.05 \pm 0.18 \text{ mg L}^{-1}$  of pure biologically active ScFvOx. Data collected indicate that, apart from a slight loss due to the purification step, the recombinant product obtained by the optimised psychrophilic expression system is biologically competent.

ScFvOx production at low temperatures was also performed by a continuous cultivation strategy. In particular, *P. haloplanktis* TAC125(pUCRPscfvox) strain was grown at 15 °C by a C-limited chemostat cultivation process, using the optimised LIV medium for batch growth phase and SCHATZ medium supplemented with 0.5 % (w/v) L-leucine and 0.4 % (w/v) L-malate for feeding (Giuliani et al. 2011). Applying a dilution rate of  $0.05 \text{ h}^{-1}$ , the system maintained the steady state for at least five resident times in which both the cell density and the product titre remain constant (Fig. 4). In these conditions, a specific active ScFvOx productivity of  $0.23 \pm 0.05 \text{ mg L}^{-1} \text{ h}^{-1}$  was achieved with a constant production yield of about  $4.5 \text{ mg L}^{-1}$ .

## Discussion

ScFvs are typical examples of proteins of relevant biotechnological value whose recombinant production in conventional host systems is sometimes poor. Their production in the common *E. coli*-based systems could be hampered by: (i) the need to address the ScFv production into the periplasmic space, where the disulphide bridges can be correctly formed; (ii) the tendency of these synthetic proteins to form insoluble aggregates when overproduced. In this conjunction, the development of a novel gene expression system in non-conventional microbial hosts represents a certain priority.

The aim of this work was the development of a new strategy for recombinant production of soluble scFv fragments by the psychrophilic bacterium *P. haloplanktis* TAC125.

A special attention was devoted to the choice of the suitable signal peptide sequence to be used as periplasmic addressing tag. Two are the major targeting routes that direct unfolded proteins to the Sec translocase of inner membrane in Gram-

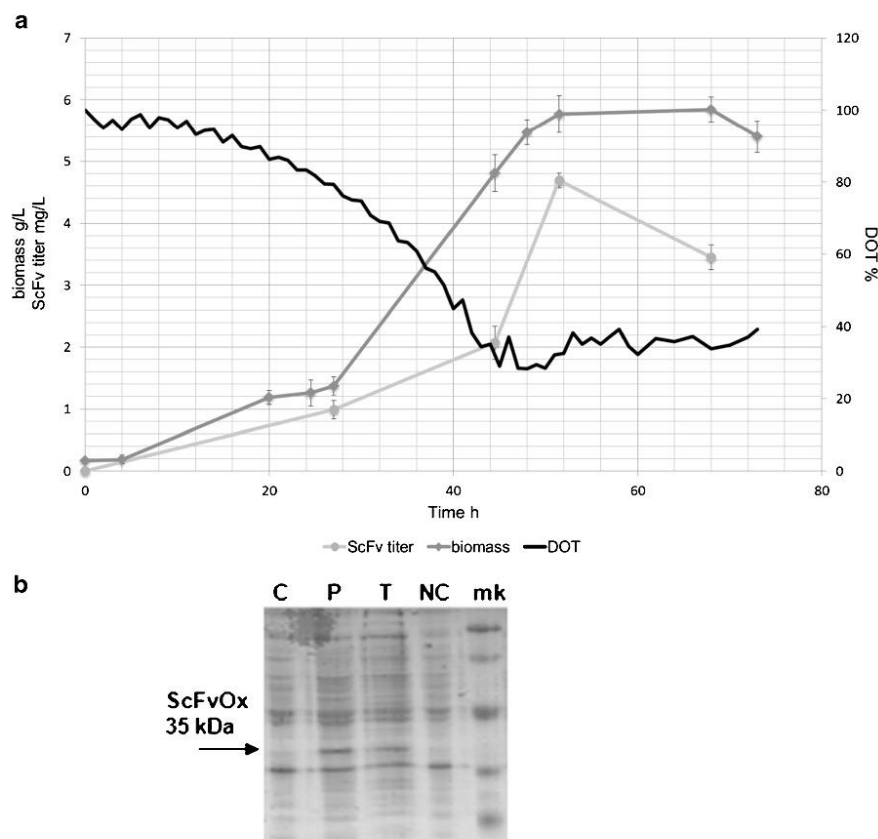


**Fig. 2** Panel a: ScFvOx titer, biomass yield and oxygen consumption profiles in *P. haloplanktis* TAC125 pUCRP-*scfv* batch cultivation in LIV medium at 15 °C. Panel b: SDS-PAGE analysis of ScFvOx cellular localization (cytoplasmic (C), periplasmic (P) and total (T) protein

extracts) produced in recombinant *P. haloplanktis* TAC125 pUCRP-*scfv* cells withdrawn after about 50 h incubation. The total soluble proteins of *P. haloplanktis* wild-type strain were used as negative control (NC). *mk* molecular weight ladder

negative bacteria, and signal peptide features (sequence and distribution of specific amino acids) define which route will be followed by a given preprotein.

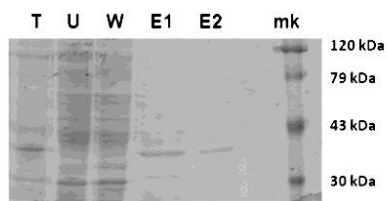


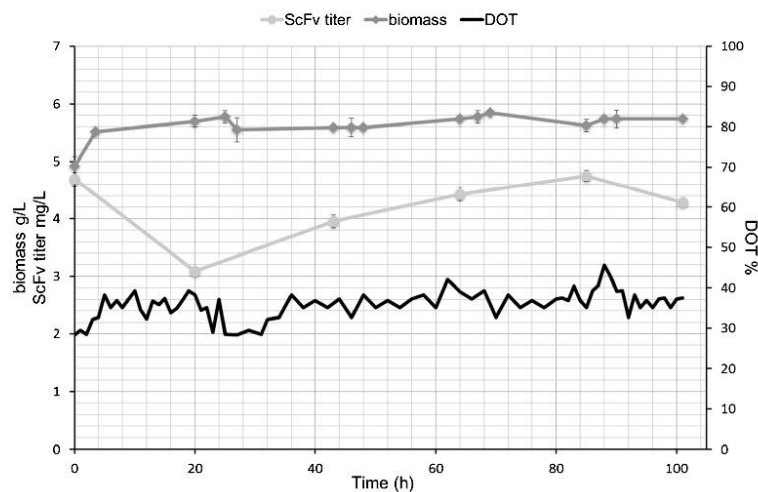
**Fig. 3** SDS-PAGE analysis of ScFvOx affinity purification. *T* total soluble extract; *U* unbound proteins fraction; *W* wash fraction; *E1* elution using 250 mM imidazole as elution buffer; *E2* elution using 500 mM imidazole as elution buffer; *mk* molecular weight protein ladder

The most frequently occurring is the SecB-dependent process (Wickner and Leonard 1996), in which the polypeptide is post-translationally translocated in the periplasmic space, i.e. after its complete synthesis (Dalbey and Chen 2004). To allow the recognition of the preprotein by the SecYEG machinery, the unfolded state of protein is required and therefore some translocation problems could be experienced by those proteins whose folding kinetic is faster than recognition event by the export system. Indeed, if the protein acquires any three-dimensional structure, it becomes an inadequate substrate for the translocation machinery and it is retained in the cytoplasm where it is often degraded (Chatzi et al. 2013). *P. haloplanktis* TAC125 contains a classical Sec translocation system (Medigue et al. 2005).

On the other side, bacteria have an equivalent of the eukaryotic signal recognition particle (SRP), which is able to



**Fig. 4** ScFvOx titer, biomass yield and oxygen consumption profiles during *P. haloplanktis* TAC125 pUCRP-*scfv* chemostat cultivation at a dilution rate of  $D=0.05\text{ h}^{-1}$



translocate the preprotein by a co-translational mechanism. The bacterial SRP system (Schierle et al. 2003) recognises hydrophobic regions displayed by the signal peptide of the nascent preprotein during synthesis, and its translation and translocation result to be simultaneous. In *E. coli*, SRP is composed by Ffh protein, which interacts with a small 4.5S RNA, while its receptor into the inner membrane is the integral inner membrane protein FtsY (Grudnik et al. 2009). A *P. haloplanktis* TAC125 genome search looking for the psychrophilic homologues of Ffh and FtsY retrieved the ORFs PSHAa0942 and PSHAa0354 respectively, indicating that an SRP-dependent translocation system is present in the cold-adapted bacterium.

With the aim of defining which of the two routes results to be the most proficient in scFvOx periplasmic production in *P. haloplanktis* TAC125, two preproteins were produced, detaining a SecB-dependent signal peptide (PsA from alpha amylase) or a SRP-dependent signal sequence (PsD from DsbA). In the most common *E. coli* production host, it has been reported that both translocation routes are effective in the scFv recombinant production (Thie et al. 2008). Data presented here demonstrate that only the co-translational molecular signal (PsD) allows the scFvOx production, its periplasmic translocation and accumulation in fully soluble and active form. The total absence of protein in the cytoplasmic fraction indicates a proper recognition and an efficient translocation. On the other side, some hypotheses can be formulated to justify the failure in production of the SecB-dependent preprotein, most pointing toward the folding pathway likely experienced by scFvOx in *P. haloplanktis* TAC125 cytoplasm prior the Sec-dependent translocation.

The optimal combination between addressing signals, gene expression system and fermentation strategy allowed us to reach a production yield of  $4.69 \pm 0.12\text{ mg L}^{-1}$  of soluble and biologically active ScFvOx, which is the highest reported so far by conventional prokaryotic expression systems even after inclusion bodies refolding (Patil et al. 2008). Moreover, performances of our optimised process led to a high specific productivity ( $Y_{P/X} = 0.94 \pm 0.03\text{ mg gX}^{-1}$ ) suggesting that a further increase in specific biomass yield would lead to higher ScFvOx production titers.

It is widely accepted that scFv and Fab antibody fragments folding rely on the activity of peptidyl prolyl *cis-trans* isomerases (PPIases) (Feige et al. 2010). Indeed, study of antibody folding pathway demonstrated that after the formation of variable and constant domain intra-chain disulphide bonds (Vinci et al. 2004), the *cis-trans* isomerization of a peptidyl prolyl bond directs folding into the native conformation, allowing formation of the inter-chain disulphide bonds. PPIases activity is also involved in the prevention of antibody fragments aggregation. Kappa light chain variable domains ( $V_K$ ) have two conserved prolines in the *cis* conformation at positions L8 and L95 (Bothmann and Pluckthun 2000). *cis-trans* isomerization of Pro-L95 residue is a rate-limiting step in  $V_K$  domains folding and it is necessary for VL/VH docking and consequently for the conformation of native protein. Remarkably, co-expression of the periplasmic *E. coli* PPIase, FkpA, resulted in a noteworthy improvement in secretion into periplasm of functional scFv fragments containing either  $V_K$  chains, which contain *cis*-prolines, or  $V_L$  chains which do not contain *cis*-prolines, suggesting that it has both PPIase enzymatic and molecular chaperone activities (Levy et al. 2013).

*cis-trans* isomerization reaction can become a rate-limiting step in protein folding when environmental temperature approaches water freezing point. A recent differential proteomics analysis carried out on *P. haloplanktis* TAC125 demonstrated that ribosome-bound trigger factor is the main up-regulated protein at low temperature (Piette et al. 2010). Virtually all nascent polypeptides interact with this chaperone, which is also endowed with a PPIase activity and can be regarded as the primary folding factor for the growth of *P. haloplanktis* TAC125 (Piette et al. 2010).

Furthermore, one of the often-observed adaptations to cold lifestyle in bacteria genome is the amplification of the number of genes coding for PPIases and/or the reduction of the proline distribution amongst psychrophilic proteins (Feller 2013). The genome of the mesophilic host *E. coli* is characterized by the presence of 10 genes, encoding a set of PPIase, localised either in the cytoplasm, in the periplasm or membrane associated. When the same analysis was carried out on the *P. haloplanktis* TAC125 genome, 15 genes were retrieved (see supplementary Table S1). Interestingly, besides the presence of homologues of each mesophilic gene, other five genes were found in the psychrophilic genome encoding a duplication of cytoplasmic SlyD and PpiC and three other PPIases, predicted to be localised one in the cytoplasm and two in the periplasmic space. The comparison between the two bacteria therefore results in the presence of three more cytoplasmic PPIase and two more periplasmic PPIase, making *P. haloplanktis* TAC125 a naturally optimised host for the recombinant production of antibody fragments.

In conclusion, our results demonstrated that the production of recombinant proteins in psychrophilic bacteria is not only a mature and reliable technology but it is also a successful strategy to overcome the product solubility problems or incorrect folding issues often occurring in conventional systems such as in *E. coli*. In this context, *P. haloplanktis* TAC125 and the set-up gene expression strategies have a valuable biotechnological potential as non-conventional systems for the production of “difficult” proteins and biopharmaceuticals such as recombinant antibody fragments.

**Acknowledgments** This work was supported by Programma Nazionale di Ricerche in Antartide PDR 2010/A1.05.

## References

- Baneyx F (1999) Recombinant protein expression in *Escherichia coli*. *Curr Opin Biotechnol* 10(5):411–421
- Birolo L, Tutino ML, Fontanella B, Gerday C, Mainolfi K, Pascarella S, Sannia G, Vinci F, Marino G (2000) Aspartate aminotransferase from the Antarctic bacterium *Pseudoalteromonas haloplanktis* TAC 125. Cloning, expression, properties, and molecular modelling. *Eur J Biochem* 267(9):2790–2802
- Bothmann H, Pluckthun A (2000) The periplasmic *Escherichia coli* peptidylprolyl *cis, trans*-isomerase FkpA. I. Increased functional expression of antibody fragments with and without *cis*-prolines. *J Biol Chem* 275(22):17100–17105. doi:10.1074/jbc.M910233199
- Bradford MM (1976) A rapid and sensitive method for the quantitation of microgram quantities of protein utilizing the principle of protein-dye binding. *Anal Biochem* 72:248–254
- Carrio M, Gonzalez-Montalban N, Vera A, Villaverde A, Ventura S (2005) Amyloid-like properties of bacterial inclusion bodies. *J Mol Biol* 347(5):1025–1037. doi:10.1016/j.jmb.2005.02.030
- Chatzi KE, Sardis MF, Karamanou S, Economou A (2013) Breaking on through to the other side: protein export through the bacterial Sec system. *Biochem J* 449(1):25–37. doi:10.1042/BJ20121227
- Coleman ME, Tamplin ML, Phillips JG, Mamer BS (2003) Influence of agitation, inoculum density, pH, and strain on the growth parameters of *Escherichia coli* O157:H7—relevance to risk assessment. *Int J Food Microbiol* 83(2):147–160
- Corchero JL, Gasser B, Resina D, Smith W, Parrilli E, Vazquez F, Abasolo I, Giuliani M, Jantti J, Ferrer P, Saloheimo M, Mattanovich D, Schwartz S Jr, Tutino ML, Villaverde A (2013) Unconventional microbial systems for the cost-efficient production of high-quality protein therapeutics. *Biotechnol Adv* 31(2):140–153. doi:10.1016/j.biotechadv.2012.09.001
- Dalbey RE, Chen M (2004) Sec-translocase mediated membrane protein biogenesis. *Biochim Biophys Acta* 1694(1–3):37–53. doi:10.1016/j.bbamcr.2004.03.009
- Dragosits M, Frascotti G, Bernard-Granger L, Vazquez F, Giuliani M, Baumann K, Rodriguez-Carmona E, Tokkanen J, Parrilli E, Wiebe MG, Kunert R, Maurer M, Gasser B, Sauer M, Branduardi P, Pakula T, Saloheimo M, Penttilä M, Ferrer P, Luisa Tutino M, Villaverde A, Porro D, Mattanovich D (2011) Influence of growth temperature on the production of antibody Fab fragments in different microbes: a host comparative analysis. *Biotechnol Prog* 27(1):38–46. doi:10.1002/btpr.524
- Duilio A, Madonna S, Tutino ML, Pirozzi M, Sannia G, Marino G (2004) Promoters from a cold-adapted bacterium: definition of a consensus motif and molecular characterization of UP regulative elements. *Extremophiles* 8(2):125–132. doi:10.1007/s00792-003-0371-2
- Feige MJ, Hendershot LM, Buchner J (2010) How antibodies fold. *Trends Biochem Sci* 35(4):189–198. doi:10.1016/j.tibs.2009.11.005
- Feller G (2013) Psychrophilic enzymes: from folding to function and biotechnology. *Scientifica* 2013:28. doi:10.1155/2013/512840
- Feller G, Lonhienne T, Deroanne C, Libioulle C, Van Becunem J, Gerday C (1992) Purification, characterization, and nucleotide sequence of the thermolabile alpha-amylase from the antarctic psychrotroph *Alteromonas haloplanktis* A23. *J Biol Chem* 267(8):5217–5221
- Fiedler U, Conrad U (1995) High-level production and long-term storage of engineered antibodies in transgenic tobacco seeds. *Biotechnology (N Y)* 13(10):1090–1093
- Gasser B, Saloheimo M, Rinas U, Dragosits M, Rodriguez-Carmona E, Baumann K, Giuliani M, Parrilli E, Branduardi P, Lang C, Porro D, Ferrer P, Tutino ML, Mattanovich D, Villaverde A (2008) Protein folding and conformational stress in microbial cells producing recombinant proteins: a host comparative overview. *Microb Cell Fact* 7:11. doi:10.1186/1475-2859-7-11
- Giuliani M, Parrilli E, Ferrer P, Baumann K, Marino G, Tutino ML (2011) Process optimization for recombinant protein production in the psychrophilic bacterium *Pseudoalteromonas haloplanktis*. *Process Biochem* 46(4):953–959. doi:10.1016/j.procbio.2011.01.011
- Giuliani M, Parrilli E, Pezzella C, Rippa V, Duilio A, Marino G, Tutino ML (2012) A novel strategy for the construction of genomic mutants of the Antarctic bacterium *Pseudoalteromonas haloplanktis* TAC125. *Methods Mol Biol* 824:219–233. doi:10.1007/978-1-61779-433-9\_11



- Grudnik P, Bange G, Sinning I (2009) Protein targeting by the signal recognition particle. *Biol Chem* 390(8):775–782. doi:10.1515/BC.2009.102
- Hanahan D (1983) Studies on transformation of *Escherichia coli* with plasmids. *J Mol Biol* 166(4):557–580
- Lange C, Patil G, Rudolph R (2005) Ionic liquids as refolding additives: *N*-alkyl and *N*-(omega-hydroxyalkyl) *N*-methylimidazolium chlorides. *Protein Sci* 14(10):2693–2701. doi:10.1110/ps.051596605
- Levy R, Ahluwalia K, Bohmann DJ, Giang HM, Schwimmer LJ, Issafras H, Reddy NB, Chan C, Horwitz AH, Takeuchi T (2013) Enhancement of antibody fragment secretion into the *Escherichia coli* periplasm by co-expression with the peptidyl prolyl isomerase, FkpA, in the cytoplasm. *J Immunol Methods* 394(1–2):10–21. doi:10.1016/j.jim.2013.04.010
- Madonna S, Papa R, Birolo L, Autore F, Doti N, Marino G, Quemeneur E, Sannia G, Tutino ML, Duilio A (2006) The thiol-disulfide oxidoreductase system in the cold-adapted bacterium *Pseudoalteromonas haloplanktis* TAC 125: discovery of a novel disulfide oxidoreductase enzyme. *Extremophiles* 10(1):41–51. doi:10.1007/s00792-005-0470-3
- Medigue C, Krin E, Pascal G, Barbe V, Bemsel A, Bertin PN, Cheung F, Cruveiller S, D'Amico S, Duilio A, Fang G, Feller G, Ho C, Mangenot S, Marino G, Nilsson J, Parrilli E, Rocha EP, Rouy Z, Sekowska A, Tutino ML, Vallenet D, von Heijne G, Danchin A (2005) Coping with cold: the genome of the versatile marine Antarctic bacterium *Pseudoalteromonas haloplanktis* TAC125. *Genome Res* 15(10):1325–1335. doi:10.1101/gr.4126905
- Papa R, Rippa V, Sannia G, Marino G, Duilio A (2007) An effective cold inducible expression system developed in *Pseudoalteromonas haloplanktis* TAC125. *J Biotechnol* 127(2):199–210. doi:10.1016/j.jbiotec.2006.07.003
- Parrilli E, De Vizio D, Cirulli C, Tutino ML (2008a) Development of an improved *Pseudoalteromonas haloplanktis* TAC125 strain for recombinant protein secretion at low temperature. *Microb Cell Fact* 7:2. doi:10.1186/1475-2859-7-2
- Parrilli E, Duilio A, Tutino M (2008b) Heterologous protein expression in psychrophilic hosts. In: Margesin R, Schinner F, Marx J-C, Gerday C (eds) *Psychrophiles: from Biodiversity to Biotechnology*. Springer Berlin, pp 365–379
- Parrilli E, Giuliani M, Giordano D, Russo R, Marino G, Verde C, Tutino ML (2010) The role of a 2-on-2 haemoglobin in oxidative and nitrosative stress resistance of Antarctic *Pseudoalteromonas haloplanktis* TAC125. *Biochimie* 92(8):1003–1009. doi:10.1016/j.biochi.2010.04.018
- Patil G, Rudolph R, Lange C (2008) In vitro-refolding of a single-chain Fv fragment in the presence of heteroaromatic thiols. *J Biotechnol* 134(3–4):218–221. doi:10.1016/j.jbiotec.2008.01.009
- Piette F, D'Amico S, Struvay C, Mazzucchelli G, Renaut J, Tutino ML, Danchin A, Leprince P, Feller G (2010) Proteomics of life at low temperatures: trigger factor is the primary chaperone in the Antarctic bacterium *Pseudoalteromonas haloplanktis* TAC125. *Mol Microbiol* 76(1):120–132. doi:10.1111/j.1365-2958.2010.07084.x
- Rippa V, Papa R, Giuliani M, Pezzella C, Parrilli E, Tutino ML, Marino G, Duilio A (2012) Regulated recombinant protein production in the Antarctic bacterium *Pseudoalteromonas haloplanktis* TAC125. *Methods Mol Biol* 824:203–218. doi:10.1007/978-1-61779-433-9\_10
- Sambrook J, Russell DW (2001) *Molecular cloning: a laboratory manual*. Joseph Sambrook, David W. Russell. Cold Spring Harbor Laboratory, Cold Spring Harbor, N.Y
- Schierle CF, Berkmen M, Huber D, Kumamoto C, Boyd D, Beckwith J (2003) The DsbA signal sequence directs efficient, cotranslational export of passenger proteins to the *Escherichia coli* periplasm via the signal recognition particle pathway. *J Bacteriol* 185(19):5706–5713
- Somerville JE Jr, Goshorn SC, Fell HP, Darveau RP (1994) Bacterial aspects associated with the expression of a single-chain antibody fragment in *Escherichia coli*. *Appl Microbiol Biotechnol* 42(4):595–603
- Tascon RI, Rodriguez-Ferri EF, Gutierrez-Martin CB, Rodriguez-Barbosa I, Berche P, Vazquez-Boland JA (1993) Transposon mutagenesis in *Actinobacillus pleuropneumoniae* with a Tn10 derivative. *J Bacteriol* 175(17):5717–5722
- Thie H, Schirmann T, Paschke M, Dubel S, Hust M (2008) SRP and Sec pathway leader peptides for antibody phage display and antibody fragment production in *E. coli*. *N Biotechnol* 25(1):49–54. doi:10.1016/j.nbt.2008.01.001
- Tutino ML, Duilio A, Parrilli R, Remaut E, Sannia G, Marino G (2001) A novel replication element from an Antarctic plasmid as a tool for the expression of proteins at low temperature. *Extremophiles* 5(4):257–264
- Vigentini I, Merico A, Tutino ML, Compagno C, Marino G (2006) Optimization of recombinant human nerve growth factor production in the psychrophilic *Pseudoalteromonas haloplanktis*. *J Biotechnol* 127(1):141–150. doi:10.1016/j.jbiotec.2006.05.019
- Vinci F, Catharino S, Frey S, Buchner J, Marino G, Pucci P, Ruoppolo M (2004) Hierarchical formation of disulfide bonds in the immunoglobulin Fc fragment is assisted by protein-disulfide isomerase. *J Biol Chem* 279(15):15059–15066. doi:10.1074/jbc.M311480200
- Wickner W, Leonard MR (1996) *Escherichia coli* preprotein translocase. *J Biol Chem* 271(47):29514–29516
- Wilmes B, Hartung A, Lalk M, Liebecke M, Schweder T, Neubauer P (2010) Fed-batch process for the psychrotolerant marine bacterium *Pseudoalteromonas haloplanktis*. *Microb Cell Fact* 9:72. doi:10.1186/1475-2859-9-72
- Yang AS, Sharp KA, Honig B (1992) Analysis of the heat capacity dependence of protein folding. *J Mol Biol* 227(3):889–900

## Strategies for the production of difficult-to-express full-length eukaryotic proteins using microbial cell factories: production of human alpha-galactosidase A

Ugutx Unzueta · Felicitas Vázquez · Giulia Accardi · Rosa Mendoza ·  
Verónica Toledo-Rubio · Maria Giuliani · Filomena Sannino · Ermenegilda Parrilli ·  
Ibane Abasolo · Simo Schwartz Jr. · Maria L. Tutino · Antonio Villaverde ·  
José L. Corchero · Neus Ferrer-Miralles

Received: 10 September 2014 / Revised: 12 December 2014 / Accepted: 14 December 2014 / Published online: 24 January 2015  
© Springer-Verlag Berlin Heidelberg 2015

**Abstract** Obtaining high levels of pure proteins remains the main bottleneck of many scientific and biotechnological studies. Among all the available recombinant expression systems, *Escherichia coli* facilitates gene expression by its relative simplicity, inexpensive and fast cultivation, well-known genetics and the large number of tools available for its biotechnological application. However, recombinant expression in *E. coli* is not always a straightforward procedure and major obstacles are encountered when producing many eukaryotic proteins and especially membrane proteins, linked to missing

posttranslational modifications, proteolysis and aggregation. In this context, many conventional and unconventional eukaryotic hosts are under exploration and development, but in some cases linked to complex culture media or processes. In this context, alternative bacterial systems able to overcome some of the limitations posed by *E. coli* keeping the simplicity of prokaryotic manipulation are currently emerging as convenient hosts for protein production. We have comparatively produced a “difficult-to-express” human protein, the lysosomal enzyme alpha-galactosidase A (*hGLA*) in *E. coli* and in the

**Electronic supplementary material** The online version of this article (doi:10.1007/s00253-014-6328-9) contains supplementary material, which is available to authorized users.

U. Unzueta · F. Vázquez · G. Accardi · R. Mendoza ·  
V. Toledo-Rubio · A. Villaverde · J. L. Corchero ·  
N. Ferrer-Miralles (✉)  
Institut de Biotecnologia i de Biomedicina,  
Universitat Autònoma de Barcelona,  
Bellaterra, 08193 Barcelona, Spain  
e-mail: neus.ferrer@uab.cat

U. Unzueta · G. Accardi · A. Villaverde · J. L. Corchero ·  
N. Ferrer-Miralles  
Departament de Genètica i de Microbiologia,  
Universitat Autònoma de Barcelona,  
Bellaterra, 08193 Barcelona, Spain

U. Unzueta · F. Vázquez · R. Mendoza · V. Toledo-Rubio ·  
I. Abasolo · S. Schwartz Jr. · A. Villaverde · J. L. Corchero ·  
N. Ferrer-Miralles  
CIBER de Bioingeniería, Biomateriales y Nanomedicina  
(CIBER-BBN), Barcelona, Spain

M. Giuliani · F. Sannino · E. Parrilli · M. L. Tutino  
Dipartimento di Scienze Biochimiche, Facoltà di Medicina  
e Chirurgia, Università degli studi di Palermo,  
90127 Palermo, Italy

F. Sannino  
Institute of Protein Biochemistry, CNR, Via Pietro Castellino 111,  
I-80131 Naples, Italy

I. Abasolo · S. Schwartz Jr.  
VHIR Vall d'Hebron Inst Recerca, CIBBIM Nanomed,  
08035 Barcelona, Spain

**Present Address:**  
F. Vázquez  
GREENALTECH S.L., 08028 Barcelona, Spain

G. Accardi  
Department of Pathobiology and Medical and Forensic  
Biotechnology, University of Palermo, 90134 Palermo, Italy

V. Toledo-Rubio  
BioIngenium S.L., 08028 Barcelona, Spain

M. Giuliani  
Novartis Vaccines and Diagnostics, via Fiorentina 1, 53100 Siena,  
Italy



psychrophilic bacterium *Pseudoalteromonas haloplanktis* TAC125 cells (*P. haloplanktis* TAC125). While in *E. coli* the production of active hGLA was unreachable due to proteolytic instability and/or protein misfolding, the expression of hGLA gene in *P. haloplanktis* TAC125 allows obtaining active enzyme. These results are discussed in the context of emerging bacterial systems for protein production that represent appealing alternatives to the regular use of *E. coli* and also of more complex eukaryotic systems.

**Keywords** Recombinant protein · Expression systems · *Escherichia coli* · *Pseudoalteromonas haloplanktis* TAC125 · Human alpha-galactosidase A · Fabry's disease

## Introduction

The deep genetic and physiological characterization, short generation time, ease of handling, established fermentation know-how and finally the capacity to accumulate foreign proteins to a high percentage of the total cellular protein content have made *Escherichia coli* the most widely used prokaryotic organism for recombinant protein production. However, there are disadvantages in using *E. coli* as an expression host. For instance, *E. coli* is not capable of producing eukaryotic posttranslational modifications, such as glycosylation, phosphorylation or disulphide bridge formation in the reducing cytoplasm, which can be critical for the production of folded, active proteins. Even so, several strategies can be implemented to obtain specific posttranslational modifications as the use of *E. coli* strains which have been engineered to maintain oxidizing conditions in the cellular milieu or to send the recombinant protein to the periplasmic space to allow cysteine bridging (Inaba 2009; Nozack et al. 2013; Prinz et al. 1997). In addition, a N-linked protein glycosylation system has been recently identified in the human enteropathogen *Campylobacter jejuni* that can be transferred to *E. coli* (Wacker et al. 2006), opening up the possibility of engineering recombinant products needing glycosylation for research and industrial applications.

On the other hand, some proteins, especially large and membrane proteins, simply fail to be produced in *E. coli*, and they occur as proteolysed species or deposited in inclusion bodies (Vallejo and Rinas 2004). Others are subjected to premature termination of translation in the presence of repetitive DNA sequences or rare codons (Daly and Hearn 2005; Sallach et al. 2009) or have a low rate of internal translation initiation (Ferreira et al. 2013; Nakamoto 2009). A large number of studies describe the conversion of proteins accumulated in inclusion bodies into soluble forms. Mainly, these methods can be categorized into three alternative approaches. In the first one, factors influencing the amount of recombinant protein present in the insoluble fraction can be modified through

careful optimization and control of the production conditions, leading to the expression of the recombinant protein in its soluble version. In this context, conventional approaches include gene expression at low temperature, use of promoters with different transcriptional strengths, modifications of growth media and the use of folding modulators (Kolaj et al. 2009). Alternatively, the protein can be extracted from inclusion bodies either under native or denaturing conditions (Martinez-Alonso et al. 2009). Finally, the target protein can be engineered to achieve soluble expression through fusion of solubility-enhancing tags (Sahdev et al. 2008; Torres et al. 2012).

In the recent years, a novel prokaryotic expression system has been developed based on the use of the psychrophilic bacterium *Pseudoalteromonas haloplanktis* TAC125 by driving the expression of genes of interest by both basal or inducible promoters (Duilio et al. 2004a, b). In addition, as was established for *E. coli* expression system, mutation of genes coding for proteases greatly reduces proteolysis of the recombinant protein (Parrilli et al. 2008). The system has demonstrated to be especially useful in improving protein solubility in relation to the widely used *E. coli* expression system and gives higher protein yield for secreted proteins (Cusano et al. 2006; Giuliani et al. 2014; Vigentini et al. 2006). Proteomics analysis points out the trigger factor chaperone as the main factor involved in protein folding during recombinant protein expression under cold temperatures (Piette et al. 2010).

The human  $\alpha$ -galactosidase A (EC 3.2.1.22;  $\alpha$ -Gal A or GLA) is the lysosomal exoglycosidase responsible for the hydrolysis of terminal  $\alpha$ -galactosyl moieties from various glycoconjugates. In the late 1980s, the full-length complementary DNA (cDNA) and the entire genomic sequence encoding mammalian GLA were isolated and characterized (Calhoun et al. 1985; Gotlib et al. 1996). The 1.4-kb full-length cDNA encodes a peptide of 429 residues, which includes a 31-residue amino-terminal signal peptide. This enzyme precursor is a glycopeptide (of approx. 55 kDa) that is processed by cleavage of the signal peptide and by oligosaccharide modifications in the Golgi and lysosomes to form the mature, active, homodimeric enzyme (approx. 100 kDa). After cleavage of the signal peptide, the glycopeptide undergoes modification of its N-linked oligosaccharide moieties in the Golgi apparatus, and then it is transported to the lysosome via the mannose-6-phosphate receptor (M6PR)-mediated pathway. Mutations in the hGLA gene resulting in deficient or absent enzymatic activity are the basis of Fabry's disease, a disorder characterized by progressive glycosphingolipid deposition in vascular lysosomes leading to early demise from renal, cardiac or cerebral vascular disease (Garman and Garboczi 2002).

The subunits of the glycosylated mature enzyme contain four putative N-glycosylation consensus sites at positions



Asn139, Asn192, Asn215 and Asn408 and five disulphide bonds between residues Cys52–Cys94, Cys56–Cys63, Cys142–Cys172, Cys202–Cys223 and Cys378–Cys382 (Garman and Garboczi 2004; Saito et al. 2013). The human enzyme has been purified from a variety of sources, and its physical and kinetic properties have been also characterized (Chen et al. 2000a, b; Corchero et al. 2011, 2012; Yasuda et al. 2004). However, the *h*GLA obtained from prokaryotic expression systems has neither been fully characterized nor purified (Hantzopoulos and Calhoun 1987). Therefore, the objective of this work is the production and purification of active *h*GLA from prokaryotic cell factories.

## Material and methods

### Bacterial strains and plasmids

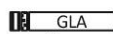
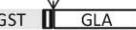


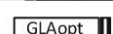
The *E. coli* strains used in this work were DH5 $\alpha$  for plasmid cloning and maintenance; BL21(DE3), *Rosetta* 2(DE3) and *Rosetta-gami* B(DE3) (Novagen) for recombinant protein expression and S17-1( $\lambda$ pir) were used as donor in interspecific conjugation experiments (Tascon et al. 1993). *P. haloplanktis* TAC125 is a Gram-negative bacterium isolated from Antarctic seawater and is deposited and available at the Institut Pasteur Collection (CIP 108707) (Medigue et al.

2005). Antarctic bacteria transformation was achieved by intergeneric conjugation as previously reported (Duilio et al. 2004b).

The four *E. coli* expression vectors used in this work (Fig. 1a) are as follows: (a) pReceiver-B01-GLA (product EX-Q0172-B01, OmicsLink ORF Expression Clone), encoding a full-length version of *h*GLA under the control of the T7 promoter; in this vector, 6 $\times$ His-tag is fused to the N-terminus of the *h*GLA open reading frame (ORF) for further detection and purification purposes; (b) pGEX4T2-GLA, encoding the mature form of the *h*GLA with a glutathione S-transferase (GST) fused at its N-terminus; a His-tag and a Tobacco etch Virus protease (TEVp) cleavage site were also added in the designed PCR oligonucleotides of the *h*GLA gene for purification purposes; (c) pGEX4T2-Opt-GLA, synthetic, codon optimized *h*GLA gene (GeneArt, Invitrogen; KF500099) cloned into pGEX4T2 as previously described; and (d) pGEX4T2-GLA-GFP, derived from pGEX4T2-GLA in which the green fluorescent protein (GFP) coding sequence was inserted into the *Eco*RI cloning site. Some other four expression vectors used in *E. coli* strains are described in Suppl. Fig. S1a.

Finally, the psychrophilic gene expression vector pPM13psDs-GLA (e) was constructed as follows: the pPM13psDs shuttle vector, containing the strong constitutive promoter PM13 (Duilio et al. 2004a) correctly located with

**Fig. 1** **a** Expression vectors used in recombinant *h*GLA production assays. Expression vectors used in *E. coli* strains: **a–d** Expression vector used in *Pseudoalteromonas haloplanktis* is shown in **e**. *GST*, glutathione S-transferase; *GLA*, *h*GLA gene; *GLAopt*, *h*GLA gene codon optimized for *E. coli* in **c** and gene codon optimized for *Pseudoalteromonas haloplanktis* in **e**. Tobacco Etch Virus protease cleavage site (TEVp) location is marked by an arrow tip. His-tag is marked by a striped box. Signal peptide of *h*GLA in **a** is marked by a stippled box. **b** Amino acid sequence of *h*GLA. The first 31 amino acids correspond to the peptide signal that is marked in *italics*. The residues coded by rare codons are shown in *bold*. Putative translation termination sequence is *underlined*

a	Plasmid name	Recombinant GLA	Cell compartment	Size	Molecular weight
a)	pReceiver-B01-GLA		cytoplasm	435 aa	49.6 kDa
b)	pGEX4T2-GLA		cytoplasm	640 aa	73.6 kDa
c)	pGEX4T2-Opt-GLA		cytoplasm	640 aa	73.6 kDa
d)	pGEX4T2-GLA-GFP		cytoplasm	876 aa	100.1 kDa
e)	pPM13psDs-GLA		periplasm	405 aa	46.3 kDa

<b>b</b>	1. <i>MQLRNPELHL</i>	<i>GCALALRFLA</i>	<i>LVSWDIPGAR</i>
	31. <i>ALDNGLARTP</i>	<i>TMGWLHWERF</i>	<i>MCNLDQCQEEP</i>
	61. <i>DSCISEKLFM</i>	<i>EMAELMVSEG</i>	<i>WKDAGYEYLC</i>
	91. <i>IDDCWMAQPR</i>	<i>DSEGRLQADP</i>	<i>QRFPHGIRQL</i>
	121. <i>ANYVHSGGLK</i>	<i>LGIYADVGNK</i>	<i>TCAGFPGSFG</i>
	151. <i>YYDIDAQTF</i>	<i>DWGVLLKFD</i>	<i>GCYCDLLENL</i>
	181. <i>ADGYKHMSLA</i>	<i>LNRTGRSIVY</i>	<i>SCEWPLYMMP</i>
	211. <i>FQKPNYTEIR</i>	<i>QYCNHWRNFA</i>	<i>DIDDSWKSIA</i>
	241. <i>SILDWTSFNQ</i>	<i>ERIVDVAGPG</i>	<i>GWNDPDMIVI</i>
	271. <i>GNFGLSWNQ</i>	<i>VTQMALWAIM</i>	<i>AAPLFMSNDL</i>
	301. <i>RHISPAKAL</i>	<i>LQDKDVIAIN</i>	<i>QDPLGKQGYQ</i>
	331. <i>LRQGDNFEVW</i>	<i>ERPLSGLAWA</i>	<i>VAMINRQIEG</i>
	361. <i>GPRSYTIAVA</i>	<i>SLKGIVACNP</i>	<i>ACFITTQLLEPV</i>
	391. <i>KRLGFEYEW</i>	<i>SRIRSHINPT</i>	<i>GTVLLQLENT</i>
	421. <i>MQMSLKDLL</i>		

respect to a psychrophilic Shine-Dalgarno sequence and the 93-bp encoding the signal peptide of *P. haloplanktis* TAC125 DsbA was double digested by *Sall-EcoRI*. The synthetic codon optimized *hGLA* gene (KF500099) was double digested by *Sall-EcoRI* and cloned into pPM13psDs corresponding sites (Fig. 1a).

#### Recombinant human GLA production and cellular fractionation

The production process in recombinant *E. coli* cells was performed by the Protein Production Platform (<http://ibb.uab.es/ibb>) of the Institute of Biotechnology and Biomedicine (IBB-UAB) and the Biomedical Networking Center (CIBER-BBN). In short, shake flask cultures were set at 37 °C and 250 rpm in LB-rich medium, plus 100 µg/mL of ampicillin for plasmid maintenance in all expression *E. coli* vectors. Expression of recombinant *hGLA* gene was induced when the absorbance at 550 nm reached values around 0.5, adding isopropyl β-D-1-thiogalactopyranoside (IPTG) at concentrations ranging from 0.1 to 1 mM. Incubation proceeded then at different temperatures of 16, 20, 25 and 37 °C depending on the strain as indicated. After induction of gene expression, 1.5-mL culture samples were withdrawn at different times and soluble and insoluble fractions were separated. In short, cells were harvested by centrifugation at 5000g (at 4 °C) for 15 min and resuspended in 200 µL of phosphate-buffered saline (PBS) (7.5 mM Na<sub>2</sub>HPO<sub>4</sub>, 110 mM NaCl, 2.5 mM NaH<sub>2</sub>PO<sub>4</sub>, pH 7.4) and further sonicated. Soluble and insoluble fractions were separated by centrifugation at 15,000g for 15 min at 4 °C. Insoluble fractions were resuspended in PBS (same volumes than those from their respective soluble fractions). Both fractions were stored at −80 °C until further analysis.

*P. haloplanktis* TAC125 (pPM13psDs-GLA) recombinant cells were cultured in aerobic conditions at 4 and 15 °C in TYP broth (16 g/L yeast extract, 16 g/L bacto tryptone, 10 g/L marine salt mix) at pH 7.5, supplemented with 100 µg/mL ampicillin, and the recombinant *hGLA* production and its cellular localization were evaluated in cell samples withdrawn at different growth phases. Cell pellets (corresponding to OD<sub>600 nm</sub>=10) were resuspended in 1 mL of 50 mM Tris-HCl at pH 8.0, 50 mM EDTA and disrupted by ultrasonic treatment consisting of six cycles of 30 s on/1 min off on ice. The mixture was centrifuged for 15 min at 10,000g at 4 °C; the resulting supernatant and pellet were collected as soluble and insoluble fractions, respectively. Total *P. haloplanktis* TAC125 (pPM13psDs-GLA) cell extract was obtained by resuspending 0.5 OD<sub>600 nm</sub> cell pellet into 400 µL of sodium dodecyl sulphate (SDS) loading dye, followed by 30 min treatment at 90 °C.

The periplasmic cell extract was obtained by resuspending bacterial pellets in 1/20 of culture volume of borate buffer

(200 mM Na<sub>2</sub>B<sub>4</sub>O<sub>7</sub>, 130 mM NaCl, 5 mM EDTA, pH 8) and incubating the mixture for 18 h at 4 °C. The suspension was then centrifuged at 8000 rpm for 15 min at 4 °C. The supernatant was stored as periplasmic extract, while the pellet was resuspended in 1/20 of original culture volume of SDS loading dye, followed by 30 min of treatment at 90 °C and stored as cytoplasmic extract.

#### Recombinant protein detection

Total cell extracts, soluble, insoluble and periplasmic cell fractions were analysed by SDS-polyacrylamide gel electrophoresis (PAGE) and Coomassie staining. For Western blot studies, upon SDS-PAGE proteins were blotted onto nitrocellulose membranes, *hGLA* immunoreactive bands were developed using either a rabbit polyclonal anti-GLA serum from Santa Cruz Biotechnology, Inc. (α-gal A H-104: sc-25823) raised against an epitope corresponding to amino acids 316–429 at the C-terminus of the mature form of *hGLA* (Fig. 1b), a rabbit polyclonal anti-GLA serum from Sigma Prestige Antibodies (product HPA000237) raised against amino acids 302–412 of the mature form of *hGLA*, or a monoclonal antibody anti-His-tag from GE Healthcare (product 27-471001), and the corresponding secondary antibodies. GST was detected with mouse monoclonal anti-GST antibody (Santa Cruz Biotechnology, Inc.; SC-138) and GFP with rabbit polyclonal anti-GFP antibodies (Santa Cruz Biotechnology, Inc.; SC-8334).

For comparison purposes, gels were loaded with sample volumes adjusted according to the OD of the culture. Samples for quantitative comparison were run in the same gel and processed as a set. Bands were analysed with the Quantity One analysis software (BioRad).

#### Protein purification

GST-containing *hGLA* recombinant proteins were purified from Rosetta-gami B cell cultures induced at 0.1 mM IPTG for 16 h at 20 °C at 250 rpm. Cell pellets were resuspended in PBS buffer (7.5 mM Na<sub>2</sub>HPO<sub>4</sub>, 110 mM NaCl, 2.5 mM NaH<sub>2</sub>PO<sub>4</sub>, pH 7.4) in the presence of EDTA-free protease inhibitors (Roche Applied Science), and cells were lysed using a French Press (Thermo FA-078A) at 1100 psi. The soluble fraction was separated by centrifugation at 15,000g for 45 min at 4 °C, filtered through 0.22-µm filters and loaded onto a 1-mL GSTrap HP column (GE Healthcare, 17-5281-05). Bound GST-GLA protein was eluted with five column volumes of elution buffer (50 mM Tris-HCl and 10 mM reduced glutathione, pH 8.0). Positive fractions were collected and dialysed against 0.01 M acetic buffer (pH 4.5), and protein concentration was estimated using the Bradford method.

The pellets of *E. coli* or *P. haloplanktis* TAC125 cells containing His-tagged *hGLA* proteins were resuspended in



buffer A (20 mM Tris–HCl pH 7.5, 500 mM NaCl and 10 mM imidazole) and cells disrupted by sonication in the presence of EDTA-free protease inhibitors (Complete, 11873580001 from Roche). The soluble cell fraction was separated by centrifugation at 15,000g for 15 min at 4 °C. After filtration through 0.22- $\mu$ m filters, recombinant proteins were purified by affinity chromatography in  $\text{Ni}^{2+}$  columns (HiTrap Chelating HP columns, 17-0408-01 from GE Healthcare) in an ÄKTA™ Purifier (GE healthcare) fast protein liquid chromatography system. Positive fractions in elution buffer (20 mM Tris–HCl pH 7.5, 150 mM NaCl and 500 mM Imidazole) were collected and dialyzed against 0.01 M acetic buffer (pH 4.5). Protein concentration was estimated using the Bradford method.

Purified proteins were characterized by N-terminal sequencing by Edman's automated degradation using in an Applied Biosystems Procise 492 protein sequencer, and molecular weight was experimentally determined by mass spectrometry (UltraFlex MALDI-TOF mass spectrometer, Bruker Daltonics, Bremen, Germany). Both analyses were performed at the Proteomics and Bioinformatics Unit of the Scientific Technical Service, SepBioEs, of the Autonomous University of Barcelona.

#### Time course of TEV cleavage reaction of GST-GLA-GFP

Purified GST-GLA-GFP was dialysed against reaction buffer (50 mM Tris–HCl, pH 8.0, 0.5 mM EDTA). Ten units of TEVp (Invitrogen, 12575-015) was added to 20  $\mu$ g of GST-GLA-GFP and incubated at 30 °C; 30- $\mu$ L aliquots were removed at specified incubation times. Reaction was stopped by adding 30  $\mu$ L of stop solution (125 mM Tris–HCl, pH 6.8; 4 % SDS; 1.4 M  $\beta$ -mercaptoethanol; 20 % (v/v) glycerol; 0.01 % bromophenol blue), and samples were stored at –20 °C until gel electrophoresis analysis. Protein samples when performing hGLA activity assays were used without buffer addition after protease incubation.

#### Enzyme assay of $\alpha$ -galactosidase A activity

The enzymatic hGLA activity was assayed with 4-methylumbelliferyl  $\alpha$ -D-galactoside (4MU- $\alpha$ -Gal, ref. M7633, Sigma Chemical, St. Louis, MO) as a substrate, at a concentration of 2.46 mM in 0.01 M acetic buffer (pH 4.5). A typical 4MU- $\alpha$ -Gal assay was performed with a reaction mixture containing 100  $\mu$ L of substrate and 25  $\mu$ L of enzyme solution. Enzymatic reactions took place in agitation, at 37 °C for 1 h. Reaction was stopped adding 1.25 mL of 0.2 M glycine–NaOH buffer (pH 10.4). The released 4-methylumbelliferone (4-MU) was determined by fluorescence measurement at 365 and 450 nm as excitation and emission wavelengths, respectively. Samples ranging from 5 to 500 ng/mL of 4-MU (ref. M1381, Sigma, St. Louis, MO) in 0.2 M glycine–NaOH buffer (pH 10.4) were used as standard curve.

One unit of enzyme activity was defined as the amount of enzyme releasing 1 nmol of 4-MU per milligram of enzyme and per hour. hGLA obtained from human fibroblasts or HEK-293 T cells were used as positive controls (Corchero et al. 2011).

## Results

### Recombinant expression of human GLA ORF in *E. coli*

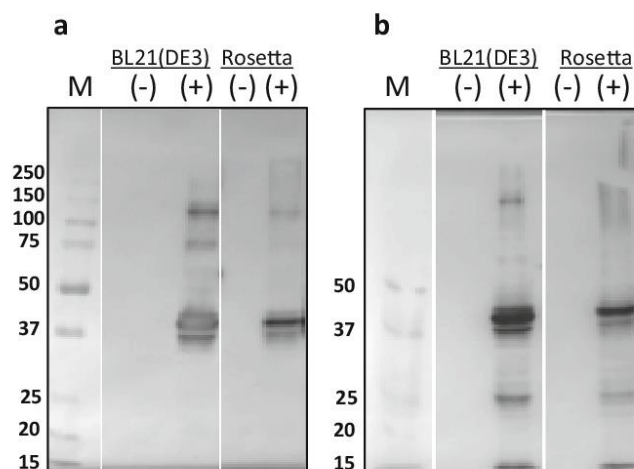
Plasmid pReceiver-B01-GLA, which contains the complete ORF of hGLA gene, was transformed in *E. coli* BL21(DE3) and Rosetta(DE3) *E. coli* strains (Fig. 1a). The Rosetta strain is able to compensate low concentrations of certain tRNAs of *E. coli* and to improve recombinant protein translation. It should be noticed that in the hGLA ORF, at least four critical arginine codons are present in the DNA sequence (Fig. 1b). Strains BL21(DE3) and Rosetta(DE3), with and without the expression plasmid, were submitted to gene expression induction conditions and analysed by SDS-PAGE followed by Western blot. Nitrocellulose membranes were developed either with a polyclonal anti-GLA antibody (Sigma-Aldrich Co.) raised against an epitope corresponding to amino acids 302–412 of the hGLA protein or with the monoclonal anti-His-tag (Fig. 2a, b). Results showed that the polyclonal antibody from Sigma and the anti-His antibody detect a main protein band corresponding to the degradation product of about 40–42 kDa (expected MW 49.6 kDa), both antibodies detecting this band as the main immunoreactive product, while samples from not transformed cells did not show any immunoreactive band. Also, both antibodies detected bands that might be associated to protein aggregates or oligomers, while proteolysis fragments were detected with the anti-His-tag monoclonal antibody but not with the polyclonal antibody, indicating a specific C-terminal cleavage. Finally, equivalent protein bands were detected upon tRNA supplementation. According to these results, only a product of approximately 42 kDa and probably other aggregated and degraded protein products, recognized by the monoclonal anti-His-tag and the anti-GLA antibodies, could be obtained in these strains transformed with the pReceiver-B01-GLA expression vector.

In addition, cell fractionation studies performed in *E. coli* BL21(DE3)/pReceiver-B01-GLA cultures showed that the hGLA produced at different induction temperatures was exclusively detected in the insoluble cell fraction (Suppl. Fig. S2).

### Recombinant production of mature form of hGLA in *E. coli*

hGLA ORF present in pReceiver-B01-GLA codes for the 429 amino acid hGLA precursor including 31 amino acid residues corresponding to the signal peptide, which is naturally processed in the ER to a 398-amino acids

**Fig. 2** Crude extracts of induced *E. coli* strains BL21(DE3) and Rosetta(DE3), not transformed (*minus sign*) or transformed with pReceiver-B01-GLA (*plus sign*). Samples were collected 3 h postinduction at 30 °C, and equivalent amounts of protein sample were loaded in each lane. **a** Western blot developed with polyclonal anti-GLA from Sigma. **b** Western blot developed with monoclonal anti-His-tag. Molecular weight marker standards are indicated in kilodaltons (Dual color, BioRad)



mature form (Lemansky et al. 1987) (Fig. 1b). Since eukaryotic signal peptides are not processed in prokaryotic hosts, nucleotides coding exclusively for the mature form of the *hGLA* ORF (32–429; Fig. 1b) were amplified by PCR and transferred to *E. coli* expression vectors to improve protein folding in the heterologous expression system (Suppl. Fig. S1a, expression vectors a and b). In addition, to promote the formation of disulphide bonds in the *hGLA* product, the experiments were performed in either Rosetta-gami *E. coli* strain or the protein was sent to the oxidizing environment present in the periplasm. Expression of the mature form of *hGLA* in *E. coli* under these conditions produced aggregated forms of the recombinant protein and protein bands compatible with degradation products (Suppl. Fig. S3 and Suppl. Fig. S4).

It has been reported that purification of full-length human proteins can be achieved by fusion to soluble proteins as GST in *E. coli* (Braun et al. 2002). This DNA fragment was also inserted into pGEX4T-2, which adds a GST fusion protein at the N-terminal end of the desired protein product (Fig. 1a).

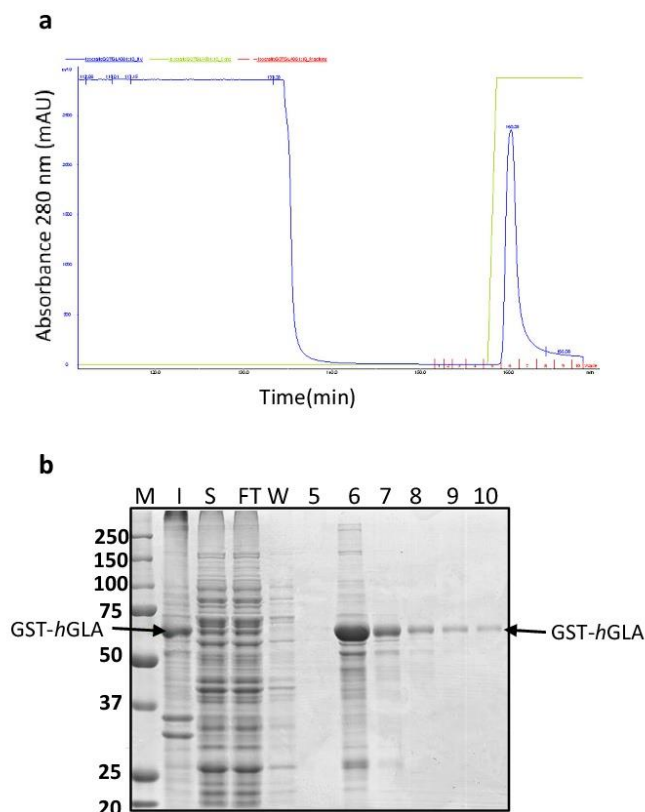
Protein expression experiments were carried out with transformed Rosetta-gami B(DE3) cells with pGEX4T2-GLA with the aim of using the fused GST for solubilization and purification purposes. Several protein induction conditions were assayed (Suppl. Fig. S5). Specific protein bands were detected in all tested conditions in both soluble and insoluble fractions. A predominant band was observed in the insoluble fraction with an apparent weight below 75 kDa that would correspond to the expected GST tagged recombinant *hGLA*, apart from other protein bands compatible with aggregates and proteolysed forms.

#### Purification and characterization of the produced human GLA

Soluble GST-fused protein was purified by affinity chromatography using a GSTrap HP 1 mL column (GE Healthcare). Elution peak contains highly pure protein sample obtained in one single chromatographic step, indicating that the chosen purification strategy was appropriate (Fig. 3). However, molecular weight of the purified protein was again smaller than expected. N-terminal sequencing of the protein band demonstrated that corresponded to the initial amino acids of the recombinant protein, although the first methionine was only partially removed. In *E. coli*, methionine aminopeptidase removes initial methionine with variable efficiency depending on the penultimate amino acid, and it has been demonstrated that the presence of an acidic residue as L present in *hGLA* reduces its activity up to 20 % (Liao et al. 2004; Xiao et al. 2010a). Moreover, mass spectrometry of the affinity purified sample revealed that the exact molecular weight of the product was 68.9 kDa (theoretical weight 73.6 kDa). This size reduction in 4.7 kDa is compatible with the elimination of 29 amino acids at the C-terminus of the protein since as it has been demonstrated, the N-terminal end remains intact. Therefore, in this proteolysed *hGLA* protein, the last amino acid corresponded then to S401 after which an arginine coded by a rare codon has to be added at position 402. In addition, at position 392, another arginine rare codon is present (Fig. 1b).

On the basis of the above-mentioned results, and to avoid the presence of rare codons close to the proteolytic point of the polypeptide chain, site-directed mutagenesis of the mentioned arginine residues in the *hGLA* (R402 and R392 rare codons) were performed using the QuikChange Lightning site-directed mutagenesis kit (Stratagene) with oligonucleotides designed by PrimerX ([www.Bioinformatics.org](http://www.Bioinformatics.org)). The resulting mutant

**Fig. 3** **a** Chromatogram of recombinant GST-GLA protein on GSTrap FF 1 mL column obtained from soluble cellular fraction of Rosetta-gami B(DE3) induced cell culture. **b** Coomassie blue stained SDS-PAGE of soluble, insoluble cell fractions and protein samples of affinity chromatography. Flow through (FT), wash (W), fractions 5–10 of elution peak. Molecular weight marker standards are indicated in kilodaltons (Dual color, BioRad)



pGEX4T2-GLA (pGEX4T2-GLAmut1; Suppl. Fig. S1a) was sequenced and used in expression experiments. Western blot analyses of the resulting protein samples showed that a GST-hGLA protein could be obtained, but its molecular weight corresponded to the 69-kDa truncated protein previously obtained (data not shown).

Further analysis of the RNA sequence of the *hGLA* revealed the presence of a putative *E. coli* transcriptional terminator motif surrounding the nucleotide position at which translation seems to finish (Nudler and Gottesman 2002) (Suppl. Fig. S1b). Oligonucleotides were designed to eliminate hairpin loop secondary structures in that region and were used to mutate the pGEX4T2-GLA DNA sequence using the QuikChange Lightning site-directed mutagenesis kit (Stratagene) generating pGEX4T2-GLAmut2 (Suppl. Fig. S1a). Protein expression experiments showed that under these conditions, the resulting recombinant protein was still

truncated, showing an apparent molecular weight of 69 kDa (data not shown). Protein aggregation was observed in protein samples stored at 4 °C for 2 weeks and confirmed in Superdex 200 10/300 GL (GE Healthcare) gel filtration chromatography since a protein peak was obtained in the void volume of the column. Activity assays of purified GLA protein fused to GST were performed using purified human GLA from a mammalian expression system as positive control (Corchero et al. 2012) as well as cellular extracts of *E. coli* cells transformed with pReceiver-B01-GLA and pET22b-GLA but enzymatic activity was not detected in any sample (Table 1).

A global codon optimisation of *hGLA* gene was attempted next. For this purpose, a synthetic GLA gene was designed and constructed (GeneArt; Invitrogen) which was cloned within the pGEX4T2 vector to produce a pGEX4T2-Opt-GLA expression vector with an optimized codon usage



**Table 1** Enzymatic activity of purified *h*GLA obtained from different cell origins

Sample	Origin	Enzymatic activity ( $\mu\text{mol/h/mg GLA}$ )
Replagal	Human fibroblasts	1945.8 $\pm$ 24.2
GLA-HEK	Human embryonic kidney	1398.6 $\pm$ 47.7
GLA- <i>E. coli</i>	<i>E. coli</i>	ND
GLA- <i>P. haloplanktis</i>	<i>P. haloplanktis</i>	77.4 $\pm$ 0.3

ND not detected

(Fig. 1a, expression vector c). In that construct, the His-tag purification module was fused at the C-terminus to differentiate from the previous GST-*h*GLA constructs in which the His-tag module was located at the N-terminus of *h*GLA. The resulting expression vector was used to transform the Rosetta-gami B(DE3) strain. Protein expression experiments of the resulting strain indicated that once again, a truncated protein was produced and hence, production of the intact *h*GLA does not depend on optimized codon usage (Fig. 4a). In addition, the detection of the GST-GLA recombinant protein with anti-GST antibodies demonstrated the presence of GST in the final protein product (Fig. 4b). However, the same samples were not detected by anti-His antibodies, indicating that truncation of GLA protein occurred at the C-terminus (Fig. 4c). On the other hand, GST-GLA obtained from the expression of the non-optimized gene contained in pGEX4T2-GLA was detected by both anti-GST and anti-His antibodies since in this construction, His-tag peptide was located N-

terminally between the GST and GLA coding sequences (Fig. 1a).

Since an incomplete product was obtained regardless of the strategies attempted so far, a protease cleavage analysis was carried out using the ExPaSy PeptideCutter program. However, no specific protease cleavage site was found at the C-terminal end of the truncated GLA product obtained. Nevertheless, to confirm these findings, the next attempted strategy was the fusion of another protein (GFP (Hsieh et al. 2010)) at the C-terminus of the GST-GLA with the aim to protect GLA from a possible proteolysis at this end (Murby et al. 1991). pGEX4T2-GLA-GFP (Fig. 1a, expression vector d) was obtained and transformed into Rosetta-gami B(DE3). Protein expression assays using anti-GLA (Fig. 5a) and specifically anti-GFP Western blot experiments (Fig. 5b) demonstrated that the whole fused protein GST-His-GLA-GFP could be produced by this strain in contrast to previous experiments. Purification and subsequent TEV proteolysis of the fused protein (Fig. 5c) did not succeed in producing an active *h*GLA product despite the strategies attempted (GST and His-tag affinity chromatography), and only background signal was detected when determining the enzymatic activity of the obtained product corresponding to the signal background of the negative control (data not shown).

#### Recombinant production of mature form of *h*GLA in *P. haloplanktis* TAC125

Recombinant *P. haloplanktis* (ppM13psDs-GLA) cells were aerobically grown in complex rich medium at two different

**Fig. 4** Detection of GST-GLA protein in Rosetta-gami B(DE3)/pGEX4T2-Opt-GLA induced cell cultures by Western blot analysis using **a** polyclonal anti-GLA antibody (Sigma), **b** polyclonal anti-GST, **c** monoclonal anti-His. NC, non-induced cell cultures; C, purified GST-GLA protein; T, total cellular fraction; S, soluble fraction; I, insoluble fraction. Molecular weight marker standards are indicated in kilodaltons (Dual color, BioRad)

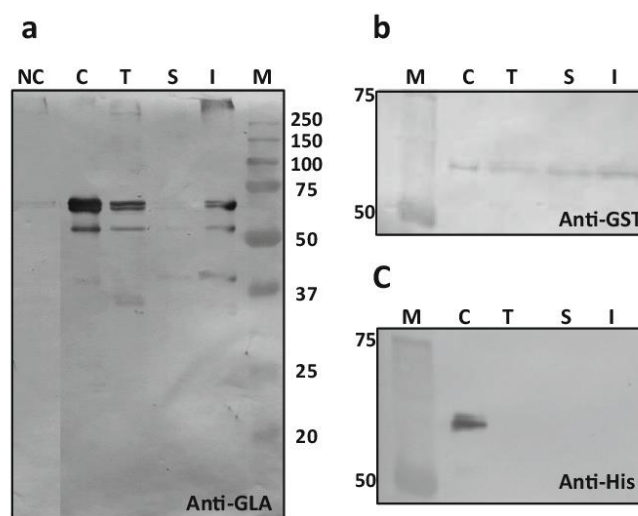
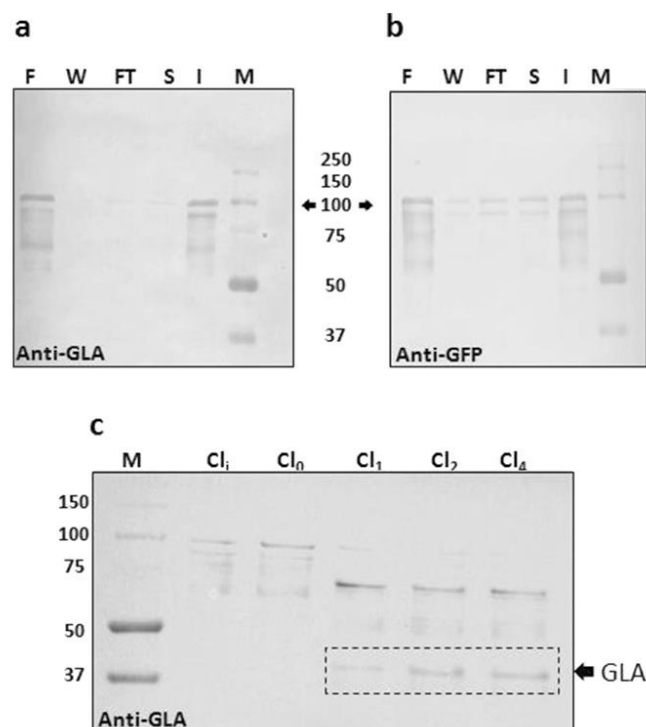


**Fig. 5** Detection of GST-GLA-GFP protein in Rosetta-gami B(DE3)/pGEX4T2-GLA-GFP induced cell cultures by Western blot analysis. **a** polyclonal anti-GLA antibody (Sigma). **b** Polyclonal anti-GFP antibody. *F*, pooled positive protein fractions obtained in GST affinity chromatography; *W*, wash fraction; *FT*, flow through; *S*, soluble cell fraction; *I*, insoluble cell fraction. **c** Release of *h*GLA protein from purified GST-GLA-GFP recombinant protein by Tobacco Etch Protease cleavage. *Cl<sub>i</sub>*, initial protein sample after protein purification; *Cl<sub>0</sub>*, protein sample at time 0; *Cl<sub>1</sub>*–*Cl<sub>4</sub>*, protein sample at 1–4 h. Molecular weight marker standards are indicated in kilodaltons (Dual color, BioRad)



temperatures (4 and 15 °C), and samples were withdrawn at different times of cultivation. The *h*GLA production was evaluated by SDS-PAGE followed by Western blotting analysis (using specific anti-GLA polyclonal antibodies) of total soluble protein extracts, and it revealed the highest protein yield after 24 h of cultivation at 15 °C (Fig. 6a, b). No recombinant GLA protein was detected in insoluble protein extracts (data not shown). A cell fractioning followed by Western blotting analysis demonstrated that recombinant GLA produced at higher temperature is also fully localized in the bacterial periplasm (Fig. 6c), while when produced at 4 °C, a fraction of the protein was still associated to the cytoplasm, likely deriving from a less efficient translocation across bacterial inner membrane. Furthermore, at the lower temperature, the recombinant *h*GLA translocated in the periplasm was also subjected to host encoded proteolytic cleavage, as demonstrated by the appearance of a lower molecular weight specific band on Western blotting analysis shown in Fig. 6c.

Soluble protein extracts from *P. haloplanktis*/pPM13psDs-GLA grown at 15 °C for 24 h were used for His-trap affinity purification (His-trap 1 mL column, GE Healthcare)

according to the protocol reported in the methods section. A linear gradient was used for elution (20–500 mM imidazole in 15 min at 0.5 mL/min flow), thus obtaining a partial purified protein (about 70 % purity) which has been used for the determination of enzymatic activity (Fig. 6d). Although the purified enzyme has the tendency to precipitate, it turned out to be active and a value of  $77.4 \pm 0.3 \mu\text{mol h}^{-1} \text{mg}^{-1}$  prot of activity was recorded (Table 1).

## Discussion

Recombinant protein production in heterologous expression systems represents a major bottleneck in the development of biopharmaceutical, industrial and research applications (Liras 2008). Even though high throughput techniques for cloning and protein production have been already described (Barnard et al. 2010; Nettleship et al. 2010; Savitsky et al. 2010; Xiao et al. 2010b), purification of challenging proteins is still a matter of trial-and-error approaches. As expression system, *E. coli* offers many advantages over eukaryotic systems

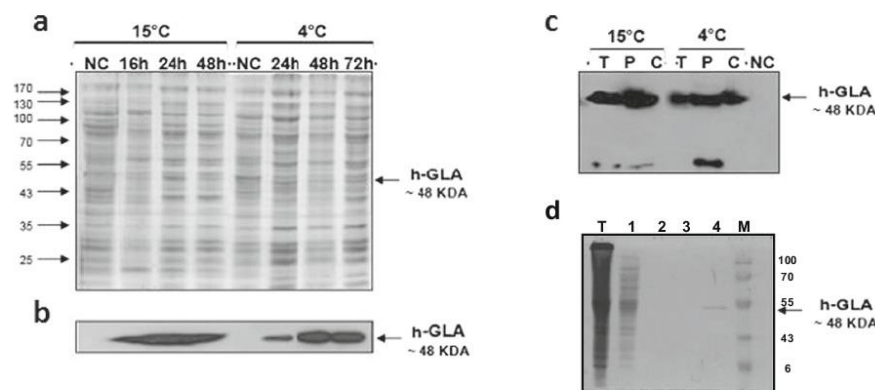


**Fig. 6** **a** Coomassie blue stained SDS-PAGE of soluble cell fractions of *P. haloplanktis* transformed with pPM13psDs-GLA at different temperatures. **b** Western blot analysis of the same samples using a polyclonal anti-GLA antibody (Santa Cruz Biotechnology). **c** Detection of recombinant hGLA in induced *P. haloplanktis* cell cultures. T, total cell

extract; P, periplasm; C, cytoplasm; NC, negative control. **d** Coomassie blue stained SDS-PAGE of hGLA purification by affinity chromatography. T, total cell extract; 1, unbound protein; 2 and 3, washes; 4, eluted protein

referring to rapidity, simplicity and expenditure (Demail and Vaishnav 2009). However, it has some disadvantages which, in some cases, are difficult to override as the lack of many posttranslational modifications and high tendency to form aggregated species (Panda 2003). In the present study, a human full-length protein, GLA, which has been purified from eukaryotic expression systems (Chen et al. 2000a, b; Corchero et al. 2012; Yasuda et al. 2004) and non-prokaryotic source (Hantzopoulos and Calhoun 1987), has been selected to try available expression methods in *E. coli* and the Antarctic psychrophilic bacterium *P. haloplanktis* TAC125. In 1987, Hantzopoulos and coauthors described the production of an active hGLA in *E. coli* (Hantzopoulos and Calhoun 1987). However, such results have not been reproduced or continued since then, and moreover, no purification protocol has been published to date. The interest in developing a production and purification system of human GLA from a prokaryotic source relies on the high cost of the actual enzymatic replacement therapy in Fabry's disease treatment which consists in recombinant protein obtained from mammalian cells having a great economical impact in patient expenditure. We have shown that hGLA can be detected in *E. coli* as either aggregated and proteolytically cleaved forms in any experimental condition tested. Aggregation of proteins seems to be driven by the presence of specific amino acid sequences (Espargaro et al. 2012), saturation of the folding machinery (Kolaj et al. 2009) or to the lack of the required posttranslational modifications as glycosylation (Ioannou et al. 1998). However, full-length recombinant hGLA has been produced when fused to GST and GFP, although purified protein is not correctly folded lacking biological activity. The absence of

enzymatic activity might be related to either unfolded protein species or deletion of the C-terminal end of the protein which seems to be critical (Miyamura et al. 1996). In addition, GLA has four glycosylation sites added after signal peptide removal in the Golgi apparatus. This sugar moieties (especially glycosylation site located at residue Asn215) play a crucial role in both folding and solubility and consequently in enzymatic activity (Ioannou et al. 1998). However, when producing hGLA in the psychrophilic expression system based in the use of the Antarctic bacteria *P. haloplanktis* TAC125, the functional full-length enzyme can be produced and purified. It has been described in comparative studies that recombinant protein production at low temperature has a positive effect in protein yield (Dragosits et al. 2011; Duilio et al. 2004a) as well as in protein conformation (Vigentini et al. 2006). The ability of the *P. haloplanktis* TAC125 to produce active hGLA over the proteolytic and aggregation tendency of the protein in *E. coli* might be related to the presence of high peptidyl prolyl *cis-trans* isomerases genes found in *P. haloplanktis* TAC125 genome and more specifically to the upregulation of the main molecular chaperone, trigger factor (Giuliani et al. 2014; Piette et al. 2010). The folding activity in the psychrophilic expression system can counteract the high tendency of the hGLA to adopt unsuitable conformations. On the other hand, in the *E. coli* cellular environment, the nascent hGLA polypeptides adopt unstable conformational species that are detected by cellular proteases, mainly at the C-terminus of the protein, leading to the formation of inactive aggregation-prone protein species. Even though the full-length protein can be produced in *E. coli*, the limited chaperone activity in this expression system renders inactive protein. Therefore,



microbial host range might be expanded to psychrophilic expression systems when difficult-to-express proteins such as full-length mammalian proteins are to be produced.

**Acknowledgments** This work was supported by ERANET-IB08-007 project from the European Union and its linked national project EUI2008-03610 to AV. We also appreciate the support from EME2007-08 to NFM from Universitat Autònoma de Barcelona, from Antartide 2010 to MLT and EP, from MIUR Azioni Integrate Italia-Spagna 2010 Prot. IT10LECLM9 to MLT, from MINECO (IT2009-0021) to AV and LT, from AGAUR (2009SGR-108) to AV. AV is also supported by The Biomedical Research Networking Center in Bioengineering, Biomaterials and Nanomedicine (CIBER-BBN, Spain), an initiative funded by the VI National R&D&I Plan 2008–2011, Iniciativa Ingenio 2010, Consolider Program, CIBER Actions and financed by the Instituto de Salud Carlos III with assistance from the European Regional Development Fund. PS has received predoctoral fellowship from ISCIII, and AV has been distinguished with an ICREA ACADEMIA award (Catalonia, Spain).

**Conflict of interests** The authors declare no conflict of interests.

## References

- Barnard GC, Kull AR, Sharkey NS, Shaikh SS, Rittenhour AM, Burnina I, Jiang Y, Li F, Lynaugh H, Mitchell T, Nett JH, Nylen A, Potgieter TI, Prinz B, Rios SE, Zha D, Sethuraman N, Stadheim TA, Bobrowicz P (2010) High-throughput screening and selection of yeast cell lines expressing monoclonal antibodies. *J Ind Microbiol Biot* 37:961–971
- Braun P, Hu YH, Shen BH, Halleck A, Koundinya M, Harlow E, LaBaer J (2002) Proteome-scale purification of human proteins from bacteria. *Proc Natl Acad Sci U S A* 99:2654–2659
- Calhoun DH, Bishop DF, Bernstein HS, Quinn M, Hantzopoulos P, Desnick RJ (1985) Fabry disease: isolation of a cDNA clone encoding human alpha-galactosidase A. *Proc Natl Acad Sci U S A* 82:7364–7368
- Chen YS, Jin M, Egborge T, Coppola G, Andre J, Calhoun DH (2000a) Expression and characterization of glycosylated and catalytically active recombinant human alpha-galactosidase A produced in *Pichia pastoris*. *Protein Expr Purif* 20:472–484
- Chen YS, Jin M, Goodrich L, Smith G, Coppola G, Calhoun DH (2000b) Purification and characterization of human alpha-galactosidase A expressed in insect cells using a baculovirus vector. *Protein Expr Purif* 20:228–236
- Corchero JL, Mendoza R, Lorenzo J, Rodriguez-Sureda V, Dominguez C, Vazquez E, Ferrer-Miralles N, Villaverde A (2011) Integrated approach to produce a recombinant, His-tagged human alpha-galactosidase A in mammalian cells. *Biotechnol Prog* 27:1206–1217
- Corchero JL, Mendoza R, Ferrer-Miralles N, Montras A, Martinez LM, Villaverde A (2012) Enzymatic characterization of highly stable human alpha-galactosidase A displayed on magnetic particles. *Biochem Eng J* 67:20–27
- Cusano AM, Parrilli E, Marino G, Tutino ML (2006) A novel genetic system for recombinant protein secretion in the Antarctic *Pseudoalteromonas haloplanktis* TAC125. *Microb Cell Fact* 5:40
- Daly R, Hearn MT (2005) Expression of heterologous proteins in *Pichia pastoris*: a useful experimental tool in protein engineering and production. *J Mol Recognit* 18:119–138
- Demain AL, Vaishnav P (2009) Production of recombinant proteins by microbes and higher organisms. *Biotechnol Adv* 27:297–306
- Dragosits M, Frascotti G, Bernard-Granger L, Vazquez F, Giuliani M, Baumann K, Rodriguez-Carmona E, Tokkanen J, Parrilli E, Wiebe MG, Kunert R, Maurer M, Gasser B, Sauer M, Branduardi P, Pakula T, Saloheimo M, Penttilä M, Ferrer P, Tutino ML, Villaverde A, Porro D, Mattanovich D (2011) Influence of growth temperature on the production of antibody Fab fragments in different microbes: a host comparative analysis. *Biotechnol Prog* 27:38–46
- Duilio A, Madonna S, Tutino ML, Pirozzi M, Sannia G, Marino G (2004a) Promoters from a cold-adapted bacterium: definition of a consensus motif and molecular characterization of UP regulative elements. *Extremophiles* 8:125–132
- Duilio A, Tutino ML, Marino G (2004b) Recombinant protein production in Antarctic Gram-negative bacteria. *Methods Mol Biol* (Clifton, N J) 267:225–237
- Espargaro A, Villar-Pique A, Sabate R, Ventura S (2012) Yeast prions form infectious amyloid inclusion bodies in bacteria. *Microb Cell Factories* 11:89
- Ferreira JP, Overton KW, Wang CL (2013) Tuning gene expression with synthetic upstream open reading frames. *Proc Natl Acad Sci U S A* 110:11284–11289
- Garman SC, Garboczi DN (2002) Structural basis of Fabry disease. *Mol Genet Metab* 77:3–11
- Garman SC, Garboczi DN (2004) The molecular defect leading to Fabry disease: structure of human alpha-galactosidase. *J Mol Biol* 337:319–335
- Giuliani M, Parrilli E, Sannino F, Apuzzo GA, Marino G, Tutino ML (2014) Recombinant production of a single-chain antibody fragment in *Pseudoalteromonas haloplanktis* TAC125. *Appl Microbiol Biotechnol* 98:4887–4895
- Gotlib RW, Bishop DF, Wang AM, Zeidner KM, Ioannou YA, Adler DA, Disteché CM, Desnick RJ (1996) The entire genomic sequence and cDNA expression of mouse alpha-galactosidase A. *Biochem Mol Med* 57:139–148
- Hantzopoulos PA, Calhoun DH (1987) Expression of the human Alpha-galactosidase-A in *Escherichia coli*-K-12. *Gene* 57:159–169
- Hsieh JM, Besserer GM, Madej M, Bui HQ, Kwon S, Abramson J (2010) Bridging the gap: a GFP-based strategy for overexpression and purification of membrane proteins with intra and extracellular C-termini. *Protein Sci* 19:868–880
- Inaba K (2009) Disulfide Bond formation system in *Escherichia coli*. *J Biochem* 146:591–597
- Ioannou YA, Zeidner KM, Grace ME, Desnick RJ (1998) Human alpha-galactosidase A: glycosylation site 3 is essential for enzyme solubility. *Biochem J* 332:789–797
- Kolaj O, Spada S, Robin S, Wall JG (2009) Use of folding modulators to improve heterologous protein production in *Escherichia coli*. *Microb Cell Factories* 8:9
- Lemansky P, Bishop DF, Desnick RJ, Hasilik A, Vonfigura K (1987) Synthesis and processing of alpha-galactosidase A in human fibroblasts. Evidence for Different Mutations in Fabry Disease. *J Biol Chem* 262:2062–2065
- Liao YD, Jeng JC, Wang CF, Wang SC, Chang ST (2004) Removal of N-terminal methionine from recombinant proteins by engineered *E. coli* methionine aminopeptidase. *Protein Sci* 13:1802–1810
- Liras A (2008) Recombinant proteins in therapeutics: haemophilia treatment as an example. *Int Arch Med* 1:4
- Martinez-Alonso M, Gonzalez-Montalban N, Garcia-Fruitos E, Villaverde A (2009) Learning about protein solubility from bacterial inclusion bodies. *Microb Cell Fact* 8:4
- Medigue C, Krin E, Pascal G, Barbe V, Bernsel A, Bertin PN, Cheung F, Cruveiller S, D'Amico S, Duilio A, Fang G, Feller G, Ho C, Mangenot S, Marino G, Nilsson J, Parrilli E, Rocha EPC, Rouy Z, Sekowska A, Tutino ML, Vallenet D, von Heijne G, Danchin A (2005) Coping with cold: the genome of the versatile marine

- Antarctica bacterium *Pseudoalteromonas haloplanktis* TAC125. *Genome Res* 15:1325–1335
- Miyamura N, Araki E, Matsuda K, Yoshimura R, Furukawa N, Tsuruzoe K, Shirotani T, Kishikawa H, Yamaguchi K, Shichiri M (1996) A carboxy-terminal truncation of human alpha-galactosidase A in a heterozygous female with Fabry disease and modification of the enzymatic activity by the carboxy-terminal domain—increased, reduced, or absent enzyme activity depending on number of amino acid residues deleted. *J Clin Invest* 98:1809–1817
- Murby M, Cedergren L, Nilsson J, Nygren PA, Hammarberg B, Nilsson B, Enfors SO, Uhlen M (1991) Stabilization of recombinant proteins from proteolytic degradation in *Escherichia coli* using a dual affinity fusion strategy. *Biotechnol Appl Biochem* 14:336–346
- Nakamoto T (2009) Evolution and the universality of the mechanism of initiation of protein synthesis. *Gene* 432:1–6
- Nettleship JE, Assenberg R, Diprose JM, Rahman-Huq N, Owens RJ (2010) Recent advances in the production of proteins in insect and mammalian cells for structural biology. *J Struct Biol* 172:55–65
- Nozach H, Fruchart-Gaillard C, Fenaile F, Beau F, Ramos OHP, Douzi B, Saez NJ, Moutiez M, Servent D, Gondry M, Thai R, Cuniasse P, Vincentelli R, Dive V (2013) High throughput screening identifies disulfide isomerase DsbC as a very efficient partner for recombinant expression of small disulfide-rich proteins in *E. coli*. *Microb Cell Fact* 12:37
- Nudler E, Gottesman ME (2002) Transcription termination and anti-termination in *E. coli*. *Genes Cells* 7:755–768
- Panda AK (2003) Bioprocessing of therapeutic proteins from the inclusion bodies of *Escherichia coli*. *Adv Biochem Eng Biotechnol* 85:43–93
- Parrilli E, De VD, Cirulli C, Tutino ML (2008) Development of an improved *Pseudoalteromonas haloplanktis* TAC125 strain for recombinant protein secretion at low temperature. *Microb Cell Fact* 7:2
- Piette F, D'Amico S, Struvay C, Mazzucchelli G, Renaut J, Tutino ML, Danchin A, Leprince P, Feller G (2010) Proteomics of life at low temperatures: trigger factor is the primary chaperone in the Antarctic bacterium *Pseudoalteromonas haloplanktis* TAC125. *Mol Microbiol* 76:120–132
- Prinz WA, Aslund F, Holmgren A, Beckwith J (1997) The role of the thioredoxin and glutaredoxin pathways in reducing protein disulfide bonds in the *Escherichia coli* cytoplasm. *J Biol Chem* 272:15661–15667
- Sahdev S, Khattar SK, Saini KS (2008) Production of active eukaryotic proteins through bacterial expression systems: a review of the existing biotechnology strategies. *Mol Cell Biochem* 307:249–264
- Saito S, Ohno K, Sakuraba H (2013) Comparative study of structural changes caused by different substitutions at the same residue on alpha-galactosidase A. *PLoS One* 8:e84267
- Sallach RE, Conticello VP, Chaikof EL (2009) Expression of a recombinant elastin-like protein in *Pichia pastoris*. *Biotechnol Prog* 25: 1810–1818
- Savitsky P, Bray J, Cooper CD, Marsden BD, Mahajan P, Burgess-Brown NA, Gileadi O (2010) High-throughput production of human proteins for crystallization: the SGC experience. *J Struct Biol* 172:3–13
- Tascon RI, Rodriguez-Ferri EF, Gutierrez-Martin CB, Rodriguez-Barbosa I, Berche P, Vazquez-Boland JA (1993) Transposon mutagenesis in *Actinobacillus pleuropneumoniae* with a Tn10 Derivative. *J Bacteriol* 175:5717–5722
- Torres LL, Ferreras ER, Cantero A, Berenguer J (2012) Strategies for the recovery of active proteins through refolding of bacterial inclusion body proteins. *Microb Cell Fact* 11:105
- Vallejo LF, Rinas U (2004) Strategies for the recovery of active proteins through refolding of bacterial inclusion body proteins. *Microb Cell Fact* 3:11
- Vigentini I, Merico A, Tutino ML, Compagno C, Marino G (2006) Optimization of recombinant human nerve growth factor production in the psychrophilic *Pseudoalteromonas haloplanktis*. *J Biotechnol* 127:141–150
- Wacker M, Feldman MF, Callewaert N, Kowarik M, Clarke BR, Pohl NL, Hernandez M, Vines ED, Valvano MA, Whitfield C, Aebi M (2006) Substrate specificity of bacterial oligosaccharyltransferase suggests a common transfer mechanism for the bacterial and eukaryotic systems. *Proc Natl Acad Sci U S A* 103:7088–7093
- Xiao Q, Zhang F, Nacev BA, Liu JO, Pei D (2010a) Protein N-terminal processing: substrate specificity of *Escherichia coli* and human methionine aminopeptidases. *Biochem-US* 49:5588–5599
- Xiao R, Anderson S, Aramini J, Belote R, Buchwald WA, Ciccosanti C, Conover K, Everett JK, Hamilton K, Huang YJ, Janjua H, Jiang M, Kornhaber GJ, Lee DY, Locke JY, Ma LC, Maglaqui M, Mao L, Mitra S, Patel D, Rossi P, Sahdev S, Sharma S, Shastry R, Swapna GV, Tong SN, Wang D, Wang H, Zhao L, Montelione GT, Acton TB (2010b) The high-throughput protein sample production platform of the Northeast Structural Genomics Consortium. *J Struct Biol* 172: 21–33
- Yasuda K, Chang HH, Wu HL, Ishii S, Fan JQ (2004) Efficient and rapid purification of recombinant human alpha-galactosidase A by affinity column chromatography. *Protein Expr Purif* 37:499–506



Article

## Structural Investigation of the Oligosaccharide Portion Isolated from the Lipooligosaccharide of the Permafrost Psychrophile *Psychrobacter arcticus* 273-4

Angela Casillo <sup>1</sup>, Ermenegilda Parrilli <sup>1</sup>, Sannino Filomena <sup>1,2</sup>, Buko Lindner <sup>3</sup>, Rosa Lanzetta <sup>1</sup>, Michelangelo Parrilli <sup>4</sup>, Maria Luisa Tutino <sup>1</sup> and Maria Michela Corsaro <sup>1,\*</sup>

<sup>1</sup> Dipartimento di Scienze Chimiche, Università degli Studi di Napoli Federico II, Complesso Universitario Monte S. Angelo, Via Cintia 4, Napoli 80126, Italy; E-Mails: angela.casillo@unina.it (A.C.); erparril@unina.it (E.P.); filomena.sannino2@unina.it (S.F.); lanzetta@unina.it (R.L.); tutino@unina.it (M.L.T.)

<sup>2</sup> Institute of Protein Biochemistry, CNR, Via Pietro Castellino 111, Napoli 80131, Italy

<sup>3</sup> Division of Bioanalytical Chemistry, Research Center Borstel, Leibniz-Center for Medicine and Biosciences, Parkallee 10, Borstel D-23845, Germany; E-Mail: blindner@fz-borstel.de

<sup>4</sup> Dipartimento di Biologia, Università degli Studi di Napoli Federico II, Complesso Universitario Monte S. Angelo, Via Cintia 4, Napoli 80126, Italy; E-Mail: parrilli@unina.it

\* Author to whom correspondence should be addressed; E-Mail: corsaro@unina.it; Tel.: +39-081-674149; Fax: +39-081-674393.

Academic Editor: Antonio Trincone

Received: 22 June 2015 / Accepted: 14 July 2015 / Published: 22 July 2015

**Abstract:** Psychrophilic microorganisms have successfully colonized all permanently cold environments from the deep sea to mountain and polar regions. The ability of an organism to survive and grow in cryoenvironments depends on a number of adaptive strategies aimed at maintaining vital cellular functions at subzero temperatures, which include the structural modifications of the membrane. To understand the role of the membrane in the adaptation, it is necessary to characterize the cell-wall components, such as the lipopolysaccharides, that represent the major constituent of the outer membrane. The aim of this study was to investigate the structure of the carbohydrate backbone of the lipooligosaccharide (LOS) isolated from the cold-adapted *Psychrobacter arcticus* 273-4. The strain, isolated from a 20,000-to-30,000-year-old continuously frozen permafrost in Siberia, was cultivated at 4 °C. The LOS was isolated from dry cells and analyzed by means of chemical methods. In particular, it was degraded either by mild acid hydrolysis or by hydrazinolysis and

investigated in detail by  $^1\text{H}$  and  $^{13}\text{C}$  NMR spectroscopy and by ESI FT-ICR mass spectrometry. The oligosaccharide was characterized by the substitution of the heptose residue, usually linked to Kdo in the inner core, with a glucose, and for the unusual presence of *N*-acetylmuramic acid.

**Keywords:** *Psychrobacter arcticus* strain 273-4; glycoconjugates; lipopolysaccharide; *N*-acetylmuramic acid; structural determination; NMR spectroscopy

---

## 1. Introduction

Cold environments are arguably the most widespread on our planet and in our solar system [1]. At least 80% of terrestrial habitats and oceans are permanently cold, together with six of the other eight planets of our solar system. Hence, understanding life's adaptation to cold environments on our planet could be useful in the search for and understanding of life on other planets [2].

Many microorganisms populate Arctic and Antarctic regions [3], and those inhabiting permafrost in particular are good candidates to study cold-adaptation, due to the mean annual temperature between  $-10$  and  $-12$  °C in the Arctic and between  $-18$  and  $-27$  °C in the Antarctic [4]. Although living microorganisms can be successfully recovered either from ice or permafrost, the latter is a more proficient environment to sustain longer growth time due to its heterogeneous soil particles and larger reservoirs of nutrients [5–7].

One physiological response to the cold environment is the alteration of membrane components, such as the presence of unsaturated and branched fatty acids in phospholipids that maintain membrane fluidity [8], and the different phosphorylation of membrane proteins and lipopolysaccharides [9–14].

The lipopolysaccharides (LPSs) are the major component of the outer membrane (OM) of almost all Gram-negative bacteria and of some cyanobacteria [15–18], constituting approximately 75% of the outer surface. The LPSs are heat-stable amphiphilic molecules indispensable for the viability and survival of Gram-negative bacteria, as they heavily contribute to the structural integrity of the OM and to the protection of the bacterial cell envelope [19].

The structure of an intact smooth (*S*)-type bacterial LPS molecule can be divided into three covalently linked domains: the glycolipid anchor, called lipid A, the intermediate core oligosaccharide (core), and the *O*-specific polysaccharide (*O*-chain) [20]. However, the rough (*R*)-type LPSs (also called lipooligosaccharides, LOSs) are completely devoid of the *O*-specific polysaccharide chain either due to genetic mutation or the inherent nature of bacteria [21].

Extreme habitats drive microbial components to fulfill cell homeostasis through the maintenance of membrane integrity. Thus, the structural characterization of LPSs of cold-adapted Gram-negative bacteria grown at low temperatures could give insight into the cryo-adaptation phenomena understanding.

Until now, only LPSs from marine Arctic [11,22] and Antarctic [12,23] Gram-negative microorganisms have been characterized, but very little is known about isolates from permafrost. It has been shown that viable bacteria are abundant in Siberian permafrost [6,24], and the most frequently isolated from the Kolyma permafrost of northeast Siberia include *Arthrobacter*, *Exiguobacterium*, *Flavobacterium*, *Sphingomonas*, and *Psychrobacter* [4–6]. *Psychrobacter* is considered an indicator

genus for permafrost and other polar environments [25], suggesting that many of its members are adapted to low temperatures and have evolved molecular-level changes that aid survival at low temperatures.

*Psychrobacter arcticus* 273-4 is a Gram-negative bacterium isolated from a 20,000-to-30,000-year-old continuously frozen permafrost horizon in the Kolyma region in Siberia that was not exposed to temperatures higher than 4 °C during isolation [5].

In this paper, we report the structural characterization of the carbohydrate backbone of the LOS of *Psychrobacter arcticus* 273-4 grown at 4 °C.

The lipooligosaccharide was degraded both by mild hydrazinolysis (*O*-deacylation) and by acetic acid hydrolysis. The products were investigated by means of chemical analysis, by <sup>1</sup>H and <sup>13</sup>C NMR spectroscopy and by electrospray ionization Fourier transform ion cyclotron resonance mass spectrometry (ESI FT-ICR MS).

## 2. Results and Discussion

### 2.1. LPS Extraction and Purification

*Psychrobacter arcticus* strain 273-4 cells were grown at 4 °C and removed from the medium by centrifugation. Dried bacteria cells were extracted using a phenol/chloroform/light petroleum (PCP) mixture to obtain the crude LPS. Due to the very low amount of LPS<sub>PCP</sub> (0.03%), cells were extracted by phenol/water method, and the aqueous phase was dialyzed and freeze-dried. In order to purify LPS<sub>w</sub> from other cell contaminants, the sample was treated with DNase, RNase, and protease followed by dialysis (LPS<sub>w</sub>, 3.1%). The purified sample (LPS<sub>w</sub>) was analyzed by DOC-PAGE electrophoresis, and the silver nitrate staining showed bands at low molecular masses, thus revealing a rough LPS (LOS, Figure 1).



**Figure 1.** Analysis of the LPS<sub>w</sub> (Lane **b**) fraction from *P. arcticus* strain 273-4 by 14% DOC-PAGE. The gel was stained with silver nitrate and was compared with LPS from *E. coli* O127: B8 (Lane **a**).

The sugar composition of the intact LOS was obtained by GC-MS analysis of the acetylated methyl glycosides and revealed the occurrence of rhamnose (rha), galactose (gal), glucose (glc), *N*-acetylmuramic acid (NAM), and 3-deoxy-D-*manno*-oct-2-ulosonic acid (Kdo). Methylation analysis

indicated the presence of 3-substituted Rha, terminal Glc, 4-substituted Glc, 3-substituted Gal, terminal NAM, 3,4,6-trisubstituted Glc, 3,4-disubstituted Glc, terminal Kdo, and 4,5-disubstituted Kdo. The methylation data also revealed a pyranose ring for all the residues. The absolute configurations of the sugar residues were determined by GC-MS analysis of the corresponding acetylated 2-octyl glycosides; all the hexoses were founded to be in the D-configuration, while rhamnose residue in the L-configuration. The absolute configuration of *N*-acetylmuramic acid was supported by the NMR data (see below).

Fatty acids analysis revealed the presence of the following main components: 3-hydroxy dodecanoic 12:0(3OH), 3-hydroxy tetradecanoic 14:0(3OH), tetradecanoic 14:0, tetradecenoic 14:1, pentadecanoic 15:0, and pentadecenoic 15:1 acids.

## 2.2. Deacylation of the LPS

The LOSw was *O*-deacylated with anhydrous hydrazine and the product obtained (LOS-OH) was analyzed by ESI FT-ICR mass spectrometry. The charge deconvoluted mass spectrum showed various K-adducts  $[M + n(K - H)]$  of four main ion populations M1–M4 (Figure 2), the composition of which is reported in Table 1. The most abundant ion population with a mass of 2633.927 u was attributed to the following composition: DeoxyHexHex<sub>5</sub>Kdo<sub>2</sub>NAMHexN<sub>2</sub>P<sub>2</sub> [14:0(3OH)] [12:0(3OH)]  $[M1 + (K - H)]$ , calculated monoisotopic mass: 2633.934 u). The signal of M3, occurring at 162.052 u lower than M1, suggested the presence of ion populations containing one hexose less. In addition, the intensity of the signal of M3 suggests very low abundance of this glycoform. The ion populations M2 and M4 were attributed the same sugar composition as M1 and M3, respectively, whereas the mass difference of 28.03 u is due to a 3-hydroxy dodecanoic in place of the 3-hydroxy tetradecanoic acid.

In addition, the methylation data revealed that the lack of the hexose residue for the ion populations M3 and M4 was from the position *O*-6 of the 3,4,6-trisubstituted glucose.

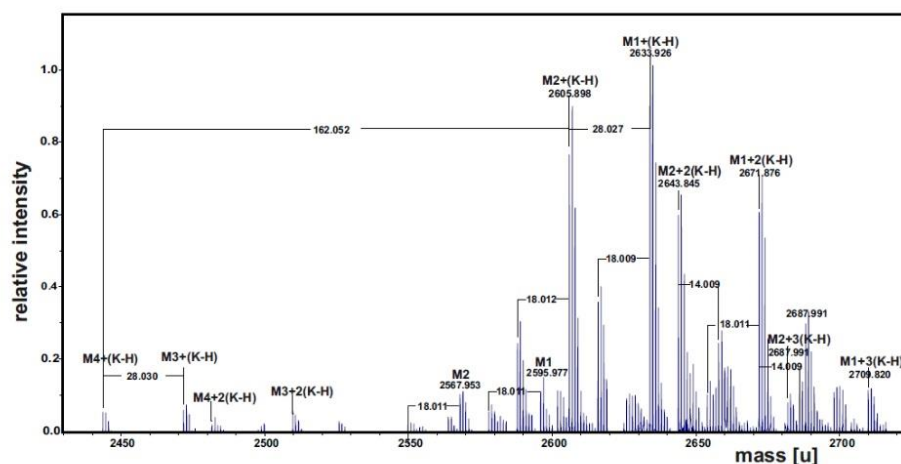


**Figure 2.** Charge deconvoluted ESI FT-ICR mass spectrum of the LOS-OH fraction isolated from *P. arcticus* 273-4. The spectrum was acquired in the negative ion mode.

**Table 1.** Composition of the main species observed in the charge deconvoluted ESI FT-ICR mass spectrum of the *O*-deacylated LOS from *P. arcticus* 273-4. Mass numbers given refer to the monoisotopic masses.

Species	Observed Mass [u]	Calculated Mass [u]	Composition <sup>a</sup>
M1-H + K	2633.926	2633.934	NAMDeoxyHexHex <sub>5</sub> Kdo <sub>2</sub> HexN <sub>2</sub> P <sub>2</sub> [14:0(3OH)] [12:0(3OH)]
M2-H + K	2605.898	2605.903	NAMDeoxyHexHex <sub>5</sub> Kdo <sub>2</sub> HexN <sub>2</sub> P <sub>2</sub> [12:0(3OH)] [12:0(3OH)]
M3-H + K	2471.875	2471.882	NAMDeoxyHexHex <sub>4</sub> Kdo <sub>2</sub> HexN <sub>2</sub> P <sub>2</sub> [14:0(3OH)] [12:0(3OH)]
M4-H + K	2443.845	2443.851	NAMDeoxyHexHex <sub>4</sub> Kdo <sub>2</sub> HexN <sub>2</sub> P <sub>2</sub> [12:0(3OH)] [12:0(3OH)]

<sup>a</sup> All molecular species were revealed as K salts.

### 2.3. Mild Acid Hydrolysis of the LPS

The well-known ability of the LOS to form micellar aggregates in aqueous solution did not allow the direct structural NMR analysis. Thus, the LOS was hydrolyzed under mild acidic conditions to cleave the unstable Kdo glycosidic linkage between the lipid A and the saccharidic region. After centrifugation, the supernatant containing the core oligosaccharidic portion of the LOS was separated from a precipitate constituted by the lipid A. The supernatant was analyzed by ESI FT-ICR MS. The charge deconvoluted mass spectrum displayed the presence of two main ion populations (N1 and N2, Figure 3). As expected, for the most abundant N1, occurring at 1469.501 u (calculated monoisotopic mass: 1469.48 u), it was found the following composition: NAMDeoxyHexHex<sub>5</sub>Kdo<sub>1</sub>. Again, the difference of 162.056 u with N2 confirmed the presence of an ion population lacking one hexose residue. No peaks with two Kdo residues were found, since the ketosidic bond is much more acid-labile than the common aldoidic bonds. Signals at 46.00 and 18.01 u lower mass values with respect to N1 were both assignable to Kdo artifacts [26].

The supernatant mixture was further purified on a Bio-Gel P-10 chromatography column (Bio-Rad Laboratories S.r.l., Milano, Italy), using pyridinium acetate buffer as eluent. The main obtained fraction, named OS, was studied by two-dimensional NMR spectroscopy.



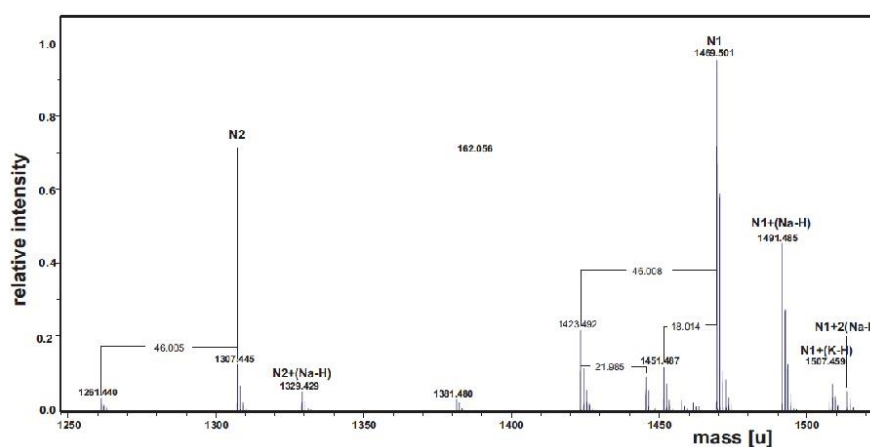


**Figure 3.** Charge deconvoluted ESI FT-ICR mass spectrum of the supernatant of acetic acid hydrolysis of *P. arcticus* 273-4 LOS. The spectrum was acquired in the negative ion mode.

#### 2.4. NMR Spectroscopic Analysis of OS

To characterize the core oligosaccharide OS fraction, it was analyzed by one- and two-dimensional NMR spectroscopy. In particular,  $^1\text{H}$ - $^1\text{H}$  DQF-COSY (double quantum-filtered correlation spectroscopy),  $^1\text{H}$ - $^1\text{H}$  TOCSY (total correlation spectroscopy),  $^1\text{H}$ - $^1\text{H}$  ROESY (rotating-frame nuclear Overhauser enhancement spectroscopy),  $^1\text{H}$ - $^{13}\text{C}$  DEPT-HSQC (distortionless enhancement by polarization transfer-heteronuclear single quantum coherence), and  $^1\text{H}$ - $^{13}\text{C}$  HMBC (heteronuclear multiple bond correlation) experiments were performed.

The  $^1\text{H}$ -NMR spectrum of the OS fraction, recorded at 310 K, is shown in Figure 4. Seven anomeric proton signals (A–G), attributable to core monosaccharide residues, were present in the region between  $\delta$  4.5 and  $\delta$  5.4 ppm (Table 2).

The  $^1\text{H}$ -NMR spectrum of OS was also recorded at 318 K (data not shown) in order to reduce the anomeric signals overlapping. In this experiment, the anomeric proton signal of E was clearly visible. Moreover, the integration of all anomeric signals showed a relative ratio of 1:1 except for the signal at 4.51 ppm. In fact, the peak area for this signal was twice the amount of every other proton anomeric signal, thus indicating the coincidence of H-1 of F with H-1 of G chemical shifts.

By considering all the two-dimensional NMR experiments, the spin systems of all the monosaccharides were identified (Table 2).

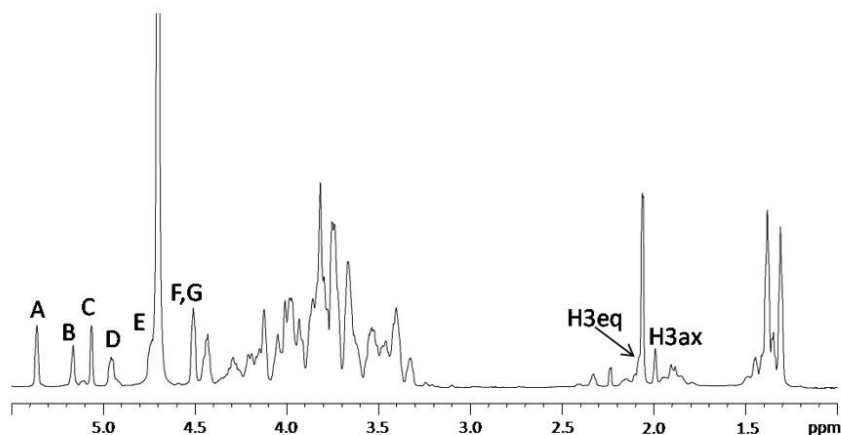


**Figure 4.**  $^1\text{H}$  NMR spectrum of the core oligosaccharide (OS) obtained by mild hydrolysis of LOS. The spectrum was recorded in  $\text{D}_2\text{O}$  at 310 K at 600 MHz. The letters refer to the residues as described in Table 2 and Scheme 1.

**Table 2.**  $^1\text{H}$  and  $^{13}\text{C}$  NMR assignments of the oligosaccharide OS obtained from acetic acid hydrolysis of the LOS from *P. arcticus* strain 273-4. The spectra were recorded at 310 K at 600 MHz.

Residue	H1	H2	H3	H4	H5	H6	H7	H8	
	C1	C2	C3	C4	C5	C6	C7	C8	
Lactyl							C1' <sup>a</sup>	H2' <sup>a</sup> C2'	H3' C3'
A	5.36	3.72	3.78	3.66	3.98	3.64/3.81	-	4.43	1.40
<i>α</i> -D-MurNAc <sup>b</sup>	95.1	55.0	78.3	71.8	73.5	64.5	183.2	79.8	20.0
B	5.16	3.84	4.28	3.98	4.44	4.04/4.19			
3,4,6- <i>α</i> -D-Glcp	100.9	73.6	78.0	75.2	71.4	68.8			
C	5.06	4.12	3.86	3.57	3.82	1.30			
3- <i>α</i> -L-Rhap	103.5	68.6	77.2	71.7	70.8	18.8			
D	4.95	3.38	3.52	3.43	3.47	3.74/3.93			
<i>β</i> -D-Glcp	102.9	74.8	77.2	71.5	77.1	62.2			
E	4.75	3.41	3.67	3.67	3.61	3.82/3.97			
4- <i>β</i> -D-Glcp	102.2	74.3	75.6	79.7	76.1	61.5			
F	4.52	3.66	3.72	4.01	3.75	3.74/3.92			
3- <i>β</i> -D-Galp	104.2	71.6	81.6	69.6	76.5	62.2			
G	4.51	3.33	3.52	3.41	3.46	3.74/3.92			
<i>β</i> -D-Glcp	103.8	74.4	77.1	74.3	77.3	62.2			
H	n.d.	-	1.89/2.09	4.16	4.11	3.87	4.06	3.78/3.80	
5-Kdo		97.8	35.5	67.3	77.0	72.8	70.0	64.5	

Additional chemical shifts: <sup>a</sup> All lactyl resonances of MurNAc are labelled prime: 1', carboxylate; 2', linkage point; 3', methyl; <sup>b</sup> NAc resonances:  $\delta$  2.07/23.0 ppm ( $\text{CH}_3$ ), 175.5 ppm (CO); n.d.: not determined.

Residue A with H-1/C-1 signals at  $\delta$  5.36/95.1 ppm was identified as a 3-*O*-(1-carboxyethyl) ether of 2-acetamido-2-deoxy glucopyranosyl residue (namely *N*-acetylmuramic acid (NAM)), with an  $\alpha$ -anomeric configuration, as suggested by the low  $^3J_{H-1,H-2}$  value (3.1 Hz). Moreover, its H-2 proton at  $\delta$  3.72 ppm was correlated, in the DEPT-HSQC experiment (Figure 5), with a C-2 resonance occurring at  $\delta$  55.0 ppm, thus indicating a nitrogen-bearing carbon atom. In addition, the HMBC spectrum showed a long range scalar coupling between the signal of H-3 at  $\delta$  3.78 ppm with the signal at  $\delta$  79.8 ppm, attributed to C-2' of 1-carboxyethyl substituent. The same experiment also revealed a correlation between the signal at  $\delta$  4.43 ppm, attributed to H-2', with both the signals of C-1' ( $\delta$  183.2 ppm) and C-3' ( $\delta$  20.0 ppm), respectively, of 1-carboxyethyl substituent. Finally, a correlation between H-2 signal at  $\delta$  3.72 ppm and the carbonyl signal of NAc group at  $\delta$  175.5 ppm was also identified.

The correlations of each H-1 to H-6 with all other protons of residues B, D, E, and G in the TOCSY spectrum provided evidence for the *gluco* configuration of all these ring systems.

Residue B with H-1/C-1 signals at  $\delta$  5.16/100.9 ppm was assigned to a 3,4,6 trisubstituted  $\alpha$ -glucose unit on the basis of the small anomeric coupling constant value ( $^3J_{H-1,H-2} = 3.7$  Hz). The downfield shift of C-3, C-4, and C-6 values of this unit at  $\delta$  78.0, 75.2, and 68.8 ppm, respectively [27], identified its substitution. This residue was linked to Kdo residue at the *O*-5 position, as shown by the correlation between H-1 B and C-5 of H in the HMBC spectrum (Figure 6, Table 3).

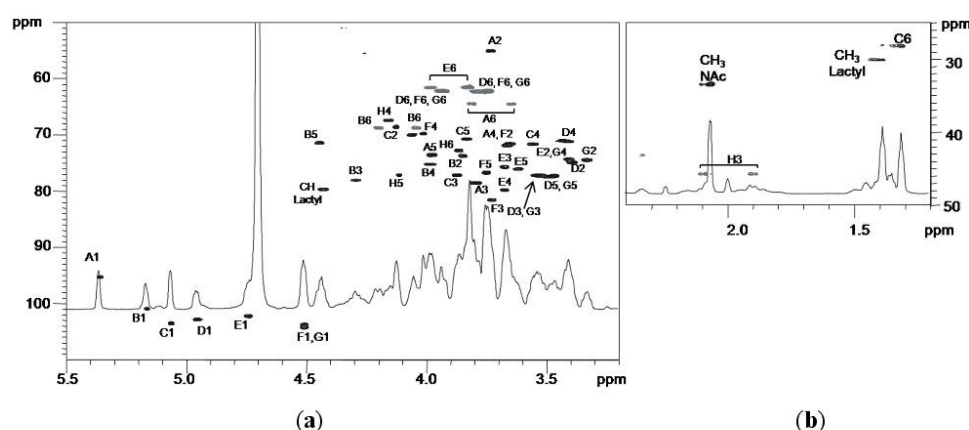


**Figure 5.** Anomeric/carbinolic (a) and aliphatic regions (b) of  $^1\text{H}$ - $^{13}\text{C}$  DEPT-HSQC spectrum of OS core of the LOS from *P. arcticus* strain 273-4. The spectrum was recorded in  $\text{D}_2\text{O}$  at 310 K at 600 MHz.

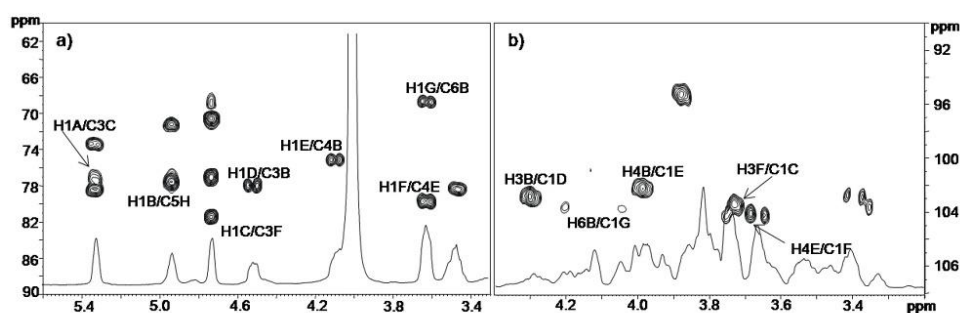


**Figure 6.** Anomeric (a) and carbinolic (b) regions of  $^1\text{H}$ - $^{13}\text{C}$  HMBC spectrum of OS core of the LOS from *P. arcticus* 273-4. The spectrum was recorded in  $\text{D}_2\text{O}$  at 310 K at 600 MHz.

**Table 3.** Correlations for H-1 and C-1 in the two-dimensional ROESY and  $^1\text{H}$ ,  $^{13}\text{C}$  HMBC spectra of the oligosaccharide OS obtained from acetic acid hydrolysis of the LOS from *P. arcticus* strain 273-4. The spectra were recorded at 310 K at 600 MHz.

Anomeric Atom in Sugar Residue ( $\delta$ )	Correlations to Atom in Sugar Residue ( $\delta$ )	
	ROESY	HMBC
A H-1 (5.36) C-1 (95.1)	C H-3 (3.86)	C H-3 (3.86)
B H-1 (5.16)	H H-5 (4.11)	H C-5 (77.0)
C H-1 (5.06)	F H-3 (3.72)	F C-3 (81.6)
D H-1 (4.95) C-1 (102.9)	B H-3 (4.28)	B H-3 (4.28)
E H-1 (4.75) C-1 (102.2)	B H-4 (3.98)	B H-4 (3.98)
F H-1 (4.52)	E H-4 (3.67)	E C-4 (79.7)
G H-1 (4.51) C-1 (103.8)	B H-6 (4.04,4.19)	B H-6 (4.04,4.19)

The lack of heptose residue, usually linked in the inner core to the Kdo, has been found so far in the Moraxellaceae [28] and Rhizobiaceae families [29,30]. The only example of a heptose-deficient core region among lipopolysaccharides from psychrophiles was found in *Colwellia psychrerythraea* strain 34H [22].

Residues D and G with H-1/C-1 signals at  $\delta$  4.95/102.9 and  $\delta$  4.51/103.8 ppm, respectively, were identified as terminal  $\beta$ -glucoses, since none of their carbons were shifted by glycosylation. For both residues the  $\beta$  configuration was inferred by the high  $^3J_{\text{H-1,H-2}}$  values (8.1 and 8.0 Hz for D and G, respectively). *Intra*-residue NOE (Nuclear Overhauser Effect) contacts of H-1 with H-3 and H-5 ( $\delta$  3.52 and 3.47 ppm, and  $\delta$  3.52 and 3.46 ppm, for D and G, respectively) were in agreement with  $\beta$ -anomeric configurations.

A  $^3J_{\text{H-1,H-2}}$  coupling constant of 8.0 Hz for residue E indicated a  $\beta$ -configuration, which was also confirmed by *intra*-residue NOEs. The C-4 of residue E was downfield shifted at  $\delta$  79.7 ppm with respect to the unsubstituted value [31], thus evidencing that this position was glycosylated. The residue F with H-1/C-1 signals at  $\delta$  4.52/104.2 was identified as a *galacto* configured residue since the TOCSY experiment showed correlations only from H-1 to H-4; in particular, it was identified as a  $\beta$ -galactose

( $^3J_{H-1,H-2} = 8.0$  Hz). Moreover, the downfield shift of proton resonance of C-3 at  $\delta$  81.6 ppm instead of  $\delta$  73.8 ppm of an unsubstituted residue [31] indicated glycosylation at this position.

The residue C with H-1/C-1 signals at  $\delta$  5.06/103.5 ppm was recognized as an  $\alpha$ -rhamnose residue, since the TOCSY spectrum showed scalar correlations of the ring protons with methyl signal in the up-field region at  $\delta$  1.30 ppm. Its  $\alpha$  configuration was suggested by the  $^3J_{H-1,H-2}$  value ( $<3$  Hz) and by the value of its C-5 chemical shift [32]. The downfield shift of carbon resonance of C-3 at  $\delta$  77.2 ppm with respect to the value of  $\delta$  71.0 ppm [31] indicated glycosylation at this position.

Finally, the Kdo (residue H) proton and carbon chemical shifts were identified starting from the diastereotopic protons H-3<sub>ax</sub> and H-3<sub>eq</sub> ( $\delta$  1.89/2.09 ppm).

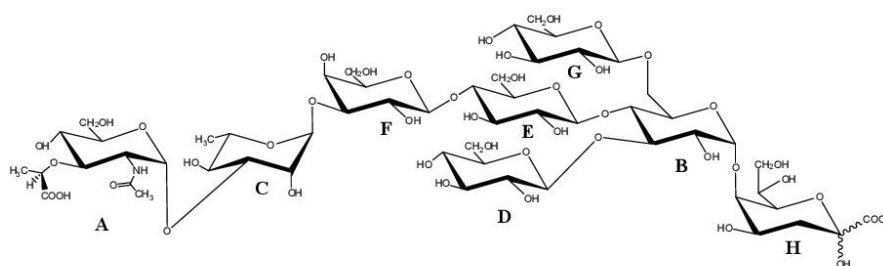
The Kdo H-5 proton was identified by vicinal scalar coupling with H-4 in the COSY spectrum. Moreover, the residue resulted to be glycosylated at O-5 position, as suggested by the downfield shift of its C-5 carbon signal at  $\delta$  77.0 ppm with respect to the value of  $\delta$  67.5 ppm for an unsubstituted Kdo [33].

The sequence of the residues was deduced from the HMBC experiment (Figure 6, Table 3) that indicated the following correlations: H-1 of B and C-5 of H, H-3 of B with C-1 of D, H-4 of B with C-1 of E, and both H-6 of B with C-1 of G. In addition, H-1 of rhamnose C displayed a correlation with C-3 of residue F, while C-1 of residue A displayed a correlation with H-3 of C. Finally, H-1 of galactose F displayed a correlation with C-4 of residue E.

Inter-residue NOE contacts, obtained from ROESY experiments (Table 3), confirmed this sequence, since dipolar couplings were observed between: H-1 of B and H-5 of H, H-1 of G and both H-6 of B, H-1 of E and H-4 of B, H-1 of F and H-4 of E, H-1 of D and H-3 of B, H-1 of A and H-3 of C, H-1 of C and H-3 of F.

The absolute configuration of residue A is based on NMR considerations. The chemical shift of C-1 at  $\delta$  95.1 ppm indicates that the *N*-acetylmuramic acid has the opposite configuration of L-rhamnose, since a value of near 103 ppm would be expected for the same absolute configuration of residue C [34]. As for 1-carboxyethyl substituent, the configuration of (*R*) for C-2' was deduced by comparing both  $^1\text{H}$  and  $^{13}\text{C}$  NMR chemical shifts of residue A with those of *N*-acetylismuramic acid [35,36], characterized by a (*S*) configuration at C-2'.

In conclusion, the complete structure of the core oligosaccharide of the LOS from *Psychrobacter arcticus* 273-4 is reported in Scheme 1.



**Scheme 1.** OS core structure of the LOS from *P. arcticus* strain 273-4.



### 3. Experimental Section

#### 3.1. Bacteria Growth and LPS Isolation

*P. arcticus* strain 273-4, isolated from permafrost soil located in Siberia. Shake flask cultivation were performed in Luria-Bertani broth [37] at 4 °C in aerobic condition. When the liquid cultures reached late exponential phase (about 90 h, OD<sub>600nm</sub> 4) cells were collected by centrifugation for 15 min at 7000 rpm at 4 °C.

Dried bacteria cells (3.1 g) were extracted first by PCP method to give very poor yield of LOS, LPS<sub>PCP</sub> (yield 0.03% w/w of dried cells) and then by hot phenol/water method [38,39]. A 240 mg amount of water extract was dialyzed (cut-off 3500 Da) and then digested with proteases, DNases, and RNases to remove contaminating proteins and nucleic acids. The sample was dialyzed (cut-off 3500 Da) in order obtaining 96 mg of sample (LPS<sub>w</sub>, yield 3.1% w/w of dried cells).

#### 3.2. Sugar and Fatty Acids Analysis

LOS (1 mg) was treated with HCl/CH<sub>3</sub>OH (1.25 M, 1 mL) and the methanolysis was performed at 80 °C for 16 h. The monosaccharides obtained were acetylated and analyzed as acetylated methyl glycosides by GC-MS. The fatty acids were analyzed as methyl esters [11].

The absolute configuration of the sugars was determined by gas chromatography of the acetylated (*S*)-2-octyl glycosides [40]. All the sample derivatives were analyzed on an Agilent Technologies gas chromatograph 6850A equipped with a mass selective detector 5973N and a Zebron ZB-5 capillary column (Phenomenex, 30 m × 0.25 mm i.d., flow rate 1 mL/min, He as carrier gas). Acetylated methyl glycosides were analyzed using the following temperature program: 140 °C for 3 min, 140 °C → 240 °C at 3 °C/min. Analysis of acetylated octyl glycosides was performed as follows: 150 °C for 5 min, 150 °C → 300 °C at 6 °C/min, 300 °C for 5 min. The temperature program for methyl esters of fatty acids is the following: 140 °C for 3 min, 140 °C → 280 °C at 10 °C/min, 280 °C for 20 min.

#### 3.3. Methylation Analysis

The linkage positions of the monosaccharides were determined by GC-MS analysis of the partially methylated alditol acetates (PMAAs).

LOS (1 mg) was methylated with CH<sub>3</sub>I (100 µL) and NaOH powder in DMSO (300 µL) for 20 h [41,42].

To identify the Kdo, the sample was then treated for the reduction of the carboxymethyl groups with sodium borodeuteride NaBD<sub>4</sub>, mildly hydrolyzed (0.1 M trifluoroacetic acid TFA, 100 °C, 30 min) to cleave ketosidic linkages, followed by a reduction (NaBD<sub>4</sub>) of hemiketal group. The product was totally hydrolyzed with 2 M TFA at 120 °C for 2 h, reduced with NaBD<sub>4</sub>, and acetylated with Ac<sub>2</sub>O and pyridine (50 µL each, 100 °C for 30 min). The mixture was analyzed by GC-MS with the following temperature program: 90 °C for 1 min, 90 °C → 140 °C at 25 °C/min, 140 °C → 200 °C at 5 °C/min, 200 °C → 280 °C at 10 °C/min, at 280 °C for 10 min.

### 3.4. Deacylation of the LOS

The LOS (70 mg) was dried over phosphorus anhydride under vacuum and then incubated with hydrazine (3.5 mL, at 37 °C for 2 h). To precipitate the LOS-OH, cold acetone was added; the pellet was recovered after centrifugation at 4 °C and 7000 rpm for 30 min, washed two times with acetone, and finally suspended in water and lyophilized (55 mg) [43].

### 3.5. Mild Acid Hydrolysis

The LOS (20 mg) was hydrolyzed with 1% aqueous CH<sub>3</sub>COOH (2 mL, 100 °C for 4 h). The resulting suspension was then centrifuged (7500 rpm, 4 °C, 30 min) and the pellet was washed twice with water. The supernatant layers obtained were combined and lyophilized. The mixture of oligosaccharides was then fractionated on a Bio-Gel P-10 column (Biorad, 1.5 × 110 cm, flow rate 15 mL/h, fraction volume 2 mL) and eluted with water buffered with 0.05 M pyridine and 0.05 M AcOH, obtaining the oligosaccharide fraction named OS (6 mg).

### 3.6. Mass Spectrometry Analysis

Electrospray ionization Fourier transform ion cyclotron (ESI FT-ICR) mass spectrometry was performed in negative ion mode using an APEX QE (Bruker Daltonics GmbH, Bremen, Germany) equipped with a 7 Tesla actively shielded magnet. The LOS sample was dissolved at a concentration of ~10 ng/μL, sprayed at a flow rate of 2 μL/min, and analyzed as described previously [44]. Mass spectra obtained were charge-deconvoluted and the mass numbers given refer to the monoisotopic masses of the neutral molecules.

### 3.7. NMR Spectroscopy

<sup>1</sup>H and two-dimensional NMR spectra were performed using a Bruker Avance 600 MHz spectrometer equipped with a cryoprobe (Bruker Italia, Milano, Italy). Two-dimensional homo- and heteronuclear experiments (COSY, TOCSY, ROESY, DEPT-HSQC, and HMBC) were performed using standard pulse sequences available in the Bruker software. <sup>1</sup>H was measured at 310 K and 318 K while two-dimensional NMR spectra were recorded at 310 K and the mixing time for TOCSY and ROESY experiments was 100 ms. The <sup>13</sup>C NMR spectrum was recorded in D<sub>2</sub>O at 298 K Bruker Avance 400 MHz spectrometer (data not shown).

## 4. Conclusions

In this paper, the complete structure of the sugar backbone of the LPS from the permafrost isolate *Psychrobacter arcticus* 273-4 is reported. The structure shows a particular inner core region, with a residue of glucose linked to the Kdo in place of a *manno*-heptose. This structural feature has been found only in another psychrophile, namely *Colwellia psychrerythrae* 34H, which showed a mannose residue linked to the Kdo.

Generally, the oligo- and polysaccharides produced by marine bacteria are distinguished by the acidic character [45] and by the occurrence of unusual sugars [46], non-sugar substituents [22,47–49] or

structures that are highly phosphorylated [10]. Although *P. arcticus* 273-4 was isolated from Arctic permafrost, it displays similar characteristics of cold-adapted marine isolates, due to the presence of the unusual residue of NAM. *N*-acetylmuramic acid, commonly encountered as a component of bacterial cell-wall peptidoglycan, has been already found in the *O*-specific polysaccharide of *Yersinia ruckerii* [50] and *Proteus penneri* [51], but to the best of our knowledge, this is the first time that it has been found in a core oligosaccharide.

It is well known that cold-adapted microorganisms are able to modify the fluidity of the cellular membrane in response to a lowering of temperature by producing a higher content of unsaturated, polyunsaturated, and methyl-branched fatty acids [52,53]. Instead, how bacteria modify the LPS structures in response to the cold stress is still poorly understood.

Even though only few LPS structures from cold-adapted bacteria have been characterized [11,12,22,23], their attractive feature is the production of rough lipopolysaccharides. Moreover, it is worth noting that *Psychrobacter arcticus* 273-4, a permafrost isolate, shares this feature with marine isolates. To the best of our knowledge, only two examples of smooth lipopolysaccharides isolated from psychrophiles have been reported so far [54,55], even if the isolates were grown at 24 °C.

By increasing the number of characterized LPS structures from psychrophiles, it will be conceivable in the future to find a connection between the lack of the polysaccharidic portion and the Gram-negative membrane cold adaptation.

### Acknowledgments

The authors thank the Centro Interdipartimentale Metodologie Chimico Fisiche, University of Naples, “Federico II”, and BioTekNet for the use of the 600 MHz NMR spectrometer. This work was supported by Regione Campania, Progetto Operativo Campania 2007/2013 (Progetto BIP, BioIndustrial Processes). Dedicated to the memory of Professor Matteo Adinolfi.

### Author Contributions

A.C. performed chemical analysis and NMR spectra; E.P. and S.F. grew bacterium cells; B.L. provided mass spectra; R.L., M.P. and M.M.C. contributed for NMR data interpretation; M.L.T. and M.M.C. conceived and designed the experiments; A.C. and M.M.C. wrote the paper.

### Conflicts of Interest

The authors declare no conflict of interest.

### References

1. Rodrigues, D.F.; Tiedje, J.M. Coping with our cold planet. *Appl. Environ. Microb.* **2008**, *74*, 1677–1686.
2. Parrilli, E.; Sannino, F.; Marino, G.; Tutino, M.L. Life in icy habitats: Novel insights into panspermia theory. *Rend. Fis. Acc. Lincei* **2011**, *22*, 375–383.
3. Chattopadhyay, M.K.; Reddy, G.S.; Shivaji, S. Psychrophilic Bacteria: Biodiversity, Molecular Basis of Cold Adaptation and Biotechnological Implications. *Curr. Opin. Biotech.* **2014**, *3*, 100–116.

4. Rodrigues, D.F.; Jesus, E.C.; L'Ayala-del-Río, H.C.; Pellizari, V.H.; Gilichinsky, D.; Sepulveda-Torres, L.; Tiedje, J.M. Biogeography of two cold-adapted genera: *Psychrobacter* and *Exiguobacterium*. *ISME J.* **2009**, *3*, 658–665.
5. Rivkina, E.M.; Friedmann, E.I.; McKay, C.P.; Gilichinsky, D.A. Metabolic activity of permafrost bacteria below the freezing point. *Appl. Environ. Microbiol.* **2000**, *66*, 3230–3233.
6. Vishnivetskaya, T.; Kathariou, S.; McGrath, J.; Gilichinsky, D.A.; Tiedje, J.M. Low-temperature recovery strategies for the isolation of bacteria from ancient permafrost sediments. *Extremophiles* **2000**, *4*, 165–173.
7. Vishnivetskaya, T.A.; Petrova, M.A.; Urbance, J.; Ponder, M.; Moyer, C.L.; Gilichinsky, D.A.; Tiedje, J.M. Bacterial community in ancient Siberian permafrost as characterized by culture and culture-independent methods. *Astrobiology* **2006**, *6*, 400–414.
8. Chattopadhyay, M.K. Mechanism of bacterial adaptation to low temperature. *J. Biosci.* **2006**, *31*, 157–165.
9. Ummarino, S.; Corsaro, M.M.; Lanzetta, R.; Parrilli, M.; Peter-Katalinić, J. Determination of phosphorylation sites in lipooligosaccharides from *Pseudoalteromonas haloplanktis* TAC 125 grown at 15 °C and 25 °C by nano-electrospray ionization quadrupole time-of-flight tandem mass spectrometry. *Rapid Commun. Mass Spectrom.* **2003**, *17*, 2226–2232.
10. Corsaro, M.M.; Lanzetta, R.; Parrilli, E.; Parrilli, M.; Tutino, M.L.; Ummarino, S. Influence of Growth Temperature on Lipid and Phosphate Contents of Surface Polysaccharides from the Antarctic Bacterium *Pseudoalteromonas haloplanktis* TAC 125. *J. Bacteriol.* **2004**, *186*, 29–34.
11. Corsaro, M.M.; Pieretti, G.; Lindner, B.; Lanzetta, R.; Parrilli, E.; Tutino, M.L.; Parrilli, M. Highly phosphorylated core oligosaccharide structures from cold-adapted *Psychromonas arctica*. *Chem. Eur. J.* **2008**, *14*, 9368–9937.
12. Carillo, S.; Pieretti, G.; Parrilli, E.; Tutino, M.L.; Gemma, S.; Molteni, M.; Lanzetta, R.; Parrilli, M.; Corsaro, M.M. Structural Investigation and Biological Activity of the Lipooligosaccharide from the Psychrophilic Bacterium *Pseudoalteromonas haloplanktis* TAB 23. *Chem. Eur. J.* **2011**, *17*, 7053–7060.
13. Ray, M.K.; Kumar, G.S.; Shivaji, S. Phosphorylation of membrane proteins in response to temperature in an Antarctic *Pseudomonas syringae*. *Microbiology* **1994**, *140*, 3217–3223.
14. Ray, M.K.; Kumar, G.S.; Shivaji, S. Phosphorylation of lipopolysaccharides in the Antarctic psychrotroph *Pseudomonas syringae*: A possible role in temperature adaptation. *J. Bacteriol.* **1994**, *176*, 4243–4249.
15. Lüderitz, O.; Freudenberg, M.A.; Calanos, C.; Lehmann, V.; Rietschel, E.T.; Shaw, D.H. Lipopolysaccharides of Gram-Negative bacteria. In *Current Topics in Membranes and Transport*; Razin, S., Rottem, S., Eds.; Academic Press Inc.: New York, NY, USA, 1982; Volume 17, pp. 79–51.
16. Westphal, O.; Lüderitz, O.; Galanos, C.; Mayer, H.; Rietschel, E.T. *Advances in Immunopharmacology*; Chedid, L., Hadden, J.W., Spreafico, F., Eds.; Pergamon Press: Oxford, UK, 1986; pp. 13–34.
17. Wilkinson, S.C. *Surface Carbohydrates of the Prokaryotic Cell*; Sutherland, I.W., Ed.; Academic Press Inc.: New York, NY, USA 1977; pp. 97–105.
18. Carillo, S.; Pieretti, G.; Bedini, E.; Parrilli, M.; Lanzetta, R.; Corsaro, M.M. Structural investigation of the antagonist LPS from the cyanobacterium *Oscillatoria planktothrix* FP1. *Carbohydr. Res.* **2014**, *388*, 73–80.

19. Alexander, C.; Rietschel, E.T. Bacterial lipopolysaccharides and innate immunity. *J. Endotoxin Res.* **2001**, *7*, 167–202.
20. Caroff, M.; Karibian, D. Structure of bacterial lipopolysaccharides. *Carbohydr. Res.* **2003**, *338*, 2431–2447.
21. Luderitz, O.; Galanos, C.; Risse, H.J.; Ruschmann, E.; Schlecht, S.; Schmidt, G.; Wheat, R.; Westphal, O.; Schlosshardt, J. Structural relationships of Salmonella O and R antigens. *Ann. N.Y. Acad. Sci.* **1966**, *133*, 349–374.
22. Carillo, S.; Pieretti, G.; Lindner, B.; Parrilli, E.; Sannino, F.; Tutino, M.L.; Lanzetta, R.; Parrilli, M.; Corsaro, M.M. Structural Characterization of the Core Oligosaccharide Isolated from the Lipopolysaccharide of the Psychrophilic Bacterium *Colwellia psychrerythraea* Strain 34H. *Eur. J. Org. Chem.* **2013**, *2013*, 3771–3779.
23. Corsaro, M.M.; Lanzetta, R.; Parrilli, E.; Parrilli, M.; Tutino, M.L. Structural investigation on the lipooligosaccharide fraction of psychrophilic *Pseudoalteromonas haloplanktis* TAC 125 bacterium. *Eur. J. Biochem.* **2001**, *268*, 5092–5097.
24. Shi, T.; Reeves, R.; Gilichinsky, D.; Friedmann, E. Characterization of viable bacteria from Siberian permafrost by 16S rDNA sequencing. *Microb. Ecol.* **1997**, *33*, 169–179.
25. Sul, W.J. Microbial Community Analysis Assessed by Pyrosequencing of rRNA Gene: Community Comparisons, Organism Identification, and Its Enhancement. Ph.D. Dissertation, The Michigan State University, East Lansing, MI, USA, 2009.
26. Olsthoorn, M.M.A.; Haverkamp, J.; Thomas-Oates, J.E. Mass spectrometric analysis of *Klebsiellapneumoniae* ssp. *pneumoniae* rough strain R20 (O1:K20) lipopolysaccharides preparations: Identification of novel core oligosaccharide components and three 3-deoxy-D-manno-oct-2-ulopyranosonic artifacts. *J. Mass Spectrom.* **1999**, *34*, 622–636.
27. Vinogradov, E.; Duus, J.; Brade, H.; Holst, O. The structure of the carbohydrate backbone of the lipopolysaccharide from *Acinetobacter baumannii* strain ATCC 19606. *Eur. J. Biochem.* **2002**, *269*, 422–430.
28. Masoud, H.; Perry, M.B.; Brisson, J.B.; Uhrin, D.; Richards, J.C. Structural elucidation of the backbone oligosaccharide from the lipopolysaccharide of *Moraxella catarrhalis* serotype A. *Can. J. Chem.* **1994**, *72*, 1466–1477.
29. Carlson, R.W.; Krishnaiah, B. Structures of the oligosaccharides obtained from the core regions of the lipopolysaccharides of *Bradyrhizobium japonicum* 61A101c and its symbiotically defective lipopolysaccharide mutant, JS314. *Carbohydr. Res.* **1992**, *231*, 205–219.
30. Forsberg, L.S.; Carlson, R.W. The Structures of the Lipopolysaccharides from *Rhizobium etli* Strains CE358 and CE359. *J. Biol. Chem.* **1998**, *273*, 2747–2757.
31. Jansson, P.-E.; Kenne, L.; Widmalm, G. Computer-assisted structural analysis of polysaccharides with an extended version of CASPER using <sup>1</sup>H- and <sup>13</sup>C-NMR data. *Carbohydr. Res.* **1989**, *188*, 169–171.
32. CASPER. Available online: <http://www.casper.org.au/casper/> (accessed on 31 January 2011)
33. Agrawal, P.K.; Bush, C.A.; Qureshi, N.; Takayama, K. Structural analysis of lipid A and Re-lipopolysaccharides by NMR spectroscopic methods. *Adv. Biophys. Chem.* **1994**, *4*, 179–236.



34. Lipkind, G.M.; Shashkov, A.S.; Knirel, Y.A.; Vinogradov, E.V.; Kochetkov, N.K. A computer-assisted structural analysis of regular polysaccharides on the basis of  $^{13}\text{C}$ -NMR data. *Carbohydr. Res.* **1988**, *175*, 59–75.
35. Knirel, Y.A.; Paramonov, N.A.; Vinogradov, E.V.; Shashkov, A.S.; Kochetkov, N.K.; Sidorczyk, Z.; Swierczko, A. Structure of the *O*-specific polysaccharide of *Proteus penneri* 62 containing 2-acetamido-3-*O*-[(*S*)-1-carboxyethyl]-2-deoxy-D-glucose (*N*-acetylismuramic acid). *Carbohydr. Res.* **1992**, *235*, C19–C23.
36. Gunawardena, S.; Reddy, G.P.; Wanga, Y.; Kolli, V.S.K.; Orlando, R.; Morris, J.G.; Bush, A. Structure of a muramic acid containing capsular polysaccharide from the pathogenic strain of *Vibrio vulnificus* ATCC 27562. *Carbohydr. Res.* **1998**, *309*, 65–76.
37. Sambrook, J.; Russell, D.W. *Molecular Cloning: A Laboratory Manual*, 3rd ed.; Sambrook, J., Russell, D.W., Eds.; Cold Spring Harbor Laboratory Press: New York, NY, USA, 2001.
38. Galanos, C.; Lüderitz, O.; Westphal, O. New Method for the Extraction of *R* Lipopolysaccharides. *Eur. J. Biochem.* **1969**, *9*, 245–249.
39. Westphal, O.; Jann, K. Bacterial lipopolysaccharides: Extraction with phenol-water and further applications of the procedure. *Methods Carbohydr. Chem.* **1965**, *5*, 83–91.
40. Leontein, K.; Lindberg, B.; Lönnngren, J. Assignment of absolute configuration of sugars by g.l.c. of their acetylated glycosides from chiral alcohols. *Carbohydr. Res.* **1978**, *62*, 359–362.
41. Ciucanu, I.; Kerek, F. A simple and rapid method for the permethylation of carbohydrates. *Carbohydr. Res.* **1984**, *131*, 209–217.
42. Forsberg, L.S.; Ramadas Bhat, U.; Carlson, R.W. Structural characterization of the *O*-antigenic polysaccharide of the lipopolysaccharide from *Rhizobium etli* strain CE3. *J. Biol. Chem.* **2000**, *275*, 18851–18863.
43. Holst, O. De-acylation of lipopolysaccharides and isolation of oligosaccharide phosphates. In *Bacterial Toxins: Methods and Protocols, Methods in Molecular Biology*; Holst, O., Ed.; Humana Press: Totowa, NJ, USA, 2000; Volume 145, pp. 345–353.
44. Pieretti, G.; Carillo, S.; Lindner, B.; Lee, K.C.; Lee, J.S.; Lanzetta, R.; Parrilli, M.; Corsaro, M.M. Characterization of the Core Oligosaccharide and the *O*-Antigen Biological Repeating Unit from *Halomonas stevensii* Lipopolysaccharide: The First Case of *O*-Antigen Linked to the Inner Core. *Chem. Eur. J.* **2012**, *18*, 3729–3735.
45. Muldoon, J.; Perepelov, A.V.; Shashkov, A.S.; Nazarenko, L.; Zubkov, V.A.; Gorshkova, R.P.; Ivanova, E.P.; Gorshkova, N.M.; Knirel, Y.A.; Savage, A. Structure of an acidic polysaccharide from the marine bacterium *Pseudoalteromonas flavipulchra* NCIMB 2033T. *Carbohydr. Res.* **2003**, *338*, 459–462.
46. Kenne, L.; Lindberg, B. *The Polysaccharides*; Aspinall, G.O., Ed.; Academic Press: New York, NY, USA, 1983; Volume 2, pp. 287–363.
47. Komandrova, N.A.; Isakov, V.V.; Tomshich, S.V.; Romanenko, L.A.; Perepelov, A.V.; Shashkov, A.S. Structure of an Acidic *O*-Specific Polysaccharide of the Marine Bacterium *Pseudoalteromonas agarivorans* KMM 232 (*R*-form). *Biochem.-Mosc.* **2010**, *75*, 623–628.
48. Hanniffy, O.M.; Shashkov, A.S.; Senchenkova, S.N.; Tomshich, S.V.; Komandrova, N.A.; Romanenko, L.A.; Knirel, Y.A.; Savage, A.V. Structure of an acidic *O*-specific polysaccharide of *Pseudoalteromonas haloplanktis* strain ATCC 14393 containing 2-acetamido-2-deoxy-D- and

- L-galacturonic acids and 3-(*N*-acetyl-D-alanyl) amino-3,6-dideoxy-D-glucose. *Carbohydr. Res.* **1999**, *321*, 132–138.
49. Nazareno, E.L.; Komandrova, N.A.; Gorshkova, R.P.; Tomshich, S.V.; Zubkov, V.A.; Kilicoyne, M.; Savage, A.V. Structures of polysaccharides and oligosaccharides of some Gram negative marine Proteobacteria. *Carbohydr. Res.* **2003**, *338*, 2449–2457.
  50. Beynon, L.M.; Richards, J.C.; Perry, M.B. The structure of the lipopolysaccharide *O*-antigen of *Yersinia ruckeri* serotype O1. *Carbohydr. Res.* **1994**, *256*, 303–317.
  51. Zych, K.; Knirel, Y.A.; Paramonov, N.A.; Vinogradov, E.V.; Arbatsky, N.P.; Senchenkova, S.N.; Shashkov, A.S.; Sidorchuk, Z. Structure of the *O*-specific polysaccharide of *Proteus penneri* strain 41 from a new proposed serogroup O62. *FEMS Immunol. Med. Mic.* **1998**, *21*, 1–9.
  52. Chintalapati, S.; Kiran, M.D.; Shivaji, S. Role of membrane lipid fatty acids in cold adaptation. *Cell. Mol. Biol.* **2004**, *50*, 631–642.
  53. Driessen, J.M.; Van de Vossenberg, J.L.C.M.; Konigs, W.N. Membrane composition and ion-permeability in extremophiles. *FEMS Microbiol. Rev.* **1996**, *18*, 139–148.
  54. Kondakova, A.N.; Novototskaya-Vlasova, K.A.; Arbatsky, N.P.; Drutskaya, M.S.; Shcherbakova, V.A.; Shashkov, A.S.; Gilichinsky, D.A.; Nedospasov, S.A.; Knirel, Y.A. Structure of the *O*-Specific Polysaccharide from the Lipopolysaccharide of *Psychrobacter cryohalolentis* K5<sup>T</sup> Containing a 2,3,4-Triacetamido-2,3,4-trideoxy-L-arabinose Moiety. *J. Nat. Prod.* **2012**, *75*, 2236–2240.
  55. Kondakova, A.N.; Novototskaya-Vlasova, K.A.; Drutskaya, M.S.; Senchenkova, S.N.; Shcherbakova, V.A.; Shashkov, A.S.; Gilichinsky, D.A.; Nedospasov, S.A.; Knirel, Y.A. Structure of the *O*-polysaccharide chain of the lipopolysaccharide of *Psychrobacter muricolla* 2pST isolated from overcooled water brines within permafrost. *Carbohydr. Res.* **2012**, *349*, 78–81.

RESEARCH

Open Access



# Acetate: friend or foe? Efficient production of a sweet protein in *Escherichia coli* BL21 using acetate as a carbon source

Serena Leone<sup>\*</sup>, Filomena Sannino, Maria Luisa Tutino, Ermenegilda Parrilli and Delia Picone<sup>\*</sup>

## Abstract

**Background:** *Escherichia coli* is, to date, the most used microorganism for the production of recombinant proteins and biotechnologically relevant metabolites. High density cell cultures allow efficient biomass and protein yields. However, their main limitation is the accumulation of acetate as a by-product of unbalanced carbon metabolism. Increased concentrations of acetate can inhibit cellular growth and recombinant protein production, and many efforts have been made to overcome this problem. On the other hand, it is known that *E. coli* is able to grow on acetate as the sole carbon source, although this mechanism has never been employed for the production of recombinant proteins.

**Results:** By optimization of the fermentation parameters, we have been able to develop a new acetate containing medium for the production of a recombinant protein in *E. coli* BL21(DE3). The medium is based on a buffering phosphate system supplemented with 0.5% yeast extract for essential nutrients and sodium acetate as additional carbon source, and it is compatible with lactose induction. We tested these culture conditions for the production of MNEI, a single chain derivative of the sweet plant protein monellin, with potential for food and beverage industries. We noticed that careful oxygenation and pH control were needed for efficient protein production. The expression method was also coupled to a faster and more efficient purification technique, which allowed us to obtain MNEI with a purity higher than 99%.

**Conclusions:** The method introduced represents a new strategy for the production of MNEI in *E. coli* BL21(DE3) with a simple and convenient process, and offers a new perspective on the capabilities of this microorganism as a biotechnological tool. The conditions employed are potentially scalable to industrial processes and require only low-priced reagents, thus dramatically lowering production costs on both laboratory and industrial scale. The yield of recombinant MNEI in these conditions was the highest to date from *E. coli* cultures, reaching on average ~180 mg/L of culture, versus typical LB/IPTG yields of about 30 mg/L.

**Keywords:** Acetate, pH control, Lactose induction, Limiting oxygenation, MNEI

## Background

*Escherichia coli* is one of the microorganisms of choice for the production of recombinant proteins at the industrial level. Its use in high density cell cultures allows one to obtain large amounts of unglycosylated, heterologous proteins, with limited production costs and optimized volumetric yields [1, 2]. For this purpose, one of the most

common system, at least on the laboratory scale, involves the use of BL21(DE3) cells in combination with the lactose/IPTG inducible pET plasmids (Novagen) [3]. Cells are routinely grown on rich media, such as Luria-Bertani or Terrific Broth [4]. Alternatively, minimal buffered media such as M9, in combination with a wide variety of carbon sources, can be used [5]. In general, defined media are preferred in industrial applications, due to the possibility of easy scale up and careful control of all nutrients concentration [6]. Within the wide panel of possible

\*Correspondence: serena.leone@unina.it; picone@unina.it  
Department of Chemical Sciences, University of Naples Federico II, via  
Cintia, 80126 Naples, Italy



© 2015 Leone et al. This article is distributed under the terms of the Creative Commons Attribution 4.0 International License (<http://creativecommons.org/licenses/by/4.0/>), which permits unrestricted use, distribution, and reproduction in any medium, provided you give appropriate credit to the original author(s) and the source, provide a link to the Creative Commons license, and indicate if changes were made. The Creative Commons Public Domain Dedication waiver (<http://creativecommons.org/publicdomain/zero/1.0/>) applies to the data made available in this article, unless otherwise stated.

carbon sources, glucose and glycerol are the most utilized because of their convenience, efficiency and ready availability.

Besides all said advantages, batch cultures of *E. coli* in the presence of excess glucose or glycerol produce acidic fermentation by-products, in particular acetate [7, 8]. Acetate is a known inhibitor of biomass and recombinant protein production [9, 10], and the extent of its production is related to bacterial growth rate and to the availability of the carbon source [11, 12], and is directly involved in the regulation of the central carbon metabolism [13]. At pH 7.0–7.5, acetate is present in equilibrium with undissociated acetic acid. The latter, unlike charged acetate ions, can migrate uncontrolled through bacterial membranes, disrupting the transmembrane  $\Delta$ pH and impairing cells viability [14]. For this reason, several techniques have been devised to limit acetate accumulation. These include modifications of the growth medium composition through the addition of amino acids or minerals [15, 16], the design of different process strategies (i.e. fed batch or dialysis culture) [17, 18] or gene engineering on the microorganisms to reduce acetate production and consequent accumulation [10]. These methods are widely reviewed elsewhere [7, 19]. Cultures of *E. coli* K12 tend to produce more acetate compared to BL21 [20, 21]. This is one of the reasons why, although historically adopted in industrial processes, strain K12 is being gradually replaced by BL21 as the preferred microbial host for recombinant protein production. Moreover, recent multi-omics analysis have demonstrated that, compared to strain K12, BL21 possesses superior balance between amino acids production and degradation machineries, thus resulting in more efficient protein yields [22]. Lower acetate production by BL21 compared to K12 is believed to be, in part, also a consequence of a more active glyoxylate shunt, which allows recycling part of the acetate produced during the fermentation toward other gluconeogenic cycles [23, 24]. A recent paper demonstrated that the phenotypic differences between the two strains is due to the high expression of acetyl-CoA synthetase (*acs*) in glucose exponential phase in BL21, which allows the simultaneous consumption of acetate and glucose [25].

Besides being a by-product of fermentative metabolism, acetate and other short chain fatty acids can be used by *E. coli* as carbon sources in conditions of nutrient limitation. Acetate, in its anionic form, cannot diffuse through the membranes, and enters the cells through a transporter-mediated mechanism [26]. Subsequently, it is introduced in the tricarboxylic acid cycle through the glyoxylate shunt, as evidenced by gene profiling [27]. Growing BL21 cells on minimal media with acetate as the sole carbon source proceeds with a longer lag phase and only a slight decrease of the final biomass compared to

other gluconeogenic carbon sources in shake flask cultures [28]. Acetate is a quite inexpensive substrate, readily available and well suited for large scale productions. Nonetheless, to our knowledge, no attempt has ever been made to exploit acetate metabolism to express recombinant proteins at high yields.

In the process of defining an optimal condition for large scale manufacturing of the sweet protein MNEI, we tested protein production in a new complex medium containing acetate as a carbon source. The medium was initially based on a pH 7.0 phosphate buffering system containing 0.5% yeast extract as a supplement of essential micronutrients, growth factors and amino acids. A recent paper by Wang et al. [29] has shown that an alkaline shift of the medium pH (pH 7.5–8.5) helps in reducing acetate stress in BL21 when the bacteria are grown on rich media. The authors hypothesized that increasing the medium pH could help reduce the concentration of undissociated, toxic, acetic acid, therefore limiting free diffusion of acetic acid and accumulation of intracellular acetate. We decided to test the effects of pH variations on recombinant protein production when acetate was used as the only supplemental carbon source, assuming that the phenomenon could also be related to its efficient utilization.

When using BL21(DE3)/pET systems, recombinant gene expression is controlled by the T7 promoter and *lac* system. Induction is conventionally achieved with the non-digestible IPTG, although this reagent is extremely expensive and therefore rarely used in industrial scale ups. Moreover, excess IPTG introduces a metabolic burden, and its by-products can ultimately be toxic for the cells [30]. In recent years, methods that replaced IPTG induction with the safer and cheaper lactose or galactose have been developed [31–34]. Here we show that, using our acetate based medium, recombinant protein synthesis can be efficiently induced with 1 mM lactose.

We tested the performance of the new growth medium for the recombinant production of MNEI, an 11 kDa, single chain derivative of monellin, a plant sweet protein [35]. MNEI can interact with the human sweet taste receptor T1R2–T1R3 and humans perceive it as 100,000 times sweeter than glucose on a molar basis [36]. This protein is potentially devoid of adverse effects and is relatively stable at high temperatures, with a melting temperature of 81.6°C at acidic pHs [37]. For all these reasons, MNEI is a likely candidate for the design of new low calorie sweeteners, with potential applications in food and pharmaceutical industries [38]. The possibility of using MNEI as a sugar replacement in industrial preparations relies on the availability of considerable amounts of protein, therefore, much attention has been given to recombinant technologies to obtain large quantities of product,



and a variety of host/plasmid combinations have been tested, as reviewed in [39]. Reported protein yields for cultures using the BL21/pET system in rich media are in the range of ~30 mg/L of culture [34, 36, 38]. With the acetate based medium, the production of soluble, functional protein using the same expression system was increased about six folds.

## Results

### Optimization of the acetate based medium for the production of MNEI in shake flasks

In order to define a more convenient growth medium with respect to the conditions previously used in the production of MNEI for structural and functional studies [35, 37, 40, 41], we first tested whether lactose could replace IPTG induction in the control (LB) condition. We set up small scale cultures using 250 mL flasks filled with 100 mL of culture media on a rotating shaker at 250 rpm and 37°C. Results from all small scale experiments were compared qualitatively by visual inspection of the Coomassie-stained SDS-PAGE of the total protein extract. We used two different lactose concentrations within the optimal range (1 and 5 mM) [42] and different post-induction times, and found that using 1 mM lactose and prolonging expression to 20 h yielded comparable amounts of recombinant proteins in LB as IPTG induction (Figure 1). This condition was used as the standard induction procedure in all subsequent experiments. The next step was the definition of the new medium, which was initially based on a pH 7.0 phosphate buffer containing 0.25% NaCl and 0.5% yeast extract as a source of amino acids, growth factors and minerals (PY medium). This medium was supplemented with an additional carbon source to a final concentration of 0.4% and protein production was compared after 20 h of 1 mM lactose induction. We evaluated the efficiency of MNEI production when glycerol, acetate, fructose or mixtures of acetate plus glycerol or glucose were present. Total proteins were extracted and analyzed by SDS-PAGE, and all results were also compared to lactose induced expression in LB (Figure 2). Supplementation of PY medium with acetate yielded the best protein expression levels, and the efficiency of protein production in this condition was higher than with conventional carbon sources such as glycerol or fructose. Using mixtures of acetate with glycerol or glucose also decreased the performance compared to the media containing only acetate, probably due to catabolite repression [4, 43].

Having confirmed the possibility of obtaining recombinant protein with the PY-acetate (PYA) medium, we then tried to vary different growth parameters to check whether the efficiency of the protein synthesis could be improved. Our standard shake flask filling (100 mL in 250 mL flasks) was set as the low oxygenation condition,

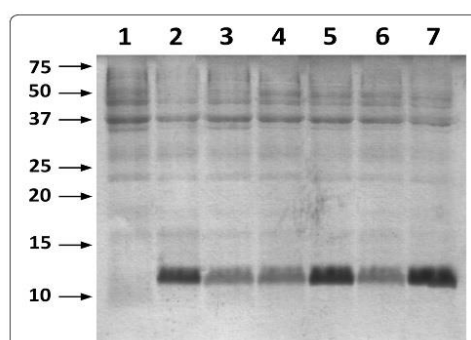


**Figure 1** Optimization of lactose concentration for induction in control conditions. Coomassie stained SDS-PAGE profile of the total protein extract from cell cultured in LB and induction with either IPTG or lactose with different post-induction times. 5  $\mu$ g of soluble protein extract were loaded in each lane. Lane 1 no induction; 2 0.4 mM IPTG, 3 h post-induction; 3 0.4 mM IPTG, 20 h post-induction; 4 1 mM lactose, 3 h post-induction; 5 1 mM lactose, 20 h post-induction; 6 5 mM lactose, 3 h post-induction; 7 5 mM lactose, 20 h post-induction.

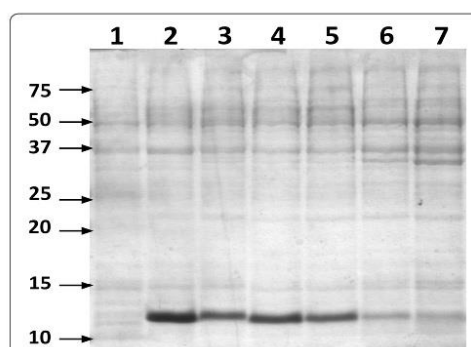
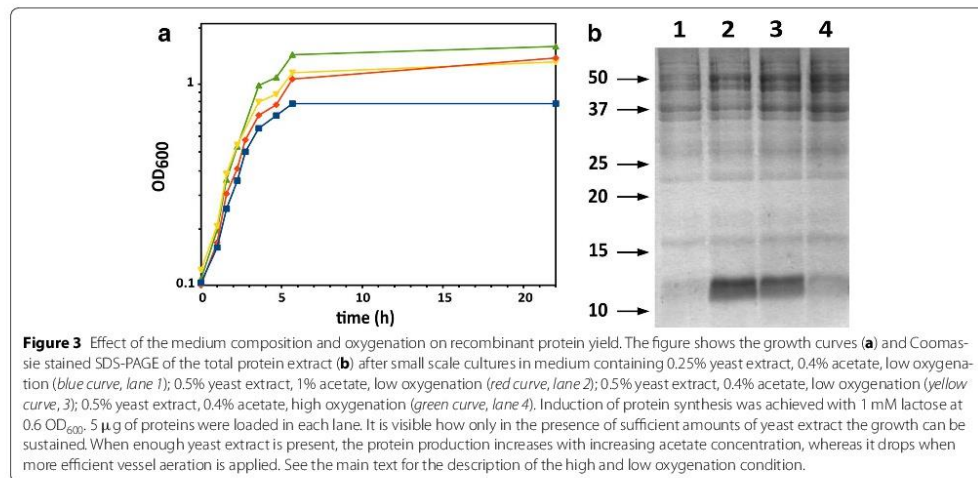


**Figure 2** Efficiency of acetate and other carbon sources with lactose induction. When using sodium acetate, the efficiency of lactose as inducer of protein synthesis is superior to other commonly used carbon sources. The Coomassie stained SDS-PAGE analysis shows 3  $\mu$ g of the total protein extract before induction (lane 1) and after 20 h post-induction with 1 mM lactose in LB (lane 2) or in PY medium supplemented with 0.4% glycerol (lane 3), 0.4% acetate (lane 4), 0.2% glycerol + 0.2% acetate (lane 5), 0.2% glucose + 0.2% acetate (lane 6) or 0.4% fructose (lane 7).

whereas higher oxygenation was achieved by reducing the flask filling level to 50 mL. We also checked the effect of yeast extract reduction (to 0.25%) or sodium acetate increase (to 1%) on biomass and protein production levels. The results of these experiments are reported in Figure 3, which presents the growth curves (panel A)



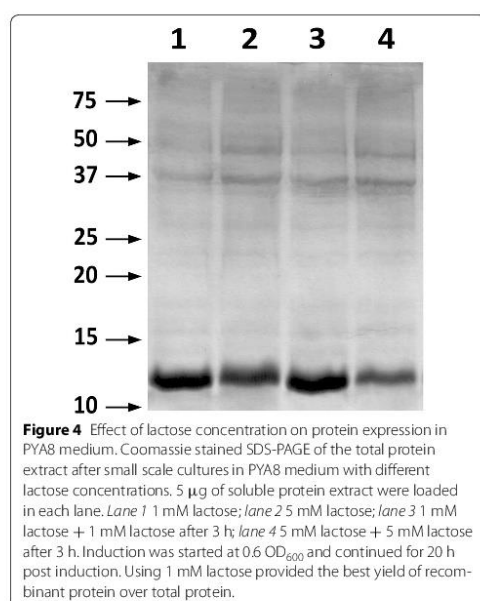


and Coomassie stained SDS-PAGE analysis of the total protein extracts obtained in these conditions (panel B). Reduction of the yeast extract concentration resulted in a sensible biomass and protein yield decrease, as expected since it is known that yeast extract supplementation to culture media is necessary to trigger acetate reduction by *E. coli* [44]. Thus, cultures in these conditions would experience lower nutrients availability, both from the diminution of the yeast extract and from the impaired ability to efficiently utilize the acetate as carbon source. On the other hand, better oxygenation resulted in slightly higher biomass accumulation, but this increase in cell density did not correspond to effective protein production, leading instead to a drop in protein synthesis, as visible in the SDS-PAGE analysis (Figure 3b). Limiting the oxygenation seems therefore required to obtain higher protein yields. In these conditions, and when 0.5% yeast extract was supplied, increasing the concentration of sodium acetate from 0.4 to 1% led to a slight gain in recombinant protein production, while leaving substantially unaffected biomass production. Further experiments with increasing concentrations of sodium acetate in the medium, from 0.4 to 2.5%, were performed, but neither biomass nor protein yield showed significant increase. These results are reported in the supplementary data (Additional file 1: Figure S1).

Recent studies by Wang et al. on BL21 tolerance to acetate [29] have shown that an alkaline shift of the medium pH helps preventing acetate stress on cell growth and protein production in cultures in rich medium. The authors suggested that increasing the medium pH could

help retaining the optimal  $\Delta$ pH between the cells and the surrounding medium, controlling acetate internalization and consequently improving cells viability. We decided to test if a pH shift could be beneficial also in the case of growth on acetate. We started from the PYA medium and adjusted its pH to obtain media with starting pH 7.5, 8.0 and 8.5. These conditions were compared with the PYA medium at pH 7.0 used in the previous experiment. Small scale experiments in these conditions did not evidence significant differences in protein production, although a slight decrease in cell density was observed for the medium at pH 7.0 compared to the other conditions (Additional file 2: Figure S2). From these results, it was apparent that a slight alkaline shift favored cell growth, and that a pH in the range 7.5–8.5 could more efficiently sustain biomass and protein production in the PYA medium.

Once this optimal growth condition had been defined, we tried to optimize lactose induction to maximize protein synthesis. We performed the experiments on PYA with a starting pH of 8.0 (PYA8), which is in the middle of the favorable pH conditions explored, and checked induction with 1 or 5 mM lactose. We also explored the effect of a second lactose pulse 3 h after the first induction. The results of these experiments are documented in Figure 4. Although it had been reported that, within the optimal 1–10 mM range, protein expression is proportional to lactose concentration in autoinducing rich media [42], from our experiment it appeared that increasing lactose concentration to 5 mM led to a drop in recombinant protein production, whereas little difference



was observed in biomass production in either condition analyzed (data not shown). The administration of one or two 1 mM lactose pulses gave comparable protein yields per total protein, and we decided to maintain the single pulse induction as our standard procedure in larger scale experiments.

#### Optimization of the downstream purification procedure

As we were looking to improve the overall process for larger scale production of MNEI, we also perfected the purification procedure. The typical strategy included two chromatographic steps, a cation exchange with a linear gradient of NaCl, followed by a size exclusion chromatography on a Sephadex G-75 column [34, 36]. This latter step is particularly time consuming and difficult to implement on large samples, as size exclusion resins are extremely sensitive to the load volumes and flow rates employed. We developed a one-step ion exchange procedure consisting in a coupled anion/cation exchange purification. The introduction of the preliminary anion exchange chromatography step, performed in a slightly acidic buffer with low ionic strength, allows for a first, rough clean up, because the proteins with acidic and neutral isoelectric points are captured on the column, together with the other negatively charged molecules. Thus, the flow through that reaches the cation resin has

already undergone a coarse purification, leading to the removal of many aspecific and secondary interactions, which in turn allows for MNEI to be recovered at high purity from the cation exchanger with a simple step gradient elution, instead of the linear anionic strength gradient used in the previous purification protocol [34, 36]. The ion exchange purification is followed by a desalting step on a Sephadex G-25 resin, which supports loading volumes up to 25% of the total column volume. By choosing to use only resins that were compatible with fast flow rates, this protocol allowed us to complete the purification from the soluble protein extract in just a few hours, and can be further sped and scaled up for larger processes. Once purified, protein was quantified by UV absorbance at 280 nm using an Abs 0.1% of 1.413, as calculated by ProtParam [45]. Purity was assessed by Coomassie stained SDS-PAGE and was always higher than 99.5%.

#### Process scale up in automatic STR fermenter

To investigate the industrial exploitability of the newly formulated system for the production of MNEI and to better grasp the influence of the different process parameters on protein production in the presence of acetate, we scaled up some of the most representative conditions used in small scale experiments to a 3 L fermentation equipment. In particular, we tested the efficiency of MNEI production in PYA medium with different oxygenation settings ( $pO_2 > 20\%$  and  $pO_2 > 10\%$ ), different starting pHs (7.0 or 8.0) and increasing acetate concentration (0.4 and 1%) (Fermenter Run, FR 1-4, Table 1). After each run, MNEI was purified and quantified according to the above procedure. The yields reported refer to the final protein recovery.

While performing cell cultures in PYA medium (FR1-2), we noticed that the pH tended to increase over the course of the run, reaching values close to 9. This phenomenon had been previously reported for cultures in rich medium [46, 47]. After depletion of the available carbon sources, amino acids from yeast extract are used by the cells as additional carbon sources with a deamination

**Table 1** Summary of the conditions used in fermenter runs (FR)

	FR1	FR2	FR3	FR4
Sodium acetate	0.4%	0.4%	0.4%	1%
Starting pH	7.0	7.0	8.0	8.0
$pO_2$	20%	10%	10%	10%
pH control	No	No	Yes	Yes
Maximum $OD_{600}/mL$	$1.3 \pm 0.1$	$1.9 \pm 0.1$	$3.2 \pm 0.1$	$5.0 \pm 0.3$
$\mu_{max}$ ( $h^{-1}$ )	0.7	0.9	1.0	1.0
DCW (g/L)	$0.7 \pm 0.1$	$1.0 \pm 0.1$	$1.7 \pm 0.1$	$2.7 \pm 0.2$



mechanism that frees ammonia and/or amines in the medium [46, 47]. When the buffering capacity of the phosphate is exhausted, the medium pH rises, reaching unphysiological values (up to 9.0) that could in principle impair biomass production. Nonetheless, we observed protein production after each run. When growing the cells in standard PYA medium (0.4% NaOAc, pH 7.0 uncontrolled,  $pO_2 > 20\%$ , FR1) we recovered only 14.0 mg of MNEI from 1 L culture. This number increased dramatically when oxygenation was reduced ( $pO_2 > 10\%$ , FR2), yielding 57.6 mg protein/L culture. Biomass production in the two runs reached 1.3 and 1.9  $OD_{600}/mL$ , respectively. When the alkaline shift was applied to the conditions used in FR2 and pH was controlled at 8.0 throughout the fermentation with the dynamic addition of acid (FR3) we noticed major improvements, mostly visible in the increment in biomass production, with a peak of 3.3  $OD_{600}/mL$  at the end of the exponential phase. However, after 20 h post induction, cells had entered the death phase and the biomass decayed, leading to non-representative biomass and protein recovery at the end of FR3. Analysis of the acetate consumption profile for this fermentation run showed that acetate was not consumed in the initial phases of the growth, during which its concentration actually increased (Figure 5a), leading to a momentary decrease in the pH. This suggests that the fast increase in biomass in the exponential phase is due to the consumption of other high efficiency carbon sources in the yeast extract. We observed a very high specific growth rate ( $\sim 1.0 h^{-1}$ ), which is consistent with the additional acetate production [48]. After about 3 h, acetate concentration reached a peak at 4.6 g/L (6.4 g/L as NaOAc) and then decreased during the whole stationary phase. When starting from a medium containing 1% sodium acetate (FR4), the temporal consumption profile appeared similar to what observed in FR3. Acetate concentration rose slightly in the first phase of the exponential growth and its consumption started only towards the end of the exponential phase, continuing throughout what could be considered a *pseudo*-stationary phase and until completion (Figure 5b). A comparison between the evolution of pH and  $pO_2$  in the four conditions analyzed is reported in the supplementary data (Additional file 3: Figure S3). The increased availability of acetate led to a noticeable gain in cell density, which reached  $5.0 \pm 0.3$   $OD_{600}/mL$  ( $2.7 \pm 0.2$  g/L DCW) at the end of the growth (Figure 5b). Soluble protein is efficiently expressed and accumulated throughout the late exponential and the *pseudo*-stationary phase, during which acetate is consumed, as showed in the temporal SDS-PAGE profile after lactose induction (Figure 5c). Recovery after purification was  $177 \pm 17$  mg of protein from 1 L culture ( $Y_{X/S} = 0.39 \pm 0.01$  g/g;  $Y_{P/S} = 0.018 \pm 0.002$  g/g;

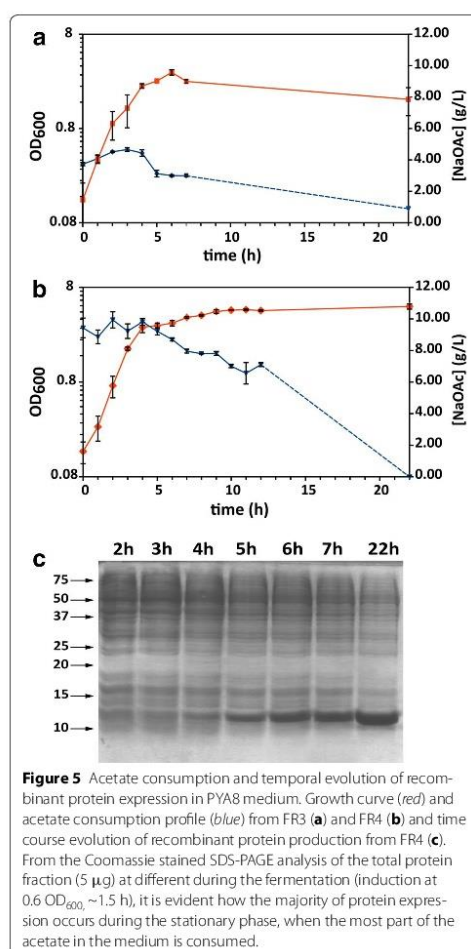
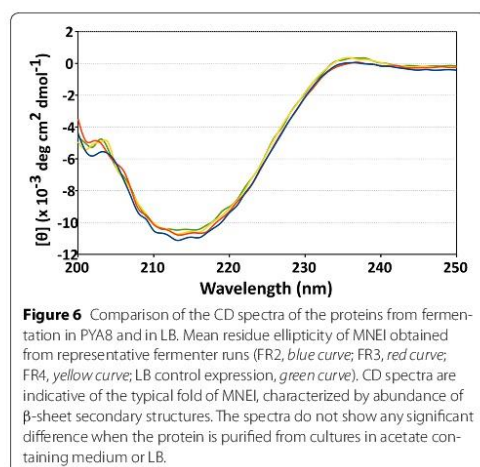


**Figure 5** Acetate consumption and temporal evolution of recombinant protein expression in PYA8 medium. Growth curve (red) and acetate consumption profile (blue) from FR3 (a) and FR4 (b) and time course evolution of recombinant protein production from FR4 (c). From the Coomassie stained SDS-PAGE analysis of the total protein fraction (5  $\mu g$ ) at different during the fermentation (induction at 0.6  $OD_{600}$ ,  $\sim 1.5$  h), it is evident how the majority of protein expression occurs during the stationary phase, when the most part of the acetate in the medium is consumed.

$Y_{P/X} = 0.07 \pm 0.01$  g/g. Yields are calculated respect to acetate, MW = 59). The protein fractions obtained from FR2-4 were analyzed by means of circular dichroism (CD) spectroscopy to verify the fold integrity. We found that, for each condition analyzed, the fold was consistent with the protein obtained from the typical LB/IPTG production, as testified by the overlap of the mean residue ellipticity plots (Figure 6).

## Discussion

The accumulation of acetate as a by-product of *E. coli* carbon metabolism has been traditionally regarded as a major limitation to the biotechnological potential of



this microorganism [7]. Despite the ascertained ability of growing on acetate as the sole carbon source, to our knowledge no attempt had been done so far to couple acetate metabolism to recombinant protein production. In our study, we have explored this possibility by setting up optimal culture conditions to obtain comparable protein yields to expression in rich media. We used this system to produce MNEI, a recombinant protein of industrial interest, which could potentially find application in the food and beverage industry as a sugar replacer [38]. The interest about this protein has been evidenced by several previous efforts to obtain it at high yields with recombinant methods [39]. We chose to employ cells of *E. coli* BL21(DE3) transformed with the pET22b + *\_MNEI* plasmid. *E. coli* BL21 has widespread utilization in laboratory scale processes, and is gaining increasing attention also in industrial scale processes. Part of the success of this strain is due to its high acetate tolerance, that allows efficient utilization in high density cell cultures with controlled feeding. Increased acetate tolerance is in turn due to an optimal acetate utilization machinery [22, 23]. We found that acetate metabolism can be employed to efficiently produce the recombinant protein in *E. coli* BL21. The choice of the BL21/pET combination also allows the use lactose induction, which is to prefer, due to reduced cost and higher biocompatibility, to conventional IPTG induction [30]. We noticed that careful control has to be applied mostly on two parameters: oxygenation and pH. In experiments with glycerol based autoinducing media, fed batch and glucose fed batch like cultures [47, 49, 50], it had already been observed that protein expression under lactose induction is more efficient in limiting oxygen concentrations. This is

also the case in the conditions explored in our study, since protein expression was completely inefficient when using higher oxygenation conditions in both small scale experiments and fermenter productions. The other parameter primarily affecting protein synthesis was the medium pH. It had been already reported that, when a primary carbon source is available, an alkaline shift could improve biomass and recombinant protein production in BL21 in the presence of acetate [29]. Our study shows that increasing the medium pH favors acetate metabolism, sustaining higher cell density in the absence of additional carbon sources. In these conditions, a concentration of sodium acetate in the medium as high as 1% (120 mM) could be consumed to completion during the *pseudo*-stationary growth that follows the exponential phase, with concomitant production of biomass and recombinant protein. This metabolism is likely coupled to the utilization of the amino acids present in the yeast extract as additional carbon sources. Use of amino acids as carbon sources proceeds through deamination and results in net ammonia and amines production, which in turn determines a pH increase [46, 47]. This trend was indeed observed in the fermentations with no pH control (FR1-2), and led to final pH values close to nine. These non-physiological conditions are likely to stop cell growth, inducing partial death and lysis, with consequent decrease of the final biomass and protein yields. By introducing pH control to 8.0, cell death is retarded and biomass accumulation continues throughout the fermentation run, leading to higher cell density and superior protein accumulation, as evidenced in FR3-4. Acetate consumption in these conditions mostly occurs during the *pseudo*-stationary phase, when the majority of the protein accumulation is observed. This system can efficiently be coupled with lactose induction. In general, lactose has been used following primary induction with IPTG [32] or in autoinducing media in the presence of a repressor of the *T7lac* promoter, such as glucose. The pioneering work by Studier on auto-inducing media [49] proved that induction by lactose can be achieved with as little as 0.005%, but is inhibited by certain sugars (primarily glucose) or amino acids. Later studies defined an optimal lactose concentration between 1 and 10 mM to be used for expression of recombinant proteins in *E. coli* BL21 in typical autoinducing media, where additional digestible carbohydrates are normally present [42]. We found that, when using PYA8 medium, optimal induction was obtained with as little as 1 mM lactose, whereas a higher concentration led to a reduction in the expression levels.

## Conclusions

In the present study, we have developed a new strategy for the production of MNEI, a sweet protein with potential application in the field of low calorie sweeteners,



obtaining higher protein titers compared to published methods employing the same expression system [39]. We have used *E. coli* BL21(DE3) as the expression host and optimized a medium containing acetate as a carbon source (PYA8) and lactose as inducer. Average protein yield with this method reached 177 mg of protein per liter of culture, which represents a sixfold increase compared to the ~30 mg/L typically obtained from the LB/IPTG protocol [34–36]. The strategy presents obvious advantages over conventional approaches, mostly linked to the affordability and availability of the reagents, and seems promising for potential scale-ups. The purification protocol of MNEI has also been redesigned and it is now suitable for applications on larger production scales. Further validation of this production system will come from the expression of other recombinant proteins with the BL21/pET combination. The batch method here presented is also likely susceptible of further improvements, with the application, for instance, of modified feed strategies, which will certainly be the object of future studies.

## Methods

### Growth conditions

All experiments were performed on *E. coli* BL21(DE3) cells freshly transformed with the pET22b + plasmid (Novagen) carrying the gene coding for MNEI as used in [35]. The gene had been cloned between the *NdeI* and *BamHI* restriction sites of the vector, thus removing the pelB leader sequence and allowing for cytoplasmic protein production. All media contained 100 mg/L Ampicillin for plasmid preservation. For small scale cultures, cells were grown on LB-Agar plates and individual colonies were inoculated in 10 mL LB (10 g/L Tryptone, 10 g/L NaCl, 5 g/L Yeast-Extract) and grown over night at 37°C on a rotating shaker at 250 rpm. Pre-cultures were then diluted at 0.1 OD<sub>600</sub> in 100 mL of the final culture medium in 250 mL flasks and incubated on a rotating shaker at 250 rpm and 37°C. Cell growth was monitored by OD<sub>600</sub> readings and protein synthesis was induced at 0.6 OD<sub>600</sub> and continued for 20 h unless otherwise specified. For fermenter runs, cells from agar plates were inoculated in 5 mL LB and growth for 6 h on a rotating shaker at 250 rpm. This starting cultures were diluted 1/100 in 100 mL of the different media, grown in 250 mL flasks at 37°C for 20 h and used to inoculate the culture in fermenter. Fermentations were carried out in a STR 3L Bioreactor connected to an ADI1030 Bio Controller (Applikon) in the final culture media (1 L working volume) and supplemented with ampicillin 100 mg/L for plasmid selection. The culture was maintained in aerobic conditions (DOT ≥ 10% unless otherwise specified) by an airflow of 60 L/h and a stirring rate of 250 rpm. When

indicated, the culture pH was maintained at 8.00 by automatic addition of H<sub>2</sub>SO<sub>4</sub> 5% v/v.

The following media were used in the different experiments:

PY medium (12.8 g/L Na<sub>2</sub>HPO<sub>4</sub>·7H<sub>2</sub>O, 3.0 g/L KH<sub>2</sub>PO<sub>4</sub>, 0.5 g/L NaCl, 5.0 g/L yeast extract), PY8 (16.1 g/L Na<sub>2</sub>HPO<sub>4</sub>·7H<sub>2</sub>O, 1.36 g/L KH<sub>2</sub>PO<sub>4</sub>, 0.5 g/L NaCl, 5.0 g/L yeast extract). Sodium acetate (A) was added from a sterile 10× stock solution to the final concentrations indicated in the main text.

Further pH adjustments were made with 0.1 M NaOH or 5% H<sub>2</sub>SO<sub>4</sub>.

Induction of protein expression was realized with 1 mM lactose at 0.6 OD<sub>600</sub>, unless differently specified in the text.

The concentration of acetate in the medium was determined spectrophotometrically [51]. Prior to spectrophotometric analyses, all samples were heated to 80°C for 20' to denature proteins and were analyzed with the K-ACE-TRM acetic acid determination kit (Megazyme). Acetate concentration was expressed as sodium salt equivalents.

Protein concentration for electrophoretic analysis was determined by Bradford Assay (Bio-Rad).

### Protein purification

After growth, cells were harvested by centrifugation (4,000×g, 4°C, 10'), washed with cold PBS and resuspended in 50 mM NaOAc, pH 5.5 to 50 OD<sub>600</sub>/mL. Cells were disrupted by intermittent sonication on ice (20') and debris were removed by centrifugation (12,000×g, 4°C, 30'). The cell lysate was applied to an anion exchange DEAE-Sepharose (20 mL, GE Lifesciences) column connected in series to a Macro-prep High-S cation exchange column (15 mL, Bio-Rad), equilibrated in the same lysis buffer. The chromatography was monitored by UV absorption at 280 nm. After loading and washing to baseline, the columns were disconnected and MNEI was eluted from the Macro-prep High-S column with 50 mM NaOAc buffer containing 100 mM NaCl. The fractions containing MNEI as assessed by SDS-PAGE were pooled and desalted on a Sephadex G-25 column in 50 mM AcOH and lyophilized. All the resins utilized in the protein purification steps allow fast flows, and a 5 mL/min flow was used in all purification steps. MNEI purity was estimated by analysis of the SDS-PAGE with the Image Lab 5.2 software (Bio-Rad).

### Circular dichroism

Protein fold integrity was assessed by circular dichroism (CD) spectra recorded on a Jasco J-715 spectropolarimeter. Molar ellipticity per mean residue [θ] in deg cm<sup>2</sup> dmol<sup>-1</sup> was calculated from the equation: [θ] = [θ]<sub>obs</sub> mrw/(10 × l × C), where [θ]<sub>obs</sub> is the



ellipticity measured in degrees,  $m_{rw}$  is the mean residue molecular weight of the protein (Da),  $C$  is the protein concentration in g/mL and  $l$  is the optical path length of the cell in cm. Cells of 0.1 cm path length were used. CD spectra were recorded with a time constant of 4 s, a 2 nm band width and a scan rate of 20 nm/min, and the signal was averaged over three scans and baseline corrected by subtracting a buffer spectrum. All spectra were recorded in 20 mM phosphate buffer, pH 2.5. A concentration of 0.25 mg/mL protein was used for each sample, as accurately determined by UV absorbance at 280 nm prior to CD measurement.

### Additional files

**Additional file 1: Figure S1.** Effect of sodium acetate concentration on biomass and recombinant protein yield. Growth curves (A) and SDS-PAGE (B) of the soluble protein extract after small scale cultures in PY medium containing different sodium acetate concentration: 0.4% (blue curve, lane 1); 1% (red curve, lane 2); 1.5% (yellow curve, lane 3); 2.0% (green curve, lane 4) and 2.5% (dark red curve, lane 5). 3  $\mu$ g of soluble protein extract were loaded in each lane. It appears that increasing acetate concentration in the medium does not affect the efficiency of protein expression, whereas, without pH or  $pO_2$  control, biomass tends to decrease with higher acetate concentrations.

**Additional file 2: Figure S2.** Effect of the medium pH on biomass and recombinant protein yield. Growth curves (A) and SDS-PAGE (B) of the soluble protein extract after small scale cultures in PYA medium varying the starting pH. Starting pH of 7.0 (blue curve, lane 1); 7.5 (red curve, lane 2); 8.0 (yellow curve, lane 3); 8.5 (green curve, lane 4). 5  $\mu$ g of soluble protein extract were loaded in each lane. In small scale experiments, variations of the starting pH above 7.5 did not result in significant changes in either biomass or protein production. A slight decrease in cell density was visible at the end of the culture starting at pH 7.0, but this effect was more significant in fermenter runs.

**Additional file 3: Figure S3.** Biomass,  $pO_2$  and pH evolution in typical fermenter runs. Growth curves (green),  $pO_2$  (red) and pH profiles relative to FR1 (panel A), FR2 (panel B), FR3 (panel C) and FR4 (panel D). In the fermentations without pH control, it is evident a drift to high pHs throughout the growth. When alkaline shift and pH control are applied (C-D), an initial slight decrease of the pH is observed, concomitant with acetate production.

### Abbreviations

IPTG: Isopropyl- $\beta$ -D-1-thiogalactopyranoside; LB: Luria Broth; PYA: phosphate/yeast extract/acetate medium; PYA8: phosphate/yeast extract/acetate pH 8.0 medium; CD: circular dichroism; NaOAc: sodium acetate; DCW: dry cell weight;  $Y_{X/S}$ : yield of biomass from substrate;  $Y_{P/S}$ : yield of protein from substrate;  $Y_{P/X}$ : yield of protein from biomass.

### Authors' contributions

SL designed and carried out the experiments, performed the data analysis and wrote the manuscript; FS performed the fermenter runs, contributed to data analysis and revised the manuscript; EP and MLT contributed to experimental design, data analysis and revised the manuscript; DP supervised the study, participated in its design and data analysis and revised the manuscript. All authors read and approved the final manuscript.

### Acknowledgements

This work has been funded by the Fondazione con il Sud (Grant 2011-PDR-19). SL would like to thank Iolanda Esposito and Jole Fonderico for the precious help with the experimental work.

### Compliance with ethical guidelines

### Competing interests

The authors declare that they have no competing interests.

Received: 22 May 2015 Accepted: 15 July 2015

Published online: 25 July 2015

### References

- Shiloach J, Fass R (2005) Growing *E. coli* to high cell density—A historical perspective on method development. *Biotechnol Adv* 23:345–357
- Tripathi NK (2009) High yield production of heterologous proteins with *Escherichia coli*. *Def Sci J* 59:137–146
- Studier FW, Daegelen P, Lenski RE, Maslov S, Kim JF (2009) Understanding the differences between genome sequences of *Escherichia coli* B strains REL606 and BL21(DE3) and comparison of the *E. coli* B and K-12 genomes. *J Mol Biol* 394:653–680
- Rosano GL, Ceccarelli EA (2014) Recombinant protein expression in *Escherichia coli*: advances and challenges. *Microbiotechnol Ecotoxicol Bioremediation* 5:172
- Sambrook J, Fritsch EF, Maniatis T (1989) Molecular cloning, vol 2. Cold spring harbor laboratory press, New York
- Huang C-J, Lin H, Yang X (2012) Industrial production of recombinant therapeutics in *Escherichia coli* and its recent advancements. *J Ind Microbiol Biotechnol* 39:383–399
- Eiteman MA, Altman E (2006) Overcoming acetate in *Escherichia coli* recombinant protein fermentations. *Trends Biotechnol* 24:530–536
- Martínez-Gómez K, Flores N, Castañeda HM, Martínez-Batallar G, Hernández-Chávez G, Ramírez OT et al (2012) New insights into *Escherichia coli* metabolism: carbon scavenging, acetate metabolism and carbon recycling responses during growth on glycerol. *Microb Cell Factories* 11:46
- Kleman GL, Strohl WR (1994) Acetate metabolism by *Escherichia coli* in high-cell-density fermentation. *Appl Environ Microbiol* 60:3952–3958
- Mey MD, Maeseneire SD, Soetaert W, Vandamme E (2007) Minimizing acetate formation in *E. coli* fermentations. *J Ind Microbiol Biotechnol* 34:689–700
- Valgepea K, Adamberg K, Nahku R, Lahtvee P-J, Arike L, Vilu R (2010) Systems biology approach reveals that overflow metabolism of acetate in *Escherichia coli* is triggered by carbon catabolite repression of acetyl-CoA synthetase. *BMC Syst Biol* 4:166
- Han K, Lim HC, Hong J (1992) Acetic acid formation in *Escherichia coli* fermentation. *Biotechnol Bioeng* 39:663–671
- Valgepea K, Adamberg K, Vilu R (2011) Decrease of energy spilling in *Escherichia coli* continuous cultures with rising specific growth rate and carbon wasting. *BMC Syst Biol* 5:106
- Axe DD, Bailey JE (1995) Transport of lactate and acetate through the energized cytoplasmic membrane of *Escherichia coli*. *Biotechnol Bioeng* 47:8–19
- Han K, Hong J, Lim HC (1993) Relieving effects of glycine and methionine from acetic acid inhibition in *Escherichia coli* fermentation. *Biotechnol Bioeng* 41:316–324
- Aristidou AA, San K-Y, Bennett GN (1999) Improvement of biomass yield and recombinant gene expression in *Escherichia coli* by using fructose as the primary carbon source. *Biotechnol Prog* 15:140–145
- Akesson M, Hagander P, Axelsson JP (2001) Avoiding acetate accumulation in *Escherichia coli* cultures using feedback control of glucose feeding. *Biotechnol Bioeng* 73:223–230
- Fuchs C, Köster D, Wiebusch S, Mahr K, Eisbrenner G, Märkl H (2002) Scale-up of dialysis fermentation for high cell density cultivation of *Escherichia coli*. *J Biotechnol* 93:243–251
- Waegeman H, De M (2012) Increasing recombinant protein production in *E. coli* by an alternative method to reduce acetate. In: Petre M (ed) *Advances in applied biotechnology*. InTech
- Son Y-J, Phue J-N, Trinh LB, Lee SJ, Shiloach J (2011) The role of Cra in regulating acetate excretion and osmotic tolerance in *E. coli* K-12 and *E. coli* B at high density growth. *Microb Cell Factories* 10:52

21. Phue J-N, Shiloach J (2004) Transcription levels of key metabolic genes are the cause for different glucose utilization pathways in *E. coli* B (BL21) and *E. coli* K (JM109). *J Biotechnol* 109:21–30. [Recombinant Proteins and Host Cell Physiology]
22. Yoon SH, Han M-J, Jeong H, Lee CH, Xia X-X, Lee D-H et al (2012) Comparative multi-omics systems analysis of *Escherichia coli* strains B and K-12. *Genome Biol* 13:R37
23. Shiloach J, Rinas U (2009) Glucose and acetate metabolism in *E. coli*—system level analysis and biotechnological applications in protein production processes. In: Lee PDSY (ed) *Systems biology and biotechnology of Escherichia coli*. Springer, Netherlands, pp 377–400
24. Phue J-N, Noronha SB, Hattacharyya R, Wolfe AJ, Shiloach J (2005) Glucose metabolism at high density growth of *E. coli* B and *E. coli* K: differences in metabolic pathways are responsible for efficient glucose utilization in *E. coli* B as determined by microarrays and Northern blot analyses. *Biotechnol Bioeng* 90:805–820
25. Castaño-Cerezo S, Bernal V, Röhrig T, Temmeier S, Cánovas M (2015) Regulation of acetate metabolism in *Escherichia coli* BL21 by protein Nε-lysine acetylation. *Appl Microbiol Biotechnol* 99:3533–3545
26. Gimenez R, Nuñez MF, Badia J, Aguilar J, Baldoma L (2003) The Gene *yjcG*, Cotranscribed with the Gene *acs*, Encodes an Acetate Permease in *Escherichia coli*. *J Bacteriol* 185:6448–6455
27. Oh M-K, Rohlin L, Kao KC, Liao JC (2002) Global expression profiling of acetate-grown *Escherichia coli*. *J Biol Chem* 277:13175–13183
28. Pally O, Gunasekera TS (2007) Growth of *E. coli* BL21 in minimal media with different gluconeogenic carbon sources and salt contents. *Appl Microbiol Biotechnol* 73:1169–1172
29. Wang H, Wang F, Wang W, Yao X, Wei D, Cheng H et al (2014) Improving the expression of recombinant proteins in *E. coli* BL21 (DE3) under acetate stress: an alkaline pH shift approach. *PLoS One* 9:e112777
30. Kosinski MJ, Rinas U, Bailey JE (1992) Isopropyl-β-D-thiogalactopyranoside influences the metabolism of *Escherichia coli*. *Appl Microbiol Biotechnol* 36:782–784
31. Gombert AK, Kilikian BV (1998) Recombinant gene expression in *Escherichia coli* cultivation using lactose as inducer. *J Biotechnol* 60:47–54
32. Kim M, Elvin C, Brownlee A, Lyons R (2007) High yield expression of recombinant pro-resilin: Lactose-induced fermentation in *E. coli* and facile purification. *Protein Expr Purif* 52:230–236
33. Kilikian BV, Suárez ID, Liria CW, Gombert AK (2000) Process strategies to improve heterologous protein production in *Escherichia coli* under lactose or IPTG induction. *Process Biochem* 35:1019–1025
34. Xu J, Banerjee A, Pan S-H, Li ZJ (2012) Galactose can be an inducer for production of therapeutic proteins by auto-induction using *E. coli* BL21 strains. *Protein Expr Purif* 83:30–36
35. Spadaccini R, Crescenzi O, Tancredi T, De Casamassimi N, Saviano G, Scognamiglio R et al (2001) Solution structure of a sweet protein: NMR study of MNEI, a single chain monellin. *J Mol Biol* 305:505–514
36. Picone D, Temussi PA (2012) Dissimilar sweet proteins from plants: oddities or normal components? *Plant Sci* 195:135–142
37. Rega MF, Di Monaco R, Leone S, Donnarumma F, Spadaccini R, Cavella S et al (2015) Design of sweet protein based sweeteners: hints from structure-function relationships. *Food Chem* 173:1179–1186
38. Kant R (2005) Sweet proteins—potential replacement for artificial low calorie sweeteners. *Nutr J* 4:5
39. Masuda T, Kitabatake N (2006) Developments in biotechnological production of sweet proteins. *J Biosci Bioeng* 102:375–389
40. Di Monaco R, Miele NA, Volpe S, Picone D, Cavella S (2014) Temporal sweetness profile of MNEI and comparison with commercial sweeteners. *J Sens Stud* 29:385–394
41. Di Monaco R, Miele NA, Picone D, Masi P, Cavella S (2013) Taste detection and recognition thresholds of the modified monellin sweetener: MNEI. *J Sens Stud* 28:25–33
42. Studier FW (2014) Stable expression clones and auto-induction for protein production in *E. coli*. In: Chen YW (ed) *Methods Mol Biol*, vol 1091. Humana Press, pp 17–32
43. Görke B, Stülke J (2008) Carbon catabolite repression in bacteria: many ways to make the most out of nutrients. *Nat Rev Microbiol* 6:613–624
44. Nancib N, Branlant C, Boudrant J (1991) Metabolic roles of peptone and yeast extract for the culture of a recombinant strain of *Escherichia coli*. *J Ind Microbiol* 8:165–169
45. Gasteiger E, Hoogland C, Gattiker A, Duvaud S, Wilkins MR, Appel RD et al (2005) Protein identification and analysis tools on the ExPASy server. In: Walker JM (ed) *The proteomics protocols handbook*. Humana Press, Totowa
46. Krause M, Ukkonen K, Haataja T, Ruottinen M, Glumoff T, Neubauer A et al (2010) A novel fed-batch based cultivation method provides high cell-density and improves yield of soluble recombinant proteins in shaken cultures. *Microb Cell Factories* 9:11
47. Ukkonen K, Veijola J, Vasala A, Neubauer P (2013) Effect of culture medium, host strain and oxygen transfer on recombinant Fab antibody fragment yield and leakage to medium in shaken *E. coli* cultures. *Microb Cell Factories* 12:73
48. Luli GW, Strohl WR (1990) Comparison of growth, acetate production, and acetate inhibition of *Escherichia coli* strains in batch and fed-batch fermentations. *Appl Environ Microbiol* 56:1004–1011
49. Studier FW (2005) Protein production by auto-induction in high-density shaking cultures. *Protein Expr Purif* 41:207–234
50. Blommel PG, Becker KJ, Duvnjak P, Fox BG (2007) Enhanced bacterial protein expression during auto-induction obtained by alteration of lac repressor dosage and medium composition. *Biotechnol Prog* 23:585–598
51. Li Z, Nimtz M, Rinas U (2014) The metabolic potential of *Escherichia coli* BL21 in defined and rich medium. *Microb Cell Factories* 13:45

**Submit your next manuscript to BioMed Central and take full advantage of:**

- Convenient online submission
- Thorough peer review
- No space constraints or color figure charges
- Immediate publication on acceptance
- Inclusion in PubMed, CAS, Scopus and Google Scholar
- Research which is freely available for redistribution

Submit your manuscript at  
[www.biomedcentral.com/submit](http://www.biomedcentral.com/submit)





## La produzione di anticorpi ricombinanti nel batterio antartico *Pseudoalteromonas haloplanktis* TAC125

MARIA GIULIANI, ERMENEGILDA PARRILLI, FILOMENA SANNINO,  
GENNARO ANTONIO APUZZO, MARIA LUISA TUTINO, GENNARO MARINO

### I. Abstract

The monoclonal antibody market represents the fastest-growing segment within the biopharmaceutical industry. Indeed, recombinant antibodies and antibody fragments are widespread tools for research, diagnostics and therapy. Large-scale production of recombinant antibodies and antibody fragments requires a suitable expression system which has to be cheap, accessible for genetic modifications, easily scaled up. Although prokaryotic expression systems can reduce production costs, recombinant antibody production in conventional bacterial hosts, such as *Escherichia coli*, often results in inclusion bodies formation. Since lowering of the expression temperature can increase product solubility facilitating its correct folding, a novel process for recombinant antibody fragments production at low temperatures was established by using the Antarctic Gram-negative bacterium *Pseudoalteromonas haloplanktis* TAC125 as recombinant expression host. To test the versatility of the newly developed process, the production of three aggregation prone model proteins, corresponding to the most common formats of antibody fragments: Fab, scFv and VHH, was evaluated. The construction of an *ad hoc* genetic expression system for each model protein followed a rational design where several critical aspects were considered including the selection of molecular signals for targeting the proteins to the periplasmic space and the choice of optimal gene-expression strategies. For Fab fragment production

in heterodimeric form an artificial operon was designed and constructed. Moreover, a new defined minimal medium was made-up to maximize bacterial growth parameters and recombinant production yields. All model proteins were obtained in soluble and biologically competent form.

The observed proficiency of the Antarctic bacterium to produce recombinant antibody fragments was related to the unusually high number of genes encoding peptidyl prolyl *cis-trans* isomerases found in the *P. haloplanktis* TAC<sub>125</sub> genome, making this bacterium the host of choice for the recombinant production of this protein class.

*Parole chiave:* frammenti anticorpali, *Pseudoalteromonas haloplanktis* TAC<sub>125</sub>, peptidil-prolil isomerasi, produzione di proteine ricombinanti, sistemi di espressione a freddo.

## 2. Introduzione

Nel panorama delle moderne biotecnologie, la produzione di proteine ricombinanti rappresenta certamente uno dei campi di maggior interesse economico. La disponibilità di numerose piattaforme cellulari per la produzione di proteine ricombinanti, ciascuna delle quali caratterizzata da proprietà peculiari, aumenta la probabilità di ottenere il prodotto ricombinante di interesse in forma solubile e biologicamente attiva, abbattendone contemporaneamente i costi di produzione. Tuttavia, la produzione di proteine ricombinanti continua ad essere un'attività molto artigianale, dal momento che non è ancora possibile prevedere *a priori* il buon esito del processo, se cioè la proteina di interesse risulterà correttamente prodotta nel sistema d'espressione scelto.

Uno dei problemi più spesso incontrati durante la produzione di una proteina ricombinante è il suo ottenimento sotto forma di aggregati insolubili, che nei procarioti assumono la definizione di "corpi inclusi". Lo studio dei processi che sono alla base dell'aggregazione proteica ha dimostrato che il fenomeno è prevalentemente dovuto alle interazioni stereospecifiche tra il solvente acquoso e le superfici idrofobiche del polipeptide neosintetizzato [43, 5]. Questo effetto, definito effetto idrofobico, è un processo sostanzialmente endotermico,

per cui risulta minimizzato in seguito all'abbassamento della temperatura del processo. Pertanto, la produzione di proteine ricombinanti in batteri psicrofili, cioè in batteri naturalmente adattati a crescere alla temperatura di 4 °C o inferiore, può rappresentare un'interessante alternativa per incrementare la qualità e la solubilità dei prodotti proteici. Una tale piattaforma cellulare potrebbe consentire l'ottenimento, in forma biologicamente attiva, di tutti quei prodotti proteici che si presentano come corpi inclusi in altri ospiti. Negli ultimi anni alcuni batteri adattati al freddo hanno attratto l'attenzione dei ricercatori in quanto dotati di interessanti proprietà che ne fanno delle potenziali fabbriche cellulari per la produzione di proteine ricombinanti. In particolare, il batterio Gram-negativo *Pseudoalteromonas haloplanktis* TAC125, isolato dall'acqua di mare dell'Antartide [3], si è rivelato di estremo interesse in quanto non solo è uno dei batteri psicrofili in grado di replicarsi più rapidamente in un intervallo ampio di temperature (0–30 °C) [45], e di raggiungere elevate densità cellulari anche a 0 °C (fino a  $A_{600}=20$ ) in condizioni ottimali di nutrizione ed aereazione.

Poiché è risultato così ben adattato alla vita a basse temperature, *P. haloplanktis* TAC125 è stato il primo batterio antartico di cui è stata completamente determinata ed annotata la sequenza genomica [29]. Lo studio del genoma e l'analisi del comportamento *in vivo* del batterio hanno consentito di mettere in evidenza alcune caratteristiche genomiche e metaboliche, che ne giustificano le eccezionali proprietà di crescita precedentemente descritte.

Tra tutte le strategie cellulari relative alla capacità del batterio di adattarsi a condizioni di vita così estreme, è utile ricordare che i) il batterio si difende dagli effetti deleteri dall'aumento della concentrazione delle specie reattive dell'ossigeno (una conseguenza delle basse temperature) non solo attivando i classici enzimi che proteggono dallo stress ossidativo (quali la superossido dismutasi SodB, la tioredossina riduttasi TrxB, o la catalasi) [50], ma anche tramite una nuova strategia che utilizza un'emoglobina batterica [37]; ii) il genoma batterico è caratterizzato da un numero inusualmente elevato di geni che codificano rRNA e tRNA (questi ultimi ammontano a 106 geni, alcune volte organizzati in lunghe ripetizioni) circostanza questa che può giustificare l'impressionante capacità di traduzione a basse temperature. Infine, recentemente sono stati messi a punto degli schemi di ingegneria genetica che hanno consentito la costruzione di mutanti genomici



sito specifici (mutanti di inserzione o di delezione). Questi hanno permesso la creazione di ceppi batterici modificati geneticamente e che mostrano migliori caratteristiche nella produzione di proteine ricombinanti [35, 37].

Un altro motivo che ha giustificato il crescente interesse scientifico nei confronti di *P. haloplanktis* TAC<sub>125</sub> è stato la messa a punto di una efficiente tecnologia per l'espressione genica ricombinante in questo microrganismo inserendo, all'interno di un vettore di clonaggio di *E. coli* opportunamente modificato [46], specifici segnali molecolari psicrofili [45, 11]. Diverse generazioni di vettori di espressione psicrofili hanno consentito di ottenere proteine ricombinanti attraverso modalità costitutive [11] o inducibili [34], e di indirizzare i prodotti ricombinanti verso uno dei compartimenti cellulari e/o di secernerli nel mezzo extracellulare [36]. I vantaggi derivanti dalla secrezione di una proteina ricombinante consistono in uno schema di purificazione generalmente più semplificato ed economico. Inoltre, la traslocazione extra-citoplasmatica rappresenta un'ottima strategia per fornire al prodotto ricombinante un residuo N-terminale autentico, dal momento che la traslocazione comporta generalmente la rimozione della sequenza segnale [30]. Tale processo consente di rimuovere il residuo iniziale di metionina la cui presenza, oltre a poter evocare una reazione immunogenica nel caso in cui la proteina sia somministrata come agente terapeutico, può ridurre l'attività biologica e la stabilità del prodotto stesso [28].

Numerosi sono gli esempi in cui l'utilizzo della piattaforma di produzione di proteine ricombinanti nel batterio psicrofilo si è dimostrato risolutivo delle problematiche riscontrate durante la produzione delle medesime proteine in *E. coli*. Molto indicativi sono due esempi di produzione di proteine ricombinanti "difficili": il fattore neurotrofico umano NGF, h-NGF, [47] e la  $\alpha$ -glucosidasi da *Saccharomyces cerevisiae* [34].

La produzione della forma matura di h-NGF presenta numerose difficoltà al microrganismo produttore: la corretta strutturazione della proteina (il processo detto di *folding*) richiede infatti la formazione di tre ponti disolfurici non consecutivi (che assumono un'organizzazione strutturale definita nodo a cisteina o *cysteine-knot fold*) e la formazione di un omodimero. I numerosi tentativi di produrre questa proteina in *E. coli* sono risultati fallimentari, determinando immancabilmente un

suo accumulo in forma insolubile [40]. Al contrario la produzione della proteina matura h-NGF in *P. haloplanktis* TAC125 ha dato luogo ad un prodotto totalmente solubile correttamente traslocato nel periplasma, dove si accumula in forma completamente dimerica [47]. Anche l'enzima  $\alpha$ -glucosidasi da *S. cerevisiae* [34], prototipo delle proteine eucariotiche di solito espresse in forma prevalentemente insolubile, quando prodotto in *P. haloplanktis* TAC125 è risultato completamente solubile e attivo [34].

L'osservazione che in *P. haloplanktis* TAC125 non siano mai stati osservati aggregati insolubili di proteina ricombinante suggerisce che le condizioni chimico-fisiche nelle cellule di questo batterio e/o i processi di *folding* sono abbastanza differenti da quanto osservato nei batteri mesofili. Sembra dar credito a questa ipotesi un lavoro recente [39] che riporta la valutazione, mediante l'impiego di un approccio di proteomica differenziale, del profilo di espressione degli *chaperone* molecolari di *P. haloplanktis* TAC125 alla temperatura di crescita ottimale (0–4 °C). In queste condizioni ambientali, il batterio produce un eccesso di uno *chaperone* associato al ribosoma, il *trigger factor*, mentre la produzione dei principali *chaperones* di risposta agli *shock* termici — DnaK, GroEL, sHSP, Hsp90, e Dsb — è ridotta ad un livello pressoché non rivelabile. Se si considera che la classica funzione attribuita a questi *chaperones* molecolari è di assistere co- o post-traduzionalmente il *folding* proteico e di prevenire o recuperare il *misfolding*, si può ragionevolmente affermare che la corretta strutturazione di polipeptidi nascenti si basa essenzialmente sulla azione del *trigger factor*. Questo *chaperone*, dotato anche di una attività *cis-trans* isomerasica dei legami peptidil-prolinici [39], interagisce praticamente con tutti i polipeptidi nascenti, potendo essere considerato a buon diritto il principale fattore di strutturazione proteica durante la crescita di *P. haloplanktis* TAC125.

È interessante osservare che l'attività delle peptidil prolil *cis-trans* isomerasi (PPIasi) è essenziale nel *folding* delle molecole anticorpali [12]. In effetti, lo studio dei percorsi di strutturazione degli anticorpi ha dimostrato che successivamente alla formazione dei legami disolfurici intra-catena nel dominio variabile e costante [48], la isomerizzazione *cis-trans* di un legame peptidil prolinico dirige la strutturazione della proteina verso la conformazione nativa, consentendo la successiva formazione di ponti disolfurici inter-catena. È stato inoltre dimostrato che l'attività delle PPIasi è particolarmente importante nella

prevenzione dell'aggregazione di frammenti anticorpali durante la loro produzione ricombinante [12].

Questa osservazione ci ha spinto ad esplorare la produzione di diversi frammenti anticorpali in *P. haloplanktis* TAC125. In questa rassegna verranno riassunti i risultati ottenuti circa la produzione in forma solubile e biologicamente attiva di frammenti anticorpali di interesse farmaceutico che, in altri sistemi di produzione batterica, tendono ad accumularsi sotto forma di aggregati proteici, in particolare:

- il frammento anticorpale a singola catena scFv anti-ossazolone [18];
- l'anticorpo da camelide VHHD6.1 [19];
- il frammento anticorpale 3H6 Fab [9, 17].

Nel panorama dei bio-farmaci, studi recenti hanno messo in evidenza il crescente significato economico del mercato degli anticorpi ricombinanti. Il mercato globale di anticorpi monoclonali risulta in costante crescita, con una tendenza che si prevede stabile nei prossimi anni [4]. Accanto alla produzione di anticorpi monoclonali, lo sviluppo delle applicazioni della tecnologia del DNA ricombinante ha consentito la progettazione di formati più piccoli di tali proteine, definiti frammenti anticorpali. Tali frammenti, pur mantenendo la specificità di legame dell'anticorpo monoclonale intero, hanno la caratteristica di possedere proprietà uniche e migliorate in un ampio spettro di applicazioni diagnostiche e terapeutiche. Infatti, in alcune applicazioni cliniche, frammenti anticorpali piccoli presentano numerosi vantaggi rispetto all'anticorpo intero. Innanzitutto, l'assenza della regione costante Fc riduce il rischio di risposta immune. Inoltre le piccole dimensioni permettono a queste molecole di penetrare nei tessuti e nei tumori solidi molto più rapidamente dell'anticorpo intero [52]. Inoltre, è possibile prevedere numerose applicazioni di questi frammenti anticorpali al di fuori dell'ambito della ricerca e della medicina, come per esempio l'uso in biosensori [21] e processi di separazione fatti su scala industriale, come la separazione di molecole chirali [20].

Affinché queste proteine di rilevante interesse economico possano trovare applicazione nei processi di cui abbiamo fatto precedentemente menzione, è necessario sviluppare degli opportuni sistemi per la

loro produzione ricombinante su larga scala. È essenziale che tali sistemi risultino economici, accessibili alla modifica genetica, facilmente dimensionabili per soddisfare la crescente richiesta ed infine sicuri per i consumatori finali. Malgrado siano stati valutati per la loro capacità di produrre anticorpi liberi e ricombinanti con diversa efficienza numerosi sistemi batterici, sia Gram-positivi che Gram-negativi, la maggior parte dei tentativi si è concentrata su *E. coli*, per una serie di ragioni di natura sia storica sia pratica [14, 1]. Tuttavia, le numerose difficoltà connesse alla qualità ed alla solubilità di frammenti anticorpali prodotti in maniera ricombinante nel batterio mesofilo rendono necessaria l'esplorazione di altre piattaforme cellulari per la produzione su larga scala di queste proteine. Di qui l'interesse a valutare la produzione di diversi frammenti anticorpali nel batterio antartico *P. haloplanktis* TAC125, al fine di valutarne le eventuali superiori capacità nella produzione ricombinante di queste molecole interessanti.

### 3. Il sistema di espressione genica psicrofilo per la produzione ricombinante di frammenti anticorpali in *Pseudoalteromonas haloplanktis* TAC125

Dal momento che la corretta strutturazione di anticorpi e frammenti anticorpali richiede la formazione di ponti disolfurici, il lavoro si è inizialmente concentrato sulla scelta di un opportuno segnale molecolare (peptide segnale) da utilizzare per l'indirizzamento del prodotto ricombinante verso lo spazio periplasmatico, il distretto cellulare in cui questa modifica post-traduzionale si realizza nei batteri Gram-negativi. Due sono le principali strade che dirigono una proteina non strutturata al sistema di traslocazione Sec della membrana interna nei batteri Gram-negativi, e le caratteristiche dei due segnali (sequenza e distribuzione di specifici aminoacidi) definisce quale delle due strade sarà seguita da una determinata preproteina.

Il sistema più frequentemente utilizzato è la traslocazione SecB-dipendente [49], in cui il polipeptide è traslocato nello spazio periplasmatico post-traduzionalmente, cioè dopo la sua sintesi completa [8]. Per consentire il riconoscimento della proteina da parte del complesso SecYEG, è essenziale lo stato non strutturato della proteina, per cui possono esserci problemi di traslocazione laddove la cinetica di *folding*

risulti essere più rapida dell'evento di riconoscimento da parte del sistema di esportazione. Infatti, se la proteina acquisisce una qualsiasi struttura tridimensionale, essa diviene un substrato non più adeguato per il macchinario di traslocazione e viene quindi confinata nel citoplasma, dove spesso subisce degradazione proteolitica [6]. L'analisi del genoma di *P. haloplanktis* TAC<sub>125</sub> ha messo in evidenza che esso contiene un sistema classico di traslocazione SecB-dipendente [29].

D'altro canto, i batteri posseggono un equivalente del sistema eucariotico di riconoscimento del segnale (SRP), il quale è in grado di traslocare la preproteina attraverso un meccanismo co-traduzionale. Il sistema batterico SRP riconosce specifiche regioni idrofobiche, presenti nella sequenza del peptide segnale della proteina nascente durante la sua sintesi, e di conseguenza la sua traduzione e traslocazione risultano essere simultanee. In *E. coli*, il sistema SRP [41] è costituito dalla proteina Ffh, che interagisce con un piccolo RNA 4.5 S, mentre il suo recettore nella membrana interna è la proteina integrale di membrana FtsY [22]. Il genoma di *P. haloplanktis* TAC<sub>125</sub> è stato analizzato alla ricerca di geni codificanti proteine omologhe a Ffh e FtsY. Tale analisi ha consentito di identificare due geni (PSHAa0942 e PSHAa0354) codificanti le proteine del sistema di traslocazione SRP-dipendente presente nel batterio psicrofilo.

Al fine di definire quale delle due vie di traslocazione risulta essere la più efficace per la produzione di frammenti anticorpali in *P. haloplanktis* TAC<sub>125</sub>, sono state prodotte due varianti della proteina scFvOx, ciascuna caratterizzata da un differente peptide segnale. Una preproteina conteneva un peptide segnale SecB-dipendente (il peptide segnale PsA della  $\alpha$ -amilasi psicrofila del batterio *P. haloplanktis* TAB23), l'altra una sequenza segnale SRP-dipendente (PsD della proteina DsbA del batterio *P. haloplanktis* TAC<sub>125</sub>). È interessante notare che, nel più comune ospite di produzione *E. coli*, in base ai dati riportati da Thie et al. [44] entrambe le vie di traslocazione sono efficaci nella produzione di scFv. I dati da noi ottenuti dimostrano al contrario che solo il segnale di traslocazione co-traduzionale consente la corretta produzione del frammento anticorpale, la sua traslocazione periplasmatica e l'accumulo in forma totalmente solubile ed attiva [18]. La totale assenza di proteina nella frazione citoplasmatica indica inoltre un perfetto riconoscimento ed una efficiente traslocazione della proteina ricombinante. Alla luce di questi dati è stato selezionato



per la produzione di altri frammenti anticorpali nel batterio psicrofilo il peptide segnale PsD.

Effettuata la scelta dell'opportuno segnale di indirizzamento periplasmatico, si è passati alla scelta dello specifico sistema di espressione ricombinante psicrofilo da utilizzare in tutti gli esperimenti di produzione in *P. haloplanktis* TAC125. Il vettore d'espressione scelto è pUCRP [34] in quanto caratterizzato dalla presenza di un promotore psicrofilo regolato la cui trascrizione è indotta dalla presenza di L-malato nel mezzo di coltura. Inoltre tale promotore mostra la più elevata efficienza trascrizionale in terreno minimo tra tutti i promotori psicrofili al momento disponibili. Per quanto riguarda la costruzione del vettore di espressione per scFvOx, il gene *psD-scFvOx-c-myc* è stato clonato *in frame* con una sequenza codificante una coda di 6 residui di istidine.

Il sistema di espressione appena descritto ha permesso di ottenere una proteina ricombinante di fusione che, accanto al peptide leader N-terminale necessario per la secrezione periplasmatica PsD, presenta due *tag* di fusione consecutivi al C-terminale, il c-Myc utile per la sua rivelazione e la coda di sei istidine per la purificazione del prodotto ricombinante (Fig. 1a).

Il medesimo vettore d'espressione modificato è stato usato anche per la produzione del VHH D6.1 (Fig. 1b), sostituendo il gene codificante scFvOx con il gene *vhhD6.1* opportunamente amplificato mediante PCR.

Per quanto riguarda la produzione del Fab 3H6, particolare attenzione è stata dedicata alla costruzione di un operone sintetico (Fig. 1c) in cui i due geni codificanti la catena leggera e quella pesante del Fab 3H6 fossero collocati opportunamente nello spazio. Per ottenere una proteina funzionale è infatti necessario il corretto assemblaggio di una catena leggera con una catena pesante in rapporto stechiometrico 1:1. Negli operoni procariotici la traduzione bilanciata di geni co-trascritti è ottenuta mediante il cosiddetto *coupling* traduzionale, per il quale è necessaria la completa traduzione del gene precedente per l'efficiente traduzione del gene distale. Geni accoppiati traduzionalmente sono caratterizzati da una particolare struttura della loro giunzione intercistronica, che venne identificata per la prima volta nell'operone del triptofano di *E. coli* [33]. È stata condotta un'analisi *in silico* dell'organizzazione strutturale di operoni naturalmente accoppiati in *cluster* nel genoma di *P. haloplanktis* TAC125. La maggior parte degli operoni ana-

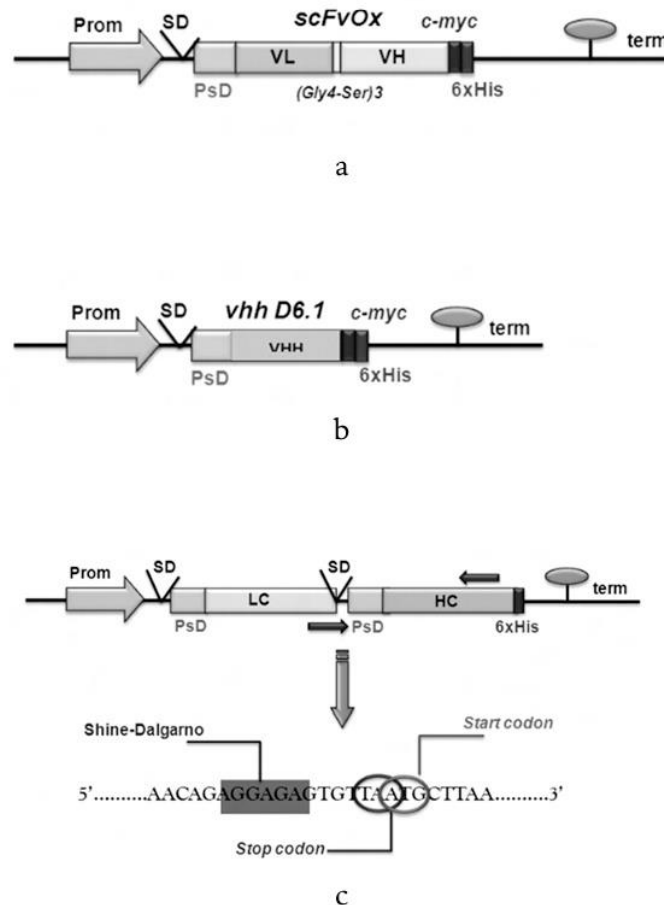


**Figura 1.** Schema delle cassette di espressione utilizzate per la produzione ricombinante dei frammenti anticorpali nel batterio *P. haloplanktis* TAC125. Pannello a: Cassetta di espressione per la produzione del ScFvOx; Pannello b: Cassetta di espressione per la produzione del VHH D6.1; Pannello c: Cassetta di espressione per la produzione del Fab3H6; Prom: promotore inducibile da L-malato; term: terminatore del gene *aat* di *P. haloplanktis* TAC125; SD: sequenza Shine-Dalgarno; PsD: sequenza codificante il peptide segnale del gene *dsbA* di *P. haloplanktis* TAC125; C-myc: sequenza codificante un tag utilizzato per immunorivelazione; 6XHis: sequenza codificante sei residui di istidina, utilizzata per la purificazione della proteina ricombinante.

lizzati ha mostrato la stessa organizzazione strutturale, in cui il codone di inizio del secondo gene del *cluster* si sovrappone al codone di stop del gene precedente, condividendo una coppia di basi. Come mostrato nella Fig. 1c, questa struttura è stata riproposta nella costruzione dell'operone artificiale per la produzione del frammento Fab 3H6. Inoltre, poiché per un'efficiente espressione del gene distale è necessario un sito di legame al ribosoma, un'identica sequenza Shine-Dalgarno è collocata sia a monte del gene *lc* sia a monte del gene *hc*.

#### **4. Ottimizzazione del terreno di coltura per la produzione ricombinante di proteine in *P. haloplanktis* TAC<sub>125</sub>**

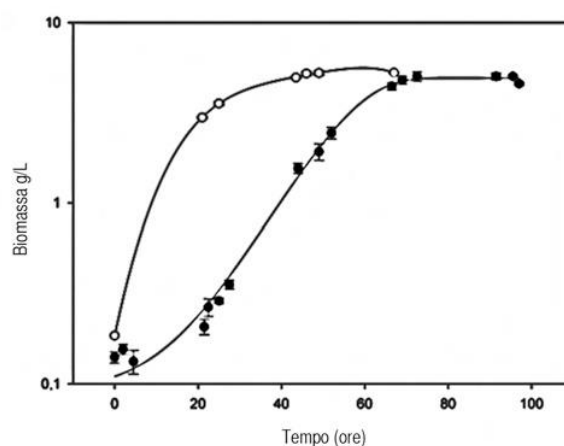
La comprensione della fisiologia cellulare e l'ottimizzazione delle strategie di coltivazione sono fattori essenziali per raggiungere l'obiettivo di un'elevata produzione di proteine ricombinanti da parte di organismi. Infatti, quando il prodotto è associato alle cellule, la produttività è correlata al livello di biomassa ottenuta durante il processo. In questo caso, l'ottimizzazione della produzione della proteina è strettamente dipendente dalla composizione del mezzo di coltura e, di conseguenza, strettamente associato alla scelta della più opportuna strategia di coltivazione da usare. Un'efficiente produzione in forma completamente solubile e cataliticamente competente di numerose proteine termolabili o tendenti alla aggregazione è stata ottenuta spesso in terreni di coltura definiti, dove i livelli di induzione e le rese di produzione sono risultati ottimizzati anche se confrontati con quelli ottenibili usando comuni mezzi di coltura ricchi e complessi [34].

Al fine di incrementare le rese di produzione delle proteine ricombinanti di interesse industriale da parte del sistema d'espressione psicrofilo, sono stati valutati: l'effetto della composizione del mezzo di coltura, la concentrazione di biomassa finale e la velocità di crescita e di produzione di proteina [17].

Inoltre è stata valutata la produzione di proteine ricombinanti di *P. haloplanktis* TAC<sub>125</sub> in un nuovo terreno di coltura sintetico ottimizzato per tale scopo.

In diversi lavori è stato riportato che il batterio psicrofilo di nostro interesse mostra una preferenza nutrizionale per gli amminoacidi come fonte di carbonio ed azoto. Per questo motivo i parametri di crescita

del batterio sono stati determinati in mezzi sintetici costituiti da una base minerale (Sali SCHATZ) con l'aggiunta di diversi aminoacidi [17]. I risultati ottenuti hanno suggerito di utilizzare L-leucina, in combinazione con L-isoleucina ed L-valina, come fonti di carbonio e d'azoto, ed hanno condotto alla formulazione del terreno LIV, il quale è stato poi impiegato in tutti i successivi tentativi di produzione di proteina ricombinante sia in coltivazione *batch* o in chemostato. In particolare il terreno LIV contiene i tre aminoacidi L-leucina, L-isoleucina ed L-valina nel rapporto molare 1:1:2. Come mostrato nella Fig. 2, la crescita del microrganismo psicrofilo in terreno LIV è caratterizzata da una fase di latenza molto breve, e da un modesto, ma significativo incremento della velocità specifica di crescita e della resa in biomassa rispetto alla crescita in terreno contenente solo L-leucina [17].



Fonte di carbonio	mmax	Resa in biomassa ( $g_{dcw} L^{-1}$ )
L-leucina	$0.10 \pm 0.01$	$3.70 \pm 0.30$
LIV	$0.13 \pm 0.01$	$5.65 \pm 0.25$

**Figura 2.** Confronto delle curve di crescita del batterio *P. haloplanktis* TAC125 in terreni sintetici definiti SCHATZ contenenti L-leucina (cerchio pieno) e una miscela di L-leucina, L-isoleucina e L-valina in rapporto molare 1:1:2 (cerchio aperto).

## 5. Produzione del frammento anticorpale a singola catena scFv anti-ossazolone

ScFv (*Single chain variable Fragment* o frammento anticorpale a singola catena variabile) è il principale frammento (30 kDa) che continua a mantenere l'unità attiva di legame all'antigene delle immunoglobuline. Le applicazioni cliniche di queste molecole richiedono la disponibilità di notevoli quantità di ScFv funzionali ed a basso costo. Tuttavia, la produzione ricombinante di questa famiglia di proteine nell'ospite batterico convenzionale, *E. coli*, presenta diverse difficoltà, essenzialmente connesse con la tendenza degli ScFvs a formare aggregati insolubili quando sono prodotti in questo sistema [42]. Al fine di risolvere queste problematiche, sono stati esplorati diversi approcci sperimentali ad esempio la possibilità di produrre queste proteine con *chaperone* molecolari [27, 12], o abbassando la temperatura di espressione.

Quest'ultimo approccio è utilizzato spesso quando il prodotto ricombinante tende ad accumularsi sotto forma di corpi inclusi [2], dal momento che, come detto precedentemente, l'abbassamento della temperatura minimizza le interazioni idrofobiche [51], la forza trainante coinvolta nella formazione dei corpi inclusi [5]. Tuttavia, la coltivazione di *E. coli* a temperature sub-ottimali generalmente provoca una diminuzione della produttività in biomassa, dovuta all'effetto dell'abbassamento della temperatura sulla velocità di crescita specifica batterica, e quindi alla risposta fisiologica da *cold-shock* [7]. Per quanto detto finora, risulta evidente che l'uso di batteri naturalmente adattati al freddo come ospiti per la produzione di proteine ricombinanti potrebbe rappresentare un'efficace alternativa per migliorare la qualità conformazionale e la solubilità di questi prodotti proteici farmaceutici.

Per valutare quindi l'efficacia del sistema d'espressione psicrofilo nella produzione ricombinante di un frammento anticorpale, si è scelto di produrre come modello ScFvOx, il frammento variabile a singola catena anti-2-fenil-5-ossazolone [15]. ScFvOx è il tipico esempio di frammento anticorpale a singola catena tendente all'aggregazione, ed infatti esso è stato usato per anni come modello per lo sviluppo di protocolli di risolubilizzazione dai corpi inclusi [38]. La produzione ricombinante è stata indirizzata verso spazio periplasmatico per consentire la formazione dei ponti disolfurici dell'anticorpo. La produzione



e la localizzazione cellulare della proteina ricombinante è stata valutata tramite un'analisi di Western blotting, ed è stato messo a punto un processo di fermentazione su scala da laboratorio. Come mostrato nella Fig. 3, la proteina è interamente traslocata nello spazio periplasmatico e prodotta in forma solubile. Combinando opportunamente i segnali di indirizzamento, il sistema di espressione genica e la strategia di fermentazione, è stato possibile raggiungere una resa di produzione di  $4,69 \pm 0,12$  mg/L di ScFvOx solubile, che rappresenta la resa più elevata finora riportata per un sistema di espressione procariotico convenzionale anche in seguito alla risolubilizzazione di corpi inclusi [38]. Molto elevata è stata, inoltre, la resa in prodotto ( $Y_{P/X}$ ) registrata ( $Y_{P/X} = 0,94 \pm 0,03$  mg gX<sup>-1</sup>). Questo aspetto suggerisce che un ulteriore incremento nella resa di biomassa specifica consentirebbe di ottenere livelli di produzione più elevati di ScFvOx [18].

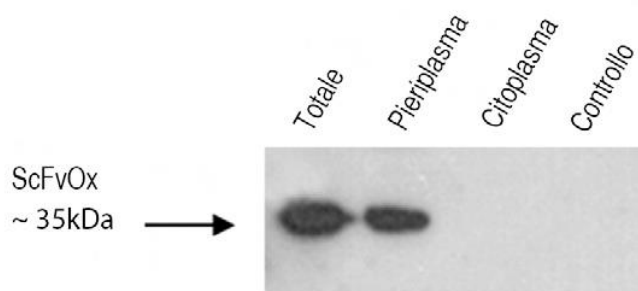


**Figura 3.** Produzione e localizzazione cellulare del frammento anticorpale ScFvOx prodotto nel batterio *P. haloplanktis* TAC125. Le cellule ricombinanti sono state recuperate, ed il loro estratto totale (estratto totale), le due sub-frazioni di estratto periplasmatico (periplasma) e l'estratto citoplasmatico (citoplasma) sono stati analizzati mediante Western Blotting, usando l'anticorpo primario anti-c-myc. Controllo, campione corrispondente ad estratto totale di cellule del batterio antartico non ricombinanti.

## 6. Produzione dell'anticorpo da camelide VHHD6.1

Fin dalla loro prima descrizione [23], gli anticorpi IgG da camelidi (cioè da cammelli, dromedari e lama) hanno attratto l'interesse degli scienziati, sia da un punto di vista della scienza di base che applicata, per via della loro caratteristica di "anticorpi a catena pesante" o HCAb (*Heavy-Chain Antibodies*). Questi anticorpi sono naturalmente privi delle catene leggere, il che rende le loro dimensioni significativamente più piccole di quelle degli anticorpi convenzionali. Come conseguenza, il loro dominio di legame sono costituiti unicamente dai domini variabili della catena pesante, a cui si fa generalmente riferimento come VHHs [32], per distinguerli dai convenzionali VHs. Il VHH, quindi, rappresenta il frammento di legame all'antigene più piccolo (~15 kDa) e intatto a nostra disposizione, ed ha pertanto un grosso potenziale in applicazioni terapeutiche e diagnostiche come prodotto di fusione multi specifico [25].

Per la loro ridotta complessità strutturale, i VHHs sono generalmente prodotti con successo nelle piattaforme microbiche convenzionali, come *E. coli*. Tuttavia, c'è una frazione di VHHs che sfugge ai test di valutazione della capacità di legame in quanto manifesta una scarsa stabilità in forma solubile nell'ospite della produzione ricombinante. Queste molecole seppure dotate di un potenziale interessante sono fatalmente destinate ad essere trascurate, dal momento che la piattaforma di produzione microbica non ha caratteristiche ottimizzate per la produzione di anticorpi.

Al fine di valutare la capacità di *P. haloplanktis* TAC125 di produrre con successo in forma solubile un frammento anticorpale da camelide è stato scelto come proteina modello il VHHD6.1 *anti-human fibroblast growth factor receptor 1* (hFGFR1). Tale frammento anticorpale deriva da un processo di selezione mediante *phage display* su una *library naive* di VHHs di lama [31] ma la sua produzione in larga scala in *E. coli* è risultata inefficace in quanto la proteina ricombinante si accumula nei corpi inclusi (De Marco A., comunicazione personale). È stato quindi necessario sviluppare un nuovo processo produttivo che consentisse di ottenere VHHD6.1 in forma solubile di al fine di consentirne una più approfondita caratterizzazione.

La produzione del frammento anticorpale VHHD 6.1 anti-hFGFR1 è stata condotta in cellule di *P. haloplanktis* TAC125 ricombinanti con

il vettore pUCRP-*vhh*, in modalità *batch* nel terreno LIV ed nelle condizioni di crescita ed induzione precedentemente ottimizzate. L'analisi della produzione e della localizzazione cellulare del frammento anticorpale ricombinante è stata condotta mediante *Western blotting* semi quantitativo su estratti totali delle proteine solubili e su frazioni periplasmatiche di campioni collezionati a diversi tempi di crescita (Fig. 4). L'immunorivelazione, realizzata mediante l'utilizzo di anticorpi anti c-Myc, ha evidenziato la produzione solubile del VHHD6.1 ricombinante durante tutte le fasi della fermentazione e la sua corretta localizzazione periplasmatica durante la fase di crescita esponenziale precoce (22h) e media (29h). Al contrario non vi è traccia di proteina ricombinante nella frazione periplasmatica ottenuta da campioni collezionati in tarda fase esponenziale (42h) ed in fase stazionaria (60h). Il livello di produzione sembra incrementare durante la fase di crescita esponenziale, raggiungendo il massimo valore di resa in tarda fase esponenziale (42h). Inoltre, negli estratti solubili totali è possibile osservare la presenza di un segnale specifico dell'apparente peso molecolare di circa 30 kDa, molto probabilmente assegnabile alla formazione di complessi dimerici dell'anticorpo. La formazione di dimeri non è sorprendente alla luce della spiccata tendenza alla multimerizzazione manifestata sia da questo che da altri formati anticorpali quando

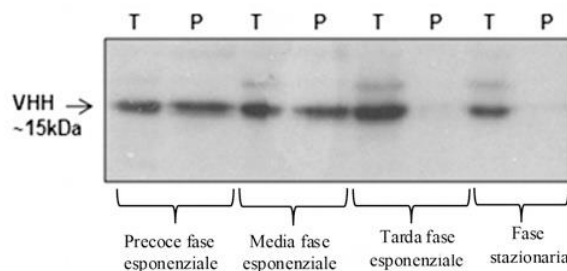


**Figura 4.** Produzione e localizzazione cellulare del frammento anticorpale VHH D6.1 prodotto nel batterio *P. haloplanktis* TAC125. Aliquote di cellule ricombinanti sono state recuperate a fasi successive della crescita cellulare e il loro estratto proteico totale (T) e la corrispondente frazione periplasmatica (P) sono state analizzate mediante Western Blotting usando l'anticorpo primario anti-c-myc.

la concentrazione locale nell'ospite della produzione ricombinante raggiunge livelli critici [24].

Un'altra osservazione interessante è la correlazione inversa tra l'aumento dell'intensità del segnale relativo al prodotto a più elevato peso molecolare e la diminuzione dell'efficienza della secrezione del prodotto ricombinante nello spazio periplasmatico. Una possibile interpretazione cinetica di questo fenomeno ipotizza che la velocità di dimerizzazione del VHH sia molto più rapida rispetto a quella di reclutamento del prodotto da parte del sistema di secrezione periplasmatico.

## 7. Produzione del frammento anticorpale 3H6 Fab

L'anticorpo anti-idiotipo Ab2/3H6 Fab è diretto contro l'anticorpo 2F5 [26], un neutralizzante ad ampio spettro del virus HIV-1, potenziale componente chiave nella formulazione di un vaccino contro HIV. Inoltre, tale proteina è stata scelta come modello nell'ambito di un progetto europeo teso all'analisi comparativa nella produzione proteica ricombinante in differenti ospiti microbici in quanto era nota la sua capacità di evocare il fenomeno detto UPR (*unfolded protein response*) quando prodotta in cellule di lievito [16].

Come precedentemente accennato, i frammenti anticorpali Fab sono eterodimeri costituiti da una catena leggera ed una pesante. Per questo motivo, per la produzione del 3H6 Fab in cellule di *P. haloplanktis* TAC125, è stato scelto di costruire un operone artificiale in cui i geni codificanti le due catene sono stati organizzati in modo da ottenerne una sintesi bilanciata grazie al fenomeno del *coupling* traduzionale (vedi Fig. 1). L'analisi della produzione ricombinante è stata condotta mediante esperimenti ELISA su estratti proteici solubili totali ottenuti da campioni di colture di *P. haloplanktis* (pUCRP-*fab*) prelevati a diversi tempi di coltura di un processo in *batch*, condotto in condizioni ottimizzate a 15°C. I risultati ottenuti dimostrano che il 3H6 Fab si accumula efficacemente durante la fermentazione, raggiungendo una concentrazione massima di  $3.99 \pm 0.11$  mg/L dopo circa 48 ore di crescita [17]. Alla fine del processo la resa di prodotto ricombinante è risultata pari a  $0.89 \pm 0.15$  mg/g<sup>-1</sup> di biomassa espressa come peso secco cellulare. Tale valore di resa è di circa 5 volte più

elevato di quanto ottenibile in *Pichia pastoris* e più di 50 volte maggiore della resa in *E. coli* e *S. cerevisiae* così come riportato in un recente lavoro [9]. Una successiva analisi della localizzazione cellulare e della corretta struttura quaternaria acquisita dal 3H6 Fab ricombinante prodotto nel batterio antartico è stata condotta mediante esperimenti di *Western blotting* di frazioni periplasmatiche e citoplasmatiche da campioni raccolti durante la fermentazione. La separazione elettroforetica del campione è stata effettuata in condizioni non-riducenti mentre l'immunorivelazione è stata realizzata usando anticorpi specifici anti-catena leggera anticorpale (Fig. 5). I risultati hanno evidenziato la presenza di segnali specifici corrispondenti al 3H6 Fab in forma eterodimerica (il peso molecolare apparente del complesso è pari a 50kDa) esclusivamente nelle frazioni periplasmatiche, a dimostrazione che il Fab non solo è prodotto efficientemente in forma solubile, ma è traslocato totalmente nello spazio periplasmatico. Infine, alla luce del peso molecolare apparente corrispondente al prodotto evidenziato nel *Western blotting* e, soprattutto, la completa assenza di segnali relativi alla catena leggera in forma libera (circa 25 kDa), suggeriscono che il prodotto ricombinante assume la corretta struttura quaternaria [17].

## 8. Conclusioni

In questa rassegna sono stati riassunti risultati recenti, ottenuti nei nostri laboratori sulla produzione ricombinante di frammenti anticorpali nel batterio antartico *P. haloplanktis* TAC125, che dimostrano come questo microrganismo possa essere considerato a buon diritto un ospite d'elezione per la sintesi di queste proteine dal particolare rilievo economico. Infatti, tutti e tre i frammenti anticorpali selezionati per la produzione ricombinante nell'ospite antartico sono stati prodotti in forma solubile e correttamente assemblata, anche in virtù della scelta del percorso di secrezione periplasmatica co-traduzionale SRP-dipendente. Infatti, solo nel caso della produzione dell'anticorpo da camelide VHHD6.1 il sistema di traslocazione attraverso la membrana interna è risultato in qualche maniera inefficace quando la crescita raggiunge elevate densità cellulari. In tutti e tre i processi, comunque, l'ospite psicrofilo è stato in grado di produrre i frammenti anticorpali con rese paragonabili, se non largamente superiori, a quanto ottenuto nei sistemi di



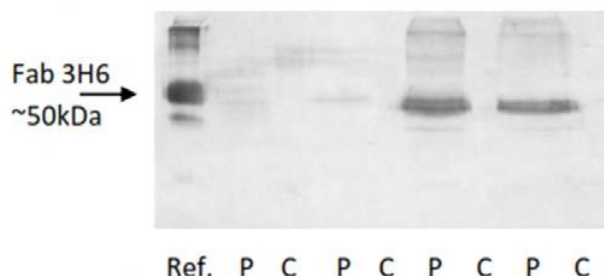


**Figura 5.** Produzione e localizzazione cellulare del frammento anticorpale Fab3H6 prodotto nel batterio *P. haloplanktis* TAC<sub>125</sub>. Aliquote di cellule ricombinanti sono state recuperate a fasi successive della crescita cellulare; il loro estratto proteico citoplasmatico (C) e la corrispondente frazione periplasmatica (P) sono state analizzate mediante Western Blotting usando l'anticorpo primario anti-c-myc. RIF, campione di Fab3H6 prodotto in maniera ricombinante in *Pichia pastoris*. L'analisi elettroforetica SDS-PAGE è stata condotta in condizioni non riducenti per cui l'analisi di immunorivelazione evidenzia il Fab3H6 in forma eterodimerica (50 kDa).

espressione convenzionali, quali *E. coli*, *S. cerevisiae* o *P. pastoris*. La particolare capacità di *P. haloplanktis* TAC<sub>125</sub> di produrre frammenti anticorpali ricombinanti di elevata qualità ha comunque indotto ad approfondire, laddove possibile, l'analisi delle caratteristiche cellulari che possano giustificarla. A tal riguardo, numerosi studi dei processi di *folding* delle molecole anticorpali hanno evidenziato il ruolo critico svolto dalle PPIasi, una classe di enzimi coinvolti nell'isomerizzazione *cis-trans* del legame X-Pro in polipeptidi. In un recente lavoro, Levy e coautori [27] hanno dimostrato che la co-espressione di FkpA, una PPIasi periplasmatica di *E. coli*, ha determinato in questo batterio un aumento significativo della secrezione periplasmatica di frammenti scFv funzionali, derivanti sia da catene V $\kappa$  (e, quindi, contenenti proline in conformazione *cis*) che catene V $\lambda$ , non dotate di *cis*-proline. Tali risultati hanno anche suggerito che l'effetto di FkpA sia legato oltre che alla sua attività enzimatica PPIasi anche a quella di *chaperone* molecolare.

La velocità della reazione di isomerizzazione *cis-trans* del legame X-Pro può comunque divenire un processo limitante durante il *folding*

proteico quando la temperatura si approssima al punto di congelamento dell'acqua. La recente osservazione che all'abbassamento della temperatura di crescita, *P. haloplanktis* TAC125 sovraesprime il *trigger factor*, lo *chaperone* molecolare che interagisce con il ribosoma ed è dotato anche di attività PPIasica, sembra ricondurre alla centralità di questo fenomeno nell'adattamento alla crescita alle basse temperature di questo microorganismo [39].

Un'altra interessante ipotesi di strategia adattativa alla psicrofilia deriva dallo studio di genomi di batteri polari, nei quali è spesso osservato un aumento nel numero di geni codificanti PPIasi che può accompagnarsi ad una riduzione della distribuzione dei residui di prolina nel proteoma codificato [13]. Per questo motivo, il genoma di *P. haloplanktis* TAC125 è stato analizzato alla ricerca di geni codificanti enzimi ad attività PPIasica. I risultati di tale analisi sono riassunti nella Tab. 1 dove sono riportati anche i 10 geni che codificano PPIasi nel batterio mesofilo *E. coli*. In accordo con quanto precedentemente ipotizzato, il genoma del batterio antartico contiene un numero superiore (15) di geni codificanti PPIasi, 10 dei quali codificano l'omologo psicrofilo delle proteine mesofile [18]. Dei 5 geni aggiuntivi posseduti da *P. haloplanktis* TAC125, due rappresentano duplicazioni dei geni codificanti le proteine SlyD e PpiC, mentre gli altri tre geni codificano una PPIasi citoplasmatica e due periplasmatiche (Tab. 1). In sintesi, alla luce della comparazione della distribuzione di enzimi ad attività PPIasi tra i due batteri, è possibile concludere che il batterio antartico possiede tre PPIasi citoplasmatiche e due PPIasi periplasmatiche in più rispetto a *E. coli*, osservazione che può giustificare le peculiari proprietà di *P. haloplanktis* TAC125 come ospite naturalmente ottimizzato per la produzione ricombinante di proteine o frammenti proteici stabilizzati da ponti disolfurici [18].

Più in generale, i nostri risultati dimostrano definitivamente che la produzione di proteine ricombinanti in questo batterio psicrofilo non è solo una tecnologia ormai affidabile, ma può essere una valida strategia per attenuare i problemi di solubilità o di *folding* scorretto che si sperimentano talora in sistemi di espressione convenzionali, come *E. coli*. Inoltre, *P. haloplanktis* TAC125 e la strategia di espressione genica messa a punto hanno dimostrato un interessante potenziale biotecnologico come piattaforma non convenzionale di produzione di proteine ricombinanti di valore significativo, come i frammenti anticorpali.

**Tabella 1.** Distribuzione dei geni codificanti enzimi ad attività peptidil-prolil cis-trans isomerasica nel genoma del batterio antartico *P.haloplanktis* TAC125 consultabile attraverso la piattaforma Mage\*.

Nome del gene	PhTAC125	Annotazione riportata in MAGE Gene	Localizzazione cellulare
slyDB	PSHAa0292	Peptidil-prolil cis-trans isomerasi, famiglia delle FKBP	citoplasma
slyDA	PSHAa0721	Peptidil-prolil cis-trans isomerasi, famiglia delle rotamasi	citoplasma
fkpB	PSHAa0920	Peptidil-prolil cis-trans isomerasi, famiglia delle rotamasi	citoplasma
	PSHAa1034	Peptidil-prolil cis-trans isomerasi, famiglia delle rotamasi	citoplasma
fkIB	PSHAa1414	Peptidil-prolil cis-trans isomerasi, famiglia delle rotamasi	citoplasma
ppiC	PSHAa2488	peptidil-prolil cis-trans isomerasi C (rotamasi C)	citoplasma
ppiC	PSHAa0308	peptidil-prolil cis-trans isomerasi C (rotamasi C)	citoplasma
tig	PSHAa2063	peptidil-prolil cis-trans isomerasi ( <i>trigger factor</i> ), <i>chaperone</i> molecolare coinvolto nella divisione cellulare	citoplasma
ppiB	PSHAa2066	peptidil-prolil cis-trans isomerasi B (rotamasi B)	citoplasma
ppiD	PSHAa2058	peptidil-prolil cis-trans isomerasi D (PPlasi D) (Rotamasi D)	associata alla membrana interna
fkpA	PSHAa2901	putativa peptidil-prolil cis-trans isomerasi	associata alla membrana interna
surA	PSHAa2633	peptidil-prolil cis-trans isomerasi (PPlasi D)	spazio periplasmatico
ppiA	PSHAa0347	putativa peptidil-prolil cis-trans isomerasi	spazio periplasmatico
	PSHAa1981	putativa peptidil-prolil cis-trans isomerasi (PPlasi)	spazio periplasmatico
	PSHAa2247	putativa peptidil-prolil isomerasi	spazio periplasmatico

\*<https://www.genoscope.cns.fr/agc/microscope/mage/viewer.php>

## References

- [1] ARBABI-GHAHROUDI M., TANHA J., R. MACKENZIE, 2005. *Prokaryotic expression of antibodies*. Cancer and Metastasis Reviews, 24, 501–519.
- [2] BANEYX F., 1999. *Recombinant protein expression in Escherichia coli*. Current Opinion in Biotechnology, 10, 411–421.
- [3] BIROLO L., TUTINO M.L., FONTANELLA B., GERDAY C., MAINOLFI K., PASCARELLA S., SANNIA G., VINCI F., G. MARINO, 2000. *Aspartate aminotransferase from the Antarctic bacterium Pseudoalteromonas haloplanktis TAC125. Cloning, expression, properties, and molecular modelling*. European Journal of Biochemistry, 267, 2790–2802.
- [4] CABEINER L.M., SURANA R., WANG S., 2010. *Monoclonal antibodies: versatile platforms for cancer immunotherapy*. Nature Reviews Immunology, 10, 317–327.
- [5] CARRIO M., GONZALEZ-MONTALBAN N., VERA A., VILLAYERDE A., S. VENTURA, 2005. *Amyloid-like properties of bacterial inclusion bodies*. Journal of Molecular Biology, 347, 1025–1037.
- [6] CHATZI K.E., SARDIS M.F., KARAMANOU S., A. ECONOMOU, 2013. *Breaking on through to the other side: protein export through the bacterial Sec system*. Biochemical Journal, 449, 25–37.
- [7] COLEMAN M.E., TAMPLIN M.L., PHILLIPS J.G., B.S. MARMER, 2003. *Influence of agitation, inoculum density, pH, and strain on the growth parameters of Escherichia coli O157:H7—relevance to risk assessment*. International Journal of Food Microbiology, 83, 147–160.
- [8] DALBEY R.E., M. CHEN, 2004. *Sec-translocase mediated membrane protein biogenesis*. Biochimica et Biophysica Acta, 1694, 37–53.
- [9] DRAGOSITS M., FRASCOTTI G., BERNARD-GRANGER L., VAZQUEZ F., GIULIANI M., BAUMANN K., RODRIGUEZ-CARMONA E., TOKKANEN J., PARRILLI E., WIEBE M. G., KUNERT R., MAURER M., GASSER B., SAUER M., BRANDUARDI P., PAKULA T., SALOHEIMO M., PENTTILA M., FERRER P., TUTINO M.L., VILLAYERDE A., PORRO D., D. MATTANOVICH, 2011. *Influence of growth temperature on the production of antibody Fab fragments in different microbes: a host comparative analysis*. Biotechnology Progress, 27, 38–46.
- [10] DUILIO A., TUTINO M.L., G. MARINO, 2004. *Recombinant protein production in Antarctic Gram negative bacteria*. Methods in Molecular Biology, 267, 225–237.
- [11] DUILIO A., MADONNA S., TUTINO M.L., PIROZZI M., SANNIA G., G. MARINO,

2004. *Promoters from a cold-adapted bacterium: definition of a consensus motif and molecular characterization of UP regulative elements*. *Extremophiles*, 8, 125–132.
- [12] FEIGE M.J., HENDERSHOT L.M., J. BUCHNER, 2010. *How antibodies fold*. *Trends in Biochemical Sciences*, 35, 189–198.
- [13] FELLER G., 2013. *Psychrophilic Enzymes: From Folding to Function and Biotechnology*. Scientifica (Cairo). 2013;2013:512840.
- [14] FERRER-MIRALLES N., DOMINGO-ESPÍN J., CORCHERO J.L., VÁZQUEZ E., A VILLAVARDE, 2009. *Microbial factories for recombinant pharmaceuticals*. *Microbial Cell Factories*, 8, 17.
- [15] FIEDLER U., CONRAD U., 1995. *High-level production and long-term storage of engineered antibodies in transgenic tobacco seeds*. *Biotechnology (N Y)* 13, 1090–1093.
- [16] GASSER B., MAURER M., RAUTIO J., SAUER M., BHATTACHARYYA A., SALO-HEIMO M., PENTTILÄ M., D. MATTANOVICH, 2007. *Monitoring of transcriptional regulation in Pichia pastoris under protein production conditions*. *Bio Med Central Genomics*, 8, 179.
- [17] GIULIANI M., PARRILLI E., FERRER P., BAUMANN K., MARINO G., M.L. TUTINO, 2011. *Process optimization for recombinant protein production in the psychrophilic bacterium Pseudoalteromonas haloplanktis*. *Process Biochemistry*, 46, 953–959.
- [18] GIULIANI M., PARRILLI E., SANNINO F., APUZZO G.A., MARINO G., TUTINO M.L., 2014. *Recombinant production of a single-chain antibody fragment in Pseudoalteromonas haloplanktis TAC125*. *Applied Microbiology Biotechnology*. 2014 Feb 18. [Epub ahead of print].
- [19] —, 2014. *Soluble recombinant protein production in Pseudoalteromonas haloplanktis TAC125*. *Methods Molecular Biology*, In press.
- [20] GOT P.A., J.M. SCHERRMANN, 1997. *Stereoselectivity of antibodies for the bioanalysis of chiral drugs*. *Pharmaceutical Research*, 14, 1516–1523.
- [21] GRAHAM B.M., PORTER A.J., W.J. HARRIS, 1995. *Cloning, expression and characterization of a single chain antibody fragment to the herbicide paraquat*. *Journal of Chemical Technology and Biotechnology*, 63, 279–289.
- [22] GRUDNIK P., BANGE G., I. SINNING, 2009. *Protein targeting by the signal recognition particle*. *Biological Chemistry*, 390, 775–782.
- [23] HAMERS-CASTERMAN C., ATARHOUGH T., MUYLDERMANS S., 1993. *Naturally occurring antibodies devoid of light chains*. *Nature* 363, 446–448.



- [24] HOLLINGER P., HUDSON P.J., 2005. *Engineered antibody fragments and the rise of single domains*. Nature Biotechnology, 23, 1126–1136.
- [25] JOOSTEN V., LOKMAN C., C. VAN DEN HONDEL, 2003. *The production of antibody fragments and antibody fusion proteins by yeasts and filamentous fungi*. Microbial Cell Factories, 2, 1.
- [26] KUNERT R.E., WEIK R., FERKO B., STIEGLER G., H. KATINGER, 2002. *Anti-idiotypic antibody Ab2/3H6 mimics the epitope of the neutralizing anti-HIV-1 monoclonal antibody 2F5*. AIDS; 16, 667–668.
- [27] LEVY R., AHLUWALIA K., BOHMANN D.J., GIANG H.M., SCHWIMMER L.J., ISSAFRAS H., REDDY N.B., CHAN C., HORWITZ A.H., T. TAKEUCHI, 2013. *Enhancement of antibody fragment secretion into the Escherichia coli periplasm by co-expression with the peptidyl prolyl isomerase, FkpA, in the cytoplasm*. Journal of Immunological Methods, 394, 10–21.
- [28] LIAO Y.D., JENG J.C., WANG C.F., WANG S.C., S.T. CHANG, 2004. *Removal of N-terminal methionine from recombinant proteins by engineered E. coli methionine aminopeptidase*. Protein Science, 13, 1802–1810.
- [29] MEDIGUE C., KRIN E., PASCAL G., BARBE V., BERNSEL A., BERTIN P. N., CHEUNG F., CRUVEILLER S., D'AMICO S., DUILIO A., FANG G., FELLER G., HO C., MANGENOT S., MARINO G., NILSSON J., PARRILLI E., ROCHA E.P., ROUY Z., SEKOWSKA A., TUTINO M.L., VALLENET D., VON, H.G., A. DANCHIN, 2005. *Coping with cold: the genome of the versatile marine Antarctica bacterium Pseudoalteromonas haloplanktis TAC125*. Genome Research, 15, 1325–1335.
- [30] MERGULHAO F.J., SUMMERS D.K., G.A. MONTEIRO, 2005. *Recombinant protein secretion in Escherichia coli*. Biotechnology Advances, 23, 177–202.
- [31] MONEGAL A., AMI D., C. MARTINELLI, 2009. *Immunological applications of single-domain llama recombinant antibodies isolated from a naïve library*. Protein Engineering, Design and Selection, 22, 273–280.
- [32] MUYLDERMANS S., M. LAUWEREYS, 1999. *Unique single-domain antigen binding fragments derived from naturally occurring camel heavy-chain antibodies*. Journal of Molecular Recognition, 12, 131–140.
- [33] OPPENHEIM D., C. YANOFSKY, 1980. *Translational coupling during expression of the tryptophan operon in Escherichia coli*. Genetics, 95, 785–795.
- [34] PAPA R., RIPPA V., SANNIA G., MARINO G., A. DUILIO, 2007. *An effective cold inducible expression system developed in Pseudoalteromonas haloplanktis TAC125*. Journal of Biotechnology, 127, 199–210.
- [35] PARRILLI E., CUSANO A.M., GIULIANI M., M.L. TUTINO, 2006. *Cell engi-*

- neering of *Pseudoalteromonas haloplanktis* TAC<sub>125</sub>: construction of a mutant strain with reduced *exo*-proteolytic activity. *Microbial Cell Factories*, 5(Suppl 1), P36.
- [36] PARRILLI E., DE VIZIO D., CIRULLI C., M.L. TUTINO, 2008. Development of an improved *Pseudoalteromonas haloplanktis* TAC<sub>125</sub> strain for recombinant protein secretion at low temperature. *Microbial Cell Factories*. 7, 2.
- [37] PARRILLI E., GIULIANI M., MARINO G., M.L. TUTINO, 2010. Influence of production process design on inclusion bodies protein: the case of an Antarctic flavohemoglobin. *Microbial Cell Factories* 9, 19.
- [38] PATIL G., RUDOLPH R., C. LANGE, 2008. In vitro-refolding of a single-chain Fv fragment in the presence of heteroaromatic thiols. *Journal of Biotechnology*, 134, 218–221.
- [39] PIETTE F., D'AMICO S., STRUVAY C., MAZZUCHELLI G., RENAUT J., TUTINO M.L., DANCHIN A., LEPRINCE P., G. FELLER 2010. Proteomics of life at low temperatures: trigger factor is the primary chaperone in the Antarctic bacterium *Pseudoalteromonas haloplanktis* TAC<sub>125</sub>. *Molecular Microbiology*, 76, 120–132.
- [40] RATTENHOLL A., LILIE H., GROSSMANN A., STERN A., SCHWARZ E., R. RUDOLPH, 2001. The pro-sequence facilitates folding of human nerve growth factor from *Escherichia coli* inclusion bodies. *European Journal of Biochemistry*, 268, 3296–3303.
- [41] SCHIERLE C.F., BERKMEN M., HUBER D., KUMAMOTO C., BOYD D., J. BECKWITH, 2003. The DsbA signal sequence directs efficient, cotranslational export of passenger proteins to the *Escherichia coli* periplasm via the signal recognition particle pathway. *Journal of Bacteriology*, 185, 5706–5713.
- [42] SOMERVILLE J.E. JR., GOSHORN S.C., FELL H.P., R.P. DARVEAU, 1994. Bacterial aspects associated with the expression of a single-chain antibody fragment in *Escherichia coli*. *Applied Microbiology and Biotechnology*, 42, 595–603.
- [43] SPEED M.A., WANG D.I., J. KING, 1996. Specific aggregation of partially folded polypeptide chains: the molecular basis of inclusion body composition. *Nature Biotechnology*, 14, 1283–1287.
- [44] THIE H., SCHIRRMANN T., PASCHKE M., DUBEL S., M. HUST, 2008. SRP and Sec pathway leader peptides for antibody phage display and antibody fragment production in *E. coli*. *Nature Biotechnology* 25, 49–54.
- [45] TUTINO M.L., DUILIO A., PARRILLI R., REMAUT E., SANNIA G., G. MARINO, 2001. A novel replication element from an Antarctic plasmid as a tool for the

- expression of proteins at low temperature*. *Extremophiles*, 5, 257–264.
- [46] TUTINO M.L., PARRILLI E., GIAQUINTO L., DUILIO A., SANNIA G., FELLER G., G. MARINO, 2002. *Secretion of alpha-amylase from Pseudoalteromonas haloplanktis TAB23: two different pathways in different hosts*. *Journal of Bacteriology*, 184, 5814–5817.
- [47] VIGENTINI I., MERICO A., TUTINO M.L., COMPAGNO C., G. MARINO, 2006. *Optimization of recombinant human nerve growth factor production in the psychrophilic Pseudoalteromonas haloplanktis*. *Journal Biotechnology*, 127, 141–150.
- [48] VINCI F., CATHARINO S., FREY S., BUCHNER J., MARINO G., PUCCI P., M. RUOPPOLO, 2004. *Hierarchical formation of disulfide bonds in the immunoglobulin Fc fragment is assisted by protein-disulfide isomerase*. *The Journal of Biological Chemistry*, 279, 15059–15066.
- [49] WICKNER W., M.R. LEONARD, 1996. *Escherichia coli preprotein translocase*. *The Journal of Biological Chemistry*, 271, 29514–29516.
- [50] WILMES B., HARTUNG A., LALK M., LIEBEKE M., SCHWEDE, T., P. NEUBAUER, 2010. *Fed-batch process for the psychrotolerant marine bacterium Pseudoalteromonas haloplanktis*. *Microbial Cell Factories*, 9, 72.
- [51] YANG A.S., SHARP K.A., B. HONIG, 1992. *Analysis of the heat capacity dependence of protein folding*. *Journal of Molecular Biology*, 227, 889–900.
- [52] YOKOTA T., MILENIC D.E., WHITLOW M., J. SCHLOM, 1992. *Rapid tumor penetration of a single-chain Fv and comparison with other immunoglobulin forms*. *Cancer Research*, 52, 3402–3408.

Maria Giuliani, Ermenegilda Parrilli, Filomena Sannino, Gennaro Antonio Apuzzo, Maria Luisa Tutino, Gennaro Marino  
Dipartimento di Scienze Chimiche, Università “Federico II”, Napoli  
Istituto di Biochimica delle Proteine, Consiglio Nazionale delle Ricerche, Napoli  
maria.giuliani@ymail.com; erparril@unina.it; filomena.sannino2@unina.it  
gen.apuzzo@gmail.com; marino@unina.it; tutino@unina.it

# Chapter 13

## Soluble Recombinant Protein Production in *Pseudoalteromonas haloplanktis* TAC125

Maria Giuliani, Ermenegilda Parrilli, Filomena Sannino,  
Gennaro Apuzzo, Gennaro Marino, and Maria Luisa Tutino

### Abstract

Solubility/activity issues are often experienced when immunoglobulin fragments are produced in conventional microbial cell factories. Although several experimental approaches have been followed to solve, or at least minimize, the accumulation of the recombinant proteins into insoluble aggregates, sometimes the only alternative strategy is changing the protein production platform.

In this chapter we describe the use of Antarctic bacterium *Pseudoalteromonas haloplanktis* TAC125 as host of choice for the production of the heavy-chain antibody fragment VHHD6.1. Combining the use of a regulated psychrophilic gene expression system with an optimized fermentation process in defined growth medium, we obtained the recombinant VHHD6.1 in fully soluble form and correctly translocated into host periplasmic space.

**Key words** *Pseudoalteromonas haloplanktis* TAC125, VHHD6.1, Psychrophilic gene expression system, LIV medium, Batch fermentation

---

### 1 Introduction

Till their first description [1], IgG antibodies from Camelidae (camels, dromedaries, and llamas) attracted attention of either basic or applied scientists due to their feature of “heavy-chain antibody” or HCAb. Indeed these antibodies are naturally devoid of light chains and it makes their size significantly lower than conventional IgG antibodies. Consequently, their binding domains consist only of the heavy-chain variable domains, referred to as VHHs [2], to distinguish them from conventional VHs. VHH is the smallest available intact antigen-binding fragment (~15 kDa) and it has a great potential in therapeutic and diagnostic application as multispecific fusion product [3].

Due to their reduced structural complexity, VHHs are often successfully produced in conventional microbial cell factories, such as *Escherichia coli* [4]. However, there may be still a fraction of

VHHs which escapes the binding evaluation tests due to poor stability in soluble form in the recombinant production host. These potentially valuable molecules are committed to be fatally overlooked, if the microbial production platform does not display optimized features for antibodies production.

Over the last years, our research group has been focused on the exploitation and implementation of the unconventional marine bacterium *Pseudoalteromonas haloplanktis* TAC125 as recombinant protein production host [5–7]. This psychrophilic Gram-negative bacterium, isolated from Antarctic sea water [8], displays several metabolic and physiological traits that justify a moderate interest as alternative protein production platform to be used when the other conventional microbial systems fail [9, 10].

Indeed, the combination of its optimal growth performances at reduced temperature—where hydrophobic interactions are significantly minimized—and a rich arsenal of folding factors and catalysts—supporting high-quality protein folding at low temperatures—allowed us to produce in soluble and active forms several difficult-to-express proteins [9–11]. Amongst them, a Fab antibody fragment [12] and a single-chain antibody fragment (unpublished results from this laboratory) highlighted an interesting proficiency of this bug in producing immunoglobulin-derived molecules.

To prove the ability of *P. haloplanktis* TAC125 to successfully produce soluble antibody fragments, an anti-human fibroblast growth factor receptor 1 (FGFR1) VHHD6.1 was chosen as model protein. It was selected by phage display from a pre-immune llama library [13] but its large-scale production in conventional *E. coli* expression systems was unsatisfactory due to inclusion bodies formation (De Marco A, personal communication). A new production process leading to improve soluble production of VHHD6.1 is therefore required for its further characterization.

In the present chapter, we describe the procedure for the cloning of *vhhD6.1* gene into a modified pUCRP psychrophilic gene expression system and its mobilization into *P. haloplanktis* TAC125 cells. Recombinant Antarctic strain was then grown at 15 °C in optimized culture conditions (LIV medium, batch cultivation in a 3 L STR automatic fermenter) and protein production followed by monitoring VHHD6.1 production and cellular localization over 60 h cultivation process, leading to the definition of optimal process conditions for the production of VHHD6.1 in soluble and fully periplasmic form.

---

## 2 Materials

### 2.1 Bacterial Strains

1. *P. haloplanktis* TAC125. This strain was kindly provided by C. Gerday, University of Liege, Belgium. The strain was isolated from the sea water in the surrounding of the Dumont



d'Urville Antarctic station (66°40'S, 40°01'E) during the 1988 summer campaign of the "Expeditions Polaires Françaises" in Terre Adélie [14].

2. *E. coli* DH5 $\alpha$  [*supE44*,  $\Delta$ *lacU169* ( $\phi$ 80 *lacZ* $\Delta$ M15) *hsdR17*, *recA1*, *endA1*, *gyrA96*, *thi-1*, *relA1*]. This strain was used as host for the gene cloning.
3. *E. coli* strain S17-1( $\lambda$ *pir*) [*thi*, *pro*, *hsd* (*r*<sup>+</sup> *m*<sup>+</sup>) *recA*::RP4:2-TC':Mu Km<sup>r</sup>::Tn7 Tp<sup>r</sup> Sm<sup>r</sup>  $\lambda$ *pir*]. This strain was used as donor in intergeneric conjugation experiments [7].

## 2.2 Solutions

1. 100 mg/mL ampicillin stock solution: dissolve 1 g of ampicillin powder in 8 mL of deionized H<sub>2</sub>O. Adjust the volume of the solution to 10 mL with deionized H<sub>2</sub>O and sterilize by filtration through a 0.22  $\mu$ m sterile filter. Split the obtained stock solution in 10 aliquots of 1 mL each in sterile polypropylene tubes and store them at -20 °C.
2. 1 $\times$  TAE buffer for agarose gel electrophoresis: 40 mM Tris-acetate, 1 mM EDTA, pH 8. Make a 50 $\times$  TAE stock solution by mixing 242 g of Tris base, 57.1 mL of glacial acetic acid, 100 mL of 0.5 M EDTA, pH 8, and adjust the volume of the solution to 1 L with deionized H<sub>2</sub>O. Store at room temperature (RT) up to 1 year.
3. 0.5 M EDTA, pH 8: dissolve 186.1 g of EDTA in 800 mL of deionized H<sub>2</sub>O. Adjust the pH to 8 with NaOH (about 20 g of NaOH pellets) and adjust the volume of the solution to 1 L with deionized H<sub>2</sub>O.
4. 3 M NaCl stock solution: dissolve 87.6 g of NaCl in 500 mL of dH<sub>2</sub>O.
5. 6 $\times$  agarose gel-loading buffer: 0.25 % bromophenol blue, 0.25 % xylene cyanol FF, and 30 % glycerol (Fermentas).
6. 10 mg/mL ethidium bromide: add 1 g of ethidium bromide to 100 mL of deionized H<sub>2</sub>O. Stir on a magnetic stirrer for several hours to ensure that the dye has dissolved. Wrap the container in aluminum foil and store it at 4 °C.
7. 20 % (w/v) L-malate stock solution: Dissolve 10 g of L-malic acid in 40 mL of deionized H<sub>2</sub>O. Adjust the pH to 7.0 with 5 M NaOH. Adjust the volume of the solution to 50 mL with dH<sub>2</sub>O and sterilize by filtration through a 0.22  $\mu$ m sterile filter. Store at 4 °C up to 2 months.
8. 1 M DTT stock solution: Dissolve 3.09 g of DTT in 20 mL of deionized H<sub>2</sub>O. Sterilize by filtration. Dispense into 1 mL aliquots and store them at -20 °C.
9. 1 $\times$  SDS-PAGE loading buffer: 62.5 mM Tris-HCl, pH 6.8, 10 % glycerol, 2 % SDS, 100 mM DTT, and 0.1 % bromophenol blue. This buffer lacking DTT can be stored at RT.

DTT should then be added just before that the buffer is used from a 1 M stock.

10. 0.5 M Tris-HCl, pH 6.8: Dissolve 60.55 g of Tris base in 800 mL of deionized H<sub>2</sub>O. Adjust the pH to 6.8 with HCl and add dH<sub>2</sub>O to make up a final volume of 1 L.
11. 0.5 % (w/v) bromophenol blue: Dissolve 0.25 g bromophenol blue powder in 45 mL of dH<sub>2</sub>O. Shake well to dissolve the dye and then adjust the volume of the solution to 50 mL with dH<sub>2</sub>O. Store at RT.
12. 5× Running buffer: Dissolve 15.1 g of Tris base, 94 g of glycine, and 5 g of SDS in 900 mL of dH<sub>2</sub>O. Adjust the volume of the solution to 1 L with dH<sub>2</sub>O.
13. 0.5 M Phosphate buffer: Dissolve 68.9 g of NaH<sub>2</sub>PO<sub>4</sub> in 900 mL of dH<sub>2</sub>O. Adjust the pH to 7.3 with NaOH and add dH<sub>2</sub>O to make up a final volume of 1 L.
14. Borate buffer: Dissolve 7.63 g of Na<sub>2</sub>B<sub>4</sub>O<sub>7</sub>, 0.76 g of NaCl in 90 mL of dH<sub>2</sub>O. Add 1 mL EDTA 0.5 M, pH 8, shake and adjust the volume of the solution to 100 mL with dH<sub>2</sub>O.
15. Western blot 1× Transfer buffer: Dissolve 3.03 g Tris base, 14.41 g glycine in 800 mL of deionized H<sub>2</sub>O. Add 200 mL methanol. Adjust the volume of the solution to 1 L with dH<sub>2</sub>O.
16. Western blot blocking buffer: Dissolve 50 g Skimmed Milk in 1 L of PBS buffer (5 % w/v). Add 1 mL Triton X-100 (0.1 % v/v) and mix.
17. Western blot washing buffer: Add 1 mL of Triton X-100 in 1 L of PBS buffer (0.1 % v/v) and mix.
18. 1× PBS: Dissolve 8 g NaCl, 0.2 g KCl, 1.44 g Na<sub>2</sub>HPO<sub>4</sub>, and 0.24 g KH<sub>2</sub>PO<sub>4</sub> in 800 mL of distilled H<sub>2</sub>O. Adjust the pH to 7.4 with HCl. Add H<sub>2</sub>O to 1 L. Sterilize by autoclaving.
19. 20× SCHATZ Salts: Dissolve 20 g of KH<sub>2</sub>PO<sub>4</sub>, 20 g of NH<sub>4</sub>NO<sub>3</sub>, 4 g of MgSO<sub>4</sub>·7H<sub>2</sub>O, 0.2 g of FeSO<sub>4</sub>, and 0.2 g of CaCl<sub>2</sub>·2H<sub>2</sub>O in 1 L dH<sub>2</sub>O. Adjust the pH to 7.0 by HCl addition. Sterilize by filtration through a 0.22 µm sterile filter. Store at 4 °C up to 2 months.

### 2.3 Media

1. LB medium (1 L) [15]: 10 g Bacto-Tryptone, 5 g Bacto-Yeast Extract, 10 g NaCl. Adjust 950 mL with deionized H<sub>2</sub>O. Shake until the solutes have dissolved. Adjust the volume to 1 L with dH<sub>2</sub>O. Sterilize by autoclaving for 20 min at 1 atm on liquid cycle. Let it cool down and store at RT. When required, add 1 mL of sterile ampicillin stock solution. After antibiotic addition store the medium at 4 °C up to 2 weeks. To prepare solid medium, add 15 g/L Bacto-Agar just before autoclaving.
2. TYP medium (1 L) [7]: 16 g Bacto-Tryptone, 16 g Bacto-Yeast Extract, 10 g Marine mix, add 950 mL of deionized H<sub>2</sub>O.

Shake until the solutes have dissolved. Adjust the pH to 7.5 with 5 N NaOH. Adjust the volume of the solution to 1 L with deionized H<sub>2</sub>O. Sterilize by autoclaving for 20 min at 1 atm on liquid cycle. When required, add 1 mL of sterile ampicillin stock solution. After antibiotic addition store the medium at 4 °C up to 2 weeks. To prepare solid medium, add 15 g/L Bacto-agar just before autoclaving.

3. LIV medium (1 L) [12]: 1 g KH<sub>2</sub>PO<sub>4</sub>, 1 g NH<sub>4</sub>NO<sub>3</sub>, 10g NaCl, 0.2 g MgSO<sub>4</sub>·7H<sub>2</sub>O, 10 mg FeSO<sub>4</sub>, 10 mg CaCl<sub>2</sub>·2H<sub>2</sub>O, 5 g L-leucine, 5 g L-isoleucine, 10 g L-valine, add 900 mL of deionized H<sub>2</sub>O. Shake until the solutes have dissolved, adjust the volume to 1 L with dH<sub>2</sub>O, and sterilize by filtration through a 0.22 µm sterile filter. Store at 4 °C. When required, add 1 mL of sterile ampicillin stock solution. After antibiotic addition store the medium at 4 °C up to 2 weeks. For protein induction add 2 mL of sterile 20 % w/v L-malate stock solution.

#### 2.4 Reagents for Molecular Biology

- Phusion™ DNA Polymerase.
- Taq DNA Polymerase.
- Restriction enzymes.
- Calf Intestinal Phosphatase, CIP.
- T4 DNA ligase.
- PCR Product Purification Kit.
- Miniprep Kit.
- Nucleotide Removal Kit.
- pGem®-T Easy Vector System I.
- Anti c-Myc mAb produced in mouse.
- Peroxidase conjugated anti-mouse IgG.
- SuperSignal West Femto Chemiluminescent Substrate.

#### 2.5 Storage Medium

Bacteria can be stored indefinitely in cultures containing 39 % of sterile glycerol (sterilize by autoclaving for 20 min at 1 atm on liquid cycle). At low temperature (from –20 to –70 °C).

---

### 3 Methods

#### 3.1 VHHD6.1 Expression Vector Construction

For L-malate-inducible VHHD6.1 production in *P. haloplanktis* TAC125 cells, *vhhD6.1* gene was cloned in pUCRP cold expression vector [16] previously modified by the addition of the sequences encoding the N-terminal *PbDsbA* leader peptide for periplasmic secretion and C-terminal *c-myc* tag and 6xHis-tag (Fig. 1).



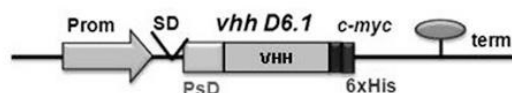


**Fig. 1** Schematic representation of VHHD6.1 expression cassettes. *SD* Shine Dalgarno sequence, *Prom* psychrophilic L-malate inducible promoter, *term* psychrophilic terminator, *PsD* *PhDsbA* signal peptide

The pUCRP-inducible expression vector [5] is a pUCLT/Rterm derivative [17] containing the transcription promoter region of the *PSHAb0363* gene, which responds to the presence of L-malate into the culture medium. The pUCLT/Rterm plasmid, deriving from the pUC18 plasmid, is characterized by the presence of (1) the pJB3-derived OriT [18], a DNA fragment responsible for the initiation of the conjugative transfer between *E. coli* S17-1  $\lambda$ pir strain (donor) and the psychrophilic cells (acceptor); (2) a pUC18-derived polylinker wherein the target gene can be cloned; (3) *E. coli blaM* gene, encoding a mesophilic  $\beta$ -lactamase which is used for the selection of the recombinant clones; (4) OriC, the origin of replication allowing the plasmid to replicate in *E. coli*; (5) the T/R box, a DNA fragment containing the cold-adapted origin of replication (OriR) [19]; (6) the *TaspC*, the transcription termination signal of the aspartate aminotransferase gene (*aspC*) isolated from *P. haloplanktis* TAC125 [14].

The addition of the molecular signal for periplasmic addressing is necessary in order to facilitate the correct folding of the recombinant product. The VHs, like the other antibodies and antibody fragments, contain disulfide bonds in their immunoglobulin domains required for the binding activity. The oxidizing environment and the dedicated chaperones present in bacterial periplasm can prevent cysteine reduction and aid to the correct disulfide bond isomerization. In addition, the use of the leader peptide isolated from *P. haloplanktis* DsbA [20] addresses the recombinant secretion through a co-translational SRP-like secretion system [21], limiting the fast protein aggregation often observed in the cytoplasm of bacteria expressing recombinant antibody fragment secreted by posttranslational Sec-dependent mechanism.

The addition of C-terminal tandem tag will allow the easy protein detection by Western blot using monoclonal anti-c-Myc tag antibodies and IMAC purification through the 6xHis-tag (Fig. 1).

1. The *vhhD6.1* gene is amplified on pHEN-D6.1 source vector (kindly provided by Dr. A. De Marco, IFOM-IEO campus Milan), in order to insert a 5' *SalI* and a 3' *NotI* restriction site by using primers VH-S-fw (5'-ATCGTGTCGACATGGC TGAGGTGC-3') and VH-N-rv (5'-ATATATGCGGCCGC AATGGAGACGGTG-3'), respectively. PCR reaction is carried

out by Phusion® High-Fidelity DNA Polymerase following the manufacturer's protocols.

2. The amplified product is purified using a commercial purification kit and then digested with *Sall* and *NotI*. Restriction hydrolyses are performed by using five enzyme units/μg of DNA, in the reaction conditions defined by the manufacturer.
3. The pUCRP vector is digested with *Sall* and *NotI*.
4. The 5' phosphate groups of the cleaved vector are dephosphorylated by treatment with calf intestinal alkaline phosphatase (0.5 U/pmol of 5' phosphate ends) for 15 min at 37 °C and 45 min at 55 °C by using the appropriate buffer delivered with the enzyme. The CIP is heat-inactivated at 75 °C for 10 min.
5. The dephosphorylated DNA is then loaded on a 1 % agarose gel (containing ethidium bromide as fluorescent marker for the migrating DNA). The DNA is cut out of the gel and purified using a commercial gel-purification kit following the manufacturer's instructions.
6. The cleaved dephosphorylated vector is then ligated to the digested amplification products by using two consecutive ligation reactions, by the means of T4 DNA ligase according to the supplier's instructions.
7. The ligation reaction mixture is used directly for transformation of the chemically competent bacteria (DH5α *E. coli* strain) according to the procedure described by Hanahan [22].
8. Recombinant clones are selected on LB agar plates containing 100 μg/mL ampicillin as selection agent.
9. Plasmids are isolated from ampR clones and the presence of the appropriate insert is verified by restriction digestion analysis (see Note 1).
10. Finally the nucleotide sequences of the inserts are checked by DNA sequencing to rule out the occurrence of any mutation during synthesis.

The resulting expression vector, pUCRP-*vhhD6.1*, contains the *vhhD6.1* gene in-frame to N-terminal PsD and C-terminal c-Myc and 6xHis tag coding sequences.

### **3.2 Construction of *P. haloplanktis* TAC125 pUCRP-*vhhD6.1* Recombinant Strain**

1. The resulting vector pUCRP-*vhhD6.1* is mobilized into *P. haloplanktis* TAC125 by intergeneric conjugation [7]. Cells are plated on TYP solid medium containing 50 μg/mL ampicillin and incubated at 4 °C to select recombinant *P. haloplanktis* TAC125 (the low temperature avoid *E. coli* growth as colony).
2. Three colonies are picked and inoculated in 3 mL of TYP liquid medium containing 100 μg/mL ampicillin and incubated at 15 °C under shaking (250 rpm) for 24 h.



3. Plasmidic DNA is extracted from each clone by using a commercial kit and recombinant plasmid clones were screened by PCR amplification of *vhhD6.1* gene.

### 3.3 VHHD6.1 Production

VHHD6.1 production is carried out according to the optimized protocol described in [12]. In detail, recombinant *P. haloplanktis* (pUCRP-*vhhD6.1*) batch cultivation was performed in a STR 3 L fermenter connected to a Bio-controller with a working volume of 1 L, in SCHATZ mineral medium supplemented with 0.5 % w/v L-leucine, 0.5 % w/v L-isoleucine, and 1.0 % w/v L-valine (LIV medium), 100 µg/mL ampicillin with additional 0.4 % w/v L-malate as inducer. The culture was carried out at 15 °C in aerobic conditions (Dissolved Oxygen Tension (DOT) ≥ 30 %), airflow of 20 L/h, and a stirring rate of 500 rpm. The culture pH was maintained at 7.00 by automatic addition of H<sub>2</sub>SO<sub>4</sub> 5 % v/v. The cell biomass from a pre-inoculum, performed in shaken flask with the same medium and temperature used for the successive experiment in batch, was used to inoculate batch cultures.

The controller automatically registers DOT, pH, and temperature values every minute during the whole process and acts on acid pump or the water bath connected to the water jacket to keep pH and temperature within the set point range. Cell growth was monitored by measuring the optical density at 600 nm (OD<sub>600nm</sub>) using a spectrophotometer.

#### 3.3.1 Process Setup

1. Fill the vessel with the media carbon sources and NaCl dissolved in 1 L of dH<sub>2</sub>O.
2. Insert the pH and DOT probes (the pH electrode must be previously calibrated according to manufacturer's instructions) and the stirrer.
3. Connect the tubes for sampling and for the inoculum and seal it with a clamp. Seal the open connections with aluminum foil. Connect a sterile 0.22 µm filter to the air inlet tube.
4. Fill in the water jacket.
5. Prepare a 250 mL Pyrex bottle with two ports cover containing H<sub>2</sub>SO<sub>4</sub> 5 % (v/v), connect a tube and seal it with a clamp.
6. Sterilize both the vessel and the acid bottle at high temperature (120 °C for 50 min at 1 atm) in autoclave.
7. After autoclaving, discard the water from the jacket and let the vessel cool down to a comfortable handling temperature then connect the pH and DOT electrodes to the bio-controller and the temperature probe to the vessel. Connect the water jacket to a thermostated water bath set at 15 °C. Connect the tube from acid bottle to the peristaltic pump and to the vessel.
8. Complement the medium by adding 50 mL of SCHATZ Salts stock solution (20×) and 1 mL of ampicillin stock solution (1,000×) through the inoculum tube using a 50 mL syringe.

9. Turn on the Bio-controller and set the following parameters:  
 (DOT)  $\geq 30\%$ .  
 pH  $7.00 \pm 0.2$ .  
 Temperature  $15\text{ }^{\circ}\text{C} \pm 0.5$ .
10. When the system reaches the desired temperature and pH, calibrate the DOT electrode by connecting the airflow inlet first to a nitrogen tank and setting the 0 % DOT when nitrogen saturation is obtained; then let the air in at maximum stirring rate to set the 100 % DOT.
11. After DOT calibration set the airflow at 20 L/h and stirring rate at 500 rpm.

### 3.3.2 Preculture

The viability of the precultured cells is crucial for a satisfying process outcome. The growth phase must be in middle exponential phase in the same medium that will be used for the fermentation.

1. From a glycerol stock streak the *P. haloplanktis* TAC125 pUCRP-*nhhD6.1* strain on a TYP agar plate containing 100 mg/L of ampicillin. Incubate it at  $15\text{ }^{\circ}\text{C}$  for about 36 h. The plate can be stored up to 3 days at  $4\text{ }^{\circ}\text{C}$ , carefully sealed with Parafilm to avoid oxygen availability to the cells (*see Note 2*).
2. Pick a single colony and inoculate it in 2 mL of liquid TYP medium supplemented with ampicillin 100 mg/L in a 14 mL snap-cap inoculation tube and incubate at  $15\text{ }^{\circ}\text{C}$  under vigorous shaking (250 rpm) for 36 h (*see Note 3*).
3. Dilute the inoculum in 50 mL of LIV medium supplemented with ampicillin 100 mg/L in a 250 mL flask and incubate for 16–18 h at  $15\text{ }^{\circ}\text{C}$  under vigorous shaking (250 rpm). The final biomass concentration should be 5–7 OD<sub>600nm</sub>.

### 3.3.3 Fermentation Process

The fermentation process will follow the general procedure described below. However, each clone can behave differently needing further optimization depending on the properties of the protein to be produced. In the following procedure, the parameters set up at the beginning of the process can be changed according to specific requirements of individual processes. For instance, the airflow is set to 20 L/h at the beginning of the process but to guarantee the sufficient oxygen supply to the growing cells (DOT > 30 %) it can be increased manually during the process up to 40 L/h. The stirring rate indeed cannot be increased over 500 rpm due to system limitation and therefore the optimal DOT can be achieved only by playing with the airflow inlet.

1. Inoculate the amount of preculture required in order to obtain a starting concentration of OD<sub>600nm</sub> = 0.2. To calculate it, register the optical density of the preculture at 600 nm using a spectrophotometer. Since the culture working volume in

bioreactor is 1 L, calculate the volume of inoculum by using the following formula:

$$\text{mL inoculum} = (\text{Culture OD}_{600\text{nm}} \times \text{mL culture volume}) / \text{Preculture OD}_{600\text{nm}}.$$

Use a 50 mL syringe connected to the inoculum tube. Carefully remove the aluminum seal and rapidly insert the syringe (to keep sterility, it can be useful to operate near the flame of a Bunsen burner). Remove the clamp before inserting the inoculum in the tube. Pipet up and down with the syringe several times to be sure that nothing lasts in the tube dead volume.

2. Wait a couple of minutes until the suspension becomes homogeneous, letting the stirrer on, then take a sample from the bioreactor to register the actual starting optical density at 600 nm. Use a 20 mL syringe connected to the sampling tube and pipet up and down several times to be sure to sample from the inside of the culture and not the dead volume of the tube.
3. Monitor the cell growth by measuring the  $\text{OD}_{600\text{nm}}$  as described above. Register the data of at least two measurements to avoid the technical error. When the cell density reaches an  $\text{OD}_{600\text{nm}}$  of 0.6–0.8 which corresponds to early exponential phase induce the recombinant gene expression by L-malate addition. Add 20 mL of 20 % w/v L-malate sterile stock solution to obtain the optimal inducer concentration of 0.4 % w/v using a syringe connected to the inoculum tube.
4. At different times after induction collect a sample corresponding to an  $\text{OD}_{600\text{nm}}$  of 25 in triplicate. Calculate the volume of each sample using the following formula:

$$\text{mL sample} = 25 / \text{Culture optical density } \text{OD}_{600\text{nm}}.$$

Collect samples after about 24, 30, 42, and 60 h after induction by centrifuging the calculated volume for 15 min at  $200 \times g$  at 4 °C. Discard the supernatant and store the biomass indefinitely at –80 °C.

5. Plot the optical density values versus the time of cultivation in graph. In a typical process (Fig. 2) the growth profile shows a diauxic growth due to the differential consumption of carbon sources during growth. During the first exponential the highest specific growth rate is reached ( $\mu_{\text{max}} = 0.13 \text{ h}^{-1}$ ); the L-valine is rapidly consumed within the first 24 h (data not shown). The second exponential growth phase starts at about 24 h of cultivation and lasts for the next 24 h with a very low specific growth rate. The total time of the process is about 60 h; afterwards the DOT increases and cell lysis starts (data not shown). Sampling point corresponds to the different phases of the fermentation process.

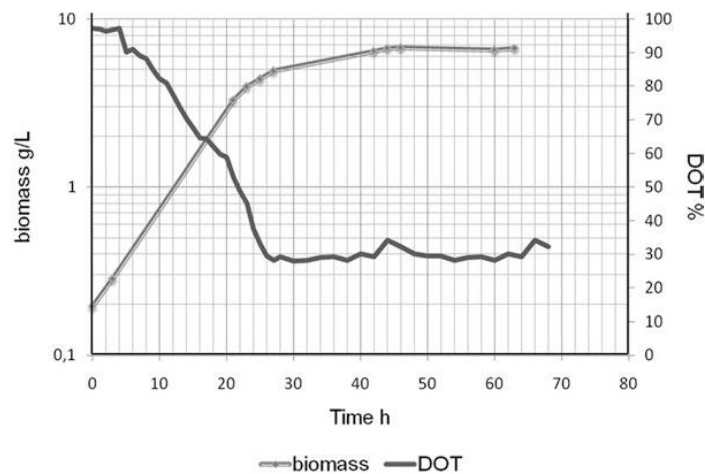


**Fig. 2** *P. haloplanktis* TAC125 (pUCRP-*vhhD6.1*) fermentation profiles. The biomass concentration is reported as g/L of dry cell weight calculated according to [12]

### 3.4 VHH D6.1 Production Analysis

To test the process efficiency, the protein detection itself is not sufficient. In order to obtain a correctly folded and, consequently, a biologically active antibody fragment product, the protein should be localized in periplasmic compartment where, due to the proper chemical-physical properties and chaperones, the correct formation of disulfide bonds contained in VHH immunoglobulin domains can be achieved.

To analyze the VHH D6.1 production and periplasmic secretion, a cellular fractionation followed by Western blotting analysis is required.

#### 3.4.1 Cell Lysis

1. Prepare 100 mL of Lysis buffer by diluting 10 mL of 0.5 M phosphate buffer stock solution and 10 mL of NaCl stock solution in 80 mL of dH<sub>2</sub>O.
2. Resuspend the bacterial pellet collected ( $OD_{600nm} = 25$ ) at different fermentation time point in 1 mL of lysis buffer by pipetting or vortexing.
3. Add 10  $\mu$ L of 100 mM PMSF stock solution and 1  $\mu$ L of 0.5 M EDTA stock solution and mix (see **Note 4**).
4. Apply five cycles of a benchtop French Press at 1.8 kbar to each sample.
5. Centrifuge the suspension at  $8,200 \times g$  for 20 min at 4 °C. Recover the resulting supernatant containing the total soluble protein extract for further analysis. Keep the protein extract on ice or store it at 4 °C for no longer than 2 h.



### 3.4.2 Periplasm Extraction

1. Resuspend an aliquot of bacterial pellet collected ( $OD_{600nm} = 25$ ) at different fermentation time point in 0.2 mL of borate buffer by gently pipetting.
2. Incubate for 16–18 h at 4 °C.
3. Centrifuge at  $8,200 \times g$  for 15 min at 4 °C and store the supernatant containing the periplasmic protein extract for further analysis. Keep the extract on ice or store it at 4 °C for no longer than 2 h.

### 3.4.3 Western Blot Protein Detection

1. Mix 12  $\mu$ L of each sample prepared at Subheadings 3.4.1 and 3.4.2 with 4  $\mu$ L of 4 $\times$  SDS-PAGE loading buffer. Boil the samples for 5 min at 95 °C and load on 15 % SDS-PAGE gel. Load 16  $\mu$ L of the samples coming from increasing time points alternating total protein extracts with periplasmic protein extracts. Run the gel for 45 min at constant 50 mA.
2. Wash the gel three times with transfer buffer for 10 min.
3. Transfer the protein on a 0.2  $\mu$ m PVDF membrane previously activated in methanol according to the manufacturer's instruction.
4. Block the membrane for 1 h in blocking buffer under shaking at RT.
5. Dilute the anti-c-Myc monoclonal antibody (*see* Subheading 2) 1:5,000 in blocking buffer by diluting 2  $\mu$ L of antibody in 10 mL. Incubate the membrane with the primary antibody solution for 1 h at RT under shaking.
6. Discard the primary antibody solution and wash the membrane three times with Western blot washing buffer for 10 min.
7. Dilute HRP anti-mouse antibody (*see* Subheading 2) 1:10,000 in blocking buffer by diluting 1  $\mu$ L of antibody in 10 mL. Incubate the membrane with the primary antibody solution for 1 h at RT under shaking.
8. Discard the secondary antibody solution and wash the membrane five times with Western blot washing buffer for 10 min.
9. Develop the Western blot using chemiluminescence.

The analysis (Fig. 3) reveals VHHD6.1 production in soluble form during all fermentation and its correct periplasmic localization during early (22 h) and middle (29 h) exponential growth phase. In contrast, no recombinant VHHD6.1 was found in periplasmic fraction extracted from samples collected at late exponential growth phase (42 h) and stationary phase (60 h) while production titers seem to increase during exponential growth reaching the highest yield at late exponential phase (42 h). Furthermore, another specific signal showing an apparent molecular weight of about 30 kDa was detected in total soluble protein extracts probably corresponding to VHHD6.1 dimers. It is not



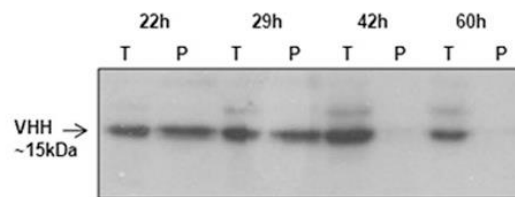


**Fig. 3** Western blotting analysis. VHHD6.1 soluble production and cellular localization on total protein extracts (T) and periplasmic fraction (P) of recombinant *P. haloplanktis* TAC125 (pUCRP-*vhhD6.1*) cells collected at different times of fermentation. Expected recombinant VHHD6.1 molecular weight: 15 kDa

surprising since a strong tendency of multimerization has been reported for this and other formats of antibody fragments in vivo when their local concentration in recombinant host cells reaches a critical value [23]. It is worth noticing that as far as the high molecular weight signal relative intensity increases the secretion efficiency of recombinant product into periplasmic space seems to decrease. One explanation can be found in VHHs dimerization kinetics that could be faster than the product recruitment by the periplasmic secretion system. On the other hand, VHH dimers formation could be a consequence of its cytoplasmic localization. If protein secretion does not occur, its correct folding cannot be achieved and hydrophobic interactions can take place among partly folded intermediates thus causing protein molecules aggregation in soluble dimeric complexes. Although the co-translational SRP-mediated secretion system was successfully employed for Fab [12] and ScFv (unpublished results) formats model proteins, VHHD6.1 translocation across the inner membrane results to be somehow inhibited at high cell densities. Further investigation has to be carried out in order to find out the reason of this phenomenon and the best strategy to overcome it.

#### 4 Notes

1. Alternatively, screen for recombinant plasmid clones by using PCR to directly amplify the insert from each bacterial recombinant colony.
2. The psychrophilic bacteria are able to grow at temperature as low as 4 °C. Limiting oxygen availability can reduce the growth but not avoid it.
3. This passage is optional but helps to overcome a long lag phase due to the adaptation of bacteria coming from a complex rich culture medium (TYP) to the defined LIV medium.
4. Add PMSF and EDTA to the lysis buffer to prevent proteolytic degradation of recombinant product.

## Acknowledgement

This work was supported by Programma Nazionale di Ricerca in Antartide 2009 (Grant PNRA 2010/A1.05) to G.M. and M.L.T.

## References

1. Hamers-Casterman C, Atarhouch T, Muyldermans S et al (1993) Naturally occurring antibodies devoid of light chains. *Nature* 363:446–448
2. Muyldermans S, Lauwereys M (1999) Unique single-domain antigen binding fragments derived from naturally occurring camel heavy-chain antibodies. *J Mol Recognit* 12:131–140
3. Joosten V, Lokman C, van den Hondel C et al (2003) The production of antibody fragments and antibody fusion proteins by yeasts and filamentous fungi. *Microb Cell Fact* 2:1
4. Harmsen MM, De Haard HJ (2007) Properties, production, and applications of camelid single-domain antibody fragments. *Appl Microbiol Biotechnol* 77:13–22
5. Rippa V, Papa R, Giuliani M et al (2012) Regulated recombinant protein production in the Antarctic bacterium *Pseudoalteromonas haloplanktis* TAC125. *Methods Mol Biol* 824:203–218
6. Giuliani M, Parrilli E, Pezzella C et al (2012) A novel strategy for the construction of genomic mutants of the Antarctic bacterium *Pseudoalteromonas haloplanktis* TAC125. *Methods Mol Biol* 824:219–233
7. Duilio A, Tutino ML, Marino G (2004) Recombinant protein production in Antarctic Gram negative bacteria. *Methods Mol Biol* 267:225–237
8. Médigue C, Krin E, Pascal G et al (2005) Coping with cold: the genome of the versatile marine Antarctica bacterium *Pseudoalteromonas haloplanktis* TAC125. *Genome Res* 15:1325–1335
9. Corchero JL, Gasser B, Resina D et al (2013) Unconventional microbial systems for the cost-efficient production of high-quality protein therapeutics. *Biotechnol Adv* 31:140–153
10. Gasser B, Saloheimo M, Rinas U et al (2008) Protein folding and conformational stress in microbial cells producing recombinant proteins: a host comparative overview. *Microb Cell Fact* 7:11
11. Vigentini I, Merico A, Tutino ML et al (2006) Optimization of recombinant human nerve growth factor production in the psychrophilic *Pseudoalteromonas haloplanktis*. *J Biotechnol* 127:141–150
12. Giuliani M, Parrilli E, Ferrer P et al (2012) Process optimization for recombinant protein production in the psychrophilic bacterium *Pseudoalteromonas haloplanktis*. *Process Biochem* 46:953–959
13. Monegal A, Ami D, Martinelli C et al (2009) Immunological applications of single-domain llama recombinant antibodies isolated from a naïve library. *Protein Eng Des Sel* 22:273–280
14. Birolo L, Tutino ML, Fontanella B et al (2000) Aspartate aminotransferase from the Antarctic bacterium *Pseudoalteromonas haloplanktis* TAC 125. Cloning, expression, properties, and molecular modelling. *Eur J Biochem* 267:2790–2802
15. Sambrook J, Russell DW (2001) Molecular cloning: a laboratory manual, 3rd edn. Cold Spring Harbor Laboratory, Cold Spring Harbor
16. Papa R, Rippa V, Sannia G et al (2007) An effective cold inducible expression system developed in *Pseudoalteromonas haloplanktis* TAC125. *J Biotechnol* 127:199–210
17. Tutino ML, Parrilli E, Giaquinto L et al (2002) Secretion of  $\alpha$ -amylase from *Pseudoalteromonas haloplanktis* TAB23: two different pathways in different hosts. *J Bacteriol* 184:5814–5817
18. Blatny JM, Brautaset T, Winther-Larsen HC et al (1997) Construction and use of a versatile set of broad-host-range cloning and expression vectors based on the RK2 replicon. *Appl Environ Microbiol* 63:370–379
19. Tutino ML, Duilio A, Parrilli E et al (2001) A novel replication element from an Antarctic plasmid as a tool for the expression of proteins at low temperature. *Extremophiles* 5:257–264
20. Madonna S, Papa R, Birolo L et al (2006) The thiol-disulphide oxidoreductase system in the cold-adapted bacterium *Pseudoalteromonas haloplanktis* TAC 125: discovery of a novel disulfide oxidoreductase enzyme. *Extremophiles* 10:41–51

21. Schierle CF, Berkmen M, Huber D et al (2003) The DsbA signal sequence directs efficient, cotranslational export of passenger proteins to the *Escherichia coli* periplasm via the signal recognition particle pathway. *J Bacteriol* 185: 5706–5713
22. Hanahan D (1983) Studies on transformation of *Escherichia coli* with plasmids. *J Mol Biol* 166:557–580
23. Hollinger P, Hudson PJ (2005) Engineered antibody fragments and the rise of single domains. *Nat Biotechnol* 23:1126–1136